University of Zabol

Agriculture, Environment & Society

انجمن علمی ماشین های کشاورزی و مکانیزاسیون ایران

Biannual, Volume 5, Issue 1, June 2025

Agriculture, Environment & Society (AES)

Volume 5, Issue 1, June 2025

Publisher: University of Zabol

Editorial Office: ***Faculty of Agriculture, University of Zabol, Zabol, Iran, P.O. Box 538-98615***

Tel: +98-54-31232102

Website: http://aes.uoz.ac.ir

Email: aes@uoz.ac.ir, aes.uoz.journal@gmail.com

Aims and Scopes

Agriculture, Environment and Society is a peer-reviewed, open-access international journal that deals with the interactions between agricultural systems and the life-supporting environment on which human well-being ultimately depends. This journal is biannually published by the *University of Zabol* (UOZ) and is scientifically supported by the *Iranian Society of Agricultural Machinery Engineering and Mechanization* (ISAMEM). The journal publishes original articles, short communications and review article. The journal's focus should capture the current needs of the agricultural systems with the goal of advancing the well-being of people. The papers in the journal should address the critical issues that will move agricultural systems forward and improve the living conditions of people. In this regard, the three critical systems that we need to understand to accomplish this end are the environment, agriculture and society. The role of the journal is to provide a forum to agricultural scientists to deliberate on important issues of agricultural research, education and extension and to present the views of the scientific community as policy inputs to planners and decision/opinion makers at various levels.

Agriculture, Environment and Society honors scientists at various levels, and encourages cutting edge research in a variety of agricultural disciplines. The journal's mission is to publish papers on new and emerging disciplines and concepts in order to provide future directions for agricultural research across the world. It is a unique journal that promotes inter-disciplinary research by encompassing all fields of crop sciences, animal sciences, fishery sciences, forestry sciences, agricultural machinery and natural resources management sciences, to stimulate interest in inter-disciplinary research.

The following should be included in all manuscripts submitted to *Agriculture, Environment and Society:*

- ***Generally, manuscripts should focus on the critical issues that will move agricultural systems forward and improve the living conditions of people.***
- ***Substantial natural science material (particularly at the farm- or landscape-level, sometimes coupled with social sciences)***
- ***A thorough examination and discussion of the interconnections between agricultural system components and other systems.***

Agriculture, Environment & Society (AES)

Volume 5, Issue 1, December 2025

Contents

Agriculture, Environment & Society

Journal homepage: www.aes.uoz.ac.ir

Detection of sugar content in sugar beets using hyperspectral imaging

Mohsen Mahdiani [a], Mehdi Khojastehpour [*b], Mahmood Reza Golzarian [c]

[a] Ph.D. Student, Department of Biosystems Engineering, Ferdowsi University of Mashhad, Mashhad, Iran
[b] Department of Biosystems Engineering, Ferdowsi University of Mashhad, Mashhad, Iran
[c] School of Engineering and IT, Murdoch University, WA 6150, Australia

ARTICLE INFO

Article history:
Received: 4 October 2024
Accepted: 15 November 2024
Available online: 1 June 2025

Keywords:
Hyperspectral imaging
Rapid detection
Regression analysis
Sugar beet
Sugar content

ABSTRACT

Measuring the sugar content in sugar beet is challenging because of the labor, expenses, and chemicals required. Hence, there is a necessity for a more efficient method to measure this content. This study aims to establish an efficient, non-invasive method for detecting sugar content in sugar beets using hyperspectral imaging, which could revolutionize quality control in the sugar beet industry. This study used hyperspectral imaging to analyze 400-950 nm sugar beet paste. Pre-processing techniques such as SNV (Standard Normal Variate) and SG (Savitzky-Golay), along with wavelength selection methods such as SPA (Successive Projection Algorithm) and CARS (competitive adaptive reweighted sampling), were applied. Furthermore, various regression models including MLR (multiple linear regression), PLS (Partial Least Squares regression) , and SVR (Support Vector Regression) were employed for prediction. Evaluating these models based on R^2 and RMSE criteria, the PLS regression model with SNV pre-processing and SPA wavelength selection stood out, achieving an R^2 value of 0.91% and RMSE of 0.24. These findings suggest the potential of hyperspectral imaging as a rapid and accurate means of determining sugar content in sugar beet across the VIS-NIR spectrum.

Highlights

- The analysis of hyperspectral images was investigated to predict the sugar content.
- SG and SNV algorithms were used for preprocessing.
- CARS and SPA algorithms were used to select the effective wavelengths.
- Models for prediction have been created by MLR, PLS and SVR algorithms.
- The best model for prediction of sugar content were selected.

1. Introduction

Assessing the sugar content in sugar beet is essential for both sugar factories and farmers, particularly in regions where payments to farmers are based on sugar content (Uygan et al., 2021; Wang et al., 2022). Since sucrose comprises C–H, O–H, C–C, and C–O bonds, various methods such as enzymatic analysis, HPLC, and polarimetry have been employed for their measurement (Pan et al., 2015a). Among these, the polarimetric method is favored for its simplicity and is commonly used in sugar factories. This method involves mixing 26 grams of sugar beet paste with 177 grams of lead acetate solution to measure sugar content through polarization (Roggo et al., 2004; Shabani and Sepaskhah, 2019).

Researchers have concentrated on developing precise and rapid methods for determining sugar content without relying on chemical reagents. Spectroscopy techniques, including hyperspectral imaging, have emerged as effective solutions. One of the pioneering studies in this area is by Roggo (Roggo et al., 2004), who employed an NIR spectrometer covering the 400 to 2498 nm wavelength range. This study demonstrated that spectroscopy can serve as a fast and straightforward method for assessing the sugar content in sugar beets. Additionally, the study highlighted the potential of this technique for simultaneously identifying other parameters. In Pan's research (Pan et al., 2015a; Pan et al., 2013; Pan et al., 2015b), two portable spectrometers with working ranges of 400-1100 nm and

* Corresponding author.
E-mail address: mkhpour@um.ac.ir
https://doi.org/10.22034/jelsa.2024.473159.1081

900-1600 nm were employed to obtain spectral data from the beets in intact and sliced conditions. The study, which considered interactance mode, consistently confirmed that sugar content could be accurately identified under all tested conditions (sliced beet and intact beet). In a separate study conducted by Babaei (Babaee et al., 2019), a near-infrared (NIR) spectrometer was employed in the wavelength range of 942-1576 nm in interactance mode to investigate the effects of spectroscopic location and sugar beet skin on the spectrometer's performance. Utilizing ANOVA analysis, the results indicated that within this spectral range, the wavelength of 1393 nm exhibited the highest correlation. Furthermore, spectral measurements taken from four locations—Northwest (NW), Southwest (SW), Northeast (NE), and Southeast (SE)—approximately one centimeter above and below the root neck, where the root diameter is greatest, did not yield significant differences. However, a notable distinction was observed between the spectroscopy of the skin and flesh of the sugar beet root, with measurements from the flesh demonstrating greater accuracy. Also in Bagharpur's study (Bagherpour et al., 2014), the quantification of sugar content was validated through the application of infrared spectroscopy within the wavelength range of 900-1600 nm on sugar beet samples, along with the implementation of pre-processing techniques.

Hyperspectral imaging is a technique that enables the extraction of internal compositional information from materials through imaging. This approach has demonstrated promising outcomes in numerous studies focused on agricultural products aimed at identifying their internal constituents. For instance, research conducted on mulberry fruits (305-1090nm wavelength in reflectance mode) has indicated that this method can effectively quantify anthocyanin levels (Li et al., 2023), while another study assessed the soluble solids content in Tribute Citru using the same technique (400–1000 nm wavelength in reflectance mode) (Li et al., 2023). In investigations carried out by Pan (Pan et al., 2014; Pan et al., 2016a), hyperspectral imaging was utilized on sugar beet slices within the spectral range of 500-1000 nm, resulting in relative reflectance data that demonstrated considerable accuracy. These results suggest that hyperspectral imaging may be an effective substitute for traditional methods of determining sugar content. In Wang's study (Wang et al., 2022), he effectively employed an Unmanned Aerial Vehicle (UAV) to evaluate the sugar levels in fields by combining hyperspectral imagery with RGB, multispectral, and thermal infrared images. His findings demonstrated that hyperspectral imaging can be used by UAVs for remote sensing to accurately measure sugar content. Nonetheless, many factories are unable to adopt these technologies widely due to their high costs thus posing problems of accessibility hence limited usage. As such, the cost-effective ways of applying hyperspectral imaging in determining sugar content levels of beet paste could greatly impact sugar processing companies. This would lead to more accurate measurements in the sugar factories.

In light of the research context, several pertinent questions arise: Firstly, is it feasible to ascertain sugar content through hyperspectral imaging of sugar beet paste? Secondly, can a regression-based methodology be developed for accurately determining sugar levels in sugar beet? How can we enhance identification accuracy by implementing efficient wavelength selection algorithms? The present study aims to address these inquiries.

2. Material and methods

2.1. Sampling and imaging

An automated machine randomly samples a portion of the sugar beets delivered to the factories. These beets undergo a process of washing, shredding, and combining to create a uniform mixture. This mixture is then analyzed to determine the sucrose content and other elements (Fasahat et al., 2022). In the Torbat-Heydarieh Sugar factory located in Torbat-Heydarieh, Khorasan Razavi, Iran, a total of 150 samples were prepared using this method. Each sample was divided into two segments: one segment was sent to an imaging lab (Automation and Computer Vision Laboratory -ACVL) at Ferdowsi University of Mashhad for imaging, while the other segment was sent to the Agricultural Research, Education and Extension Organization (AREEO) in Mashhad, Khorasan Razavi, Iran, to obtain data on sucrose content using a Betalizer (Figure 1), the sugar content (SC) was determined using the polarimetric method.

The linear scan-type imaging device utilized in this study is a Desktop Scanner manufactured by Parto Afzar Sanat Co. (Zanjan, Iran). It possesses several key specifications, including a scan length of 200mm, a scan resolution of 0.05mm, a vertical arm height of 400mm, and four halogen light sources that ensure uniform illumination. The imaging spectral range of this device spans from 400nm to 950nm, with a spectral interval of 2nm between consecutive spectral images. To ensure accurate calibration, the device was calibrated by imaging a white standard plate, which serves as the device standard, and obtaining a dark reference image by covering the lens with the cap. In addition to its ability to manually store and display the average spectrum of a selected region, the device also can store spectroscopic images. The primary focus of this study is the analysis of the stored images. The images within the device create a spectroscopic cube with dimensions of 114 x 36 x 516. Here, 516 represents the spectral resolution of the image, which corresponds to the number of acquired spectra ranging from 400nm to 950nm. Furthermore, the values 36 and 114 represent the spatial resolution—specifically the width and height—of the captured images. For data analysis, MATLAB software (VER 2022b, MathWorks Inc, US) was employed on an ACER ASPIRE laptop equipped with 20GB RAM and a core i7 CPU processor.

After preparation, each sample was placed in a tightly sealed container with minimal air exchange and stored in a refrigerator at -4 degrees Celsius. The samples were then quickly transported to the laboratory, taking less than 24 hours. A precise 2 cm stainless-steel cube mold was created to ensure standardization in laboratory analysis. This mold was used to shape the mixed sugar beet paste into uniform

sample blocks, ensuring all samples had identical dimensions and height to maintain consistency during sampling. The samples were carefully inserted into the molds and flattened with a knife to address any potential height variations during the sampling process (Figure 2). Without this mold, smoothing the surface would have required significant effort, and the color would have changed in the process. However, the small dimensions of the mold allowed for quick smoothing with a knife. If the sample's color changed during sampling, some material was removed from the middle and placed into the mold. Determining the appropriate sample size was essential to achieve a sample with a specific thickness quickly. Additionally, applying pressure at the end of the mold and removing some material from the sample's surface allowed for faster imaging and minimized color changes. Each sample was sampled at least twice, and the average of the spectra was used as the final sample spectrum. Subsequently, the sample was positioned beneath the imaging device, and a region of interest (ROI) measuring 51x51 pixels was designated at the center of each sample surface using the associated imaging software application. The spectral images across all spectral bands were then captured from this defined ROI.

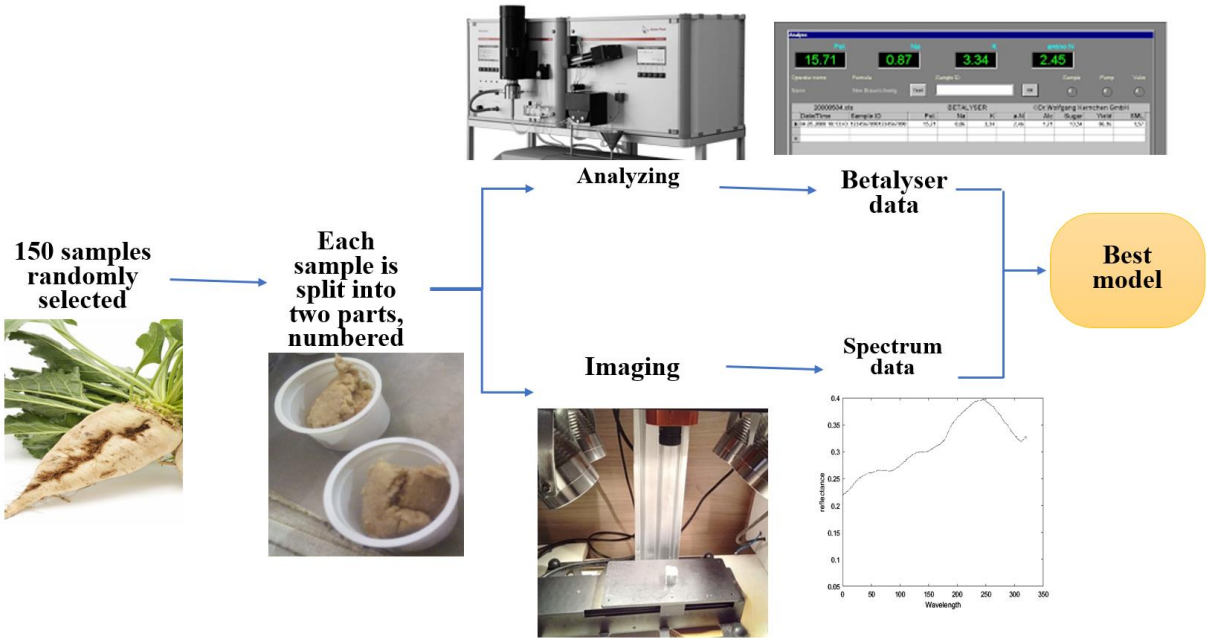

Figure 1. Flowchart of model building

Figure 2. A 2x2x2 cm sampling mold and a manual rectangular Region of Interest (ROI) on the sample after the spectral image is captured

2.2 Data processing

In spectroscopic devices, the existence of device noise in both low and high spectral ranges necessitates the exclusion of specific spectra during the processing stage. For instance, in a particular device, the initial and final spectra were eliminated as reported by Yang et al. (Yang et al., 2014), leading to a total of 321 spectra out of the original 516 spectra captured. The remaining 321 spectra were then utilized in the subsequent processing procedures, as illustrated in Figure 3. In subsequent analyses, we utilized data cubes, each with dimensions of 321 × 51 × 51 and comprising a total of 150 samples—a complete dataset.

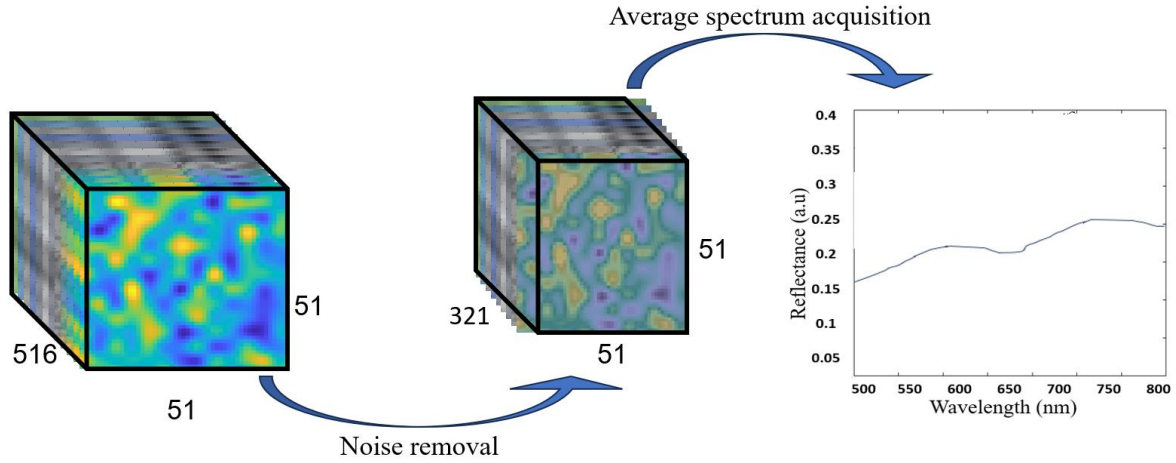

Figure 3. Noise removal and average spectrum acquisition

To address the impact of outliers on predictive models caused by instrument and operational errors, the researchers in this study employed the Monte Carlo Partial Least Squares (MCPLS) method (Zhang et al., 2015). To begin with, a calibration set was created by randomly selecting sample fractions, while the remaining fractions were designated as the prediction set. PLS models were then generated repeatedly to ensure that each sample was utilized multiple times in the prediction set. As a result, each sample produced a series of predictive residual errors (PRE). For each sample in the prediction set, the Mean of Predicted Residual Errors (MPRE) and the Standard Deviation of Predicted Residual Errors (STDPRE) were calculated (Figure 4) (Guo et al., 2012).

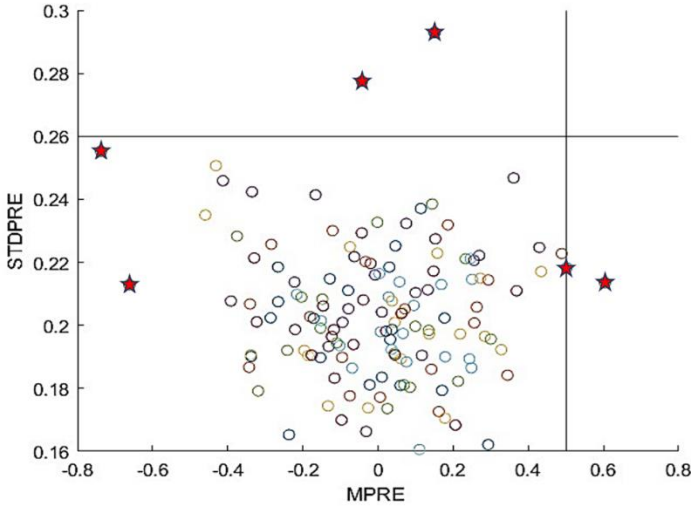

Figure 4. MPRE versus STDPRE plot for determining outliers

2.2.1. Preprocessing

Data acquired from spectroscopic imaging systems can be influenced by various factors, including light scattering resulting from the interaction between the sample and the detector, changes in sample size, surface roughness of the sample, noise generated due to an increase in system temperature, and other factors. These unintended factors have the potential to affect the accuracy of models and lead to significant discrepancies in the interpreted data. These elements introduce additional noise that may mask true spectral signals, thus compromising the reliability of analytical outcomes (Zhang et al., 2021). Ensuring the integrity of the data not only strengthens calibration models but also fosters greater confidence in subsequent interpretations and applications across various scientific fields. Therefore, to achieve stable, accurate, and reliable validation models, it is necessary to preprocess the data (Rossel, 2008). In this particular study, two common

preprocessing techniques (Sim et al., 2024), namely Standard Normal Variate (SNV) and Savitzky-Golay (SG) smoothing, were utilized. SNV and SG are. These preprocessing techniques are employed to mitigate the influence of multiplicative effects such as baseline shifts and intensity changes in spectral data. SNV involves transforming each data point by subtracting the mean and dividing it by the standard deviation across all data points. On the other hand, Savitzky-Golay (SG) smoothing is used to remove random noise while preserving important features of the captured spectra. The SG smoothing technique applies a convolution process with a set of predefined coefficients to a moving window of data points. SNV was performed with a degree of 3 and a window size of 5. The SG method, which utilizes a window size of 5 and a degree of 3, is widely employed for noise reduction (Yu et al., 2021). SNV, on the other hand, is useful in eliminating the scattering effect caused by light and particle size. Furthermore, the impact of these preprocessing methods on the performance of the predictive model was evaluated and compared with the performance metrics obtained when only the raw data, without any preprocessing, was fed into the model.

2.2.2. Selection of effective wavelengths

To enhance modeling accuracy and reduce computational time, employing different algorithms for selecting effective wavelengths is crucial. This study investigated two commonly used methods: Competitive Adaptive Reweighted Sampling (CARS) and Successive Projection Algorithm (SPA). The CARS method, inspired by the concept of "survival of the fittest" from Darwinian Theory, utilizes Monte Carlo sampling to select a subset of wavelengths through iterative processes and competition. This method evaluates wavelengths based on their absolute coefficient value in PLS modeling by optimizing variables with an exponential decreasing penalty function and adaptive weighted resampling (Ji et al., 2020). The subset with the smallest RMSEV is identified as characteristic wavelengths, obtained through repetitions of sampling (Shao et al., 2020).

On the other hand, the SPA is a valuable tool for forward variable selection, enhancing modeling speed and accuracy by reducing collinearity and extraneous information among variables. SPA operates by selecting the optimal wavelength with the highest design value in each iteration until the desired number of wavelengths is reached. The number of variables is determined by minimizing the root mean square error (RMSE) in multiple linear regression (MLR) calibration (Shao et al., 2020), contributing to improved modeling outcomes.

In general, the SPA method involves adding one wavelength at a time based on correlation, while the CARS algorithm samples and re-weights wavelengths according to their performance in predicting the target property. This study aims to compare these two methods in terms of their effectiveness and efficiency in spectral data analysis.

MLR is a widely used technique for establishing a linear relationship between spectral data and chemical components. Despite being an older algorithm, MLR remains efficient, especially when the number of features is less than the observations (Fei et al., 2023). Additionally, PLSR is a method that utilizes full-spectrum data to predict sample composition by identifying the highest covariance between reference values and spectral data. PLSR combines various statistical analysis methods to model the relationship between dependent and independent variables, making it particularly useful in scenarios with more variables than observations and when multicollinearity is present among the X values (Nie et al., 2023). Support Vector Regression (SVR) is another supervised Machine Learning technique that focuses on structural risk minimization and demonstrates high-performance (Ahmad et al., 2020), especially with multidimensional data and high-dimensional datasets (Mesut et al., 2023).

Given the wide utilization and satisfactory outcomes of these three regression methods in hyperspectral image studies (Mitku et al., 2024; Shao et al., 2020; Soltanikazemi et al., 2022), all three methods were employed in this study to assess the most effective prediction models (Figure 5).

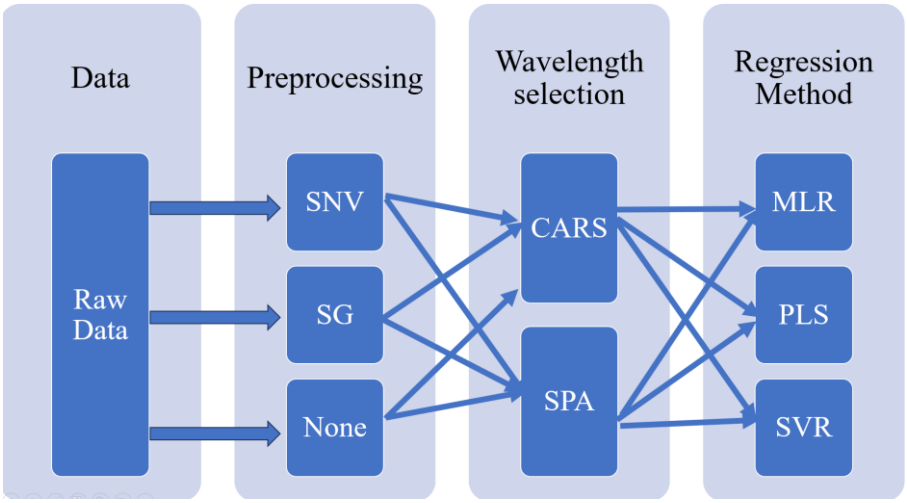

Figure 5. Workflow of finding regression method

2.3. Model evaluation

In this study, due to the limited amount of data, the cross-validation method was employed. The data was split into two groups: 80% for training and 20% for validation. Regression model evaluation metrics include the correlation coefficient (R) and root mean square error (RMSE). R indicates the goodness of fit, while RMSE measures the difference between predicted and actual values (eq. 1-2). A value of R^2 close to 1 suggests high stability and fit, whereas an RMSE close to 0 indicates stronger predictive ability (Li et al., 2023):

$$R = \sqrt{1 - \frac{\sum_{i=1}^{n}(\hat{y}_i - y_i)^2}{\sum_{i=1}^{n}(y_i - y_m)^2}} \quad (1)$$

$$RMSE = \sqrt{\frac{\sum_{i=1}^{n}(\hat{y}_i - y_i)^2}{n}} \quad (2)$$

In these equations,

y_i = measured value of the attribute for the ith sample in the category;

$\hat{y}_i$ =predicted value of the attribute for the ith sample in the category;

y_m= The average measured values of attributes in the category;

n= the number of category samples;

3. Results

After analyzing the Betalyser result shows that the SC ranges from 10.10 to 23.65%. This range is consistent with the typical SC range of 10 to 24 % in sugar factories, indicating a close resemblance to real-world samples. In the spectrum (Figure 3), there is a noticeable dip at 650 nanometers and a peak at 620 nm, associated with the chlorophyll level in the paste (Governici et al., 2017; Tian et al., 2019). This range is also recognized by Pan et al. as a crucial factor in determining chlorophyll in sugar beet (Tian et al., 2019). Additionally, a noticeable peak at 750 nm, suggested by Pan, is likely linked to the third overtone of water(Pan et al., 2016b) or the fourth overtone of C–H (Wei et al., 2017). The O–H and C–H functional groups are associated with the concentration of specific internal compositions, such as soluble solid contents.

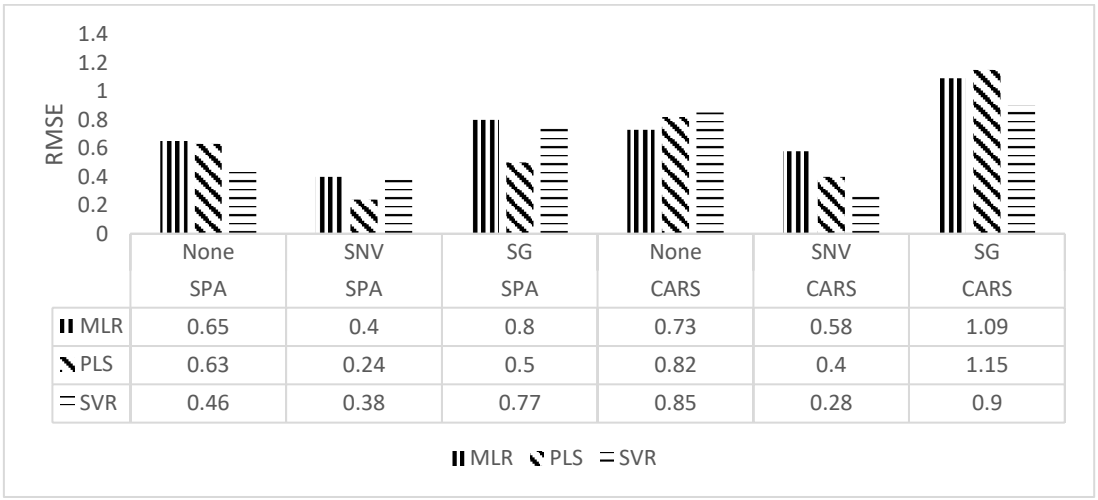

	None SPA	SNV SPA	SG SPA	None CARS	SNV CARS	SG CARS
MLR	0.65	0.4	0.8	0.73	0.58	1.09
PLS	0.63	0.24	0.5	0.82	0.4	1.15
SVR	0.46	0.38	0.77	0.85	0.28	0.9

(a)

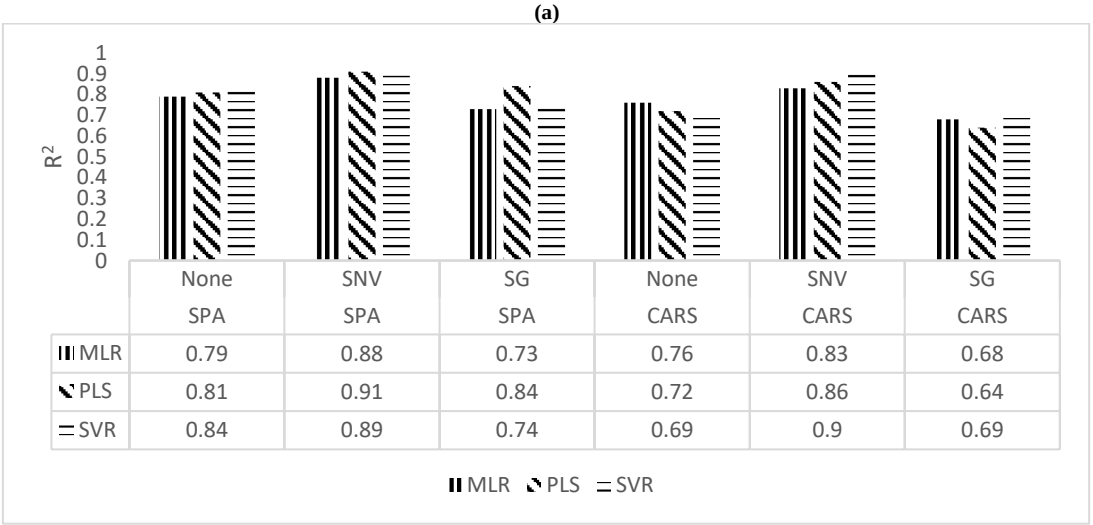

	None SPA	SNV SPA	SG SPA	None CARS	SNV CARS	SG CARS
MLR	0.79	0.88	0.73	0.76	0.83	0.68
PLS	0.81	0.91	0.84	0.72	0.86	0.64
SVR	0.84	0.89	0.74	0.69	0.9	0.69

(b)

Figure 6. Comparison of different regression, a) comparison of RMSE b) comparison of R^2

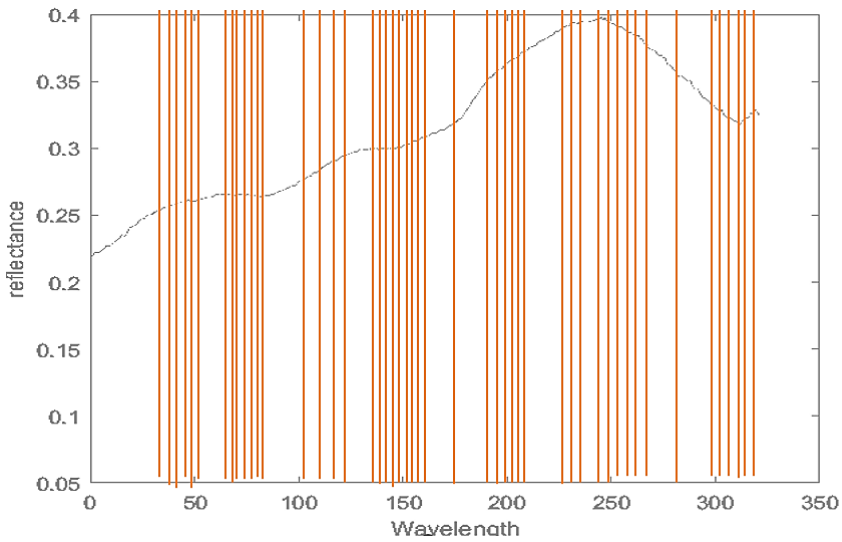

Figure 7. Selected wavelengths for determining sucrose

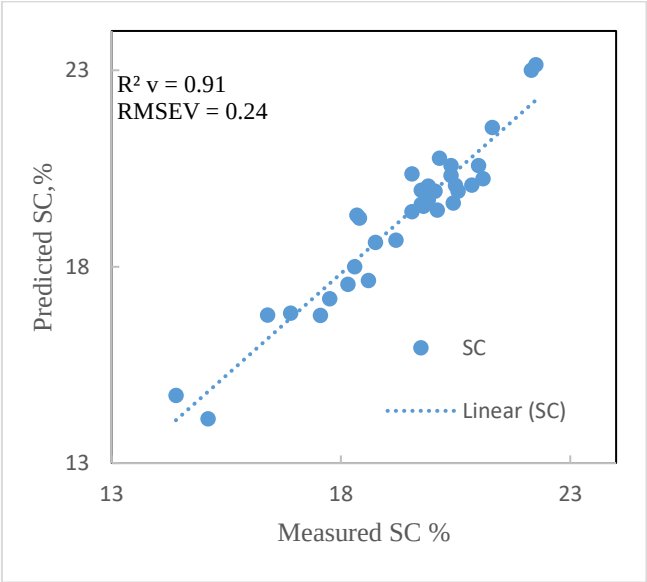

Figure 8. Measured vs predicted value

The MCPLS method was utilized to detect outliers, following a similar approach to Zhang's study (Zhang et al., 2023). For running MCPLS 75% of the selected samples were assigned randomly to the calibration set, whereas the remaining 25% were allocated to the prediction set. This iterative procedure was repeated 5000 times, leading to the generation of a scatter plot that visually depicts the correlation between MPRE and STDPRE. Figure 4 Demonstrates that six samples were identified as outliers. Specifically, any values of MPRE out of range (-0.5, 0.5) and values of STDPRE surpassing 0.26 were classified as outlier data.

The spectral data contained excessive information, linearity, and overlapping, which negatively affected the performance of multivariate calibration models. This study utilized SPA and CARS to identify particular wavelengths with minimal linearity and redundancy, enhancing modeling efficiency.

The number of effective wavelengths was selected after applying effective wavelength selection methods (CARS and SPA) to each type of preprocessing data (None, SNV, SG) then prediction models were created using MLR, PLS, and SVR regression methods, and the results are shown in Figure 6.

In Figure 6, the combination of the SPA and SG algorithms exhibits the highest RMSE value and the lowest R^2 value. Conversely, the combination of the SPA algorithm with SNV demonstrates the lowest RMSE value and the highest R^2 value. Figure 6 illustrates the capability of the SPA algorithm to decrease the RMSE value. This comparison between the SPA algorithm without preprocessing and the CARS algorithm without preprocessing is evident. The best model for identifying effective wavelengths as input for the PLS algorithm is the combination of SNV preprocessing and the SPA algorithm that selects 50 wavelengths (Figure 7). This model achieved a validation R^2 of 0.91, RMSEV of 0.24. Figure 8 also illustrates the performance of the best model for predicting sugar content in the calibration set and validation set.

4. Discussion

In this study, different regression models were employed (PLSR, MLR, and SVR) to analyze hyperspectral data within the visible-near-infrared (vis-NIR) spectral range (400-950nm). The present model successfully determined the sugar content in sugar beet. This study found that the SNV and SG pre-processing algorithms significantly improved model accuracy in most cases, based on validation data. Additionally, algorithms for selecting effective wavelengths, such as CARS and SPA, enhanced model performance. While the CARS algorithm chose fewer wavelengths, its accuracy was lower than SPA. Among the regression methods in this study, MLR and PLS algorithms exhibited better performance than the SVR algorithm in predicting SC. Results are consistent with previous studies (Pan et al., 2014; Pan et al., 2016a) that demonstrated the ability to determine sucrose content within the 500-1000 nm wavelength range using the PLS algorithm with an R^2 of 0.76. Pan's study (Pan et al., 2013; Pan et al., 2015b), revealed that the optimal model for intact beet was 0.81, while for sliced beet it was 0.89, within the wavelength range of 400-1100 nm. One possible reason for the difference in the results could be attributed to the use of sugar beet paste in this study, which provided a more homogeneous sample. Findings align with other studies that determine sugar content in fruit paste and employ hyperspectral images. For instance, Maraphum (Maraphum et al., 2020) identified the amount of sugar in sugarcane within the same wavelength range (400-1000 nm) and showed that using the PLS algorithm with first derivative preprocessing achieved an R2 of 0.66, which is superior to their proposed method. Liu (Liu et al., 2017) demonstrated that using multispectral imaging of tomato paste within the range of 405-970 nm can determine sugar content with an R^2 of 0.93. In this study, the optimal method for predicting the SC level involves employing SNV preprocessing in conjunction with the SPA algorithm to determine the relevant wavelengths for the PLS algorithm. This approach resulted in a validation R2 of 0.91 and a minimal RMSEV of 0.24. These values are significantly higher and lower, respectively than those reported in previous studies (Maraphum et al., 2020; Pan et al., 2016a), indicating the model's higher performance and robustness in predicting sugar content. This research demonstrates, for the first time, that the SC of sugar beet paste can be evaluated through hyperspectral imaging. These findings have promising implications for the agricultural industry, as they can lead to improved crop management practices and enhanced product quality. By leveraging various algorithms such as SPA, PLS, and MLR, scientists can build robust models that provide accurate and reliable results. Furthermore, this study emphasizes the significance of selecting effective wavelengths, with the SPA method emerging as a particularly valuable tool in this regard. Overall, these results contribute to the growing body of knowledge on the application of hyperspectral imaging for quality assessment in agricultural products, highlighting its potential for enhancing efficiency and precision in various industrial processes.

5. Conclusion

The current study sought to measure the sugar content in sugar beet using hyperspectral images of sugar beet paste within the spectral range from 400 to 950 nm. To achieve this, dough samples were taken from the shipments received at the sugar factory. The sugar content of each sample was assessed using a Betalyzer, and hyperspectral imaging of the sugar beet paste was also captured. In this study, pre-processing methods such as SNV and SG were utilized, along with effective algorithms for wavelength selection, specifically CARS and SPA. The results were then fed into MLR, PLS, and SVR algorithms, resulting in the creation of eighteen regression models that combined these approaches. Among the eighteen developed models, the best model was selected with the minimum RMSE and maximum R^2 values. These results indicated that all models were acceptable, but the best performance was achieved when SNV preprocessing was carried out along with the SPA algorithm as an input method for PLS regression. Such results would enable fast, chemical-free evaluation of sugar content, thereby benefiting sugar factories while also assisting farmers in assessing the size of their crops' sugar content. Since this research is quite at the beginning, it would be of great use to extend the project for more general results with more samples involved. Moreover, techniques beyond those applied could still provide further precision. For instance, deep learning techniques may be considered to learn features of the hyperspectral data.

Declaration of Competing Interest

The authors declare that they have no conflicts of interest.

Acknowledgments

The authors also wish to express their gratitude to Torbat_Heydarieh Sugar Factory for their collaboration.

Funding: This work was supported by Ferdowsi University of Mashhad (FUM) [Grant No. 59736].

References

Ahmad, M. S., Adnan, S. M., Zaidi, S., & Bhargava, P. (2020). A novel support vector regression (SVR) model for the prediction of splice strength of the unconfined beam specimens. *Construction and Building Materials, 248*, 118475. https://doi.org/10.1016/j.conbuildmat.2020.118475

Babaee, B., Khanmohammadi, M., Garmarudi, A. B., & Abdollahin Noghabi, M. (2019). Effect of peeling and point of spectral recording on sucrose determination in sugar beet root using near infrared spectroscopy. *Infrared Physics & Technology, 103*, 103065. https://doi.org/10.1016/j.infrared.2019.103065

Bagherpour, H., Minaei, S., & Abdollahian Noghabi, M. (2014). Non-destructive determination of sugar content in root beet by near infrared spectroscopy (nirs). *Journal of Food Science & Technology (2008-8787), 12*(46).

Fasahat, P., Rezaei, J., Sharifi, M., Azizi, H., Fatouhi, K., Mahdikhani, P., Pedram, A., Jalilian, A., & Babaei, B.

(2022). Assessment of root and white sugar yield stability of sugar beet genotypes.

Fei, S., Xu, D., Chen, Z., Xiao, Y., & Ma, Y. (2023). Mlr-based feature splitting regression for estimating plant traits using high-dimensional hyperspectral reflectance data. *Field Crops Research*, *293*, 108855. https://doi.org/10.1016/j.fcr.2023.108855

Governici, J. L., Faria, R. M., dos Reis Tinini, R. C., & Mederos, B. J. T. (2017). Tomatoes maturation analysis with reflectance spectral images. *Journal of Agricultural Science and Technology B.*

Guo, W.-L., Du, Y.-P., Zhou, Y.-C., Yang, S., Lu, J.-H., Zhao, H.-Y., Wang, Y., & Teng, L.-R. (2012). At-line monitoring of key parameters of nisin fermentation by near infrared spectroscopy, chemometric modeling and model improvement. *World Journal of Microbiology and Biotechnology*, *28*, 993-1002. https://doi.org/10.1007/s11274-011-0897-x

Ji, H., Wang, W., Chong, D., & Zhang, B. (2020). Cars algorithm-based detection of wheat moisture content before harvest. *Symmetry*, *12*(1), 115. https://doi.org/10.3390/sym12010115

Li, C., He, M., Cai, Z., Qi, H., Zhang, J., & Zhang, C. (2023). Hyperspectral imaging with machine learning approaches for assessing soluble solids content of tribute citru. *Foods*, *12*(2), 247. https://doi.org/10.3390/foods12020247

Li, S., Song, Q., Liu, Y., Zeng, T., Liu, S., Jie, D., & Wei, X. (2023). Hyperspectral imaging-based detection of soluble solids content of loquat from a small sample. *Postharvest Biology and Technology*, *204*, 112454. https://doi.org/10.1016/j.postharvbio.2023.112454

Li, X., Wei, Z., Peng, F., Liu, J., & Han, G. (2023). Non-destructive prediction and visualization of anthocyanin content in mulberry fruits using hyperspectral imaging. [Original Research]. *Frontiers in Plant Science*, *14*. https://doi.org/10.3389/fpls.2023.1137198

Liu, C., Hao, G., Su, M., Chen, Y., & Zheng, L. (2017). Potential of multispectral imaging combined with chemometric methods for rapid detection of sucrose adulteration in tomato paste. *Journal of Food Engineering*, *215*, 78-83. https://doi.org/10.1016/j.jfoodeng.2017.07.026

Maraphum, K., Saengprachatanarug, K., Wongpichet, S., Phuphaphud, A., & Posom, J. (2020). In-field measurement of starch content of cassava tubers using handheld vis-near infrared spectroscopy implemented for breeding programmes. *Computers and Electronics in Agriculture*, *175*, 105607. https://doi.org/10.1016/j.compag.2020.105607

Mesut, B., Başkor, A., & Aksu, N. B. (2023). Role of artificial intelligence in quality profiling and optimization of drug products *A handbook of artificial intelligence in drug delivery* (pp. 35-54): Elsevier. https://doi.org/10.1016/B978-0-323-89925-3.00003-4

Mitku, A. A., Titshall, L., Zewotir, T., & North, D. (2024). Application of support vector machine regression and partial least-square regression models for predicting sugarcane leaf nutrients content using near infra-red spectroscopy. *Communications in Soil Science and Plant Analysis*, *55*(2), 196-207. https://doi.org/10.1080/00103624.2023.2265426

Nie, B., Du, Y., Du, J., Rao, Y., Zhang, Y., Zheng, X., Ye, N., & Jin, H. (2023). A novel regression method: Partial least distance square regression methodology. *Chemometrics and Intelligent Laboratory Systems*, *237*, 104827. https://doi.org/10.1016/j.chemolab.2023.104827

Pan, L., Lu, R., Tu, K., & Cen, H. (2014). *Detection of moisture, soluble solids, and sucrose content and mechanical properties of sugar beet by hyperspectral scattering imaging.* Paper presented at the 2014 Montreal, Quebec Canada July 13–July 16, 2014.

Pan, L., Lu, R., Zhu, Q., McGrath, J. M., & Tu, K. (2015a). Measurement of moisture, soluble solids, sucrose content and mechanical properties in sugar beet using portable visible and near-infrared spectroscopy. *Postharvest Biology and Technology*, *102*, 42-50. https://doi.org/10.1016/j.postharvbio.2015.02.005

Pan, L., Lu, R., Zhu, Q., Tu, K., & Cen, H. (2016a). Predict compositions and mechanical properties of sugar beet using hyperspectral scattering. *Food and Bioprocess Technology*, *9*, 1177-1186. https://doi.org/10.1007/s11947-016-1710-5

Pan, L., Lu, R., Zhu, Q., Tu, K., & Cen, H. (2016b). Predict compositions and mechanical properties of sugar beet using hyperspectral scattering. *Food and Bioprocess Technology*, *9*(7), 1177-1186. https://doi.org/10.1007/s11947-016-1710-5

Pan, L., Zhu, Q., Lu, R., & McGrath, J. M. (2013). *Detection of sucrose content of sugar beet by visible/near infrared spectroscopy.* Paper presented at the 2013 Kansas City, Missouri, July 21-July 24, 2013.

Pan, L., Zhu, Q., Lu, R., & McGrath, J. M. (2015b). Determination of sucrose content in sugar beet by portable visible and near-infrared spectroscopy. *Food Chemistry*, *167*, 264-271. https://doi.org/10.1016/j.foodchem.2014.06.117

Roggo, Y., Duponchel, L., & Huvenne, J.-P. (2004). Quality evaluation of sugar beet (beta vulgaris) by near-infrared spectroscopy. *Journal of agricultural and food chemistry*, *52*(5), 1055-1061. https://doi.org/10.1021/jf0347214

Rossel, R. A. V. (2008). Parles: Software for chemometric analysis of spectroscopic data. *Chemometrics and Intelligent Laboratory Systems*, *90*(1), 72-83. https://doi.org/10.1016/j.chemolab.2007.06.006

Shabani, A., & Sepaskhah, A. R. (2019). Optimal amounts of water and nitrogen applied to sugar beet when crop price depends on its sugar content. *Spanish Journal of Agricultural Research*, *17*(3), e1202. https://doi.org/10.5424/sjar/2019173-14487

Shao, Y., Liu, Y., Xuan, G., Wang, Y., Gao, Z., Hu, Z., Han, X., Gao, C., & Wang, K. (2020). Application of hyperspectral imaging for spatial prediction of soluble solid content in sweet potato. *RSC advances*, *10*(55), 33148-33154. https://doi.org/10.1039/c9ra10630h

Sim, J., McGoverin, C., Oey, I., Frew, R., & Kebede, B. (2024). Optimisation of vibrational spectroscopy instruments and pre-processing for classification

problems across various decision parameters. *Food Innovation and Advances*, *3*(1), 52-63. https://doi.org/10.48130/fia-0024-0004

Soltanikazemi, M., Minaei, S., Shafizadeh-Moghadam, H., & Mahdavian, A. (2022). Field-scale estimation of sugarcane leaf nitrogen content using vegetation indices and spectral bands of sentinel-2: Application of random forest and support vector regression. *Computers and Electronics in Agriculture*, *200*, 107130. https://doi.org/10.1016/j.compag.2022.107130

Tian, X., Li, J., Wang, Q., Fan, S., Huang, W., & Zhao, C. (2019). A multi-region combined model for non-destructive prediction of soluble solids content in apple, based on brightness grade segmentation of hyperspectral imaging. *Biosystems Engineering*, *183*, 110-120. https://doi.org/10.1016/j.biosystemseng.2019.04.012

Uygan, D., Cetin, O., Alveroglu, V., & Sofuoglu, A. (2021). Improvement of water saving and economic productivity based on quotation with sugar content of sugar beet using linear move sprinkler irrigation. *Agricultural Water Management*, *255*, 106989. https://doi.org/10.1016/j.agwat.2021.106989

Wang, Q., Che, Y., Shao, K., Zhu, J., Wang, R., Sui, Y., Guo, Y., Li, B., Meng, L., & Ma, Y. (2022). Estimation of sugar content in sugar beet root based on uav multi-sensor data. *Computers and Electronics in Agriculture*, *203*, 107433. https://doi.org/10.1016/j.compag.2022.107433

Wei, X., He, J.-C., Ye, D.-P., & Jie, D.-F. (2017). Navel orange maturity classification by multispectral indexes based on hyperspectral diffuse transmittance imaging. *Journal of Food Quality*, *2017*. https://doi.org/10.1155/2017/1023498

Yang, Y., Ren, J., Zheng, X.-Q., Zhao, L.-Y., & Li, M.-M. (2014). Rapid determination of beet sugar content using near infrared spectroscopy. *Guang pu xue yu guang pu fen xi= Guang pu*, *34*(10), 2728-2731.

Yu, Y., Zhang, Q., Huang, J., Zhu, J., & Liu, J. (2021). Nondestructive determination of ssc in korla fragrant pear using a portable near-infrared spectroscopy system. *Infrared Physics & Technology*, *116*, 103785. https://doi.org/10.1016/j.infrared.2021.103785

Zhang, C., Liu, F., Kong, W., & He, Y. (2015). Application of visible and near-infrared hyperspectral imaging to determine soluble protein content in oilseed rape leaves. *Sensors*, *15*(7), 16576-16588. https://doi.org/10.3390/s150716576

Zhang, J., Guo, Z., Ren, Z., Wang, S., Yin, X., Zhang, D., Wang, C., Zheng, H., Du, J., & Ma, C. (2023). A non-destructive determination of protein content in potato flour noodles using near-infrared hyperspectral imaging technology. *Infrared Physics & Technology*, *130*, 104595. https://doi.org/10.1016/j.infrared.2023.104595

Zhang, X., Sun, J., Li, P., Zeng, F., & Wang, H. (2021). Hyperspectral detection of salted sea cucumber adulteration using different spectral preprocessing techniques and svm method. *LWT*, *152*, 112295. https://doi.org/10.1016/j.lwt.2021.112295

Agriculture, Environment & Society

Journal homepage: www.aes.uoz.ac.ir

Pollination service to faba bean agroecosystem: quantifying and valuation using field experiment

Hossein Kazemi [*a], Ahmad Nadimi [b], Christine Fürst [c, d]

[a] Department of Horticulture, Faculty of Plant Production, Gorgan University of Agricultural Sciences and Natural Resources, Gorgan, Iran
[b] Department of Plant Protection, Faculty of Plant Production, Gorgan University of Agricultural Sciences and Natural Resources, Gorgan, Iran
[c] Dept. Sustainable Landscape Development, Institute for Geosciences and Geography, Martin-Luther University Halle, Von-Seckendorff-Platz 4, 06120 Halle (Saale), Halle, Germany
[d] German Centre for Integrative Biodiversity Research (iDiv) Halle-Jena-Leipzig, Puschstraße 4, 04103 Leipzig, Germany

ARTICLE INFO

Article history:
Received: 29 August 2024
Accepted: 11 February 2025
Available online: 31 May 2025

Keywords:
Economic value
Faba bean cultivars
Insect
Pollination
Regulating service

ABSTRACT

In this study, pollination service in the faba bean agroecosystem was evaluated and valued with a field experiment. For this purpose, a factorial experiment based on a randomized complete blocks design with three replications was carried out in the research farm of Gorgan University of Agricultural Sciences and Natural Resources (Golestan province, Iran), during 2020-2021. The treatments of this experiment included cultivar as the first factor in four levels, including Feyz, Mahta, Barkat and Shadan and the second factor in two levels, including open-pollinated plants by insects and limitation of pollination by a cage. In this experiment, each plot included five planting rows with a distance between plants on each row of 15 cm, a planting depth of 5 cm and a distance between rows of 50 cm. Also, each plot had a size of 2×2.5 m and the distance between of plots was 75 cm. During the growing season, with the onset of warmer temperatures and insect activity in late March 2021, plots with limited open pollination are wholly trapped by the nets until the end of pollination. Simultaneously with the activity of insects in the field, samples of insects are collected using lattice nets. At the time of crop maturing, green yield and plant biomass were harvested. Finally, we quantified the value of pollination service by marketing price and alternative cost methods. In this study, we collected 13 pollinator species from the faba bean agroecosystem. The share of insects in the pollination of faba bean cultivars was obtained between 3.81 and 17.06 %. Results showed that the economic value of pollination in the faba bean agroecosystem was between 38,056,136 to 161,000,000 Rls.ha^{-1}. Generally, the role of pollinating insects in new faba bean cultivars was more than in the old cultivars, especially, the cultivars such as Mahta that use more pollination service than other cultivars. It is necessary that faba bean growers promote and protect pollination service to enhance their economic benefits in agroecosystems.

Highlights

- Faba bean pollination by 13 insect species boosts yield by 3.81-17.06% in Gorgan, Iran.
- Economic value of pollination ranges from 38M to 161M Rls/ha in faba bean fields.
- New cultivar Mahta relies most on insects (17.06%) vs. old cultivar Barkat (3.81%).
- Feyz and Barkat cultivars yield highest profit; Mahta benefits most from pollination.
- Study urges protecting pollinators for sustainable faba bean agroecosystem gains.

1. Introduction

Globally, agricultural ecosystems cover about 40% of the land (FAO, 2014), which are both providers and dependents on a variety of ecosystem services. They provide critical ecological services such as food production, aesthetics, carbon sequestration, soil erosion control, pest control, soil health and water regulation (Sandhu et al., 2010). At the same time, agricultural

* Corresponding author.
E-mail address: hkazemi@gau.ac.ir
https://doi.org/10.22034/jelsa.2025.475987.1083

ecosystems depend on services such as biodiversity, nutrients, soil structure and function, and water cycle (Power, 2010).

In recent decades, significant work has been done to determine the value of the functions, goods and services in the agroecosystems. Regulating services are concerned with the ability of natural and semi-natural ecosystems to regulate essential ecological processes and life support systems through bio-geochemical cycles and biosphere processes. Regulatory functions provide many services that have direct and indirect benefits to humans (Costanza et al., 1997).

The evaluation and quantification of various services and functions of agroecosystems are the most important ways to pay attention to these services and adopt appropriate strategies for their sustainability**.** For example, Andersson et al. (2014) investigated the effects of agricultural management and landscape heterogeneity on field bean pollination. Their results suggest that to maximize pollination success, it is important to improve field management and maintain natural habitats in agricultural landscapes.

In China, Zou et al. (2017) evaluated the relationships between landscape texture and pollinator communities. Their results showed that landscapes with small fields support an abundant but relatively species-poor bee community that provides pollination services to canola.

In Central Germany, Happe et al., (2018) investigated the effects of farming systems and scale agricultural landscapes on bee communities. Their results showed that organic system had the higher insect-pollinated richness. The value of insect pollination to yield of oilseed rape (*Brassica rapa*) in Bangladesh was estimated by Islam et al., (2022). They found that oilseed rape with visiting insects had a 30.8% greater yield compared to those where visitors were excluded. Also, they calculated the economic value of pollination at about $US 26.92 million per annum.

Wild bees were sampled by Carrié et al. (2018) from 43 cereal fields in southwestern France, the surrounding proportion of permanent grasslands. They found that the mean slope of surrounding grasslands was the factor that most positively influenced bee richness, abundance and trait distribution in bee communities. They also found that the mean slope of surrounding grasslands had a better predictive power of bee community structure than the proportion of permanent grasslands. In another study, Cunningham and Feuvre, (2013) provided honeybee hives to 17 faba bean fields in South Australia, and they observed that bee activity and fruits per stem decreased with increasing distance from hives. They found an effect of distance from hives on mean yield.

Faba bean (*Vicia faba* L.) is one of the oldest crops that is mostly grown in Asian, African and Europe countries. This crop can be used in human and animal nutrition, which directly and indirectly provides the protein needs of humans (Majnoon Hosseini, 1996). Faba bean is a suitable crop for rotation with oilseeds and cereals due to the high amount of nitrogen bio-fixation and breaking the cycle of diseases. One of the regulating services provided by natural ecosystems to faba bean agroecosystem is insect pollination. It is important for the productivity of grain in faba bean agroecosystems. Studies have confirmed that pollination by insects can improve plant yields. A study demonstrated that the yield benefits of additional pollination varied significantly among five faba bean cultivars, with some showing a yield increase of up to 37% under insect pollination, while others experienced a yield decrease of 51% when pollinated. This variability suggests that cultivar selection is crucial for optimizing yield through pollination (Bishop et al., 2020). Recent findings emphasize that while honeybees contribute to faba bean pollination, wild bumblebees are the most effective pollinators, accounting for approximately 70% of marketable yields in certain regions. This highlights the importance of maintaining diverse pollinator populations to maximize crop yields (Burns and Stanley, 2023). However, the importance of pollination as an ecosystem service depends on cultivar reproductive form, pollinator species and insect abundance.

In Iran, Golestan province is a suitable region for producing agricultural products. This province is one of the centers of faba bean production in the country, therefore paying attention to the pollination service can lead to development of sustainable production and more economic advantages for farmers and ecological advantages for the environment. The faba bean growers can protect the pollination service to enhance their economic benefits in agroecosystems. In this study, pollination service in a faba bean agroecosystem is evaluated, quantified and valuated.

2. Materials and methods

2.1. Experimental site

During 2020-2021, a field experiment was conducted at the research farm of Gorgan University of Agricultural Sciences and Natural Resources, located in Gorgan county, Golestan province (northeast of Iran). Gorgan county is located in 54 degrees and 30 minutes' longitude of the east and 37 degrees and 45 minutes' latitude of the north, with the average height of 120 meters above sea level. In this county, there is usually a mild and semi-humid season and a relatively warm and semi-humid season. Gorgan has a semi-arid climate. The average annual temperature is 17.8 °C and the annual precipitation is approximately 584 mm.

2.2. Field operations

In this experiment, each plot included five planting rows with a distance between plants on each row of 15 cm, a planting depth of 5 cm and a distance between rows of 50 cm. Also, each plot had a size of 2×2.5 m and the distance between of plots was 75 cm. The amount of nitrogen was 10 kg/ha from nitrogen chemical fertilizer that was applied as a starter. Faba bean seeds were sown in late November 2020 and harvested early June 2021. During the growing season, the necessary care is carried out to control pests, diseases and weeds by non-chemical methods. We used physical methods to control pests and removed some of the infected leaves and branches. Additionally, we conducted two rounds of weeding to effectively control of weeds.

Also, supplementary irrigation was done two times during the growing season as a flooding method.

2.3. Quantification of pollination service

In this study, pollination regulation in the faba bean agroecosystem was quantified and valuated by the performance of a field experiment. For this purpose, a factorial experiment was conducted as a randomized complete blocks design with three replications at the research farm of Gorgan University of Agricultural Sciences and Natural Resources, during 2020-2021. The treatment composition of this experiment included: cultivars as the first factor in four types including, Feyz, Mahta, Barkat, and Shadan and pollination treatment as the second factor in two levels including, free pollination by insects and restriction of pollination by cages (Figure1).

Plan **Cultivars**; V1: Shadan, V2: Feyz, V3: Barkat, V4: Mahta **Pollination**; p1: Free, p2: Limited				
1	$V1_{p2}$	$V3_{p1}$	$V4_{p2}$	$V2_{p1}$
2	$V2_{p2}$	$V1_{p2}$	$V4_{p1}$	$V3_{p1}$
3	$V4_{p2}$	$V1_{p1}$	$V2_{p2}$	$V3_{p1}$

Figure 1. The design performance of field experiment, Gorgan, Iran.

Each cage had a size of 2×2.50×1 m from lattice nets type. At the time of crop ripening, grain yield, green biomass and Harvest Index (HI) were harvested from an area of one square meter of each plot. Finally, the marketing price and alternative cost methods were used to value this service. The marketing price method uses actual market prices for ecosystem services when they are available. One of the key concepts in this valuation process is alternative cost, which can be assessed through various cost-based methods. Alternative cost, often referred to as opportunity cost, represents the value of the best alternative forgone when a choice is made. In the context of ecosystem services, it helps quantify what society sacrifices when choosing one land use or resource management strategy over another (Pushpam, 2005; Selivanov and Hlaváčková, 2021). Also, statistical analysis of data performed using SAS software based on ANOVA and means compared based on LSD test at 5% probability level.

2.4. Insect collection

During the growing season, with the start of flowering and with the warming of the air and the start of insect activity, the limited plots by cages be wholly trapped by lattice nets until the end of the pollination stage. Simultaneously with the activity of insects in the field, samples were collected by a net trap. Surveys were performed from 10:00 am to 12:00 pm, from late March to mid-April 2020. The samples were then collected, and all insects were transferred to jars containing 70% ethanol and glycerol. Insect samples were moved to the entomology laboratory of Gorgan University of Agricultural Sciences and Natural Resources, then, they were identified in terms of scientific names.

3. Results and discussion

3.1. Pollinator insects

We collected 13 pollinator species from the faba bean agroecosystem. We found the faba bean plants were pollinated by *Polistes gallicus, Polistes dominulu, Spilostethus sp., Eristalis tenax, Oxythyrea cinctella, Ichneumonidae, Harmonia axyridis, Syrphus ribesii, Pygopleurus* sp., *Sphecodes* sp., *Lasioglussum* sp., *Anthophora* sp. and *Apis mellifica* in Gorgan (Table 1). Some of the pollinators shown in Figure 2. Before this research, Liu et al. (2020) reported that pollination efficiencies were high for species *Apis mellifera, Apis cerana, Eristalis tenax,* and *Tiphia vernalis* in common buckwheat and adult Syrphidae flies are of second importance after bees as the second most pollinating group in the insect category. In our study, Halictid bees (*Lasioglussum* sp.) had the most abundant (25.71%),

followed by European paper wasp (*Polistes dominula*) (20.0%), *Pygopleurus* sp (11.43%) and *Spilostethus* sp. (8.57%) (Table 1). Lundin (2023) found that honeybees provide 47% of the insect pollination services for faba bean, while short-tongued bumblebees contribute 40%, long-tongued bumblebees account for 6%, and solitary bees make up 8% of the services. This indicates that both managed honeybees and wild bees, particularly short-tongued bumblebees, play a significant role in the pollination of faba beans in Sweden.

Table 1. Scientific name, family name and frequency of pollinators in faba bean agroecosystem, Gorgan, Iran.

	Scientific name	Family name	Frequency (%)
1	Polistes gallicus	Vespidae	2.85
2	Polistes dominula	Vespidae	20.00
3	Spilostethus sp.	Lygaeidae	8.57
4	Eristalis tenax	Syrphidae	2.85
5	Oxythyrea cinctella	Scarabaeidae	2.85
6	Ichneumonidae	Ichneumonidae	5.71
7	Harmonia axyridis	Coccinellidae	2.85
8	Syrphus ribesii	Syrphidae	5.71
9	Pygopleurus sp.	Glaphyridae	11.43
10	Sphecodes sp.	Halictidae	2.85
11	Lasioglussum sp.	Halictidae	25.71
12	Anthophora sp.	Apidae	5.71
13	Apis mellifera	Apidae	2.85

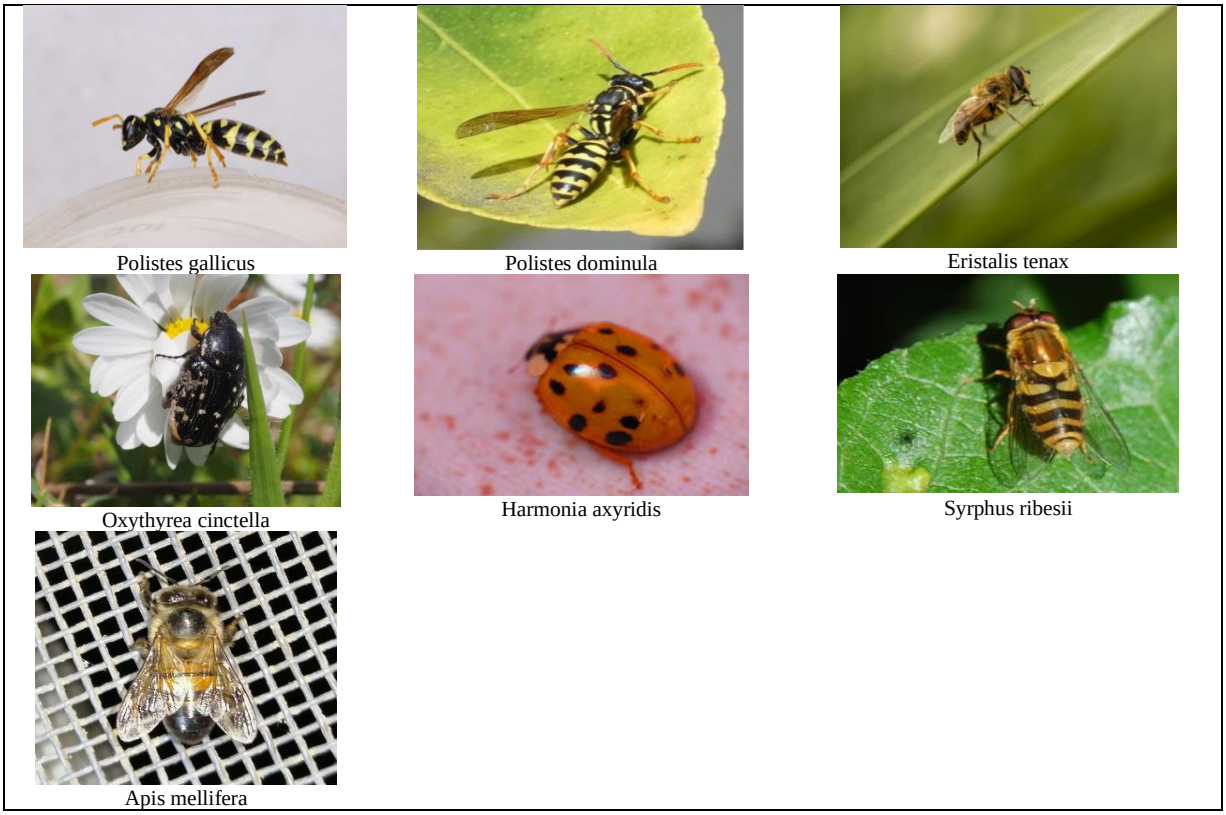

Figure 2. Some pollinators in faba bean agroecosystem (Source: GBIF)

The genus *Lasioglossum* in Halictidae is one of the largest genera of bees worldwide with an incredibly diverse array of behaviors. These bees are found worldwide, but are especially abundant in temperate regions. Halictidae are one of the six bee families in the order Hymenoptera. They are a very diverse group of metallic and non-metallic bees and certainly are more abundant than most bees except *Apis* species (Buckley et al., 2019). In Catalonia (Spain), Morrison et al., (2017) found a strong inverse relationship between wild bee abundance and surrounding landscape diversity in cereal fields margins. For example, they reported that with decreasing landscape complexity in Catalonia, the proportion of Halictidae bees increased.

In this study, European paper wasp (*Polistes dominula*) had an abundance of about 20.0%. This insect is a eusocial paper wasp native to Mediterranean Europe. Individual records for this distribution could only be found for Europe and Iran. European paper wasp lives in a wide range of habitats within temperate climates, including woodland, shrubland, grassland agricultural and urban areas and this

insect builds nests using paper and saliva (Stout, 2013).

The findings regarding pollination services to faba beans have significant implications for both productivity and agroecosystem sustainability. Enhanced pollination, particularly through managed pollinators like honeybees, has been shown to increase yields by up to 49% compared to self-pollination conditions, highlighting the critical role of insect pollinators in maximizing crop output (Gasim, and Abdelmula, 2018).

3.2. Quantification of ES related to pollination

The results showed that the cultivar types had significantly different as green yield and biomass at the level of 1% probability (Table 2). The highest grain yield was related to Barkat cultivar, which was in the same statistically class as Feyz (Table 3). The share of insects in pollination of cultivars was between 3.81 and 17.06 % (Table 4). The highest share of the pollinating insects was related to Mahta cultivar. This cultivar from the medium seed group is suitable for cultivation in moderate and cold regions. The number of pods per plant for this cultivar is 25-40, with a protein content of about 28-31%, and it is resistant to diseases. Also, this cultivar is superior to other faba bean cultivars and lines from the view of mechanized harvesting. Mahta is the first cultivar without tannins and dual-purpose faba beans in Iran and can be used in feeding livestock, poultry and aquatics (Sheikh et al., 2017c). The results showed that the role of pollinating insects in new faba bean cultivars such as Mahta was more than the old cultivar such as Barkat. Globally, there is growing confirmation that improved pollination practices can help support higher yield and reduced variability for a wide range of insect-pollinated plants (Cunningham and Feuvre, 2013). In this study, it determined that the highest Harvest Index (HI) was related to Barkat as an old cultivar, and the lowest of HI was obtained in Mahta cultivar (Table 3). Also, the share of pollination by insects was obtained by 14.51% in Shadan cultivar (Table 4). Shadan cultivar belongs to the medium grain group. It is resistant to Cercospora leaf spot (*Cercospora zonata*) disease and is suitable for mechanized harvesting. This cultivar has about 3.5-5.0 t/ha grain yield with 20-28 t/ha green yield, 25 pods per plant and 27-30% protein content. Shadan as a new cultivar is suitable for human consumption as cotyledon (Sheikh et al., 2017b).

Table 2. Results of analysis of variance (mean square) of ecosystem services related to pollination by insects in a faba bean agroecosystem, Gorgan, Iran.

Source of variables	Green yield (kg/m^2)	Green biomass (kg/m^2)	HI (%)	Economic profit (10^7 Rls/ha) *
Block	ns	ns	ns	ns
Pollination (P)	ns	ns	ns	ns
Cultivar (C)	**	*	ns	**
C*P	ns	ns	ns	ns
CV (%)	17.28	14.70	6.48	17.27

ns: Non-significant. ** Significant at 1% probability level, * Significant at 5% probability level

Table 3. Results of mean comparison of ecosystem services related to pollination by insects in a faba bean agroecosystem, Gorgan, Iran.

Treatment	Green yield (kg/m^2)	Green biomass (kg/m^2)	HI (%)	Economic profit (10^7 Rls/ha) *
Pollination				
Free pollination	2.790a	4.622a	37.54a	97.6a
Limited pollination	2.739a	4.632a	36.89a	95.7b
Cultivar				
Shadan	2.622b	4.705a	35.84bc	91.7bc
Feyz	3.142ab	5.081a	36.89b	109.9a
Barkat	3.212a	4.917a	39.41a	101.2ab
Mahta	2.073c	3.804b	35.26c	72.5c

*Rls: Rials. Means with same letters in each column don't have significant differences based on the LSD test at the 5% probability level .

Table 4. Share and economic value of pollination in faba bean agroecosystem, Gorgan, Iran.

Cultivar	Pollination percentage	Economic value of pollination (Rls/ha)*
Shadan	14.51	135,566,667
Feyz	13.64	161,000,000
Barkat	3.81	38,056,136
Mahta	17.06	135,333,333

Rls: Rials

3.3. Valuation of pollination service

Results showed that cultivars had significant difference in economic profit. The highest profit was obtained in Feyz and Barkat cultivars (Table 3). Also, results showed that the economic value of pollination in the faba bean agroecosystem was between 38,056,136 to 161,000,000 Rls/ha. Feyz and Barkat cultivars had the highest and lowest profits from insect pollination, respectively (Table 4). Feyz cultivar as a new cultivar from coarse grain faba bean, is suitable for regions with moderate and semi-moderate of Iran. The pod length of the cultivar is high with 6-9 seeds per pod, and 145 grams of 100-seeds weight (Sheikh et al., 2015a). In the study by Cunningham and Feuvre (2013), the share of pollination by insects in faba bean fields was estimated at 17%. Economically, their analysis indicated that the provision of hives was profitable for a wide range of realistic values for crop value and pollination cost. In the same direction, Islam et al., (2021) reported that the value of oilseed rape was $US 87.5 million $annum^{-1}$, of which the economic value of insect pollination was $US 26.92 million $annum^{-1}$ in Bangladesh. The application of input-output models for economic valuation

provides valuable insights into the agricultural sector's dynamics in Iran. By focusing on enhancing agribusiness productivity and implementing sustainable practices like managed hives, Iran can bolster its agricultural economy while addressing critical challenges such as food security. To focus on the characteristics of cultivars that are relevant to pollination efficiency and economic valuation, it's essential to consider how different cultivars interact with pollinators and the resultant effects on plant production and quality. A study revealed significant variations in the yield benefits of additional pollination across five different faba bean cultivars. Some cultivars experienced yield increases of up to 37% with insect pollination, while others saw a decline of 51% when pollinated. This variability highlights the importance of cultivar selection for maximizing yield through effective pollination (Bishop et al., 2020).

4. Conclusion

Our results showed that pollination by insects can improve yield of faba bean and the value of insect pollination in this crop depended on insect species, cultivar type and insect abundances. According to this, the share of insects in pollination was obtained between 3.81 and 17.06 percent. Also, cultivars had significant difference in economic profit, and the role of pollinating insects in new faba bean cultivars was more than in the old cultivars. The study on faba bean pollination highlights the significant role that insect pollinators play in enhancing crop yield, particularly emphasizing the cultivar Mahta, which exhibits a higher dependency on pollination services compared to others. This finding underscores the need for a more direct connection between these results and broader ecological and agricultural practices, particularly in relation to sustainability and biodiversity within agroecosystems. To enhance their economic benefits within the faba bean agroecosystem, it is essential for farmers to understand the crucial role of insects in pollination. By actively promoting and protecting these pollination services, growers can ensure a more productive and sustainable farming future. Taking steps to create a pollinator-friendly environment will not only boost yields but also contribute to the overall health of the ecosystem and protect of biodiversity.

Acknowledgments

We thank the Gorgan University of Agricultural Sciences and Natural Resources (GUASNR) and Dr. F. Sheikh that supported this research.

References

Andersson, G. K., Ekroos, J., Stjernman, M., Rundlöf, M., & Smith, H. G. (2014). Effects of farming intensity, crop rotation and landscape heterogeneity on field bean pollination. *Agriculture, Ecosystems & Environment*, *184*, 145-148. https://doi.org/10.1016/j.agee.2013.12.002

Bishop, J., Garratt, M. P. D., & Breeze, T. D. (2020). Yield benefits of additional pollination to faba bean vary with cultivar, scale, yield parameter and experimental method. *Scientific Reports*, *10*(1), 2102. https://doi.org/10.1038/s41598-020-58518-1

Burns, K. L. W., & Stanley, D. A. (2023). Irish faba beans (Fabales: Fabaceae) depend on wild bumblebee pollination for marketable yields. *Agricultural and Forest Entomology*. *25*(2):312-322. https://doi.org/10.1111/afe.12553

Buckley, K., Zettel, C., & Jamie Ellis, N. (2019). Sweat bees, halictid bees. *Featured Creatures*. University of Florida. Publication Number: EENY-499. https://entnemdept.ufl.edu/creatures/misc/bees/halictid_bees.htm.

Carrié, R., Lopes, M., Ouin, A., & Andrieu, E. (2018). Bee diversity in crop fields is influenced by remotely-sensed nesting resources in surrounding permanent grasslands. *Ecological Indicators*, *90*, 606-614. https://doi.org/10.1016/j.ecolind.2018.03.054

Cunningham, S. A., & Feuvre, D. L. (2013). Significant yield benefits from honeybee pollination of faba bean (Vicia faba) assessed at field scale. *Field Crops Research*. *149*: 269-275. https://doi.org/10.1016/j.fcr.2013.05.019

Costanza, K., Naeem, S., ONeill, R. V., Paruelo, J., Raskin, R. G., Sutton, P., & Van den Belt, M. (1997). The value of the worlds ecosystem services and natural capital. *Nature*, *387*(6630), 253260Daily. https://doi.org/10.1038/387253a0

FAO STAT. (2014). Food and Agriculture Organization of the United Nations. *http://www.fao.org/faostat/en/#home*

Gasim, S. M., & Abdelmula, A. A. (2018). Impact of bee pollination on yield of faba bean (Vicia faba L.) grown under semi-arid conditions. *Agricultural Sciences*, *9*(6), 729-740. https://doi: 10.4236/as.2018.96051

Happe, A. K., Riesch, F., Rösch, V., Gallé, R., Tscharntke, T., & Batáry, P. (2018). Small-scale agricultural landscapes and organic management support wild bee communities of cereal field boundaries. *Agriculture, Ecosystems & Environment*, *254*, 92-98. https://doi.org/10.1016/j.agee.2017.11.019

Islam, R., Howlett, B. G., Chapman, H., Haque, M. A., & Ahmad, M. (2022). The value of insect pollination to yield of oilseed rape (Brassica rapa) in Bangladesh. *Journal of Asia-Pacific Entomology*, *25*(1), 101844. https://doi.org/10.1016/j.aspen.2021.11.005

Liu, R., Chen, D., Luo, S., Xu, S., Xu, H., Shi, X., & Zou, Y. (2020). Quantifying pollination efficiency of flower-visiting insects and its application in estimating pollination services for common buckwheat. *Agriculture, Ecosystems & Environment*, *301*, 107011. https://doi.org/10.1016/j.agee.2020.107011.

Lundin, O. (2023). Partitioning pollination services to faba bean (Vicia faba L.) between managed honeybees and wild bees. *Basic and Applied Ecology*, *71*, 9-17. https://doi.org/10.1016/j.baae.2023.05.006

Majnoon Hosseini, N. (1996). Pulses in Iran. Jihad Publishing Institute. 240 pages.

Morrison, J., Izquierdo, J., Plaza, E. H., & González-Andújar, J. L. (2017). The role of field margins in supporting wild bees in Mediterranean cereal agroecosystems: Which biotic and abiotic factors are important?. *Agriculture, Ecosystems & Environment*,

247, 216-224. https://doi.org/10.1016/j.agee.2017.06.047

Power, A. G. (2010). Ecosystem services and agriculture: tradeoffs and synergies. Philosophical transactions of the Royal society of London, series B, *Biological Sciences. 365*, 2959–2971. https://doi.org/10.1098/rstb.2010.0143

Pushpam, K. (2005). Market for Ecosystem Services. International Institute for Sustainable Development (IISD). http://www.iisd.org

Sandhu, H. S., Wratten, S. D., & Cullen, R. (2010). Organic agriculture and ecosystem services. *Environmental science & policy*, *13*(1), 1-7. https://doi.org/10.1016/j.envsci.2009.11.002

Selivanov, E., & Hlaváčková, P. (2021). Methods for monetary valuation of ecosystem services: A scoping review. *Journal of Forest Science*, *67*(11), 499-511. https://doi.org/10.17221/96/2021-JFS

Sheikh, F., Sekhavat, R., Miri, Kh., Astaraki, H., & Aghajani, M. A. (2017). *Introduction report of new G-Faba-1-1 coarse faba bean line, suitable for temperate and semi-temperate regions (Feyz cultivar)*. Golestan Agricultural and Natural Resources Research Center Press. 35 p.

Sheikh, F., Sekhavat, R., Miri, Kh., Astaraki, H., & Aghajani, M. A. (2017). *Introduction of a new line of G-Faba-133, a faba bean resistant to diseases and mechanized harvesting (Shadan cultivar)*. Golestan Agricultural and Natural Resources Research Center Press. 35 p.

Sheikh, F., Sekhavat, R., Miri, Kh., Astaraki, H., & Aghajani, M. A. (2017). *Introduction of G-Faba-95 WRB2-6, promising faba bean line, medium grain, disease resistant, low tannin and suitable for mechanized harvesting (Mahta cultivar)*. Golestan Province Agricultural Education and Natural Resources Research Organization Press. 37 p.

Stout, E. (2013). *Polistes dominula* (online). Animal Diversity Web. http://animaldiversity.org/accounts/Polistes_dominula

Zou, Y., Bianchi, F. J. J. A., Jauker, F., Xiao, H., Chen, J., Cresswell, J., Luo, S., Huang, J., Deng, X., Hou, L., & van der Werf, W. (2017). Landscape effects on pollinator communities and pollination services in small-holder agroecosystems. *Agriculture, Ecosystems & Environment*, 246, 109–116. https://doi.org/10.1016/j.agee.2017.05.035

Agriculture, Environment & Society

Journal homepage: www.aes.uoz.ac.ir

Spatial modeling of soil saturation percentage using machine learning methods in Sistan plain

Younes Jamalzehi Samareh [a], Ali Shahriari [*b], Mohammad Reza Pahlavan-Rad [c], Alireza Ziaei Javid [d], Abolfazl Bameri [b]

[a] M.Sc Graduate of Soil Science, Department of Soil Science and Engineering, University of Zabol, Zabol, Iran
[b] Department of Soil Science and Engineering, University of Zabol, Zabol, Iran
[c] Soil and Water Research Department, Golestan Agricultural and Natural Resources Research and Education Center, AREEO, Gorgan, Iran
[d] Researcher, Devision of Soil Formation, Classification and Survey Researches, Soil and Water Research Institute, Karaj, Iran

ARTICLE INFO

Article history:
Received: 24 September 2024
Accepted: 21 February 2025
Available online: 1 June 2025

Keywords:
Deltaic soils
Hyper-arid region
Land management
Random forest

ABSTRACT

Soil maps are an urgent need for different land users and decision-makers. In recent years, attention to digital soil mapping has greatly increased, but most studies have focused on surface soil, even though land users are faced with the three-dimensional (3D) structure of soil. Saturation percentage (SP) is one of the physical attributes of soil moisture, which can be considered in land management, especially in the direction of soil water retention in connection with other attributes, in arid areas. Therefore, the present study was conducted with the aim of digital mapping of SP in 3D using some machine learning methods in the Sistan Plain, which is located on the Hirmand River delta in a hyper-arid region. To carry out this research, the information from 576 soil profiles located in the Sistan Plain was used and the percentage of saturated soil moisture was measured using the standard method at depths of 0-15, 15-30, 30-60, and 60-100 cm using the weighted average method. Random forest (RF), quantile regression forest (QRF), and cubist methods were used for spatial modeling. The results showed that the variables derived from remote sensing showed a significant correlation with the SP parameter only at the first and second depths, which were close to the ground surface, but the variables derived from DEM had a significant correlation at all depths. These variables were mainly related to alluvial activities, which had the greatest effect on soil changes in the studied area. Among the models, the RF method showed the best performance for spatial modeling of SP in all depths. The 3D modeling of the percentage of SP showed that the value of SP is the lowest in the south and medium in the middle of the area, and the highest in the north of the Sistan plain at the edge of the Hamoun wetlands. SP value is repeated with the same spatial trend, but the average value of SP increases from the surface to the depth. It seems that the changes in this attribute are in line with the 3D changes in the soil texture components in the region. Based on the results of the three-dimensional zoning of SP, it could be recommended that in the northern areas of the Sistan Plain, irrigation should be done with a longer time interval than in the southern regions for the same agricultural products. In the fields of natural resources, to manage vegetation and especially to deal with wind erosion, plants with shallow and deep roots in the northern regions, and trees and plants with deep roots in the southern regions can be considered. Machine learning methods, especially RF, can be effective in preparing digital and 3D maps of soil characteristics and can help different land users manage their land better.

Highlights

- RF model excels in 3D SP mapping in Sistan Plain, outperforming QRF and Cubist.
- SP lowest in south, highest in north near Hamoun wetlands, rises with depth.
- DEM variables key for SP at all depths; RS variables effective only at 0-30 cm.

* Corresponding author.
E-mail address: shahriari.ali@uoz.ac.ir
https://doi.org/10.22034/jelsa.2025.479520.1087

- SP aligns with soil texture changes, linked to alluvial activity in hyper-arid area.
- Suggests longer irrigation intervals in north, deep-root plants in south for management.

1. Introduction

As the foundation of terrestrial ecosystems, soil plays an important role in supporting biodiversity, agriculture, and ecosystem services (Montanarella and Panagos, 2021). It is essential to manage, utilize, and safeguard soil, while also comprehending its transformations at a landscape scale, to achieve sustainability (Mulder et al., 2011; Wulf et al., 2014). Soil studies are the main source for land use management and sustainable agriculture (Soil Science Division Staff, 2017). Soil is a controlling factor in many environmental processes such as greenhouse gas emissions, nitrate leaching, and plant and forest growth. Attributes such as acidity, salinity, texture, structure, and saturation percentage (SP) affect the physical and chemical behavior of the soil.

Saturated soil potential (SP) refers to the volume of water present in the soil when it is fully saturated. Specifically, SP is defined as the ratio of the weight of water needed to saturate the pore space to the weight of the dry soil. It serves as a critical indicator in soil hydroecological research. Additionally, SP is closely related to soil composition and can be employed as a parameter for estimating soil texture components, quantitatively assessing cation exchange capacity (CEC), and determining soil water holding capacit (Ahmad Aali et al., 2009). Also, soil SP reflects some physical properties of soil (Stivent and Khan, 1996). It is worth noting that soil SP indicates the amount of water availability for the plant, as well as the amount of movement of organic and inorganic solutes in the soil, and therefore, the processes of soil formation and the evolution of the profile affected by it (Ahmad Aali et al., 2009).

Identifying spatial changes of soil characteristics such as SP is essential for land management. Digital soil mapping (DSM) is a key method for assessing soil spatial changes and has been utilized for over two decades (Kidd et al., 2018; Kidd et al., 2020). Advances in computing technology have revolutionized soil science (Wadoux et al., 2020). DSM integrates field and laboratory methods with spatial and non-spatial inference systems to populate soil spatial information systems (IUSS, 2023). Recent years have seen a surge in DSM studies focusing on soil physical and chemical properties, driven by the increasing demand for quantitative soil data, advancements in statistical modeling and artificial intelligence, and improved access to environmental data for rapid soil mapping (Taghizadeh-Mehrjardi et al., 2021; Wadoux et al., 2020; Grunwald et al., 2012). Accurate soil datasets are essential for effective management of agriculture, water conservation, carbon stocks, and soil erosion (Adeniyi et al., 2024; Žížala et al., 2022). There are few studies in the direction of three-dimensional mapping of soil properties such as particle size distribution and soil texture class (Amirian Chekan et al., 2017; Dharumarajan and Hegde, 2022; Emami et al., 2024b), organic carbon (Jamshidi et al., 2019; Mousavi et al., 2022) and saltiness and salinity. (Filippi et al., 2020; Emami et al., 2024a) has been done. Researchers used the RF model for digital soil mapping at the province scale and showed that when the RF model was trained using conventional soil mapping (CSM), the accuracy of the resulting DSM was higher than the original CSM (Heung et al., 2022). Cao et al. (2023) used the RF model to predict the risk of cadmium contamination in the soil of an abandoned mine and showed that the RF model is an accurate and stable model for predicting the risk of toxic metal contamination. Emami et al. (2024b) Using the quantile regression forest (QRF) method, showed that environmental variables are the most important factors in predicting the distribution of soil texture components and early soil attributes such as SP. Also, the use of environmental variables as auxiliary variables is one of the important factors that influence DSM, and investigating the type of influence of these auxiliary variables can identify the type of soil, for a better understanding of soil development and preparing soil prediction maps is important and necessary (Duan et al., 2022). It is also possible to use different environmental variables that have constant application in the entire study area by considering the climatic and geographical conditions of the study area (Fan et al., 2022). Naimi Mardani et al. (2021), using synthetic soil image and machine learning made acceptable predictions using the Cubist model for sand, soil organic carbon and CCE, and the RF model for clay. They showed that the combination of high-quality RS data and DEM-derived variables can predict soil properties, and the use of RS data can reduce soil sampling costs and, as a result, soil mapping. The Sistan Plain is an alluvial plain located on the Hirmand River delta and has an extremely arid climate. SP is one of the easily available soil attributes that is related to the soil moisture level and water management in the soil. Therefore, paying attention to the 3D digital mapping of SP is very important for planning and management of water and soil in agricultural and environmental activities. So, the present study was conducted with the aim of digital mapping of the SP in 3D using some machine learning methods in the Sistan Plain

2. Materials and methods

2.1. Study area

Sistan Plain is located in the north of Sistan and Baluchistan province, southeast of Iran and southwest of the Asian continent with geographical coordinates of 61 degrees 10 minutes to 61 degrees 50 minutes of longitude and 30 degrees 18 minutes to 31 degrees 21 minutes of latitude. is (Figure 1). This deltaic plain is the result of the alluvial sediments of a river, which is known as a wide plain and originates from the Hirmand River in Afghanistan. The area of the studied area is about 218 thousand hectares (Siyasar et al., 2020; Piri, 2012). The Sistan Plain is a floodplain and does not have any orogenic activity and high elevations, and it has no special topography. The average height above sea level varies between 480-490 meters and the slope of the area varies

between 1-2% (Mirakzehi et al., 2018). According to the strategic characteristics of the Sistan plain, it has a hot, dry and desert climate, the average summer temperature is more than 40 degrees Celsius and the average winter temperature reaches 5 degrees above zero. In terms of humidity and temperature regime, the soil of the region is aridic and hyperthermic respectively. Its land use is divided into three types of agriculture, barren and unusable (salt marsh) and the predominant plant species are salt-tolerant plants and plants with deep roots (such as *Tamarix aphylla*), salt grass (*Salsola tomentosa*), heather (*Alhagi camelorum*), eucalyptus (*Eucalyptus camaldulensis*), Crete (D*esmostachya bipinnata*) (Mirakzehi et al., 2018; Delbari et al., 2019).

2.2. Sampling and laboratory methods

To estimate soil SP, the data from 576 soil profiles were used (Jamalzehi Samareh, 2022), and the method of determining the sampling points was based on the random supervised method (Figure 1). Soil SP tests have been measured in a standard way, using the weighted average method in Excel 2019 software to categorize the data and calculate the SP value at the depths of 0-15, 15-30, 30-60, and 60-100 cm was used. These depths were selected based on the method announced by the FAO organization to determine standard depths for studying and preparing soil maps (Bishop et al., 1999; Malone et al., 2009).

2.3. Environmental variables

Data obtained from remote sensing images can be used to obtain qualitative and quantitative information about soil properties and are an essential and very cost-effective data source for soil mapping (Agbu et al., 1990; Ben-Dor et al., 2009). In this study, Landsat 8 OLI images with a 27m resolution during whose cloud cover was less than 10% were downloaded from the EarthExplorer.gov site the sampling intervals, then the downloaded images were used for radiometric corrections with the Radiometric Calibration tool and atmospheric corrections with the FLAASH Atmospheric Correction tool in the software ENVI 5.3 was done. Subsequently, multiple indices were computed and derived using ArcGIS 10.4 software (Table 1). Additionally, a Digital Elevation Model (DEM) featuring a spatial resolution of 27 meters, obtained from the EarthExplorer.gov website, was utilized to extract environmental variables through SAGAGIS software (Table 2) and then in ArcGIS 10.4 software using the Extract Multi Values to Points tool, the variables of each point in the satellite images were extracted and using the Table to Excel variables were saved as a table in Excel 2019 software. After that, to determine the correlation between the studied attributes and environmental variables, Pearson's correlation coefficient was used in SPSS software, and the variables that showed a significant correlation with soil SP were included in the process of modeling and statistical analysis, and other variables were removed (Aksoy et al., 2012; Zeraatpishe et al., 2019; Shahriari et al., 2019). And then maps of each selected variable were prepared using ArcGIS 10.4 software (Wei et al., 2021; Bameri et al., 2015).

Initially, all environmental variables were incorporated into the modeling process. Subsequently, based on their relative importance, which ranges from 0 to 100%, variables with importance values below 10% were deemed insignificant and consequently excluded from the models. The remaining variables were utilized in the final models.

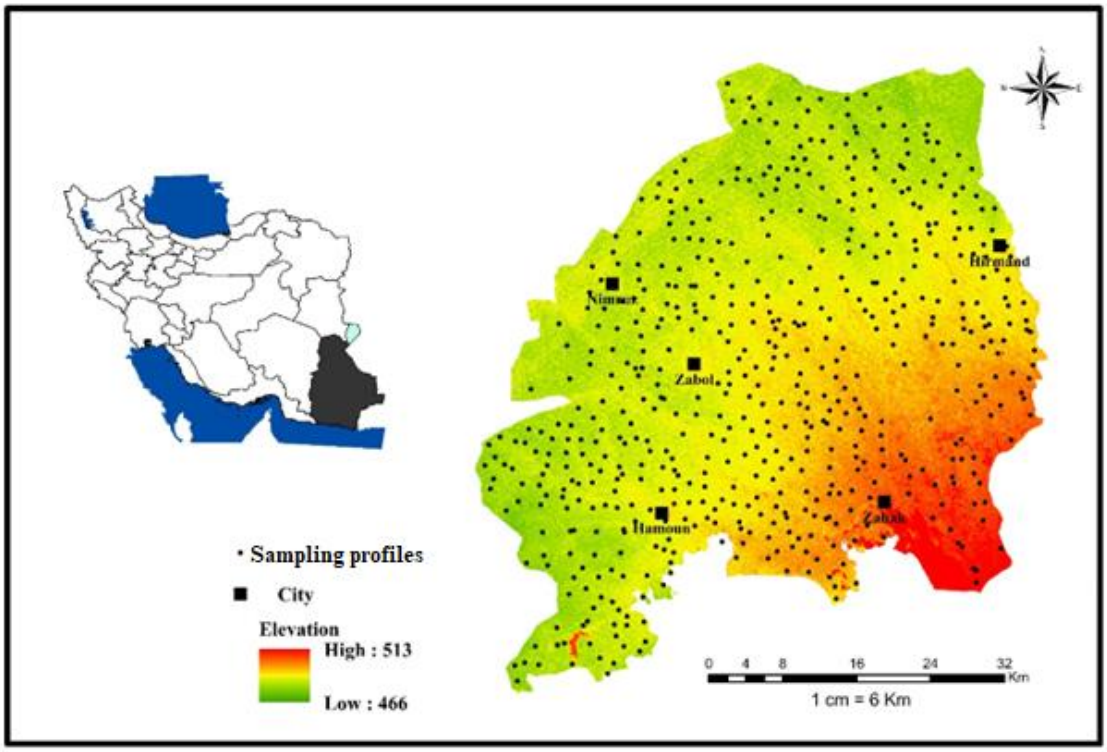

Figure 1. The location of the area and the studied soil profiles

2.4. Spatial modeling

The random forest (RF) method is a non-parametric model that builds multiple decision trees and combines them to create a more accurate classification. This method generates several trees and continuously classifies the data to find the best generalization point for each point and finally uses a voting mechanism in the forest to determine the output. This method is characterized by randomly selected samples and allows each tree in the forest to have similarities and differences (Cao et al., 2023; Shams et al., 2023).

The quantile regression forest (QRF) method as an advanced statistical modeling technique and a developed method of random forest algorithms is a flexible, non-linear, and non-parametric method that is very popular and useful as a powerful tool in machine learning methods (Gyamerah and Moyo, 2020; Athey et al., 2019; Wager and Athey, 2018). QRF has great potential to perform quantitative regressions on predictive distributions in various domains, as well as handle complex problems such as quantile regression and uncertainty estimation, and can provide users with a QRF algorithm that is widely implemented in R software (Gyamerah and Moyo, 2020; Meinshausen, 2017).

The Cubist method is a rule-based regression method that is quite effective in digital soil mapping (Zulfiqari and Abedi, 2019, Malone et al., 2016b). This algorithm is a tree model based on M5 theory (Quinlan, 1992) and prediction It divides the user into different subgroups based on "if-then" rules (Kuhn et al., 2016).

The main advantage of the Cubist method is to add multiple training committees and “reinforcement” so as to make the weights more balanced. a series of trees are produced to establish the Cubist model. The number of neighbors is used to modify the rule-based forecastsThe Cubist model employs a linear combination of the two models. The general conception about the Cubist regression model is described as follows: during the growth of a tree, many leaves and branches are grown.

The branches can be regarded as a series of “if-then” rules, while the terminal leaves can be regarded as an associated multivariate linear model. Assuming that a series of covariates comply with the condition of a rule, the associated model will be applied to calculate the predictive value. The Cubist model adds boosting with training committees (usually greater than one) which is similar to the method of “boosting” by sequentially developing a series of trees with adjusted weights. The number of neighbors in the Cubist model is applied to amend the rule-based prediction (Kuhn et al., 2016).

The key strength of the Cubist method lies in its use of multiple training committees and boosting techniques to achieve a more balanced distribution of weights. Its primary application is in analyzing large-scale databases that contain vast numbers of records and both numeric and nominal fields.

Each of the three models evaluates the importance of individual variables. During the modeling process, the values of each variable are randomly permuted while the values of the other variables remain unchanged. The difference between the Mean Squared Error (MSE) calculated from the permuted data and the original data provides a measure of variable importance. Variables that result in a relatively larger increase in MSE are considered more significant.

Initially, all environmental variables were included in the modeling process. However, based on their relative importance, which ranges from 0 to 100%, variables with importance values below 10% were deemed insignificant and subsequently removed from the models. The remaining variables were then used in the final models.

It is worth mentioning that to implement the desired models from the specialized packages "caret", "randomForest", "Cubist" and the "qrf" function was performed in R version 4.3.2 statistical software environment.

K-fold cross-validation was employed to assess model performance. Specifically, a 10-fold cross-validation approach was applied, in which the dataset was randomly divided into k=10 subsets (folds).

The model was trained using k=9 folds and validated on the remaining single fold, with accuracy metrics computed based on the test fold. This training and testing procedure was repeated k times, ensuring that each fold was used as the test set exactly once. The overall performance of the model was determined by averaging the accuracy metrics across all folds, and the results were reported accordingly.

The root mean square error (RMSE), mean error (ME), and correlation coefficient (R^2) were used to compare the models and choose the best model to obtain the dependent variables (saturated humidity). The R^2 value indicates the proportion of variation explained by the model, while the Root Mean Squared Error (RMSE) serves as a measure of prediction accuracy. The Mean Absolute Error (MAE), which is always a positive value, represents the average magnitude of errors and tends to exhibit a skewed distribution. Consequently, the closer the MAE value is to zero, the greater the accuracy of the method being evaluated.

Equation 1 was used to calculate RMSE:

$$\mathrm{RMSE} = \sqrt{\frac{1}{n}\sum_{i=1}^{n}(\mathbb{Y}i - \mathbb{Y}j)^2} \qquad \text{Equation (1)}$$

where n is the total number of data, Yi is the measured value and Yj is the predicted value.

Equation 2 was used to calculate ME:

$$\mathrm{ME} = \frac{1}{n}\sum_{i=1}^{n}[\,\mathbb{Y}^*(\mathrm{xi}) - \mathbb{Y}(\mathrm{xi})] \qquad \text{Equation (2)}$$

where n is the total number of data, Y(xi) is the predicted value at the i-th point and Y^* (xi) is the calculated value at the i-th point.

Equation 3 was used to calculate R^2:

$$\mathbb{R}^2 = \frac{S_{xy}^2}{S_{xx}S_{xy}} \qquad \text{Equation (3)}$$

where x and y are the standard deviation of the variables and are in the form of Sx and Sy and its covariance is also denoted by COVxy and can be calculated from the relationship of R^2 (Metinfar et al., 2019).

Table 1. Environmental variables extracted from Landsat 8

Symbol of covariate	Description	Symbol of covariate	Description	Definition
SWI1	SWIR Band	DVI	Difference Vegetation Index	NIR – RED
SWIR2	SWIR Band	SR	Simple Ratio	NIR/Red
NIR	NIR Band	SLAVI	Specific Leaf Area Vegetation Index	NIR/(Red + SWIR 2)
coastal	Coastal Band	SAVI	Soil Adjusted Vegetation Index	(1 + L) * (NIR - RED) / (NIR + RED + L)
GEMI	-	MNDWI	Modified normalized difference water index	(Green -Swir)/ (Green + swir)
NBRI	Normalized burn ratio	EVI	Enhanced Vegetation Index	(NIR - RED) / (NIR + C1 * RED-C2 *BLUE + L)
CTVI	-	Blue	Blue band of Landsat-8	Wavelength of 0.450–0.515 μm
SATVI	soil-adjusted total vegetation index	Red	Red band of Landsat-8	Wavelength of 0.630–0.680 μm
NRVI	Normalized Ratio Vegetation Index	Green	Green band of Landsat-8	Wavelength of 0.525–0.600 μm
B1	Landsat OLI	EVI2	Enhanced Vegetation Index	(NIR - RED) / (NIR + C1 * RED-C2 *BLUE + L)
B2	Landsat OLI	NDVI	Normalized Difference Vegetation Index	(NIR-RED) / (NIR + RED)
B3	Landsat OLI	GNDVI	Green Normalized Difference Vegetation Index	(B5 - B3)/ (B5 + B3)
B4	Landsat OLI	NDWI	Normalized difference water index	(B3 - B5)/ (B3 + B5)
B5	Landsat OLI	NDWI2	Normalized difference water index	(B3 - B5)/ (B3 + B5)
B6	Landsat OLI	SAVI_1	Soil Adjusted Vegetation Index	(1 + L) * (NIR - RED) / (NIR + RED + L)
B7	Landsat OLI	MSAVI	Modified Soil-adjusted Vegetation Index	(1+L)(NIR-Red)/ (NIR+Red+L)
RVI	Ratio Vegetation Index	MSAVI2	Modified Soil-adjusted Vegetation Index	(2*NIR+1-sqrt ((2*NIR + 1)2-8*(NIR-Red)))/2

Table 2. Environmental variables extracted from DEM

Symbol of covariate	Description	References
Wetindex	Wetness index	-
Convergen	Convergence index	-
Diurnal_Anisotropic_ Heating	Diurnal anisotropic heating	Boettinger et al., (2008)
Overland Distflow	Overland flow distance to channel network	Boettinger et al., (2008)
Wind_Effect	The Wind Effect is a dimensionless index	Boettinger et al., (2008)
Drainage	Drainage Basins	Boettinger et al., (2008)
Cluster	Study area classification into groups	Boettinger et al., (2008)
Croscurve	Cross- sectional curvature	Boettinger et al., (2008)
Slope	Slope angle (%)	-
Catchment	Catchment area	-
Landforms	Landform	-
Distriverfinal	Distance from main river	-
Relative_Slope_ Position	Relative slope position	Boettinger et al., (2008)
Analytical _Hillshading	Analytical hillshading	Boettinger et al., (2008)
Channel network	Channel networks	Boettinger et al., (2008)
Flow_Path_ Length	Flow path length	Boettinger et al., (2008)
Effective_Air_ Flow_Heights	Effective air flow heights	Boettinger et al., (2008)
Horizontal_ Overland_ Flow_Distance	Horizontal overland flow distance	Boettinger et al., (2008)
Vertical Distance Channel	Vertical distance to channel network	Taghizadeh-Mehrjardi et al., (2021)
Valey depth	Depth of valley in meters	Rodiguez et al., (2002) Taghizadeh-Mehrjardi et al., (2021)
LSfacror	Multiple flow algorithms and help to accurately estimate current accumulation	Boehner and Selige, (2006) Taghizadeh-Mehrjardi et al., (2021)
Aspect	Compass direction of the maximum rate of change	Hom, (1981)

3. Results and discussion

3.1. Statistical analysis

Characteristics such as kurtosis and skewness of the data show that at all depths the SP data are normal to almost normal (Table 3). Also, SP values in all depths have the lowest coefficient of variation. Coefficient of variation (CV), which is a measure of relative variability, if 100% > CV ≥ 50% high variability, 50% > CV ≥ 21% moderate variability, and if CV ≤ 20% indicates low variability (Karimi Nezhad et al., 2015).

In this study, the coefficient of variation of SP was 50%-21%, which showed moderate variability. Also, the average value of SP showed that the first depth (0-15 cm) had the lowest average value (33.92 percent) and the fourth depth (60-100 cm) had the highest average (39.30 percent). Regarding SP changes in Sistan plain soil, limited studies have shown that in the Miankangi area, the average (46.67%) of this characteristic is higher than the average in the surface soil of the whole plain (Gholamalizadeh Ahangar et al., 2015; Hashemi et al., 2016).

According to the changes in soil texture components in the study area (Jamalzehi Samrah et al., 2021), it seems that the role of these attributes on SP changes at the surface and depth is significant.

3.2. Auxiliary variables

Figure 2 shows the distribution map of auxiliary variables with high importance in RF and QRF methods, including valley depth, channel network, distance from the river, evaluation, and normalized difference vegetation index (NDVI). Based on RF modeling, The valley depth variable was the most important, the channel network, the distance from the river, and the evaluation were less important, and the NDVI and vertical index were the least important (Figure 3-a). The channel network variable has the most importance, evaluation, valley depth, distance from the river, band 4, band 6, surface soil particle size index, band 7, band x43 and salinity index have medium importance, NDVI index has the least importance (Figure 3- b). The valley depth variable had the most importance, the channel network, distance from the river, and evaluation had medium importance, and the vertical and salinity index had the least importance (Figure 3-c). The valley depth variable had the most importance, evaluation, distance from the river and channel network had medium importance, and vertical and NDVI index had the least importance (Figure 3-d).

Table 3. Some statistical characteristics of SP

Depth (Cm)	Average	Median	Min	Max	Variance	Skewness	Kurtosis	Standard Deviation	CV
0-15	33.96	32.99	14	61.6	53.93	0.55	0.23	7.34	21.61
15-30	35.38	33.26	14	74.3	88.83	1.03	1.02	9.42	26.62
30-60	38.07	35.67	12	74.7	124.34	0.95	0.72	11.15	29.29
60-100	39.40	36.79	16	75.4	140.70	0.81	0.07	11.86	20.10

Based on QRF modeling, the variables of the channel network, evaluation, and distance from the river are the most important, valley depth variables, NDVI index, band 5, band 4, band 6 and band x43 are of medium importance, surface soil particle size index variables, band 7 and index Salinity was the least important (Figure 4-a). The variable of the channel network has the most importance, variables of evaluation, distance from the river, NDVI index, band 4, band 5, valley depth, band 6, band x43, and surface soil particle size index have medium importance, band 7 variables, and salinity index have the least importance were (Figure 4-b). The channel network variable had the most importance, the evaluation and distance from the river variables had medium importance, and the valley depth variable had the least importance (Figure 4-c). The channel network variable, evaluation has the most importance, the distance from the river has medium importance, and the valley depth variable has the least importance (Figure 4-d).

Emami et al. (2024b) used different auxiliary variables to model soil texture components using the QRF model and found that the valley depth variable acted as one of the best auxiliary variables for clay and sand modeling. Researchers considered the distance from the river and the network of canals (Pahlavan-Rad and Akbarimoghaddam, 2018) and Bands 4 and 7 (Shahriari et al., 2019) to be important auxiliary variables in the modeling of the surface soil texture of a part of the Sistan plain. Various researchers have found that elevation has played an important role in the preparation of soil maps as an auxiliary variable for modeling (Taghizadeh-Mehrjardi et al., 2021). Mirak zehi et al. (2018) showed in the spatial modeling of Sistan plain soil classes that the channel network, valley depth, elevation, and distance from the river are important auxiliary variables.

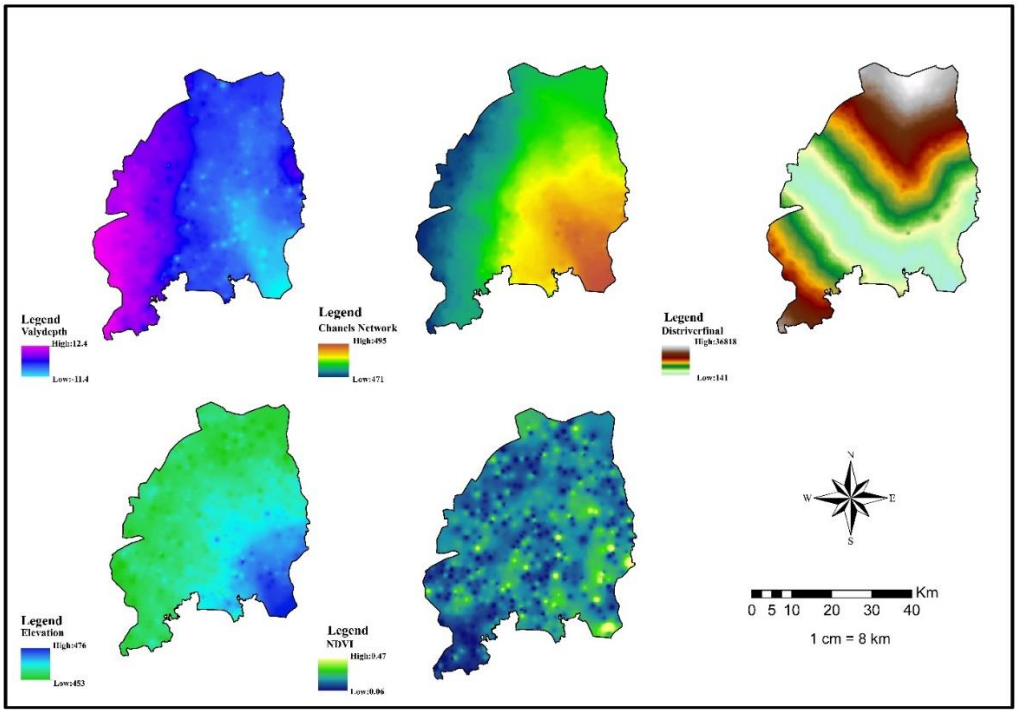

Figure 2. Distribution of auxiliary environmental variables in the study area

In general, it can be said that the variables derived from remote sensing were effective in modeling soil SP only in the first (0-15 cm) and second (15-30 cm) depths which were close to the land surface. Several studies also confirmed that in three-dimensional modeling of soil characteristics, the importance of auxiliary variables extracted from satellite images decreases with increasing depth (Amirian Chekan et al., 2017; Taghizadeh Mehrjardi et al., 2014).

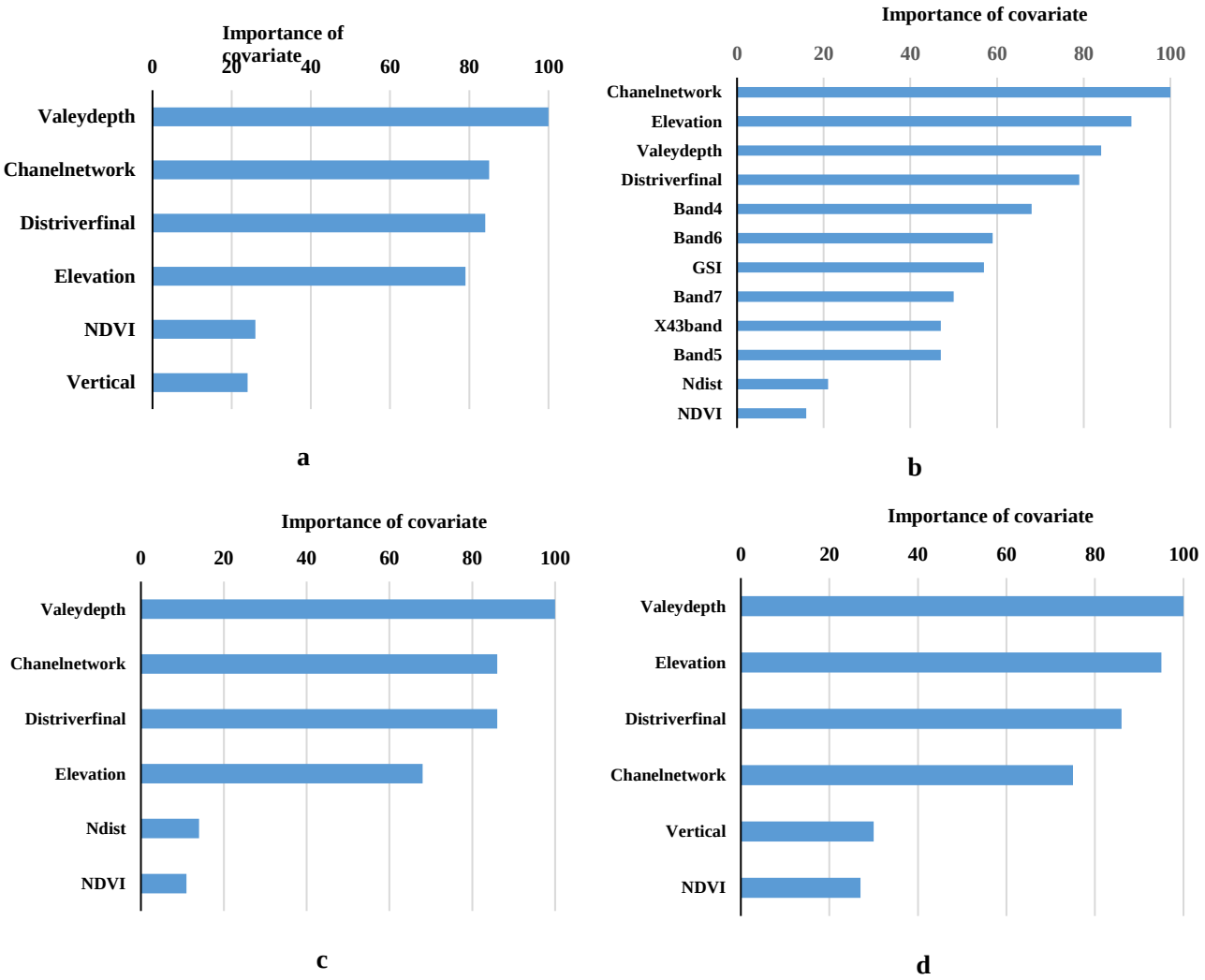

Figure 3. Importance of variables used in SP modeling with the RF model (a: 0-15 cm, b: 15-30 cm, c: 30-60 cm and d: 60-100 cm)

Also, several studies have stated that in areas with a low slope (less than 5%) due to the low variability of the variables from the DEM, other topographical parameters have less effect in predicting soil properties, especially on the surface (Amirian Chekan et al., 2017; Emami et al., 2024b). Contrary to these findings, in all studied depths, the variables derived from the DEM (terrestrial variables) were effective on SP in the area. In the third depth (30-60 cm) and the fourth depth (60-100 cm), only terrestrial variables were effective in modeling. Another point about these selected variables is that they are mainly related to alluvial activities (such as the depth of the valley, distance from the river, channel network, and elevation). The activity that has had the greatest effect on soil changes in the studied area (Mirakzehi et al., 2018; Pahlavan-rad and Akbarimoghaddam, 2018; Shahriari et al., 2019).

In other words, the selected environmental variables reflect the conditions and soil-forming factors in the Sistan Plain. On the other hand, it seems that for the physical attribute, SP, the variables derived from DEM show a higher correlation at all depths. The reason for the relationship between the variables extracted from DEM and physical characteristics such as soil texture components can be related to their effect on the vertical and lateral movement of soil particles through erosion and sedimentation (Emami et al., 2024b; Akpa et al., 2014).

3.3. Spatial modeling

Based on the highest value of R^2 and the lowest value of RMSE, the RF model for SP at depths of 0-15, 15-30, 30-60, and 60-100 was obtained as the best model for 3D spatial modeling in Sistan floodplain (Table 4). Of course, in the second depth, the QRF model has also performed better based on the MAE index. It should be mentioned that, in general, no significant difference was observed between the studied models. Also, Naimi Mardani et al.

(2021) showed that the RF model for the parameters of clay (R^2=0.48 and RMSE=6.02), silt (R^2=0.19 and RMSE=35.17), and sand (R^2=0 34.34 and RMSE=65.10) based on R^2 value and RMSE has a higher performance for predicting soil texture components. Hengl et al. (2015) predicted the spatial distribution of soil properties using the RF model and linear regression and reported that the RF model is more accurate in predicting soil properties than the linear regression model. Pahlavan-Rad and Akbarimoghaddam (2018) investigated the spatial distribution pattern of soil texture components and pH in a part of the agricultural lands of the Sistan floodplain in Zahak city by using the RF model and found that the RF model due to the large variation in the amount of soil texture in the plain Sistan flood reaches relatively high RMSE values for both soil texture and pH

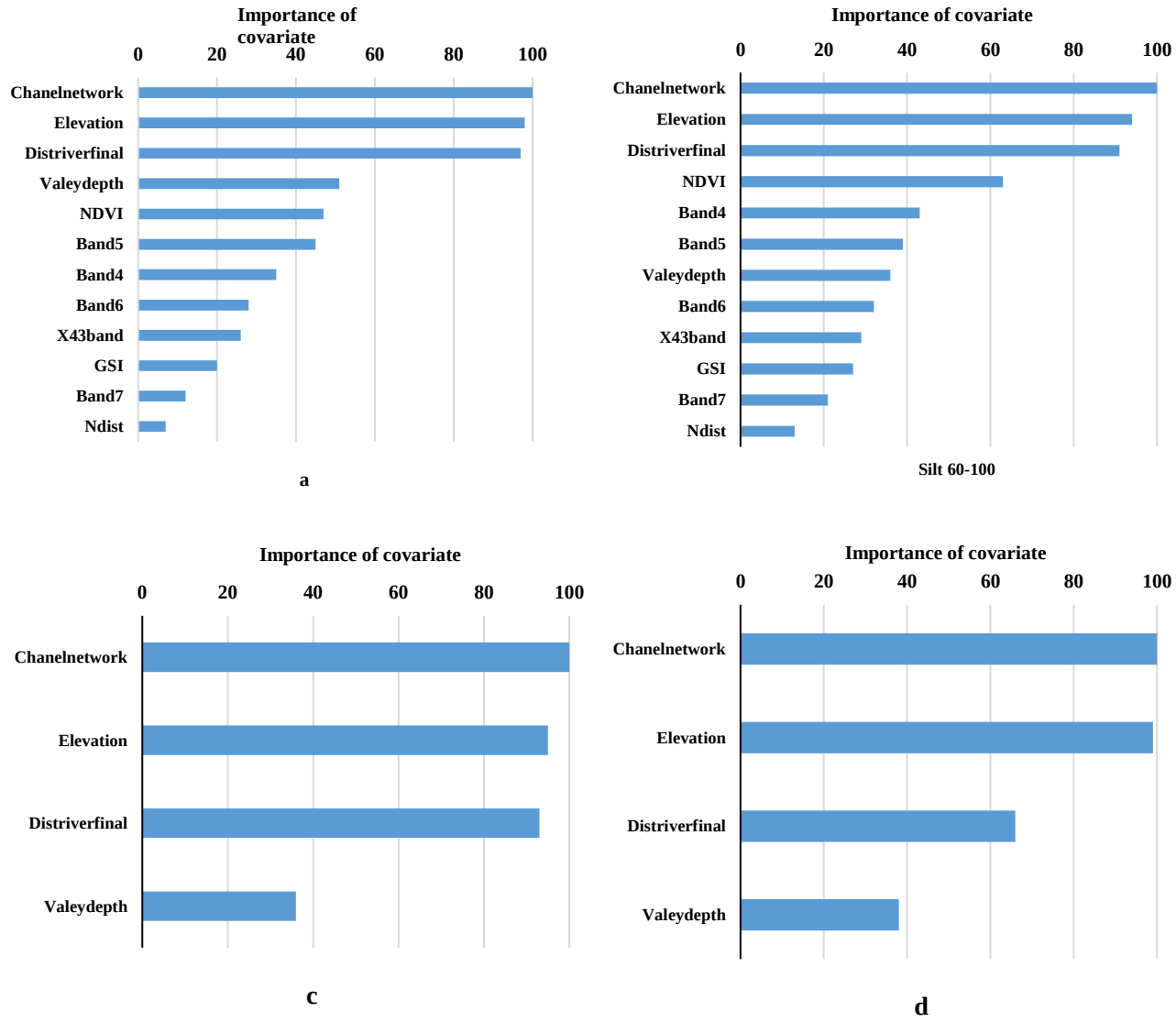

Figure 4. Importance of variables used in SP modeling with the QRF model (a: 0-15 cm, b: 15-30 cm, c: 30-60 cm and d: 60-100 cm)

Camera et al. (2017) using MLR models and RF, predicted soil properties including WRB soil groups, soil depth, and soil texture classes, and showed that the RF model compared to The MLR model performed better. Zhang et al. (2020) used the RF model to predict soil clay and showed that the RF model performs well in showing the changes from the surface to the depth and has a very good accuracy compared to other methods. Jena et al. (2023) used the RF model for digital mapping of soil texture components and their results showed that R^2 value for depths of 0-5, 5-15, 15-30, 30-60, 60-100, and -200 100 was equal to 0.30, 0.28, 0.21, 0.02, 0.02, 0.14, respectively, and in the first two depths, the accuracy of the model showed a good performance, and in the lower depths, the accuracy of the model decreased.

Lotfollahi et al. (2023) performed spatial modeling of soil texture components using the Global Soil Map and limited data and showed that the RF model with R^2 and RMSE values of 0.80 and 3.87 respectively for sand and 0.82 and 2.34 for clay and silt had the most accurate predictions of 0.85 and 2.89. Also, in this research, they showed that terrestrial-based environmental variables had a greater effect than remote-sensing variables.

Table 4. Soil SP spatial modeling results

Model	Depth (Cm)	Mtry	committees	Neighbors	RMSE	R^2	ME
RF	0-15	2	-	-	6.75	0.19	5.34
QRF		2	-	-	6.82	0.18	5.37
Cubist		-	1	9	6.99	0.17	5.47
RF	15-30	2	-	-	8.40	0.23	6.48
QRF		2	-	-	8.48	0.23	6.34
Cubist		-	10	0	8.45	0.19	6.46
RF	30-60	2	-	-	10.19	0.19	7.93
QRF		2	-	-	10.86	0.14	8.14
Cubist		-	1	0	10.54	0.15	8.03
RF	60-100	2	-	-	11.26	0.12	8.97
QRF		2	-	-	11.86	0.01	9.13
Cubist		-	1	9	11.52	0.11	9.09

The relatively high RMSE values observed in this study reflect the complexity of soil property variations and the diverse conditions influencing soil formation in floodplains (Wälder et al., 2008). Aeolian erosion and deposition are two significant processes contributing to increased spatial heterogeneity within the study area. Although challenging to incorporate, the inclusion of environmental variables related to aeolian processes could enhance the accuracy of the model.

3.4. 3D distribution of SP

As can be seen, the distribution of SP at depths of 0-15, 15-30, 30-60, and 60-100 is shown in Figure 5. The spatial changes of SP at the depth of 0-15 (first depth) has an increasing value in the northern parts and It has an average amount in the central parts of the Sistan plain and a smaller amount in the southern parts. In this depth, SP value in class more than 40% is 7.16% of lands, class 35-40% is 26.99% of lands, class 30-30% is 56.21% of lands, class 25-30 is 9.3% of lands and the class less than 25% included 0% of Sistan Plain lands. Hashemi et al. (2016) showed that the trend of SP changes in the surface soils of the Miankangi region of the Sistan Plain is similar to the pattern of distribution of silt and clay particles in the region. In other words, SP has a close and high relationship with soil texture components (Selmy et al., 2022).

According to research by Jamalzehi Samrah et al. (2021) on soil texture components in the Sistan region, a correlation analysis was done between these properties and SP at various depths (Table 5). The result showed a significant and positive correlation between silt and clay particles and SP in all depths. Conversely, a significant negative correlation was found between sand particles and SP in the studied area.

Table 5. Correlation analysis between SP and Soil texture components

	Depth	Clay%	Silt%	Sand%
SP%	0-15	0.581^{**}	0.491^{**}	-0.637^{**}
	15-30	0.631^{**}	0.442^{**}	-0.676^{**}
	30-60	0.647^{**}	0.379^{**}	-0.707^{**}
	60-100	0.655^{**}	0.324^{**}	-0.692^{**}

The significance level is marked with stars ($P < 0.01^{**}$)

The spatial changes of SP in the depth of 15-30 (second depth) have an increasing value in the northern parts, and it has an average value in the central parts of the plain and a small value in the southern parts. In this depth, SP value in class more than 40% is 22.60% of lands, class 35-40% is 20.89% of lands, class 30-30% is 50.50% of lands, class 25-30 is 73.5% of lands and the class included less than 25% of 0.01% of Sistan plain lands.

Shahriari et al. (2019) in the spatial modeling of the soil texture components of the Sistan plain at a depth of 0-30 cm showed that the amount of soil clay components is the highest in the northwestern and northern parts of the plain. Also, in the southern and central parts of the plain, which are adjacent to the Sistan River, there is more sand, and in the northwestern, northern, and western parts of the region, the amount of sand is the lowest. The amount of silt is the highest in the eastern, northeastern and western parts of the region, too. Also, Pahlavan-rad and Akbarimoghaddam (2018) in a study they conducted in the southeastern and southern parts of the Sistan plain investigated the changes in soil texture components at a depth of 0-30 cm and showed that due to the proximity to the Sistan river, the amount of sand in this area is high that the reason for that is the quick sedimentation of sand from suspension during floods. On the other hand, the high amount of sand in the area is caused by wind-blown sediments resulting from the 120-day winds that prevail in the area. These strong winds start from the beginning of June and end in the middle or end of September, when the water flow of the Hirmand River stops in the area from the north, and the northwest blows towards the south and causes the erosion of sand particles from the northern parts and the sedimentation and redistribution of sand particles in the southwestern and southern parts. Also, the amount of silt was high in the area around the Sistan River, and since the most important variable of these researchers in this study was "distance from the river", it is likely that the amount of clay is higher in these soils as a result of the slower settling of clay and silt particles from flood sediments above the river. in the region (Pahlavan-Rad and Akbarimoghaddam, 2018). Based on this, it seems that the amount of SP in this area is strongly influenced by the changes in the soil texture components and is in line with the changes in clay and silt parameters and has an opposite relationship with the sand parameter.

The spatial changes of SP in the depth of 30-60 (third depth) has an increasing value in the northern parts and has an average value in the central and southern parts of the plain. In this depth, SP value in class more than 40% is 27.33% of lands, class 40-35% is 34.49% of lands, class 30-30% is 31.23% of lands, class 25-30 is 1.01% of lands and the class less than 25% included 0% of Sistan Plain lands. The spatial distribution of SP in the depth of 60-100 (fourth depth) has an increasing value in the northern and central parts, and it has an average value in the southern parts of the plain. In this depth, SP value in class more than 40% is 39.31% of lands, class 35-40% is 37.03% of lands, class 30-30% is 23.93% of lands, class 25-30 is 0.72% of lands and the class less than 25% included 0% of Sistan Plain lands.

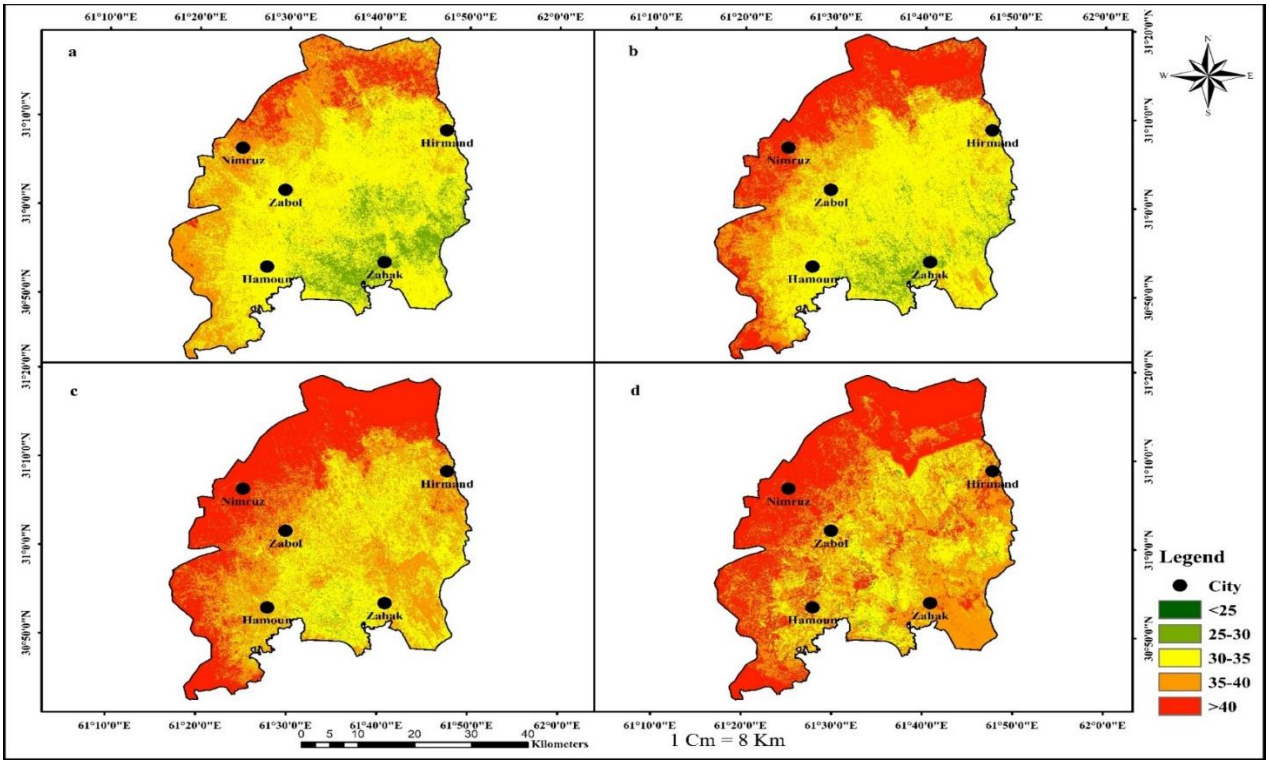

Figure 5. SP distribution at depths of a: 0-15 cm, b: 15-30 cm, c: 30-60 cm and d: 60-100 cm.

In general, the amount of SP increases from the surface to the depth of the soil in the Sistan plain. Jamalzehi Samrah et al. (2021) showed that with increasing soil depth, the proportion of fine soil components (silt and clay) increases with depth in the Sistan plain, and these changes are constant from 40 cm to 100 cm deep. Therefore, as mentioned, the changes in soil SP in the Sistan plain are in line with the changes in the soil texture components of the region (Hashemi et al., 2015; Selmy et al., 2022). On the other hand, the soil SP 3D changes are in line with the changes in the soil texture of the Sistan plain, and these changes are strongly influenced by the interactions of the prevailing alluvial and aeolian activities in the studied area, that these activities cause complexity in the relative changes of the soil characteristics of the region (Mirakzehi et al., 2018; Pahlavan-rad and Akbarimoghaddam, 2018; Shahriari et al., 2019).

Based on the results obtained regarding the three-dimensional zoning of the percentage of saturated soil moisture, it seems that in the northern areas of the Sistan plain, due to the high level of this parameter, the irrigation cycle can be done with a longer time interval than in the southern areas of the plain for agricultural products. Therefore, agricultural products or plants with more drought resistance can be recommended for the northern areas of the plain. Also, in the northern regions, both plants with shallow and deep roots can be considered to manage vegetation and deal with wind erosion, in the fields of natural resources, and in the southern regions of the plain, more trees and plants with deep roots can be used for this purpose.

4. Conclusion

3D spatial modeling of soil SP in dry areas is one of the important aspects of soil mapping that plays an important role in land management strategies. For the spatial modeling of this attribute, different methods are used, including random forest, quintile regression forest, and cubist. The results showed that the value of SP in the south was the lowest values and in the middle of the Sistan plain was the average values and in the north of the plain at the edge of the Hamoun wetlands had the highest values and the SP changed from the surface to the depth with the same spatial trend in the studied layers, and its average value increases from the surface to the depth. It seems that the changes are in line with the three-dimensional changes of the soil texture components in the region. The random forest method had the best performance in SP estimation and the environmental variables derived from satellite images and DEM (terrestrial variables) at two upper depths

(0-15 and 15-30 cm) and the terrestrial variables at all depths showed a good correlation with SP. The relationship between selected environmental variables and alluvial processes was significant. In general, the findings emphasize the importance of integrating environmental variables that reflect soil conditions and their influencing factors in conjunction with advanced modeling techniques such as RF to prepare and produce soil characteristic maps with high accuracy. For future studies, it is recommended to use new machine learning models in this regard.

References

Adeniyi, O.D., Bature, H., & Mearker, M. A. (2024). Systematic Review on Digital Soil Mapping Approaches in Lowland Areas. Land, 13, 379. https://doi.org/10.3390/land13030379.

Agbu, P. A., Fehrenbacher, D. J., & Jansen, I. J. (1990). Soil property relationships with SPOT satellite digital data in east central Illinois. *Soil Science Society of America Journal*, *54*(3), 807-812. https://doi.org/10.2136/sssaj1990.03615995005400030031x

Ahmad Aali, K., Parsinejad, M., & Rahmani, B. (2009). Estimation of Saturation Percentage of Soil Using Multiple Regression,ANN, and ANFIS Techniques. *Computer and Information Science*, *2*(3), 127-136

Akpa, S. I. C., Odeh, I. O. A. & Bishop, T. F. A. (2014). Digital mapping of soil particle-size fractions for Nigeria. *Soil Science Society of America Journal, 78*. 1953-1966. https://doi.org/10.2136/sssaj2014.05.0202

Aksoy, E., Panagos, P., & Montanarella, L. (2012). Spatial prediction of soil organic carbon of Crete by using geostatistics. In: Minasny, B., Malone, B.P., McBratney, A.B. (Eds.), Digital Soil Assessments and Beyond. *CRC Press, London*, 149–159.

Amirian Chekan, A., Taghizadeh Mehrjerdi, R., Sarmadian, F., & Heidary, A. (2017). Three-dimensional mapping of soil texture using spline depth functions and artificial neural networks. *Iranian Journal of Soil and Water Research*, *48*(1). 113-123. [In Persian]

Athey, S., Tibshirani, J., & Wager, S. (2019). Generalized random forests. https://doi.org/10.1214/18-aos1709.

Bameri, A., Khormali, F., Kiani, F., & Dehghani, A. A. (2015). Spatial variability of soil organic carbon in different hillslope positions in Toshan area, Golestan Province, Iran: Geostatistical approaches. *Journal of Mountain Science*, *12*(6), 1422-1433. https://doi.org/10.1007/s11629-014-3213-z

Ben-Dor, E., Chabrillat, S., Dematt, J., Taylor, G., Hill, J., Whiting, M., & Sommer, S. (2009). Using imaging spectroscopy to study soil properties. *Remote Sens. Environ. 113* (1), 38-55. Imaging Spectroscopy Special Issue. https://doi.org/10.1016/j.rse.2008.09.019OUCI+2

Bishop, T. F. A., McBratney, A. B. & Laslett, G. M. (1999). Modelling soil attribute depth functions with equal-area quadratic smoothing splines. *Geoderma, 91*, 27-45. https://doi.org/10.1016/s0016-7061(99)00003-8

Boehner, J., & Selige, T. (2006). Spatial prediction of soil attributes using terrain analysis and climate regionalisation. *Gottinger Geographische Abhandlungen*, *115*, 13-28

Boettinger, J. L., Ramsey, R. D., Bodily, J. M., Cole, N. J., Kienast-Brown, S., Nield, S. J., ... & Stum, A. K. (2008). Landsat spectral data for digital soil mapping. In *Digital soil mapping with limited data* (pp. 193-202). Dordrecht: Springer Netherlands. https://doi.org/10.1007/978-1-4020-8592-5_16

Camera, C., C., Zomeni, Z., Noller, J. S., Zissimos, A. M., Christoforou, I. C., & Bruggeman, A. (2017). A high resolution map of soil types and physical properties for Cyprus: A digital soil mapping optimization. *Geoderma*, *285*, 35-49. https://doi.org/10.1016/j.geoderma.2016.09.019

Cao, J., Guo, Z., Lv, Y., Xu, M., Huang, C., & Liang, H. (2023). Pollution risk prediction for cadmium in soil from an abandoned mine based on random forest model. *International Journal of Environmental Research and Public Health*, *20*(6), 5097. https://doi.org/10.3390/ijerph20065097

Delbari, M., Afrasiab, P., Gharabaghi, B., Amiri, M., & Salehian, A. (2019). Spatial variability analysis and mapping of soil physical and chemical attributes in a salt-affected soil. *Arabian Journal of Geosciences*, *12*(3), 68-86. https://doi.org/10.1007/s12517-018-4207-x.

Dharumarajan, S., & Hegde, R. (2022). Digital mapping of soil texture classes using Random Forest classification algorithm. *Soil Use and Management*, *38*(1), 135-149. https://doi.org/10.1111/sum.12668

Duan, M., Guo, Z., Zhang, X., & Wang, C. (2022). Influences of different environmental covariates on county-scale soil type identification using remote sensing images. *Ecological Indicators*, *139*, 108951. https://doi.org/10.1016/j.ecolind.2022.108951

Emami, M., Khormali, F., Pahlavan-Rad, M. R., & Ebrahimi, S. (2024). Digital modeling of surface and subsurface soil salinity in Golestan province, Iran. *Geoderma Regional*, *37*, e00800. https://doi.org/10.1016/j.geodrs.2024.e00800.

Emami, M., Khormali, F., Pahlavan-Rad, M. R., & Ebrahimi, S. (2024b). Preparation of three-dimensional maps of soil particle size fraction by combining quantile regression forest algorithm and spline functions in the north of Golestan province. Iran., *Iranian Journal of Soil and Water Research*, *55* (1), 51-68. [In Persian] https://doi.org/10.22059/ijswr.2023.366978.669594

Fan, N. Q., Zhao, F. H., Zhu, L. J., Qin, C. Z., & Zhu, A. X. (2022). Digital soil mapping with adaptive consideration of the applicability of environmental covariates over large areas. *International Journal of Applied Earth Observation and Geoinformation*, *113*, 102986. https://doi.org/10.1016/j.jag.2022.102986

Filippi, P., Jones, E., & Bishop, T.F. (2020). Catchment-scale 3D mapping of depth to soil sodicity constraints through combining public and on-farm soil databases – A potential tool for on-farm management. *Geoderma*,

374, 114396. https://doi.org/10.1016/j.geoderma.2020.114396

Gholamalizadeh Ahangar, A., Sarani, F., Hashemi, M., & Shabani, A. (2015). Comparison of linear regression methods, geostatistical and artificial neural network modeling of organic carbon in dry land of Sistan plain. *Water and Soil*, *28*(6), 1250-1260. [In Persian] https://doi.org/10.22067/jsw.v0i0.32714

Grunwald, S., Thompson, J. A., Minasny, B., & Boettinger, J. L. (2012). Digital soil mapping in a changing world. In *Digital Soil Assessments and Beyond* (pp. 301-306). CRC Press London. https://doi.org/10.1201/b12728-60

Gyamerah, S. A., & Moyo, E. (2020). Long-Term Exchange Rate Probability Density Forecasting Using Gaussian Kernel and Quantile Random Forest. *Complexity*, *2020*(1), 1972962. https://doi.org/10.1155/2020/1972962

Hashemi, M. , Gholamalizadeh Ahangar, A. , Bameri, A. , Sarani, F. & Hejazizadeh, A. (2016). Survey and Zoning of Soil Physical and Chemical Properties Using Geostatistical Methods in GIS (Case Study: Miankangi Region in Sistan). *Water and Soil*, *30*(2), 443-458. [In Persian]. https://doi.org/10.22067/jsw.v30i2.25950

Hengl, T., Heuvelink, G. B., Kempen, B., Leenaars, J. G., Walsh, M. G., Shepherd, K. D., ... & Tondoh, J. E. (2015). Mapping soil properties of Africa at 250 m resolution: Random forests significantly improve current predictions. *PloS one*, *10*(6), e0125814. https://doi.org/10.1371/journal.pone.0125814

Heung, B., Bulmer, C. E., Schmidt, M. G., & Zhang, J. (2022). Provincial-scale digital soil mapping using a random forest approach for British Columbia. *Canadian Journal of Soil Science*, *102*(03), 597-620. http://dx.doi.org/10.1139/cjss-2021-0090

Hom, B. K. (1981). Hill shading and the reflectance map. *Proceedings of the IEEE*, *69*(1), 14-47. https://doi.org/10.1109/proc.1981.11918

IUSS. 7th global digital soil mapping workshop (2016). Available online: https://projects.au.dk/digitalsoilmapping// (accessed on 1st August 2023).

Jamalzehi Samrah, Y. (2022). *Three-dimensional spatial modeling texture components and saturation percentage of soil in the Sistan plain.* MSc's thesis. Faculty of Water and Soil, University of Zabol. 186 p.

Jamalzehi Samareh, Y., Shahriari, A., Pahlavan-Rad, M., Ziaei Javaid, A. & Bameri, A. (2021). *Preparation of three-dimensional maps of the size of soil particles in the floodplain of Sistan* [Conference presentation]. The Seventeenth Iran Soil Science Congress and 4th National Farm Water Management Conference, Soil and Water Research Institute, Karaj, Iran. [In Persian]

Jamshidi, M., Delavar, M. A., Taghizadehe-Mehrjerdi, R., & Brungard, C. (2019). Evaluating digital soil mapping approaches for 3D mapping of soil organic carbon. *Iranian Journal of Soil Research*, *33*(2), 227–239. [In Persian]. https://doi.org/10.22092/ijsr.2019.119764

Jena, R. K., Moharana, P. C., Dharumarajan, S., Sharma, G. K., Ray, P., Deb Roy, P., Ghosh, D., Das, B., Alsuhaibani, A. M., & Gaber, A. (2023). Spatial prediction of soil particle-size fractions using digital soil mapping in the North Eastern region of India. *Land*, *12*(7), 1295. https://doi.org/10.3390/land12071295

Karimi Nezhad, M. T., Tabatabaii, S. M., & Gholami, A. (2015). Geochemical assessment of steel smelter-impacted urban soils, Ahvaz, Iran. *Journal of Geochemical Exploration*, *152*, 91–109. https://doi.org/10.1016/j.gexplo.2015.01.005

Kidd, D., Searle, R., Grundy, M., McBratney, A., Robinson, N., O'Brien, L., Zund, P., Arrouays, D., Thomas, M., Padarian, J., Jones, E., Bennett, J. M., Minasny, B., Holmes, K., Malone, B. P., Liddicoat, C., Meier, E. A., Stockmann, U., Wilson, P., Wilford, J., Payne, J., Ringrose-Voase, A., Slater, B., Odgers, N., Gray, J., van Gool, D., Andrews, K., Harms, B., Stower, L., & Triantafilis, J. (2020). Operationalising digital soil mapping – Lessons from Australia. *Geoderma Regional*, *23*, e00335. https://doi.org/10.1016/j.geodrs.2020.e00335

Kidd, D., Searle, R., & Wilson, P. (2018). Digital soil mapping: application, opportunity and challenges. *Soil Science Policy Journal* (1), 35–40. Available at https://www.soilscienceaustralia.org.au/publications/soil-policy-journal/

Kuhn, M. K., Weston, S., Keefer, C., & Coulter, N. (2016). *Cubist models for regression* [Computer software manual]. https://cran.r-project.org/package=Cubist

Lotfollahi, L., Delavar, M. A., Biswas, A., Jamshidi, M., Taghizadeh-Mehrjardi, R., & Fatehi, S. H. (2023). Modeling the spatial distribution of sand, silt, and clay particles based on GlobalSoilMap and limited data. *DESERT*, *28*(2), 243–263.

Malone, B. P., McBratney, A. B., Minasny, B. & Laslett, G. M. (2009). Mapping continuous depth functions of soil carbon storage and available water capacity. *Geoderma*, *154*, 138-152. https://doi.org/10.1016/j.geoderma.2009.10.007

Malone, B. P., Minasny, B., & McBratney, A. B. (2016). *Using R for digital soil mapping* (pp. 133–136). Springer. https://doi.org/10.1007/978-3-319-44327-0

Meinshausen, N. (2017). *quantregForest: Quantile regression forests* [Computer software manual]. CRAN.

Metinfar, H., Maqsoodi, Z., Mousavi, S., & Jalali, M. (2019). Evaluation of machine learning methods in digital organic carbon mapping of agricultural soils (part of Khorram Abad plain. *Water and Soil Magazine*, *24*(4), 327–343. [In Persian]

Mirakzehi, K., Pahlavan-Rad, M. R., Shahriari, A., & Bameri, A. (2018). Digital soil mapping of deltaic soils: A case of study from Hirmand (Helmand) river delta. *Geoderma*, *313*, 233–240. https://doi.org/10.1016/j.geoderma.2017.10.039

Montanarella, L., & Panagos, P. (2021). The relevance of sustainable soil management within the European Green Deal. *Land Use Policy*, *100*, 104950. https://doi.org/10.1016/j.landusepol.2020.104950

Mousavi, S. R., Sarmadian, F., Omid, M. K., & Bogaert, P. (2022). Three-dimensional mapping of soil organic carbon using soil and environmental covariates in an

arid and semi-arid region of Iran. *Measurement, 201*, 111706. https://doi.org/10.1016/j.measurement.2022.111706

Mulder, V., de Bruin, S., Schaepman, M., & Mayr, T. (2011). The use of remote sensing in soil and terrain mapping - a review. *Geoderma, 162*(1–2), 1–19. https://doi.org/10.1016/j.geoderma.2011.03.021

Naimi mardani, S., Ayoubi, S., Demattê, J., Zeraatpisheh, M., Amorim, M. T., & Oliveira Mello, F. A. (2021). Spatial prediction of soil surface properties in an arid region using synthetic soil image and machine learning. *Geocarto International*, 1–25. https://doi.org/10.1080/10106049.2021.1996639

Pahlavan-Rad, M. R., & Akbarimoghaddam, A. (2018). Spatial variability of soil texture fractions and pH in a flood plain (case study from eastern Iran). *Catena, 160*, 275–281. https://doi.org/10.1016/j.catena.2017.09.004

Piri, H. (2012). Assessment of computational methods of estimation of potential evapotranspiration using lysimeter data (Case study: Sistan Plain). *Journal of Irrigation and Water Engineering, 3*(9), 50–62. [In Persian]

Quinlan, J. R. (1992). Learning with continuous classes. In *Proceedings of the Fifth Australian Joint Conference on Artificial Intelligence* (pp. 343–348). World Scientific.

Rodiguez, F., Maire, E., Courjault-Rade, D., & Darrozes, J. (2002). The Black Top Hat function applied to a DEM: A tool to estimate recent incision in a mountainous watershed. *Geophysical Research Letters, 29*(1), 91–94. https://doi.org/10.1029/2001gl013484

Selmy, S. A., Abd El-Aziz, S., El-Desoky, A., & El-Sayed, M. A. (2022). Characterizing, predicting, and mapping of soil spatial variability in Gharb El-Mawhoub area of Dakhla Oasis using geostatistics and GIS approaches. *Journal of the Saudi Society of Agricultural Sciences, 21*(4), 383–396. https://doi.org/10.1016/j.jssas.2021.05.004

Shahriari, M., Delbari, M., Afrasiab, P., & Pahlavan-Rad, M. R. (2019). Predicting regional spatial distribution of soil texture in floodplains using remote sensing data: A case of southeastern Iran. *Catena, 182*, 104–149. https://doi.org/10.1016/j.catena.2019.104149

Shams, M. Y., Tarek, Z., Elshewey, A. M., Hany, M., Darwish, A., & Hassanien, A. E. (2023). A machine learning based model for predicting temperature under the effects of climate change. In A. E. Hassanien & A. Darwish (Eds.), *The power of data: Driving climate change with data science and artificial intelligence innovations* (pp. 61–81). Springer Nature Switzerland. https://doi.org/10.1007/978-3-031-22457-4_4

Siyasar, H., Honar, T., & Abdolahipour, M. (2020). Comparing of generalized linear models, random forest and gradient boosting trees in estimation of reference crop evapotranspiration (Case study: The Sistan Plain). *JWSS, 23*(4), 395–410. [In Persian] https://doi.org/10.47176/jwss.23.4.40631

Soil Science Division Staff. (2017). *Soil survey manual* (C. Ditzler, K. Scheffe, & H. C. Monger, Eds.) (USDA Handbook 18). Government Printing Office.

Stivent, G. A., & Khan, M. A. (1996). Saturation percentage as a measure of soil texture in the lower Indus Basin. *Journal of Soil Science, 17*(1), 255–263. https://doi.org/10.1111/j.1365-2389.1966.tb01471.x

Taghizadeh Mehrjardi, R., Minasny, B., Sarmadian, F., & Malone, B. P. (2014). Digital mapping of soil salinity in Ardakan region, central Iran. *Geoderma, 213*, 15–28. https://doi.org/10.1016/j.geoderma.2013.07.027

Taghizadeh-Mehrjardi, R., Emadi, M., Cherati, A., Heung, B., Mosavi, A., & Scholten, T. (2021). Bio-inspired hybridization of artificial neural networks: An application for mapping the spatial distribution of soil texture fractions. *Remote Sensing*, Article 1–23. https://doi.org/10.3390/rs13040612

Wadoux, A. M.-C., Minasny, B., & McBratney, A. B. (2020). Machine learning for digital soil mapping: Applications, challenges and suggested solutions. *Earth-Science Reviews, 210*, 103359. https://doi.org/10.1016/j.earscirev.2020.103359

Wager, S., & Athey, S. (2018). Estimation and inference of heterogeneous treatment effects using random forests. *Journal of the American Statistical Association, 113*(523), 1228–1242. https://doi.org/10.1080/01621459.2017.1319839

Wei, Y., Ding, J., Yang, S., Yang, X., & Wang, F. (2021). Comparisons of random forest and stochastic gradient treeboost algorithms for mapping soil electrical conductivity with multiple subsets using Landsat OLI and DEM/GIS-based data at a type oasis in Xinjiang, China. *European Journal of Remote Sensing, 54*(1), 158–181. https://doi.org/10.1080/22797254.2021.1888657

Wulf, H., Mulder, T., Schaepman, M., Keller, A., & Jörg, P. (2014). *Remote sensing of soils* (Tech. Rep. 00.0338.PZ/435-0501). University of Zurich. https://doi.org/10.5167/uzh-109992

Zeraatpisheh, M., Ayoubi, S., Jafari, A., Tajik, S., & Finke, P. (2019). Digital mapping of soil properties using multiple machine learning in a semi-arid region, central Iran. *Geoderma, 338*, 445–452. https://doi.org/10.1016/j.geoderma.2018.11.011

Zhang, Y., Ji, W., Saurette, D. D., Easher, T. H., Li, H., Shi, Z., Adamchuk, V. I., & Biswas, A. (2020). Three-dimensional digital soil mapping of multiple soil properties at a field-scale using regression kriging. *Geoderma, 366*, 114253. https://doi.org/10.1016/j.geoderma.2020.114253

Žížala, D., Minařík, R., Skála, J., Beitlerová, H., Juřicová, A., Rojas, J. R., Penížek, V., & Zádorová, T. (2022). High-resolution agriculture soil property maps from digital soil mapping methods, Czech Republic. *Catena, 212*, 106024. https://doi.org/10.1016/j.catena.2022.106024

Zulfiqari, F., & Abedi, Gh. (2019). Modeling the effective factors in the concentration of dust particles in the air using the method CUBIST. In *International Conference on Dust in Southwest Asia*, Zabol. [In Persian]

Agriculture, Environment & Society

Journal homepage: www.aes.uoz.ac.ir

The study of energy indices and greenhouse gas emissions in some crops production in the east of Golestan Province, A case study: Minoodasht township

Hasan Mamashli [a], Masoumeh Naeemi [*b], Nasibe Rezvantalab [c], Ali Rahemi Karizaki [d]

[a] M.Sc graduated in Agroecology, Plant Production Department, College of Agriculture and Natural Resources, Gonbad Kavous University, Gonbad Kavous, Iran
[b] Plant Production Department, College of Agriculture and Natural Resources, Gonbad Kavous University, Gonbad Kavous, Iran
[c] PhD graduated in Agronomy, Plant Production Department, College of Agriculture and Natural Resources, Gorgan Agricultural Sciences and Natural Resources University, Gorgan, Iran
[d] Plant Production Department, College of Agriculture and Natural Resources, Gonbad Kavous University, Gonbad Kavous, Iran

ARTICLE INFO

Article history:
Received: 7 December 2024
Accepted: 21 February 2025
Available online: 1 June 2025

Keywords:
Chemical fertilizers
Fossil fuel
Greenhouse gas emissions
Input energy
Output energy

ABSTRACT

Increasing the CO_2, N_2O and CH_4 concentrations cause the global warming. Therefore, the fuel consumption, energy and greenhouse gas emissions in wheat, canola and sunflower productions in Minoodasht township were investigated. Data were collected from 60 wheats, 25 canola and 10 sunflower fields in 2021-2022 growing season. Energy input and greenhouse gas emissions per hectare was analyzed based on the fuel and input consumptions per each agricultural operation by related coefficients. Findings revealed that 140.46, 100.00 and 158.00 l/ha fuel diesel were needed to wheat, canola and sunflower production. Land preparation in wheat and canola production and harvesting the sunflower had the highest energy requirements and greenhouse gas emissions. The output to input energy ratio was calculated as 4.84, 4.94 and 3.69 in wheat, canola and sunflower productions, respectively. Also, in the wheat, canola and sunflower production, net energy was 62,743, 39,885 and 31,177 MJ, respectively, energy efficiency was 0.21, 0.19 and 0.13 respectively, and specific energy was 4.76, 5.26, 7.69 MJ/kg, respectively. According to the results, 1238, 904 and 1070 kg $eqCO_2$/ha were emitted from wheat, canola and sunflower fields, respectively. On average, 76, 89, and 92 g greenhouse gases were emitted for one MJ/ha energy consumed in wheat, canola, and sunflower productions, which is equivalent to 16, 18, and 25 g energy output, respectively. Finally, according to the obtained results, the chemical fertilizers consumption, especially nitrogen fertilizers, as well as the fossil fuels consumption account for an important part of energy consumption and greenhouse gases emissions.

Highlights

- Wheat uses 140.46 L/ha fuel, canola 100 L/ha, sunflower 158 L/ha in Minoodasht, 2021-2022.
- Energy efficiency: wheat 4.84, canola 4.94, sunflower 3.69; net energy highest in wheat.
- GWP: wheat 1238, canola 904, sunflower 1070 kg eqCO2/ha; N-fertilizers, fuel key emitters.
- Land prep in wheat/canola, harvest in sunflower lead energy use and GHG emissions.
- Wheat emits 76 g GHG/MJ input, canola 89 g, sunflower 92 g; optimizing inputs cuts emissions.

1. Introduction

Energy consumption has become more than before in agriculture by increasing the population growth and more fossil fuels demands (Fei and Lin, 2017). In addition, it is predicted that the energy consumption will increase due to the increased economic growth, soil degradation, climate change and global warming, as well as labor shortages. It is worth mentioning that high energy consumption will be a dangerous threat to maintain the agriculture sustainability, public health and environmental functions (Bergtold et al., 2017). Efficient consumption of energy is one of the main demands for sustainable agriculture

* Corresponding author.
E-mail address: masoumeh_naeemi@yahoo.com
https://doi.org/10.22034/jelsa.2025.492657.1092

(Ghorbani et al., 2011). The higher energy efficiency will provide the natural resources saving, reducing environmental damage and developing the sustainable agriculture (Yuan et al., 2018). Energy analysis of agricultural ecosystems is a useful method to determine the energy and environmental sustainability. Furthermore, optimizing the natural resources by more energy-efficient crop cultivation technologies, is needed to enhance the cost benefits and mitigate the environmental consequences (Gong et al., 2021). Accordingly, reducing the energy consumption and increasing the energy efficiency is very necessary to ensure the food sustainability and environmental security. The analysis of energy input and output is a promising assessment for analyzing energy flow and determining the optimal use of energy in crop productions (Kizilaslan, 2008). Sustainable environment dependent on the sustainable agriculture. Environmental factors have a great contribution to agriculture as compared to other. Higher energy use efficiency will promote sustainable agriculture by minimizing environmental problems and preventing the destruction of natural resources. (Imran et al., 2020).

The agricultural sector is important because it can be useful as a global solution to reduce the greenhouse gas emissions caused by human activities (Yuan et al., 2018). The share of agricultural activities in the greenhouse gas emissions is 10-12% of the total greenhouse gas emission (Brownea et al., 2011). Increasing the greenhouse gas concentrations in the atmosphere will cause the earth to warm up, and as a result, the atmosphere and oceans average temperatures will also increase (Pishgar-Komleh, 2012).

The production, transportation, storage and distribution of inputs as well as the use of machinery causes the combustion of fossil fuels, which results the greenhouse gas emissions into the atmosphere and global warming. Therefore, it is very necessary to know the intensity of greenhouse gas emissions based on the kilogram of carbon dioxide equivalent in various tillage operations, use of chemical fertilizers and pesticides, irrigation and harvesting methods (Lal, 2004).

The share of the world's arable land for grain cultivation is about 52%, which is approximately equivalent to 707 million hectares. The most cultivated area of wheat species in the world is common wheat (Triticum aestivum L.) or bread wheat, so that it includes approximately 95% of the wheat cultivated area in the world (Pourazri et al., 2013). Canola is the second oilseed crop in the world after soybean with 68 million ton productions (FAO, 2023). Sunflower is often cultivated as a source of vegetable oil. Its nutritional value and quality are often more than other oil crops. Sunflower has 40 to 60% edible oil. At present, more than 90% of the edible oil needed in the country is supplied through imports, therefore, it is important to cultivate the oil crops, including sunflower and canola, in Iran, especially in Golestan Province (Mousavi-Avval et al., 2011).

The reports indicated the different amounts of fuel consumption in wheat production. The fuel consumption calculated 65.00, 126.00 and 93.40 l/ha by Safa et al. (2011), Taghavifar and Mardani (2015) and Wang et al. (2014), respectively. The amount of greenhouse gases emissions due to the fuel consumption was evaluated as 460.06 ± 0.15 kg eq-CO_2 ha^{-1} (Rezvantalab et al., 2015), while some researchers estimated to be 203 and 455.2 kg eq-CO_2 ha^{-1} (Safa and Samarasinghe, 2012; Mohammadi et al., 2014).

A study evaluated the energy consumption in rain-fed wheat cultivation in China, stating that 56%, 22%, 14%, 4%, and 4% of the total energy consumption in rain-fed wheat production was attributed to the use of chemical fertilizers, pesticides, seeds, machinery, and human labor, respectively. The total energy consumption and energy efficiency were calculated 18200 MJ ha^{-1} and 2.9, respectively. This study considered the use of sandy mulch to increase the rain-fed wheat grain yield, which was able to enhance the energy use efficiency and net energy (Wang et al., 2019). In the terrace region of Turkey, by comparing energy indices in wheat production, energy use efficiency was reported 3.77. The main reason for the increased energy use efficiency was attributed to the higher wheat grain yield in the region. Additionally, the chemical fertilizers and fossil fuels consumptions were among the most significant sources of energy consumption in wheat production (Unakotan and Aydin, 2018). In a study aimed at assessing the environmental impact of sunflower production in the Halilan County of Ilam Province, Iran, was observed that the global warming potential for sunflower production was 2417.42 kg eq-CO_2 ha^{-1}. Electricity consumption, diesel fuel, and nitrogen fertilizers were the main sources of greenhouse gas emissions in sunflower production. Greenhouse gas emissions from electricity consumption were higher than from other inputs due to the use of the old electric pumps in the irrigation system. The carbon efficiency coefficient for sunflower cultivation was calculated 2.06 (Azizpanah et al., 2023).

The Minoodasht twonship, located in Golestan Province, Iran, has 25200 hectares of arable lands. So, 20,800, 950, and 105 hectares are allocated annually to the cultivation of wheat, canola, and sunflower, respectively. This study will examine fuel consumption, energy use, and greenhouse gas emissions, comparing these factors across wheat, canola, and sunflower to identify the best crop in terms of fuel consumption and reducing greenhouse gas emissions.

2. Materials and Methods

2.1. Data collection

Data were collected from 60 wheats, 25 canola and 10 sunflower fields in 2021-2022 growing season. The study was conducted in Minoodasht township using a random sampling method. The required data was collected through face-to-face interviews with the producers and by taking notes on all agricultural operations. The operations included plowing, disking, cultivating, chemical spraying, etc. Information was recorded based on the duration of each agricultural operation, the amount of fuel consumed per hectare for each operation, the types of machinery used, the number of operations, the variety and seeds used amount,

the types of chemical fertilizers, the types of pesticides used to control weeds, pests, and diseases, and finally the yield of the agricultural products mentioned in each sampled fields. At the end of the survey, information such as the area under cultivation and the type of pervious crop planted was recorded in each field. After recording the mentioned information, an assessment of energy flow and greenhouse gas emissions was conducted.

2.2. Energy analysis

Energy flow in the fields can be divided into energy input and energy output which the energy input (consumable) was classified in direct and indirect energy in many studies (Rathke et al., 2007; Tipi et al., 2009; Kaltsas et al., 2007).

Direct energy (MJ/ha) includes (1) the fuel consumption in various field operations including land preparation, sowing, fertilizing, plant protection, irrigation, and harvesting; (2) electricity for water pumping; and (3) the use of human labor. Indirect energy (MJ/ha) includes (1) the energy used for manufacturing, warehousing, and transportation of chemical fertilizers; (2) the energy used for manufacturing, warehousing, and transportation of chemical pesticides; (3) the energy used to manufacture, repair and maintenance of equipment and agricultural machinery; (4) Energy in seeds, as well as the need for winnowing energy, packaging, and storage (Rathke et al., 2007).

Firstly, energy consumed in each field based on Mega Joule per hectare (MJ/ha) was calculated as follows.

In order to calculate the fuel energy, the working time of machine was recorded separately at the beginning of any operation from start to end of the production process. Then, fuel consumption was calculated by the following equation (1) according to the past experiences of machinery drivers.

$$FT=t*FH \quad (1)$$

FT: fuel needed to perform the field operation (L ha^{-1}); t: working time of the machine; FH: fuel needed to perform the field operation (L h^{-1}).

Energy conversion ratios were used to calculate the fuel amounts to the consumed energy (Table 1).

Energy for agricultural machinery and equipment was calculated as mentioned above:

$$EM=(E\times WLt)t \quad (2)$$

EM: machinery and equipment energy for farming operations (MJ ha^{-1}); E: Energy for manufacturing, repair, maintenance, and transportation of machinery and equipment (MJ kg^{-1}); W: machinery and equipment weight (kg); Lt: the useful lifetime for machinery and equipment (hours); t: time needed for operation (h ha^{-1}); E: constant value and equal to 142.7 MJ kg^{-1} (Table 1) (Kaltsas et al., 2007).

In order to assess the energy consumption for chemical pesticide application, the percentage of active ingredients was identified in each pesticide (Table 2). Also, specific gravity was determined for liquid pesticides. Then, used net weight values were calculated by multiplying the specific gravity in the percentage of the active ingredient. Afterwards, the total energy consumed for each of the pesticide was calculated based on the amount of energy used for the production of each pesticide (Table 1). Formulating the pesticides also requires energy, which added 20 MJ kg^{-1} to energy consumption. Pesticides transportation to their consumption place requires energy that is not considerable (Clements et al., 1995).

To calculate the fertilizer energy consumption, fertilizer types and amounts were recorded. Then, the main ingredient of fertilizers was determined based on nitrogen (N), phosphorus (P_2O_5) and potassium (K_2O) in each fertilizer (Table 3). Total energy consumption was calculated by multiplying the amount of consumed energy in the main substance (Table 1).

In order to calculate the energy consumption for seed, seed amount (kg) per hectare was determined. In the next stage, the energy per one kilogram of seed was determined (Table 1). The energy consumption for seed was calculated by multiplying two parameters in each field.

The energy output was assessed by multiplying the harvested seed by its energy equivalents (Table 1). Based on the total energy equivalents of the inputs and output, energy use efficiency, energy productivity, specific energy, and net energy were calculated using the following equations (4-7) (Kazemi et al., 2015b):

Energy use efficiency=Output energy (MJ/ha)/Input energy (MJ/ha) (3)

Energy use productivity (kg/MJ)=Seed yield (kg/ha)/Input energy (MJ/ha) (4)

Specific energy (MJ/kg)=Input energy (MJ/ha)/Seed yield (kg/ha) (5)

Net energy (MJ/ha)=Output energy (MJ/ha)−Input energy (MJ/ha) (6)

GHG emissions can be calculated and represented per unit of the land used in crop production, per unit weight of the produced seed, and unit of the energy input or output. Firstly, the energy amount of each fuel source used in the manufacture and transportation of production inputs including seed, machinery, fertilizer, and pesticide, and fuel consumption in production operations was obtained using proportions. Then, using CO_2, N_2O, and CH_4 gas emission factors including 1, 310, and 21 kg CO_2, the total GHG emission was calculated equivalent to CO_2 (Soltani et al., 2013).

For these calculations, it was assumed that the electricity in Iran is generated by sources in the following proportions: 0.18% from coal, 16.6% from oil, 80.8% from natural gas, 2.3% from water generators, and 0.09% from wind generators (IEA, 2009). GHG emissions were determined per one hectare, one tone of crop produced, and one MJ of total input and output energy (Soltani et al., 2013).

3. Results of discussion

3.1. Wheat

The results indicated that the filed areas under wheat cultivation varied from 1 to 22 hectares, 85 percent was less than 10 hectares. Wheat planting typically took place from 30th November to 10th December. For the initial seedbed, 90 percent of farmers used a single plowing, while 10 percent used double plowing. The number of secondary tillage operations recorded between 1 to 3 times. The most common planting tool was the row seed drill. The average amount of seed used for planting was 200 kg ha^{-1} depending on the seed quality, planting date, and type of planting equipment. Overall, farmers applied fertilizer 3 times (in the form of base and top-dressing). Most farmers used urea fertilizer as a base fertilizer (Table 3). Top-dressing was mainly applied during tillering, stem elongation, and flowering, depending on the plant's demand. A total of 3 types of pesticides were used. The pesticides used included Topik, Granstar, Tilt, and Diazinon. A boom sprayer was primarily used for weed control, while a tractor-mounted sprayer was used for pest and disease management. Wheat harvesting took place from mid to late June. The harvest date depended on the crop maturity, seed moisture content, weather conditions, and availability of the combine harvester. On average, wheat grain and straw yields were recorded at 3500 and 4000 kg ha^{-1}, respectively.

Table 1. Energy equivalents for inputs and outputs in wheat, canola and sunflower production.

Inputs	Unit		References
Wheat grain	kg	15.7	(Pimental and Pimental, 2008)
seed Canola	kg	25	(Mousavi-Avval et al., 2011)
Sunflower	kg	28.5	(Sheikh and Houshyar, 2009)
Human labor	h	1.96	(Turhan et al., 2008)
Machinery	kg	142.7	(Kaltsas et al., 2007)
N	kg	60.6	(Akcaoz et al., 2009)
P2O5	kg	11.1	(Akcaoz et al., 2009)
K2O	kg	6.7	(Akcaoz et al., 2009)
Fossil fuel	l	38	(Hydrocarbon balance sheet of Iran, 2006)
Herbicides	kg i.e	287	(Tzilivakis et al., 2005)
Fungicide	kg i.e	99	(Strapatsa et al., 2006)
Insecticides	kg i.e	237	(Tzilivakis et al., 2005)
Outputs			
Wheat grain	kg	14.7	(Singh et al., 2007)
Wheat straw	kg	6.9	(Singh et al., 2007)
Canola seed	kg	25	(Mousavi-Avval et al., 2011)
Sunflower seed	kg	28.5	(Sheikh and Houshyar, 2009)

Table 2. Specific weight and percentage of effective substance of different pesticides used in crop production.

Chemical types	Chemical name	Specific weight	Effective ingredient (%)
herbicides	Granstar	-	75
	Topik	1.6	35
	Terflan	2.5	48
	2,4,D	1.22	67.5
Fungicides	Tilt	0.99	25
	Alto100	1.3	60
	Rural	1	52
Insecticides	Diazinon	1.18	60
	Larvin	1.40	80
	Malation	1.23	57
	Cypermethrin	1.24	40
	Select super	1	1.15

Table 3. The percentage of main elements in different fertilizers used

Fertilizer types	Chemical ingredient
Diammonium phosphate	P2O5(46%), Nitrogen (18%)
Triple superphosphate	P2O5(46%)
Macro	P2O5(8%), Nitrogen (15%), Potassium (15%)
Sulfate of potassium	Potassium (48%)
Urea	Nitrogen (46%)

3.2. Canola

In canola cultivation, the field areas varied from 0.5 to 5 hectares, 80 percent was less than 5 hectares. The most common crop grown before canola was soybean. The planting date typically extended from mid-November to mid-December. All farmers used a single plowing for the initial seedbed preparation. The number of secondary tillage operations was recorded as 1 to 3 times. The seed amount used by farmers recorded 4 kg ha^{-1}. Overall, farmers applied fertilizer to canola fields 2.95 times (in both base and top-dressing). In most canola-cultivated fields, urea fertilizer was used as the base fertilizer. The average top-dressing was recorded as approximately 2 times per field in rosette and seed filling stages. The pesticides used included the herbicides Cypermethrin and Select Super, as well as the fungicide Rural. A boom sprayer was mainly used for weed control, while a tractor-mounted sprayer was used for disease management. The canola harvest took place from early to late June. On average, 2000 kg was harvested per hectare.

3.3. Sunflower

According to the findings, the field areas cultivated under sunflowers was recorded as 2-12 hectares, 90 percent of fields was less than 10 hectares. The most common crops grown before sunflowers were wheat and barley, which accounted for 80 percent of the fields. The final harvest of wheat and barley was completed by the end of June. Sunflower planting generally began in early July and completed by July 10. Only one plowing was performed to initial seedbed preparation. The number of secondary tillage operations for sunflower cultivation was 1-3 times. The most common planting method for sunflowers was hand broadcasting. The amount of seed used was 7-8 kg ha^{-1}. The Hyson cultivar was the only variety used for sunflower cultivation. Overall, farmers applied fertilizer to their sunflower fields twice (as a base and top-dressing). Most farmers used urea fertilizer as the base fertilizer. The top-dressing was mainly applied once, during the 4-5 leaf stage, depending on the plant's needs. Two types of herbicides were recorded, including Select Super and Terflan. A tractor-mounted sprayer was used for weed control before planting, and a boom sprayer was used after germination. Sunflower harvesting took place in late September. On average, 1500 kg ha^{-1} sunflower seeds were harvested.

3.4. Energy Consumption and greenhouse gas emissions from inputs

Tables 4, 5, and 6 indicate the amount of input consumption, energy consumption, and greenhouse gas emissions resulting from the use of inputs in one hectare of wheat, canola, and sunflower fields. In wheat production, the energy consumed from chemical fertilizers, fossil fuels, seed usage, machinery, pesticide consumption, and human labor were ranked from the highest to lowest energy consumption, with fossil fuel and chemical fertilizer consumption accounting for a total of 76 percent of the overall energy consumption. Consequently, the highest level of greenhouse gas emissions was attributed to the chemical fertilizers and fossil fuels consumption, followed by the machinery application and chemical pesticides. Energy consumption in the rain-fed wheat production in China indicated that 56, 22, 14, 4, and 4 percent of total energy consumption was related to the chemical fertilizer consumption, chemical pesticides, seeds for planting, machinery application, and human labor utilization, respectively (Wang et al., 2019). The present results showed that the energy derived from chemical fertilizers, fossil fuel consumption, machinery application, pesticide use, and human labor were ranked from the highest to lowest in canola production (Table 5). As a result, the chemical fertilizers consumption, fossil fuels, machinery application, and pesticide also corresponded to the highest to lowest levels of greenhouse gas emissions. In sunflower production, the highest energy consumption was attributed to fossil fuel and chemical fertilizer use, while machinery application, pesticide consumption, and human labor were evaluated in the subsequent ranks. Azizanpah et al (2023) reported that the electricity consumption, fossil fuels, and nitrogen fertilizers were the main sources of carbon dioxide emissions in sunflower production in Ilam, Iran.

The energy derived from wheat seeds accounted for 19.25% of total energy consumption (Table 4). Therefore, it is essential to avoid unnecessary use of wheat seeds for planting as much as possible. A study conducted in Gorgan reported that the combinate seeder in wheat planting was associated with lower seed consumption, while the use of a centrifugal seed broadcasting was linked to higher seed consumption. Ultimately, they stated that by using new equipment such as combinate seeder, it is possible to save on seed and input energy consumption as well as unnecessary costs in crop production (Rezvantalab et al., 2015). The share of seed energy in canola and sunflower cultivation constituted 0.61% and 1.22% of the total energy, respectively, which is very minimal (Table 5). Mousavi Avval et al., (2011) also assessed the share of seeds used in sunflower production by 2.4%.

By examining the findings in the section on energy consumption resulting from chemical fertilizers in wheat production, it can be stated that the energy consumed averaged 6624.6 MJ ha^{-1}, with nitrogen-containing fertilizers accounting for 24.89 percent. Additionally, the energy consumption from phosphorus and potassium-containing fertilizers was 17.8 and 57.2 percent, respectively (Table 5). It is worth mentioning that nitrogen fertilizers were used in all fields, while phosphorus and potassium fertilizers were used in 93 and 50 percent of the fields, respectively. The studies showed that the organic fertilizers were not used in any of the wheat-cultivated fields. The chemical fertilizers application resulted 510.35 kg eq-CO_2 ha^{-1} greenhouse gas emissions in each wheat-cultivated farms, with the highest emission levels associated with the use of nitrogen-containing fertilizers, similar to the energy consumption patterns. Other chemical fertilizers had a lesser role in greenhouse gas emissions (Table 6). Since the share of energy consumption and greenhouse gas emissions is high by nitrogen fertilizers consumption, it can be said that reducing the nitrogen-containing fertilizer consumption in each wheat-cultivated field will have a very significant impact on reducing energy consumption and greenhouse gas emissions. In canola cultivation, 49.56 percent of total energy consumption was attributed to the use of chemical fertilizers, with nitrogen fertilizer consumption estimated 83.38 percent. Phosphorus and potassium-containing fertilizers accounted for 10 and 6.24 percent of energy consumption, respectively (Table 5).

In canola cultivation, the application of chemical fertilizers resulted 15.398 kg eq-CO_2 ha^{-1} greenhouse gas emissions, was the highest by use of nitrogen-based fertilizers. Table 6 illustrate that other chemical fertilizers had a significantly lower role in greenhouse gas emissions compared to the nitrogen-based fertilizers application. Accordingly, nitrogen-based fertilizers application was a key factor in energy consumption and greenhouse gas emissions. Therefore, reducing the use of nitrogen fertilizers, a significant role can be played in decreasing energy consumption and greenhouse gas emissions in canola production.

In sunflower production, 29.5 percent of input energy was allocated to chemical fertilizers, especially nitrogen-based fertilizers, with the shares of nitrogen, phosphorus, and potassium-based chemical fertilizers evaluated 82, 11.22, and 7 percent, respectively (Table 5). Also, organic fertilizers were not used in sunflower production fields. As observed in the sunflower production, chemical fertilizers led to 17.274 kg eq-CO_2 ha^{-1} greenhouse gas emissions, was the most closely associated with the nitrogen-based fertilizers application. Other chemical fertilizers also had a minor role in greenhouse gas emissions (Table 5 and 6). In the sunflower production, the share of fossil fuel in input energy consumption and greenhouse gas emissions was determined to be 51.87 and 47.73 percent, respectively. Therefore, the fossil fuel and the greenhouse gas emitted in the sunflower production were higher compared to other inputs, including nitrogen chemical fertilizers (Tables 5 and 6).

In New Zealand, Safa and Samarasinghe (2012) estimated that the greenhouse gas emissions from the chemical fertilizers consumption in wheat production amounted to 52 percent, equivalent to 539 kg eq-CO_2 ha^{-1}, with 48 percent attributed to nitrogen-based fertilizers. Omidmehr (2018) calculated the energy consumed for nitrogen fertilizer in sunflower production as 4960 Mj ha^{-1}, which accounted for 47 percent of the total energy consumption. Jankowski et al (2015) assessed the share of energy consumption from chemical fertilizers was 80 percent of input energy in canola production. The intensity of nutrient input (N mainly) and intensity of all the inputs during the vegetation period play a role in the overall environmental impact (Bernas et al., 2023).

Various methods have been proposed to reduce energy consumption and greenhouse gas emissions originating from chemical fertilizers, particularly nitrogen-based fertilizers in agricultural production such as the proper implementation of crop rotation, attention to the production methods of chemical fertilizers that have higher fuel and energy efficiency, improving the application methods of chemical fertilizers—especially nitrogen fertilizers—such as multi-stage application and timing that aligns with the crop growth, and producing chemical fertilizers that have higher absorption efficiency and are non-leachable. Additionally, the use of nitrification inhibitors and urease inhibitors, better irrigation management conducted at appropriate times alongside the application of chemical fertilizers, soil sampling before planting to accurately determine the nutrient requirement of plants, and the selection and breeding of plants with lower nutrient requirements (Safa and Samarasinghe, 2012; Pimental and Pimental, 2008; Nemecek et al., 2008; Ahmadi and Aghajani, 2012).

According to Table 5, the energy required to control weeds, insects, and fungi with chemical pesticides was 164.31, 167.59 and 24.51 Mj ha^{-1} respectively. In total, 356.60 Mj ha^{-1} energy was consumed to control pests, diseases, and weeds during wheat production. In the wheat-producing fields that consumed the most energy with chemical pesticides, several fungicides were often used.

In the production of canola, 233.43 MJ ha^{-1} energy were consumed due to the use of chemical pesticides, with the share of insecticides being zero percent. Additionally, the greenhouse gas emissions from each hectare of canola were reported 37.61 kg eq-CO_2 ha^{-1}. In sunflower production, where only herbicides and insecticides were used, 456.65 Mj ha^{-1} energy were consumed, and greenhouse gas emissions amounted to 73.57 kg eq-CO_2 ha^{-1}. Therefore, the energy consumption and greenhouse gas emissions originating from chemical pesticides in sunflower production were estimated the highest, while in canola were the lowest (Table 6). Omidmehr (2018) also reported the amount in the Miyai County for sunflower production as 199 MJ ha^{-1}. Among the methods, the application of natural methods for controlling pests and plant diseases can be noted to reduce the use of chemical pesticides. These methods include increasing the resistance genes of crops to pests, diseases, and weeds, strengthening their natural enemies, properly implementing crop rotation, practicing conservation tillage, and producing forage plants and planting trees in fields (Pimental and Pimental, 2008; Safa et al., 2011).

Fossil fuel consumption was 140.46, 100.00, and 158.00 l ha^{-1} in wheat, canola, and sunflower production, respectively (Table 4). In various studies, fuel consumption in wheat production was evaluated 92, 126, 93, 125, and 65 l ha^{-1} (Soltani et al., 2013; Taghavifar and Mardani, 2015; Wang et al., 2019; Safa et al., 2011; Safa and Samarasinghe, 2012). Safa and Samarasinghe (2012) reported the greenhouse gas emissions from fuel in wheat production as 203 kg eq-CO_2 ha^{-1}, while Mohammadi et al. (2014) reported 2.455 kg eq-CO_2 ha^{-1}. In wheat, canola, and sunflower productions 5367, 3804, and 6004 MJ ha^{-1} energy from fossil fuel were consumed, respectively (Table 5). Consequently, 33.73%, 32.85%, and 43.70% of greenhouse gas emissions were attributed to fossil fuel consumption (Table 5, 6). According to the results, the share of machinery uses in wheat, canola, and sunflower productions were estimated 7.06%, 7.46%, and 9.69% of the total input energy, respectively (Table 5). Also, 17.90, 18.20, and 32.08 labor hours were required in wheat, canola, and sunflower production, respectively (Table 4), and the share of energy consumption was 44.37%, 210.3%, and 351% of the total input energy, respectively (Table 5).

Therefore, based on the findings presented, the use of appropriate amounts of fossil fuels and chemical fertilizers, especially nitrogen-based fertilizers to reduce energy consumption and greenhouse gas emissions in wheat production, seems essential because 71 percent of energy consumption and 66 percent of greenhouse gas emissions were attributed to the use of nitrogen fertilizers and fossil fuels. A study suggested reducing the consumption of nitrogen fertilizers and fossil fuels for cleaner wheat production in terms of energy consumption and greenhouse gas emissions in Golestan Province (Soltani et al., 2013). In canola production, optimal use of chemical fertilizers and fossil fuels can significantly save energy consumption and prevent the excessive greenhouse gas emissions. Additionally, in sunflower production, 30.00 percent and

52.04 percent of energy consumption and greenhouse gas emissions, respectively, were due to the use of chemical fertilizers and fossil fuels. By optimizing the use of chemical fertilizers, especially nitrogen fertilizers, and fossil fuels, particularly in land preparation and harvesting, energy consumption and greenhouse gas emissions can be significantly reduced.

In evaluation under Pannonian climate conditions reported that the energy efficiency indicator NEO, which shows the area-based energy gain, was estimated highest with 160.2 kg N ha^{-1} , which is from the point of soil N accumulation and potential N emission (N_2O into the atmosphere and NO_3-N leaching into the aquifer) not sustainable for this pedo-climatic region. From the ecological point of view, zero N fertilization showed the best indicators energy use efficiency, energy input, and energy productivity (Moitzi et al., 2024).

Table 4. Amounts of input consumption in wheat, canola and sunflower production in Minodasht.

Inputs	Unit (per hectare)	Wheat	Canola	Sunflower
N	kg	92	69	46
P_2O_5	kg	46	46	34.5
K_2O	kg	24	48	36
Herbicides	kg	0.58	0.63	0.78
Fungicides	kg	0.25	0.52	-
Insecticides	kg	0.71	-	0.70
Seed	kg	200	4	8
Machinery	h	26.8	19.05	26.5
Fossil fuel	l	140.46	100	158
Human labor	h	17.9	15.2	32.08
Crop yield	kg	3500	2000	1500

Table 5. Amounts of energy consumption (MJ ha^{-1}) in wheat, canola and sunflower production in Minodasht.

Energy consumption	Wheat	Canola	Sunflower
N	5575	4181	2788
P_2O_5	510.6	511	383
K_2O	161	322	241
Total energy of fertilize	6246.6	5014	3411.75
Herbicides	164.31	181.96	255.43
Fungicides	24.51	51.48	-
Insecticides	167.59	-	201.22
Pesticides	356.60	233.43	456.65
Seed	3140	100	228
Machinery	1152	755.31	1122
Fossil fuel	5367	3804	6004
Human labor	35.08	29.79	351
Input energy	16307	10115	11573
Output energy	79050	50000	42750

Table 6. Amounts of greenhouse gas emissions (kg eq-CO2 ha^{-1}) in wheat, canola and sunflower production in Minodasht.

Inputs	Wheat	Canola	Sunflower
N	446.32	329.85	223.32
P_2O_5	41.9	41.9	31.41
K_2O	13.2	26.4	19.76
Total energy of fertilize	501.38	398.15	274.17
Herbicides	26.42	29.31	41.51
Fungicides	3.95	8.30	-
Insecticides	26.99	-	32.42
Pesticides	57.36	37.61	73.57
Machinery	261.62	171.53	254.81
Fossil fuel	418.62	296.72	468.32
Total Greenhouse gasses emission	1238.98	904.01	1070.87

3.5. Energy indices

The energy consumed in wheat production was recorded as 16307 MJ ha^{-1}, with direct and indirect energy shares evaluated 68% and 32%, respectively (Table 7). In the present study, the use of nitrogen-based fertilizers and fossil fuels accounted for 70% of the total energy consumption in wheat production; therefore, reducing energy consumption in these two parameters would significantly decrease overall energy use. In Golestan Province, the total input energy consumed in wheat production was assessed 15411 MJ ha^{-1}, with direct and indirect energy shares reported 65% and 35%, respectively. In a study conducted on wheat production in northern Khuzestan Province, the total energy consumed was reported as 16500 MJ ha^{-1}, with chemical fertilizers, fossil fuels, and seeds accounting for 60%, 25%, and 15% of energy consumption, respectively. It is noteworthy that in the aforementioned study, the share of energy from nitrogen-based fertilizers constituted 95% of the total energy consumed from fertilizer application (Kiani and Houshyar, 2012). In canola production, 10115 MJ ha^{-1} energy were utilized, with direct and indirect energy shares reported at 60% and 40%, respectively (Table 7). Additionally, the results showed that the largest portions of direct and indirect energy were due to the consumption of

fossil fuels and nitrogen-based fertilizers, respectively (Table 7).

Therefore, the entry of excess energy was significantly prevented by optimizing the use of fossil fuels. The findings indicated that the total energy input consumed for the sunflower production was evaluated at 11573 MJ ha^{-1}, with direct and indirect energy contributions accounting for 55% and 45%, respectively. Additionally, based on the results, the consumption of fossil fuels and nitrogen-based fertilizers had the highest shares of direct and indirect energy, respectively (Table 7).

The energy output was estimated 79050 MJ ha^{-1}, in wheat production. Rezvantalab et al. (2015) reported an output energy was 50200 MJ ha^{-1} in wheat production in Golestan Province. The findings showed that the output energy for canola and sunflower production were 50000 and 42,750 MJ ha^{-1}, respectively. The energy output to input for wheat, canola, and sunflower production were evaluated 4.84, 4.94, and 3.69, respectively (Table 7). It can be said that the lower seed yield in sunflower compared to the two crops of wheat and canola, along with the higher consumption of fossil fuels in sunflower production, has led to a decrease in energy output and an increase in energy input, ultimately resulting in a reduced ratio of energy output to input in sunflower production.

In a study conducted in Iran, the energy efficiency in the production of irrigated and rain-fed wheat was estimated 1.32 and 1.20, respectively, from 1999 to 2006 (Beheshti Tabar et al., 2010). They also reported energy efficiency for some crops in Iran for irrigated products such as wheat (1.32), barley (1.22), potatoes (0.85), corn (1.81), onions (0.86), sugar beets (1.77), lentils (0.70), chickpeas (0.73), watermelons (0.93), soybeans (1.78), cucumbers (0.38), tomatoes (0.47), and cotton (0.49).

According to the results presented in Table 7, the net energy in wheat production compared to canola and sunflower productions was 2.63 and 4.9, respectively. This indicated that a higher total output energy led to an increase in the net energy received compared to wheat and canola. Zenter et al (2004) also reported the net energy received for wheat cultivation between 32 to 40 MJ ha^{-1}, specifically for the seed production. Higher energy output and lower energy input in crop production systems increased net energy gain (Bhunia et al., 2021). In wheat, canola, and sunflower production 0.21, 0.19, and 0.13 kilograms were produced per each mega joule of energy consumed per hectare, respectively (Table 7).

The increased use of nitrogen-based fertilizers and fossil fuels will be a significant factor in reducing the productivity. Since specific energy has an inverse relationship with energy efficiency, it can be said that by increasing yield and reducing energy consumption in the use of chemical fertilizers and fossil fuels for agricultural operations, energy consumption per kilogram of product can be reduced. Soltani et al. (2013) reported an average energy efficiency as 0.27 in six scenarios evaluated for wheat production in Gorgan. The results showed that higher yields and lower energy inputs led to increased energy efficiency and reduced specific energy. Additionally, Rezvantalab et al. (2015) found that the using more efficient machinery can reduce the duration of machinery use and ultimately fuel consumption, which can increase energy efficiency and the energy output/input ratio per hectare, thereby reducing energy consumption per kilogram of grain.

They also stated that using cultivars with higher yield potential and better agricultural management in the wheat and soybean productions, which leads to increased yields, can also enhance energy efficiency and the energy output/input ratio.

3.6. GWP indices

As the results, the total greenhouse gas emissions in wheat, canola, and sunflower production were 1238, 904, and 1070 kg eq-CO_2 ha^{-1}, respectively (Table 8). GWP per kilogram of product decreased by increasing the crop yield. Therefore, higher grain yields in wheat production resulted the lower greenhouse gas emissions per kilogram of product compared to canola and sunflower production (Table 8). The calculated GWP per one mega joule of energy input used in wheat production was higher than the other two crops due to the higher energy consumption for producing the wheat compared to canola and sunflower (Table 8). Additionally, the GWP per unit of energy output was also assessed to be greater, because higher energy output in wheat production compared to canola and sunflower production (Table 8). In Golestan Province, 160 g eq-CO_2 were emitted into the atmosphere in one kilogram of wheat produced. Furthermore, for each mega joule of energy consumed directly or indirectly in wheat production, 80 g eq-CO_2 equivalent were released, resulting in 14 g MJ^{-1} of energy output (Rezvantalab et al., 2015). Ultimately, it can be said that paying attention to the optimal use of nitrogen fertilizers and fossil fuels can play a significant role in reducing greenhouse gases emissions. As previously mentioned, using high-horsepower tractors and equipment with greater working width and penetration depth can lead to energy savings and consequently reduce greenhouse gas emissions.

Table 7. Energy indices in wheat, canola and sunflower production in Minoodasht.

Energy indices	Wheat	Canola	Sunflower
Direct energy	5411	4014	6355
Indirect energy	10869	6101	5218
Total input energy	16307	10115	11573
Total output energy	79050	50000	42750
Output energy/input energy	4.84	4.94	3.69
Net energy	62743	39885	31177
Energy productivity	0.21	0.19	0.13
Specific energy	4.76	5.26	7.69

Table 8. Energy indices in wheat, canola and sunflower production in Minoodasht.

GWP indices	Wheat	Canola	Sunflower
GWP per hectare	1238	904	1070
GWP per crop yield	0.35	0.45	0.71
GWP per input energy	0.076	0.089	0.092
GWP per output energy	0.016	0.018	0.025

4. Conclusion

The results showed that wheat production requires less energy compared to canola and sunflower, and consequently, fewer greenhouse gas will be emitted into the atmosphere. The land preparation operations for wheat and canola cultivation, as well as the harvesting of sunflower, had the highest energy requirements and greenhouse gas emissions. For each hectare of wheat, canola, and sunflower produced, 76, 89, and 92 g greenhouse gases were emitted per mega joule of energy consumed, respectively, while the estimated emissions for energy output were 16, 18, and 25 g, respectively. Finally, total energy input in wheat production was more than in canola and sunflower productions. But energy use efficiency in wheat and canola productions were more than in sunflower production. Ultimately, it can be stated that the use of chemical fertilizers, particularly nitrogen-based fertilizers, as well as fossil fuels, accounted for the majority of energy consumption and greenhouse gases emissions. If the consumption of these inputs is optimized, there will be a significant reduction in energy consumption and greenhouse gases emissions for wheat, canola, and sunflower production.

References

Ahmadi, M., & Aghajani, M. (2011). Analysis of energy consumption in cotton cultivation in Golestan Province in order to provide a solution to increase resource efficiency. *Journal of Agro-ecology. 11*(4), 151-158. (In Persian with English abstract). https://doi.org/10.22067/jag.v10i3.62349

Akcaoz, H., Ozcatalbas, O., & Kizilay, H. (2009). Analysis of energy use for pomegranate production in Turkey. *Journal of Food, Agriculture and Environment, 7*, 475-480.

Azizpanah, A., Pourmusi, M., Taki, M. (2023). Eco-environmental and sustainability evaluation of cucumber and sunflower productions in Iran**.** *Total Environment Research Themes, 6*, 100037. https://doi.org/10.1016/j.totert.2023.100037

Beheshti Tabar, I., Keyhani, A., & Rafiee, Sh. (2010). Energy balance in Iran's agronomy (1990–2006). *Renewable and Sustainable Energy Reviews, 14*(3), 849–855. https://doi.org/10.1016/j.rser.2009.10.024

Bergtold, J. S., Shanoyan, A., Fewell, J. E., & Williams, J. R. (2017). Annual bioenergy crops for biofuels production: Farmers' contractual preferences for producing sweet sorghum. *Energy, 119*, 724–731. https://doi.org/10.1016/j.energy.2016.11.032

Bernas, J., Koppensteiner, L. J., Tichá, M., Kaul, H. P., Klimek-Kopyra, A., Euteneuer, P., ... & Neugschwandtner, R. W. (2023). Optimal environmental design of nitrogen application rate for facultative wheat using life cycle assessment. *European Journal of Agronomy, 146*, 126813. https://doi.org/10.1016/j.eja.2023.126813

Bhunia, S., Karmakar, S., Bhattacharjee, S., Roy, K., Kanthal, S., Pramanick, M., ... & Mandal, B. (2021). Optimization of energy consumption using data envelopment analysis (DEA) in rice-wheat-green gram cropping system under conservation tillage practices. *Energy, 236*, 121499. https://doi.org/10.1016/ j.energy.2021.121499

Brownea, N. A., Eckarda, R. J., Behrendt, R., & Kingwell, R. S. (2011). A comparative analysis of on-farm greenhouse gas emissions from agricultural enterprises in south eastern Australia. *Animal Feed Science and Technology*, 166-167, 641-652. https://doi.org/10.1016/j.anifeedsci.2011.04.045

Clements, D. R., Weise, S. F., Brown, R., Stonehouse, D. P., Hume, D. J., & Swanton, C. J. (1995). Energy analysis of tillage and herbicide inputs in alternative weed management systems. Agriculture, Ecosystem and Environment. *52*, 119–128. https://doi.org/10.1016/01678809(94)00546-q

FAO. (2023). http://www.fao.org/faostat/en/#data/qc

Fei, R., & Lin, B. (2017). Estimates of energy demand and energy saving potential in china's 359 agricultural sector. *Energy*, 135, 865-75. https://doi.org/10.1016/j.energy.2017.06.173

Ghorbani, R., Mondani, F., Amirmoradi, S., Feizi, H., Khorramdel, S., & Teimouri, M. (2011). A case study of energy use and economic analysis of irrigated and dryland wheat production systems. *Applied Energy, 88*, 283-288. https://doi.org/10.1016/j.apenergy.2010.04.028

Gong, X., Qiu, R., Zhang, B., Wang, S., Ge, J., Gao, S., & Yang, Z. (2021). Energy budget for tomato plants grown in a greenhouse in northern China. *Agricultural Water Management*, 255, 107039. https://doi.org/10.1016/j.agwat.2021.107039

International Energy Agency (IEA). Key world energy statistics (2009). Available online at: http://iea.org/stats/electricitydata.asp.

Imran, M., Özçatalbas, O., & Khalid Bashir, M. (2020). Estimation of energy efficiency and greenhouse gas emission of cotton crop in South Punjab, Pakistan. *Journal of the Saudi Society of Agricultural Sciences, 19*, 216-224. https://doi.org/10.1016/ j.jssas.2018.09.007

Jankowski, K. J., Budzyński, W. S., & Kijewski, Ł. (2015). An analysis of energy efficiency in the production of oilseed crops of the family *Brassicaceae* in Poland. *Energy*, *81*, 674-681. https://doi.org/10.1016/j.energy.2015.01.012

Kaltsas, A. M., Mamolos, A, P., Tsatsasarelis, C. A., Nanos, G. D., & Kalburtji, K. L. (2007). Energy budget

in organic and conventional olive groves. Agriculture, *Ecosystems & Environment, 22*, 243-251. https://doi.org/10.1016/j.agee.2007.01.017

Kiani, S., & Houshyar, E. (2012). Energy Consumption of Rainfed Wheat Production in Conventional and Conservation Tillage Systems. *International Journal of Agriculture and Crop Sciences*, *4*(5), 213-219.

Kizilaslan, H. (2008). Input-output energy analysis of cherries production in Tokat province of Turkey. *Applied Energy*, *86*, 1354-8. https://doi.org/10.1016/j.apenergy.2008.07.009

Lal, R. (2004). Carbon emission from operations. *Environment International*, *30*, 981-990. https://doi.org/10.1016/j.envint.2004.03.005

Mohammadi, A., Rafiee, S., Jafari, A., Keyhani, A., Mousavi-Avval, S. H., & Nonhebel, S. (2014). Energy use efficiency and greenhouse gas emissions of farming systems in north Iran. *Renewable Sustainable Energy Review*, *30*, 724-733. https://doi.org/10.1016/j.rser.2013.11.012

Moitzi, G., Koppensteiner, L. J., Klimek-Kopyra, A., Bernas, J., Kaul, H. P., Wagentristl, H., ... & Neugschwandtner, R. W. (2024). Effects of sowing date and nitrogen applications on the energy efficiency of facultative wheat (*Triticum aestivum* L.) in a Pannonian environment. *Heliyon*, *10*(19). https://doi.org/10.1016/j.heliyon.2024.e37923

Mousavi-Avval, S. H., Rafiee, S., & Jafari, A. (2011). Sensitivity analysis of agrochemical energy inputs and their environmental impacts in rapeseed production. In *Jordan International Energy Conference*.

Nemecek, T., Richthofen, J. S., Dubois, G., Casta, P., Charles, R., & Pahl, H. (2008). Environmental impacts of introducing grain legumes into European crop. *European Journal of Agronomy*, *28*, 380-393. https://doi.org/10.1016/j.eja.2007.11.004

Omidmehr, Z. **(**2018**).** Comparison of energy efficiency and global warming potential in rainfed sunflower production systems. *Journal of Agro-ecology*, *11*(2), 739-755. (In Persian with English abstract). https://doi.org/10.22067/jag.v11i2.49739

Pimental, D., & Pimental, M. H. (2008). Food, energy and society. *Taylor & Francis*. 266 Pp.

Pishgar-Komleh, S. H., Ghahderijani, M., & Sefeedpari, P. (2012). Energy consumption and CO_2 emissions analysis of potato production based on different farm size levels in Iran. *Journal of Cleaner Production*, *33*, 183-191. https://doi.org/10.1016/j.jclepro.2012.04.008

Pourazri, F., Ehsanzadeh, P., & Jahanbin, S. (1390). The reaction of coated tetraploid wheats to nitrogen deficiency stress compared to macaroni wheat. *Journal of Crop Plant Sciences of Iran*, *42*, 294-285. (In Persian with English abstract). https://doi.org/20.1001.1.20084811.1390.42.2.8.6

Rathke, G. W., Wienhold, B. J., Wilhelm, W. W., & Diepenbrock, W. (2007). Tillage and rotation effect on corn–soybean energy balances in eastern Nebraska. *Soil and Tillage Research*, *97*, 60–70. https://doi.org/10.1016/j.still.2007.08.008

Rezvantalab, N., Soltani, A., Zeinali, E., & Daylam Salehi, R. (2015). Evaluation of fuel and energy use and greenhouse gases emissions in wheat and soybean production in Golestan province. PhD thesis, Gorgan University of Agricultural Sciences and Natural Resources. Gorgan, Iran. (In Persian with English abstract)

Safa, M., & Samarasinghe, S. (2012). CO_2 emissions from farm inputs "Case study of wheat production in Canterbury, New Zealand". *Environmental pollution*, *171*, 126-132. https://doi.org/10.1016/j.envpol.2012.07.032

Safa, M., Samarasinghe, S., & Mohsen, M. (2011). A field study of energy consumption in wheat production in Canterbury, New Zealand. *Energy Conversion Management*, *52*, 2526–2532. https://doi.org/10.1016/j.enconman.2011.01.004

Sheikh D, & Houshyar M. J. (2009). Energy consumption of canola and sunflower production in Iran. *American-Eurasian Journal of Agricultural & Environmental Sciences*, *6*(4),381–384**.**

Singh, H., Singh, A. K., Kushwaha, H. L., & Singh, A. (2007). Energy consumption pattern of wheat production in India. *Energy*, *32*(10), 1848-1854. https://doi.org/10.1016/j.energy.2007.03.001

Soltani, A., Rajabi, M. H., Zeinali, E. & Soltani, E. (2013). Energy inputs and greenhouse gases emissions in wheat production in Gorgan, Iran. *Energy*, *50*, 54 -61. https://doi.org/10.1016/j.energy.2012.12.022

Strapatsa, A. V., Nanos, G. D. & Tsatsarelis, C. A. (2006). Energy flow for integrated apple production in Greece. *Agriculture Ecosystem and Environment*, *116*, 176-180. https://doi.org/10.1016/j.agee.2006.02.003

Taghavifar, H., & Mardani, A. (2015). Energy consumption analysis of wheat production in West Azerbaijan utilizing life cycle assessment (LCA). Renewable *Energy*, *74*, 208-213. https://doi.org/10.1016/j.renene.2014.08.026

Tipi, T., Cetin, B., & Vardar, A. (2009). An analysis of energy use and input costs for wheat production in Turkey. *Agriculture, Ecosystems & Environment*, *7*, 352-356. http://www.isfae.org/scientificjournal.php

Turhan, S., Cananozbag, B., & Rehber, E. (2008). A comparison of energy uses in organic and conventional tomato production. *Journal of Food, Agriculture and Environment*, *6*, 318-321.

Tzilivakis, J., Warner, D. J., Lewis, M. K. A., & Jaggard, K. (2005). An assessment of the energy inputs and greenhouse gas emissions in sugar beet (*Beta vulgaris* L.) production in the UK. *Agricultural Systems*, *85*, 101–119. https://doi.org/10.1016/j.agsy.2004.07.015

Unakotan, G., & Aydın, B. (2018). A comparison of energy use efficiency and economic analysis of wheat and sunflower production in Turkey: A case study in Thrace Region. *Energy*, *149*, 279-285. https://doi.org/10.1016/j.energy.2018.02.033

Wang, C., Li, X., Gong, T., & Zhang, H. (2014). Life cycle assessment of wheat-maize rotation system emphasizing high crop yield and high resource use efficiency in Quzhou County. *Journal of Cleaner*

Production, *68*, 56-63. https://doi.org/10.1016/j.jclepro.2014.01.018

Wang, D., Feng, H., Li, Y., Zhang, T., Dyck, M., & Wu, F. (2019). Energy input-output, water use efficiency and economics of winter wheat under gravel mulching in Northwest China. *Agricultural Water Management*, *222*, 354–366. https://doi.org/10.1016/j.agwat.2019.06.009

Yuan, S., Peng, S., Wang, D., & Man, J. (2018). Evaluation of the energy budget and energy use efficiency in wheat production under various crop management practices in China. *Energy*, *160*, 184-191 https://doi.org/10.1016/j.energy.2018.07.006

Zentner, R. P., Lafond, G. P., Derksen, D. A., Nagy, C. N., Wall, D. D., & May, W. E. (2004). Effects of tillage method and crop rotation on non-renewable energy use efficiency for a thin Black Chernozem in the Canadian Prairies. *Soil and Tillage Research*, *77*, 125–136. https://doi.org/10.1016/j.still.2003.11.002

Agriculture, Environment & Society

Journal homepage: www.aes.uoz.ac.ir

Unveiling the most sustainable date production systems in Mirjaveh, Iran: an emergy-based approach

Soudabeh Rafsanjani [a], Mohammad Reza Asgharipour [*b], Tohid Bagherpour [b], Mohammad Ali Javaheri [c]

[a] Ph.D Student of Agroechology, Faculty of Agriculture, University of Zabol, Zabol, Iran
[b] Department of Agronomy, Faculty of Agriculture, University of Zabol, Zabol, Iran
[c] Seed and Plant Improvement Research Department, Kerman Agricultural and Natural Resources Research and Education Center, Agricultural Research Education and Extension Organization (AREEO), Kerman, Iran

ARTICLE INFO

Article history:
Received: 9 May 2024
Accepted: 21 February 2025
Available online: 10 June 2025

Keywords:
Emergy value of money
Environmental inputs
Exchange
Export
Sustainable agriculture

ABSTRACT

This study aimed to identify the most sustainable production system for Mazafati and Rabbi date palm cultivars in Mirjaveh County, Iran, during 2022-2023. Data pertaining to cultivated area, date palm production and yield, export volume, as well as the environmental and economic inputs necessary for production, were gathered through documentary and survey methods. These data were then analysed for the two study systems. The input elements were subsequently transformed into emergy equivalents, sej. The data collected indicates that the total emergy needed to sustain the Mazafati and Rabbi date palm production systems was 3.33E+16 and 2.92E+16 sej/ha/yr, respectively. The majority of inputs for both the Mazafati and Rabbi date palm production systems came from purchased sources, making up 92.69% and 71.68% of the total inputs, respectively. The findings suggest that both systems impose substantial environmental burdens as a result of their lack of utilisation of renewable resources and heavy dependence on non-renewable inputs. Hence, it is imperative and inevitable to decrease the utilisation of these resources in both date palm systems. Based on the emegy exchane ratio and emergy to money ratio indices, the Mazafati date palm system demonstrated higher values, indicating greater economic sustainability compared to the Rabbi system. Conversely, the emergy yield ratio was higher for the Rabbi date palm, suggesting that this system is more sustainable than Mazafati date palm production in terms of product yield. Overall, the Mazafati date palm system demonstrated a slight edge in terms of economic, commercial, and ecological sustainability.

Highlights

- Mazafati dates use 3.33E+16 sej/ha/yr, Rabbi 2.92E+16 sej/ha/yr in Mirjaveh, Iran.
- Purchased inputs dominate: 92.69% for Mazafati, 71.68% for Rabbi dates.
- Mazafati excels in economic sustainability (EER 4.460) over Rabbi (3.391).
- Rabbi shows higher yield sustainability (EYR 1.455) than Mazafati (1.430).
- Both systems strain environment, need less non-renewable input reliance.

1. Introduction

Over the past few decades, scientists in the field of agriculture have become more focused on clean production and environmental protection as the foundation for sustainable development. This shift in attention is a result of the growing awareness of the environment and the demand for sustainable agricultural practices (Gheicari et al., 2021; Amiri et al., 2022). Given the circumstances, it is crucial to meticulously plan and oversee agricultural ecosystems, as sophisticated systems can guarantee both sustainable and desirable production (Fallahinejad and Armin, 2022). Due to the abstract nature of sustainability, it is not feasible to directly measure it. Therefore, simpler criteria are needed to assess agricultural and agroecosystem

* Corresponding author.
E-mail address: m_asgharipour@uoz.ac.ir
https://doi.org/10.22034/jelsa.2025.456534.1064

sustainability (Shahhoseini and Kazemi, 2022).

The impact of energy consumption on various aspects such as food security, agricultural sustainability, community health, and ecosystem functions and services is widely acknowledged (Kazemi et al., 2018; Kohkan et al., 2017). Indicators based on changes in capital value have been developed to assess and compare the sustainability of different agricultural systems. Indicators used to evaluate the sustainability of agricultural systems should fulfil specific criteria, as outlined by Brown and Ulgiati in 1997. Initially, it is imperative that they exhibit consistency and conformity with one another, while also adhering to predetermined objectives for the advancement of sustainable agricultural practices. Consistency and absence of contradictions are essential for ensuring the reliability of the indicators. Furthermore, it is crucial that the indicators are precise, effectively capturing the intricacies of sustainability in agricultural systems with an adequate level of specificity. In order to be practical, data collection for these indicators should be quantifiable, indicating that it can be easily and economically carried out. Ultimately, in order to achieve widespread acceptance, the indicators must possess user-friendly characteristics and be specifically crafted to facilitate unambiguous comprehension by farmers, policymakers, and all pertinent stakeholders. The foundation of all these characteristics is the necessity for data of superior quality. For the sustainability assessment to be valid, the calculations of indicators must rely on valuable and reliable input data.

An assessment of these indicators in various agricultural ecosystems allows for the identification and quantification of their environmental, economic, and sustainability effects. The outcomes of these evaluations can provide valuable insights for farmers and local decision-makers in determining the most effective strategies for optimising resource utilisation and promoting sustainable agriculture (Jafari et al., 2018). Emergy analysis has become a useful tool for developing environmental policies and evaluating resource quality in complex environmental and economic systems over the last thirty years (Brown and Ulgiati, 1997).

The numerous emergy measurement indicators offer a more comprehensive understanding of the extent of resource renewability, the proportion of renewable and non-renewable resources, and the impact of environmental and market inputs on the overall emergy of a system (Odum, 2000). Emergy indicators can be utilised to precisely evaluate the capacity, renewability, environmental stress, and overall sustainability of a system, considering both environmental and economic aspects. Emergy analysis is a useful tool for measuring the sustainability of various agricultural systems within a shared framework. It helps identify the most environmentally sustainable system (Asgharipour et al., 2020).

Several studies have employed emergy analysis to assess the sustainability of various agricultural systems. For instance, Asgharipour et al. (2021) evaluated the sustainability of four greenhouse vegetable production systems (cucumber, tomato, bell pepper, and eggplant) in Iran. They found that the cucumber production system was the most sustainable, primarily due to its efficient use of free environmental energy and lower reliance on non-renewable inputs. Similarly, Amiri et al. (2021) investigated the sustainability of different beef cattle production systems in the Sistan region of Iran. Their study highlighted the importance of balancing economic and environmental factors in agricultural production. They concluded that a semi-intensive production system for Sistani cattle could provide a sustainable and economically viable option for livestock farmers in the region.

Developing countries prioritise achieving rapid economic growth, and exports are crucial in driving this growth and promoting economic prosperity (Frankel and Romer, 1999). Given the circumstances, it is crucial to implement export development strategies, specifically focusing on boosting non-oil exports. Agricultural exports make a substantial contribution to increasing farmers' incomes, alleviating poverty, and improving overall livelihood and economic well-being at the national level. Iran, being one of the leading exporters of dates worldwide, is encountering a notable obstacle in the form of a decreasing share of exports to the European Union market, which happens to be its most crucial export destination, despite its efforts to increase its presence in the global market.

The fluctuation in prices of agricultural products has consistently been a significant concern for agricultural economists and policymakers. According to Rafiei and MirBagheri (2017), a broader range of these fluctuations leads to more severe negative outcomes, resulting in significant losses primarily for farmers and ultimately for society as a whole. While certain economists highlight the notable effectiveness of exports, there have been concerns raised regarding the potential rise in energy consumption and subsequent environmental pollution linked to the expansion of exports. Hence, it is imperative to conduct a comprehensive empirical analysis of the correlation between exports and energy in order to develop suitable trade and environmental policies (Sadorsky, 2012).

Over the next 50 years, agricultural production in developing countries is expected to experience significant growth. This growth will result in a two- to threefold increase in the consumption of nitrogen and phosphorus, a doubling of water demand, and a tripling of pesticide use, as stated by Tilman et al. in 2001.

Iran confronts a multitude of environmental challenges, such as water scarcity, droughts, population growth, and rising demand for food production. Developing a more profound comprehension of sustainability among planners and policymakers is essential in effectively tackling these challenges. Assessing the level of sustainability and making informed choices to improve it are crucial for the country's long-term development (Nazarian et al., 2020).

The date palm is a prominent horticultural commodity in Iran, consistently ranking between third and sixth place in terms of export value in recent years. This product has substantial potential to generate foreign exchange for the country (Pejman, 2001). Nevertheless, a considerable proportion of date palm production and its derivatives in

Iran rely on conventional techniques and encounter multiple deficiencies throughout the production process and palm cultivation operations, resulting in a detrimental effect on the ultimate product's quality. In order to fully maximise food production capacities, it is crucial to effectively oversee the entire production chain, spanning from the initial production stages to the final consumption. This requires establishing the essential circumstances to optimise the country's capacity for food production (Alipour and Mahdavi, 2014).

Due to its favourable climatic conditions, Mirjaveh County in Sistan and Baluchestan Province is regarded as one of Iran's most suitable regions for date production. This region cultivates a wide variety of dates, such as Mazafati, Rabbi, Zardān, Piyū, Sang Shekan, Āshey, Shāhān, Helilī, and Dezk. Out of these different types, Mazafati and Rabbi dates are particularly esteemed for their exceptional quality. The provinces of Sistan and Baluchestan, specifically the counties of Saravan and Mirjaveh, are acknowledged as the primary cultivators of Mazafati dates in Iran. Furthermore, this particular region is the exclusive cultivator of the distinct Rabbi variety within the nation. Mazafati dates are highly sought after in the domestic market due to their exceptional quality and flavour.

They hold a prominent position in the overall production of Mazafati dates in the country. Rabbi dates, known for their distinct attributes including a chocolatey consistency, partial dryness, long shelf life, ability to be washed, deep and vibrant colour, elongated form, and small seed, are in high demand in international markets. Traders predominantly purchase and export the majority of this product to foreign countries (Mollazehi, 2013).

This study utilised an emergy-based methodology to accomplish the following aims: (a) Determine the most environmentally friendly date palm production system between the Mazafati and Rabbi cultivars grown in Mirjaveh County, Iran during the period of 2022-2023. The assessment of sustainability will involve a comprehensive evaluation of both environmental and economic factors. (b) Assess the environmental consequences of both systems by examining their dependence on renewable resources versus non-renewable inputs. (c) Assess the economic feasibility of each system using emergy yield ratio (EER) and emergy material ratio (EMR). The study aims to provide valuable insights for policymakers and date palm producers by accomplishing these objectives. The provided data can be utilised to advance sustainable methodologies and enhance the efficient utilisation of resources in the Iranian date palm industry. This will ultimately contribute to ensuring food security and improving environmental well-being.

2. Materials and Methods

2.1 Study Area

The objective of this study was to monitor the production of date palms in Mirjaveh County, located in Sistan and Baluchestan Province, throughout the cropping year of 2021-2022. Mirjaveh County is situated in the eastern part of Sistan and Baluchestan Province and shares a border that spans more than 350 kilometres with Pakistan. The county shares borders with Pakistan to the northeast, east, and southeast. It also borders Zaranj County to the north and west, and Khash County to the south and southwest. The county spans across an expansive area of more than 6,000 square kilometres and is situated at an elevation of 858 metres above sea level.

Mirjaveh is classified as one of the most arid regions in the country, with an average annual precipitation of only 30 millimetres. The climate in the central region of the county is characterised by high temperatures, low humidity, and a desert-like environment. Nevertheless, as a result of the significant altitude variation of more than 2,200 metres between the central part and the Ladiz section, this particular area experiences a more temperate climate and greater precipitation. The heights in the Ladiz section are sufficiently covered with snow during winter.

2.2 Data Collection

Data on various facets of date palm production in the region were gathered to carry out this research. This encompassed data regarding the acreage dedicated to cultivating date palms, the total output and productivity of dates, and the rate of exporting date products. In addition, information regarding the environmental and economic resources needed for date production was collected. The data were gathered through a combination of documentary research, analysis of existing records, and survey methods, which involved directly obtaining information from pertinent sources.

To ensure the robustness of our findings, we collected data from a representative sample of date palm orchards in Mirjaveh County. The sample size was determined based on statistical considerations and practical constraints. We aimed to capture the diversity of production systems and environmental conditions within the region. Specifically, we sampled 87 Mazafati date palm orchards and [insert number] Rabbi date palm orchards.

Initially, the inputs provided to the agricultural systems were transformed into emergy equivalents. Agricultural ecosystems can be classified into two distinct categories: purchased inputs and free environmental inputs. The purchased inputs encompass commodities such as electricity, fuel, agricultural machinery, fertilisers, pesticides, and other industrial products. On the other hand, environmental resources that are not restricted or limited are referred to as free environmental inputs. These include sunlight, soil, organic matter, wind energy, chemical energy, irrigation water potential, and rain.

Both systems were assessed for capital allocation and post-harvest product performance. The fair selling price of date palm products was determined using the emergy exchange ratio indicator. This method involves converting the flows associated with the sale of date palm products and the corresponding monetary transactions into emergy units, and then calculating their ratio. This ratio denotes the emergy transfer that occurs during a transaction or purchase. Furthermore, to assess the pros and cons in relation to the cost incurred for dates, the emergy of the money obtained from date sales was also computed.

2.3 Emergy Analysis

Step 1: Defining the Scope and Drawing Energy Diagrams

To begin the process of emergy analysis, it is necessary to establish the specific time and spatial limits for both systems being studied. Additionally, energy diagrams should be created to classify the inputs of the systems being assessed into categories such as renewable or non-renewable, environmental or imported sources (Odum, 2000). Energy diagrams are crucial for managing the connections between important system components and productive processes. They illustrate the environmental foundations of the system and the relationships between them.

Figure 1 displays the cumulative emergy flow diagram for the Rabbi and Mazafati date palm production systems. Agricultural systems derive inputs from two primary sources: environmental inputs and purchased inputs. The diagrams depict the extent of the production system, with environmental inputs on the left, purchased inputs at the top, and the beneficial output of the production systems on the right.

Step 2: Classifying Inputs

When analysing production systems, inputs are categorised into four distinct categories according to Lu et al. (2010).

Renewable environmental resources (R) encompass natural elements such as sunlight, wind, rain, and river water.

Non-renewable environmental resources (N) refer to resources that are not capable of being replenished, such as those related to soil erosion and the processes involved in soil formation and ground water.

Purchased renewable resources (FR): encompassing seeds, and organic fertilisers procured externally to the system.

Purchased non-renewable resources (FN): such as fertilisers, pesticides, machinery, etc.

The machinery's emergy consumption was determined by considering the quantity of steel employed, the machines' ideal lifespan, and the annual working hours (Asgharipour et al., 2019). The emergy of the consumed saplings was calculated using the emergy coefficient per unit of currency, as described by Jafari et al. (2018). The raw data was calculated in joules, grammes, or rials after estimating the input (U) and output (Y) flows for each production system, following the emergy standards in Iran (Amiri et al., 2019; Asgharipour et al., 2020).

Various emergy indices are used for emergy analysis, which is aimed at conducting environmental and economic assessments (Lu et al., 2010).

This study utilised various indices to assess different aspects of the system. These indices included the transformity (Tr), specific emergy (Se), percentage of emergy renewability (%R), emergy yield ratio (EYR), emergy investment ratio (EIR), environmental load ratio (ELR) and its modified version (ELR*), environmental sustainability index (ESI) and its modified version (ESI*), emergy exchange ratio (EER), emergy index of producti safety (EIPS), and the emergy to money ratio (EMR). Asgharipour et al. (2020) provided the descriptions and formulas for the emergy indices used in this research.

This study aimed to conduct a detailed analysis of the production and services carried out in both the Rabbi and Mazafati date palm production systems. To achieve this, all input and output values were multiplied by their respective conversion factors. This enabled the conversion of various units into a standardised unit, simplifying the computation of emergy ratios and indices.

Emergy indices serve as efficient tools for assessing the pressure and harm imposed on different systems. Furthermore, these indices have the ability to offer a thorough depiction of the functional attributes of the production system in terms of utilisation and sustainability (Campbell et al., 2005).

Choosing suitable indices for ecosystem evaluation is crucial. The chosen indices in this study are considered the most dependable indicators for assessing ecosystems (Cheng et al., 2017).

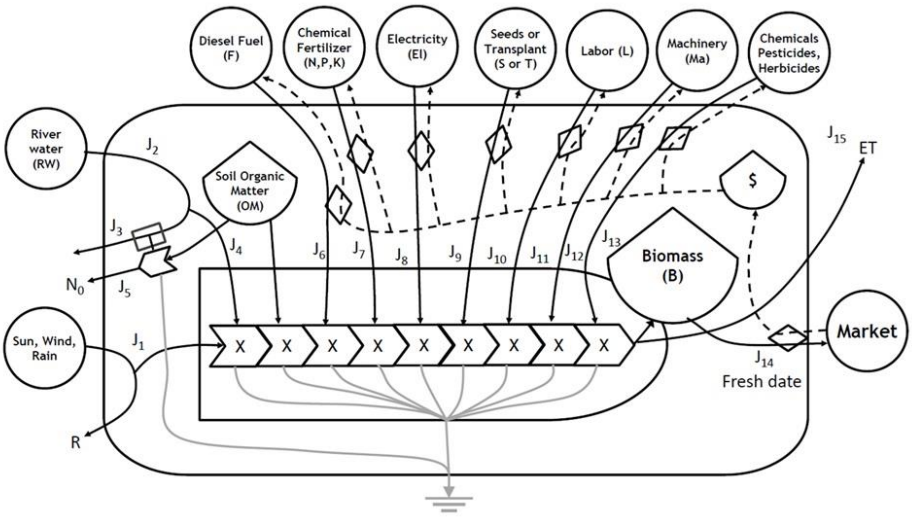

Figure 1. Emergy flow diagram of Mozafati and Rabi date production systems in Mirjaveh city

Table 1 displays the formulas and calculation methods of the emergy indices utilised for assessing the performance of research systems. By utilising these indices, it is possible to make a more precise comparison and analysis of the performance of the two production systems for Rabbi and Mazafati date palms.

Table 1. Specifications and formulas of the emergy-based indicators used to evaluate Mozafati and Rabbi date production systems in Mirjaveh city (Asgharipour et al., 2020)

Index	Formula	Specifications	Reference
Renewable inputs from free local resources	R	Renewable environmental flows	By definition
Non-renewable environmental inputs	N	Non-renewable environmental flows	By definition
Renewable purchased inputs	F_R	Renewable flows from purchased resources	By definition
Non-renewable purchased inputs	F_N	Non-renewable purchased flows	By definition
Transformity	Tr = U / AE	Amount of emergy required to produce an output unit in joules. AE is the energy content.	(Brown and Ulgiati, 2004)
Special Emargy	SE = U / PW	Amount of emergy required to produce an output unit in grams. AE is the energy content.	(Brown and (Ulgiati, 2004)
Renewable emergy ratio	%R = R+F_R / U×100	Percentage of the renewable energy used by the system	(Odum, 2000)
Emergy yield ratio	EYR = U / F_N+F_R	Ability of a process to use renewable and nonrenewable environmental resources with economic resources as a capital	(Odum, 2000)
Emergy investment ratio	EIR = F_R+F_N/R	EIR is the ratio of emergy resources purchased from outside to all free environmental emergy in the system.	(Brown and Ulgiati, 2004)
Modified Emergy Investment Ratio	= F_N+F_R /R EIR*	The adaptation rate of investment in product production is compared with environmental resources received for free.	(Amiri et al., 2019)
Environmental loading ratio	ELR = N+F_N / R+F_R	Environmental pressure produced by a process	(Lu et al., 2017)
Modified Environmental Loading Ratio	ELR* =F_N+N / R+F_R	An inverse measure of sustainability	(Lu et al., 2017)
Emergy Sustainability Index	ESI = EYR / ELR	The dependence of the system output on the environment, the greater the value, the stronger the sustainability of the system	(Lu et al., 2017)
Modified Emergy Sustainability Index	ELR* ESI* = EYR/	Alternate sustainability index that focuses on the use of renewable resources with minimal pressure on the environment.	(Lu et al., 2017)
Emergy Exchange Ratio	EER = U/YM	Economic output (A system yield) traded with money in the market (YM) on total emergy input rate (U).	(Odum, 1996)
Emergy Money Ratio	EMR = U/net profit	Emergy investment per dollar of net profit	By definition
Emergy index of product safety	EIPS=1 − [C/ (F_N + F_R)]	It assesses the effect of chemical fertilizer, pesticide and herbicide use on product safety	(Xi and Qin, 2009)

3. Results and Discussion

3.1 Input Emergy Structure

Table 2 displays the movement of natural resources and purchased inputs within the production systems of Rabbi and Mazafati dates. The inputs listed in this table have been computed using coefficients associated with solar energy over the course of the year. Additionally, the inputs have been categorised as either renewable or non-renewable, depending on their renewability percentages. Furthermore, the total energy of the systems has been converted to solar energy (sej).

The total emergy input for the production systems of Mazafati and Rabbi dates in Mirjaveh county were 3.33E+16 and 2.92E+16 sej/ha/yr respectively (Table 3). The Mazafati date production system had a higher total emergy consumption compared to the Rabbi date production system. This was primarily because the Mazafati system used more non-renewable inputs that were purchased.

As a result, the Mazafati date production system consumed a greater amount of emergy compared to the Rabbi date production system. The seedlings accounted for the highest proportion of emergy in the Mazafati date production system, contributing 19.47 percent or 6.49E+15 sej/ha/yr. Nitrogen fertiliser was the second highest contributor, accounting for 14.83 percent or 4.94E+15 sej/ha/yr.

The study by Fallahinejad et al. (2021) reported the total supportive emergy for wheat production system as 2.32E+16, for barley as 1.91E+16, for sugar beet as 4.95E+16 sej/ha/yr. The supportive emergy for the production systems of wheat, garlic, and onion was 2.45E+16, 3.12E+16, and 4.73E+16 sej/ha/yr, respectively. As a result, the garlic production systems had an emergy consumption that was approximately 90 percent greater than the wheat production systems and 50 percent greater than the onion production systems (Yasini et al., 2020). Amiri et al. (2021) focused on comparing the sustainability of various shallot production systems, including a natural habitat, a mechanized system, and a conservation system. In contrast, our study aimed to compare the sustainability of two specific date palm cultivars, Mazafati and Rabbi, under different production systems.

The production systems of Mazafati and Rabbi dates in Mirjaveh county have been classified into four categories based on the types of inputs they receive: renewable

environmental free inputs (R), non-renewable environmental free inputs (N), purchased inputs (FR & FN).

3.1.1 Renewable Environmental Inputs (R)

Renewable environmental resources encompass solar energy, wind energy, the chemical energy of precipitation, and freshwater from rivers. In the production systems for Mazafati dates, the inputs accounted for 0.21 percent of the total input energies, while for Rabbi dates, they accounted for 0.24 percent (Table 3). The proportion of these inputs was greater in the Rabbi date production system in comparison to the Mazafati date production system. The study conducted by Jafari et al. (2018) determined that in Nehbandan county, the renewable environmental inputs for date and pistachio production systems were estimated to be 13.8 percent and 10.4 percent, respectively. The study conducted by Moonilall et al. (2020) found no significant variation in the quantity of renewable environmental resource inputs across different maize cultivation production systems.

Table 2. Natural and economic flows of Mozafati and Rabbi production systems in Mirjaveh city

	Unit	Mazafati	Rabbi
Renewable environmental inputs			
Solar energy	J	3.6E+13	3.6E+13
Wind, kinetic energy	J	2.25E+09	2.25E+09
Rain, chemical	J	1.51E+09	1.51E+09
River water	J	1.15E+11	9.99E+10
Non-renewable environmental inputs			
Groundwater	J	2.89E+11	2.51E+11
SOM reduction	J	2.06E+10	2.06E+10
Soil erosion	g	1.82E+06	1.82E+06
Purchased inputs			
Human labor	J	4.88E+08	4.29E+08
Machinery	g	6.42E+03	6.42E+03
Fossil fuel and lubricant	g	3.21E+10	3.21E+10
Nitrogen fertilizer	g	1.60E+05	1.45E+05
Phosphorus fertilizer	g	1.25E+05	9.50E+04
Potash fertilizer	g	5.50E+04	3.50E+04
Micro fertilizer	g	2.50E+03	2.50E+03
Earth emergy	Rials	3.72E+15	3.72E+15
Organic fertilizer	g	2.00E+06	1.70E+06
Sapling	Rials	9.60E+07	7.15E+07
Outpu			
Economic yield	g	3.25E+06	3.75E+06
Economic yield	J	3.82E+09	4.41E+09

Table 3. Emergency analysis and input structure in Mozafati and Rabbi production systems in Mirjaveh city (sej/ha/yr)

Items	Mazafati			Rabbi	
	Emergy/Unit	Emergy	%	Emergy	%
Renewable environmental inputs					
Solar energy	1.00E+00	3.60E+13	0.11%	3.60E+13	0.12%
Wind, kinetic energy	1.24E+03	2.79E+12	0.01%	2.79E+12	0.01%
Rain, chemical	2.34E+04	3.54E+13	0.11%	3.54E+13	0.12%
River water	3.61E+04	4.16E+15	12.48%	3.61E+15	12.34%
Subtotal	2.34E+04	7.14E+13	0.21%	7.14E+13	0.24%
Non-renewable environmental inputs					
Groundwater	2.34E+04	6.76E+15	20.29%	5.88E+15	20.13%
SOM reduction	4.27E+04	8.80E+14	2.64%	8.80E+14	3.01%
Soil erosion	1.27E+09	2.31E+15	6.93%	2.31E+15	7.91%
Subtotal		9.96E+15	29.87%	9.07E+15	31.05%
Purchased inputs					
Human labor	2.22E+06	1.08E+15	3.25%	9.52E+14	3.26%
Machinery	1.01E+10	6.48E+13	0.19%	6.48E+13	0.22%
Fossil fuel and lubricant	8.60E+04	2.76E+15	8.28%	2.76E+15	9.45%
Nitrogen fertilizer	3.09E+10	4.94E+15	14.83%	4.48E+15	15.33%
Phosphorus fertilizer	2.82E+10	3.53E+15	10.57%	2.68E+15	9.17%
Potash fertilizer	2.23E+09	1.23E+14	0.37%	7.81E+13	0.27%
Micro fertilizer	3.91E+09	9.78E+12	0.03%	9.78E+12	0.03%
Earth emergy	1.00E+00	3.72E+15	11.15%	3.72E+15	12.72%
Organic fertilizer	2.96E+08	5.92E+14	1.78%	5.03E+14	1.72%
Sapling	6.76E+07	6.49E+15	19.47%	4.83E+15	16.54%
FR		1.20E+15	3.60%	9.21E+14	3.15%
FN		2.21E+16	66.32%	1.92E+16	65.56%
Subtotal		2.33E+16	69.92%	2.01E+16	68.71%
Total		3.33E+16	100.00%	2.92E+16	100.00%

3.1.2 Non-Renewable Environmental Inputs (N)

The study considered non-renewable environmental inputs such as groundwater, loss of soil organic matter, and soil erosion. In the production systems for Mazafati dates, these inputs accounted for 29.87 percent, and for Rabbi dates, they accounted for 31.05 percent of the total input

emergy (Table 3). The Rabbi date production system exhibits a greater rise in these values in comparison to the Mazafati date system, which suggests a higher level of soil erosion and loss of organic matter. Furthermore, the proportion of groundwater, which is the most substantial non-renewable resource, is noteworthy in both systems. It accounts for 20.29 percent of the total emergy input in the Mazafati date system and 20.13 percent in the Rabbi date system (Table 3). Implementing contemporary irrigation techniques can effectively decrease the utilisation of groundwater.

The study conducted on a maize farm in Kansas, USA, estimated that the proportion of non-renewable environmental inputs was 2.16E+13 sej/ha/yr (Martin et al., 2006). According to Shahhosini et al. (2020), the assessment of potato production in Golestan province revealed that the groundwater input for autumn and spring production systems was respectively 23.92 percent and 45.28 percent higher than other inputs.

The significant reliance on non-renewable resources, particularly groundwater, in both Mazafati and Rabbi date palm production systems highlights the need for sustainable management practices. Our findings corroborate those of Asgharipour et al. (2019), who also emphasized the importance of reducing reliance on non-renewable inputs in agricultural systems.

To mitigate the environmental impacts of date palm cultivation, several strategies can be implemented, such as adopting advanced irrigation systems like drip irrigation to reduce water consumption and improve water use efficiency, implementing sustainable soil management practices like cover cropping, crop rotation, and organic fertilization to improve soil health and reduce erosion, exploring the use of renewable energy sources like solar power to reduce dependence on fossil fuels and decrease greenhouse gas emissions, and developing policies that promote sustainable agricultural practices and provide incentives for farmers to adopt environmentally friendly technologies.

Future research should focus on quantifying the environmental and economic benefits of these strategies and exploring their long-term impacts on the sustainability of date palm production systems. Additionally, a more comprehensive assessment of the social and cultural factors influencing farmers' adoption of sustainable practices is needed.

3.1.3 Purchased Inputs (FN and FR)

The inputs Purchased consist of the labour force, machinery, fossil fuels and oils, chemical fertilisers (nitrogen, phosphorus, potassium, and micronutrients), land value, organic fertilisers, and consumed seedlings. The cumulative values of these inputs for the Mazafati date production systems were 2.33E+16 sej/ha/yr, while for the Rabbi dates, the total values were 2.01E+16 sej/ha/yr. The proportion of renewable resources purchased for the Mazafati date production system was 3.60 percent, and for Rabbi dates it was 3.15 percent. In contrast, the proportion of non-renewable resources purchased was 66.32 percent for Mazafati dates and 65.56 percent for Rabbi dates. The market inputs accounted for 69.92 percent of the total input emergy for Mazafati dates and 68.71 percent for Rabbi dates. These inputs were nearly equal for both date production systems, with no significant differences observed (Table 3).

The nitrogen fertiliser accounted for the largest proportion of purchased inputs in both the Mazafati and Rabbi date production systems, with 14.83 percent for Mazafati and 15.33 percent for Rabbi. This was followed by land value, which accounted for 11.15 percent for Mazafati and 12.72 percent for Rabbi. Seedlings had the third highest share, with 19.47 percent for Mazafati and 16.54 percent for Rabbi. Minimising the usage of these resources is crucial for reducing the proportion of externally purchased resources in these systems. The proportion of certain inputs was below one percent, specifically machinery (0.19 percent for Mazafati and 0.22 percent for Rabbi), potassium fertiliser (0.37 percent for Mazafati and 0.27 percent for Rabbi), and micronutrient fertilisers (0.03 percent for both types of dates) (Table 3).

The purchased inputs for the commercial rapeseed production system amounted to 1.80E+16 sej/ha/yr, while for the subsistence rapeseed production system it was 1.61E+16 sej/ha/yr. The evaluation of purchased resources in commercial and subsistence rapeseed systems reveals minor variations in the overall emergy of purchased resources between the two systems, however, there were notable disparities in the composition of these resources. As an illustration, the amount of energy required for labour in the subsistence system was almost twice as much as that in the commercial system. In the subsistence system, the amount of emergy consumed by organic fertilisers was 3.55E+15 sej/ha/yr, whereas in the commercial system, it was completely absent. In the commercial system, the combined emergy consumption for herbicides, electricity, and the establishment of the irrigation system amounted to 2.08E+15 sej/ha/yr, while it was completely absent in the subsistence system. The emergy consumed by agricultural machinery and fossil fuels in the commercial system was three times greater than that of the subsistence system, while in the subsistence system it was six times greater. The energy consumed by chemical potassium fertilisers in the commercial system was approximately three times greater than that in the subsistence system (Amiri et al., 2019). In the wheat production system, nitrogen, phosphorus, and potassium fertilisers made up 97 percent of the non-renewable resources that were bought (Hoshyar et al., 2018). According to Zhang et al. (2012), nitrogen fertiliser and labour were the inputs with the highest emergy in wheat production.

3.2 Emergy-Based Indices

Emergy analysis takes into account all available environmental resources, such as human labour and ecosystem services, which are often disregarded in other approaches. This aids in ascertaining appropriate strategies for the sustainable management of agriculture (Yue et al., 2016; Houshyar et al., 2018).

3.2.1 Transformity (Tr) and Specific Emergy (SpE)

These indices aid in assessing the efficiency of product output in terms of emergy (Brown and Ulgiati, 2004). The transformity is a measure of the profitability of a production process. A high level of this index indicates low performance and productivity in long-term environmental and economic competition (Odum, 2000). Specific emergy (SpE) is a fundamental concept in emergy studies that quantifies the amount of emergy needed to produce a single unit of biomass. The amount of supportive emergy required for each unit of biomass produced is determined by the unit of mass, either in grammes or kilogrammes (Odum, 2000; Chen et al., 2009; Li et al., 2010; Zhang et al., 2012).

The production systems of Mazafati and Rabbi dates in Mirjaveh county had transformities of 8.72E+06 and 6.63E+06 sej/J, respectively (Table 4). The emergy requirements for the production systems of Mazafati and Rabbi dates were 1.03E+10 and 7.79E+09 sej/g, respectively (Table 4).

The Mazafati date production system exhibited a lower efficiency in transformity compared to the Rabbi date system. However, when considering SpE calculation, the Rabbi date system demonstrated lower efficiency. Based on the acquired values, it can be concluded that there is a minor disparity in the transformity between the two systems, but there is a notable discrepancy in the calculated values for SpE.

The transformity for the commercial rapeseed production system was calculated as 3.08E05 sej/J, while for the subsistence rapeseed production system it was calculated as 9.48E+05 sej/J (Amiri et al., 2019). The transformity for dates in Nehbandan county was reported as 1.71E+09 sej/J, while for pistachios it was reported as 1.47E+09 sej/J. The specific emergy for date production system was 1.37E+10 sej/g, and for pistachio production system it was 2.02E+05 sej/g (Jafari et al., 2018).

Table 4. Emergy-based indices of the production systems of Mozafati and Rabbi date in Mirjaveh city

	Mazafati	Rabbi
Transformity	8.72E+06	6.63E+06
Specific emergy	1.03E+10	7.79E+09
R%	3.81%	3.40%
EYR	1.430	1.455
EIR	2.325	2.196
EIR*	326.433	281.212
ELR	139.568	127.213
ELR*	2.802	3.327
ESI	0.010	0.011
ESI*	0.510	0.437
EER	4.460	3.391
EIPS	0.945	0.963
EMR	5.86E+06	6.23E+06

3.2.2 Emergy Renewability Ratio (R%)

Production systems that have a higher proportion of renewable resources compared to those that rely more on non-renewable inputs are more likely to succeed and be sustainable in economic competition. This is because non-renewable resources are becoming increasingly scarce over time (Asgharipour et al., 2019). The production systems of Mazafati and Rabbi dates had a dependency on renewable resources of 3.81 percent and 3.40 percent, respectively, as shown in Table 4. The sustainability index of both systems is almost identical, although the Mazafati date production system is marginally more sustainable than the Rabbi date system.

The R% for shallot production in mechanised, traditional, conservation, and natural habitat systems were reported as 18.60%, 26.30%, 25.30%, and 16.30%, respectively (Amiri et al., 2021). The emergy renewability ratio for traditional rice production and intensive vegetable cultivation in China was estimated to be 52.66 percent and 12.30 percent, respectively, according to Su et al. (2020). The proportion of renewable resources in the total production resources for the rice production system in Mazandaran was documented as 8.26 percent (Amini et al., 2020).

3.2.3 Emergy Yield Ratio (EYR)

This EYR assesses the dominance of a system based on the emergy costs it incurs, serving as a sustainability indicator that encompasses both the environment and the environmental economy. It possesses the capacity to recognise agricultural ecosystems (Fallahinejad et al., 2021). The EYR is widely acknowledged as a crucial indicator in the analysis of various systems (Amiri et al., 2021). The EYR for the production systems of Mazafati and Rabbi dates were 1.430 and 1.455 respectively, as shown in Table 4.

Based on the results, the production systems of Mazafati and Rabbi dates exhibit almost identical stability. Nevertheless, the estimated EYR for Mazafati dates is marginally inferior to that of Rabbi dates, primarily because of the higher reliance on purchased emergy resources in the former system. Hence, it is imperative for farmers to prioritise the utilisation of available environmental resources, as minimising reliance on purchased resources enhances the EYR in production systems.

The EYR for rice was 5.13, as reported by Amini et al. (2020). The EYR values for cucumber, tomato, bell pepper, and eggplant production systems were documented as

1.025, 1.015, 1.014, and 1.012 respectively. The cucumber production system exhibited a greater value compared to the other three systems (Asgharipour et al., 2020).

The EYR for the Yaghuti grape production system in Sistan was reported to be 1.02, according to Koohkan et al. (2017).

3.2.4 Standard Investment Ratio (EIR) and Modified Investment Ratio (EIR*)

The EIR assesses the level of investment, economic growth, and availability of unrestricted environmental resources, as well as the agricultural system's reliance on the environment. A lower EIR value indicates that a system relies more heavily on environmental resources, incurs lower economic costs, and has a higher output dependence on environmental resources (Odum, 2000). Furthermore, the EIR* is calculated by dividing the amount of inputs purchased by the amount of renewable environmental inputs. Amiri et al. (2019) suggest that conducting a more principled comparison of production costs and competitive strength in the market is advisable. The EIR index for the production systems of Mazafati and Rabbi dates were 2.325 and 2.196, respectively, as shown in Table 4. The EIR* values for Mazafati dates were 326.433, while for Rabbi dates they were 281.212 (as shown in Table 4).

The Mazafati date production system demonstrates greater economic development as evidenced by its higher EIR and EIR* compared to the Rabbi date production system. This is attributed to a larger utilisation of market inputs, such as nitrogen fertiliser and saplings, which have contributed to the increase in these indices. Hence, by decreasing market inputs in the Mazafati date production system, it is possible to reduce these indices and enhance production efficiency.

The EIR values for different production systems of shallot, including mechanised, traditional, conservation, and natural habitat systems, were 7.721, 12.665, 23.223, and 0.785, respectively. Similarly, the EIR* indices for these systems were 21.872, 25.308, 40.932, and 3.708, as reported by Amiri et al. in 2021. A research conducted on the sustainability of the Huanjiang forest-grassland region in China revealed a consistent upward trend in the EIR index over a span of 16 years. The index value escalated from 0.12 in 2000 to 0.71 in 2015 (Zhan et al., 2020). The EIR, as reported by Zhao et al. (2019), varied from 4.15 to 7.18 across different wheat-growing regions with varying climates. The EIR for oat and wheat production systems in China was calculated as 2.94 and 1.30, respectively, according to Zhai et al. (2017).

3.2.5 Standard Environmental Load Ratio (ELR) and Modified Environmental Load Ratio (ELR*)

The ELR quantifies the environmental strain caused by the utilisation of non-renewable energies that are within human jurisdiction. Greater environmental pressure is indicated by higher ELR values, particularly when this index surpasses 10 (Su et al., 2020). The ELR is determined by dividing the total non-renewable and purchased emergy inputs by the renewable inputs. On the other hand, ELR* specifically examines the ratio of non-renewable resources to renewable resources (Ortega et al., 2002). Typically, ELRs that are less than 2 indicate a minimal impact on the environment, ELRs between 2 and 10 suggest a moderate impact, and ELRs above 10 indicate a significant strain on the environment (Brown and Ulgiati, 2004; Cavalett et al., 2006).

The ELR was calculated as 139.568 for the production system of Mazafati dates and 127.213 for the production system of Rabbi dates. In addition, the ELR for the same systems were 2.802 and 3.327 respectively, as shown in Table 4. Systems with high ELR values indicate a substantial amount of environmental pressure, mainly because they heavily rely on non-renewable environmental resources like groundwater and contribute to soil erosion. Nevertheless, the significant disparities between the ELR and ELR* values indicate that both systems impose a moderate burden on the environment.

The ELR index values for wheat, barley, sugar beetroot and saffron were reported as 63.56, 66.06, 23.56, and 79.63 respectively (Fallahinejad et al., 2021). The ELR for subsistence cultivation of rapeseed was 19.75, while for commercial cultivation it was 12.68. The ELR* for subsistence cultivation was 17.85, and for commercial cultivation it was 4 (Amiri et al., 2019). According to Wang et al. (2014), the ELR for wheat production systems was 10.59, while for maize it was 0.47.

3.2.6 Standard Environmental Sustainability Index (ESI) and Modified Environmental Sustainability Index (ESI*)

The ESI is a comprehensive measure of environmental sustainability. It is calculated by dividing the EYR index by the ELR. The assessment quantifies the advantages gained from a system in relation to the amount of space occupied (Brown and Ulgiati, 1997). The ESI and ESI* assess the ability of a process to achieve high performance while minimising its impact on the environment (Odum, 1996). A production system with an ESI value below 1 signifies a significant environmental pressure, whereas values ranging from 1 to 10 indicate a relatively sustainable production system (Su et al., 2020).

The research calculated the ESI and ESI* for the Mazafati date production system as 0.010 and 0.011 respectively. For the Rabbi date production system, the values were 0.510 and 0.437 respectively (Table 4).

The study found that both agricultural systems had environmental sustainability indices below one, which suggests a very low level of sustainability and a high degree of environmental pressure. Both the Mazafati and Rabbi date production systems heavily rely on non-renewable environmental resources.

The index for the autumn and spring potato cultivation systems was calculated as 0.05 and 0.07 respectively (Shah Hoseini et al., 2021). The environmental sustainability of the conventional forage maize production system in Denmark was reported as 0.24 (Ghaley et al., 2018). The index for dates and pistachios was computed as 0.93 and 1.30 respectively, according to Jafari et al. (2018).

Furthermore, the index for the potato production system was calculated to be 0.03, as determined by Zhai et al. (2017).

3.2.7 Emergy Exchange Ratio (EER)

The EER, a metric developed by Azizi et al. (2021), quantifies the efficiency of emergy by comparing the total emergy consumed in production to the emergy obtained from sales in the market. This index is determined by the efficiency of the product in relation to its area and assesses the emergy gain from product sales. Furthermore, it evaluates the equilibrium between the economic output traded for currency in the market (YM) in megajoules per unit area and the overall emergy input to the system (U). An EER value greater than one signifies a high level of system efficiency in converting monetary emergy into product and reflects significant purchasing power in the market (Amiri et al., 2019). The EER values for the Mazafati and Rabbi date production systems were 4.460 and 3.391 respectively, as shown in Table 4. The fact that the index is greater than one for both systems indicates their high production efficiency.

The EERs for cucumber, tomato, bell pepper, and eggplant production systems were documented as 0.72, 0.54, 0.46, and 0.33 respectively, according to Asgharipour et al. (2020). The EER values for these systems, which are below one, indicate their low efficiency. The EER index for commercial rapeseed systems was 0.94, while for subsistence rapeseed systems it was 0.31. The rapeseed production systems are considered inefficient because their EER values are less than one (Amiri et al., 2019).

3.2.8 Emergy Index of Product Safety (EIPS)

The EIPS evaluates the level of safety in agricultural product outputs by considering the contributions of chemical fertilisers and herbicides as inputs. According to Xi and Qin (2009), there is a positive correlation between the EIPS value and the security and health of the crops. In other words, as the EIPS value increases, the crops are more secure and healthy. The production safety index for the Mazafati date production system was determined to be 0.945, while for the Rabbi date system, it was found to be 0.963. The assessment of production safety for both systems yielded almost identical results (Table 4).

Nevertheless, the safety index of the Rabbi date system was marginally superior to that of the Mazafati dates. Thus, it can be asserted that the Rabbi date production system yields a more wholesome product. However, in order to augment this index, it is imperative to decrease the overall utilisation of fertilisers for both systems. The EIPS values for mechanised, traditional, conservation, and natural shallot habitat systems were 0.883, 0.906, 1.00, and 1.00 respectively (Amiri et al., 2021). The EIPS for three different models of goose farming in cornfields, conventional corn and wheat-chickpea rotation were determined to be 0.97, 0.91, and 0.94, respectively, according to a study conducted by Guan et al. (2016). According to Sha et al. (2015), the index for two production models of goose farming in cornfields and conventional corn cultivation in the southeastern region of Tibet were 0.86 and 0.70, respectively.

3.2.9 Emergy-Money Ratio (EMR)

The EMR establishes a connection between the economic attributes and the environmental inputs to an ecosystem. This indicator quantifies the monetary value of environmental flows and purchased inputs that enter the system as a result of the production of goods (products and services) at a specific point in time (Lu and Campbell, 2009). Within the realm of emergy indices, there is a requirement for an index that effectively conveys the economic worth of system outputs from an emergy standpoint. This index is known as EMR, as described by Chen et al. (2017). EMR is a measure of the amount of energy invested per unit of profit. It is calculated by dividing the emergy investment by the net profit. This concept was introduced by Zhang et al. (2012).

The EMR values for the production systems of Mazafati dates and Rabbi dates were determined to be 5.86E+06 and 6.23E+06, respectively. The analysis of EMR values in this study reveals that the Rabbi date production system has a greater emergy flow per unit of net profit compared to the Mazafati date production system (Table 4). The emergy analysis of four systems, namely corn farming, duck breeding, mushroom cultivation, and fish farming, yielded EMR values of 1.36E+13, 8.22E+13, 5.04E+13, and 4.78E+13 emrial, respectively.

The EMR values of the assessed systems demonstrate that the agricultural system (specifically maize production) has a lesser amount of emergy flow per dollar earned in comparison to the animal husbandry (duck breeding), horticulture (mushroom production), and aquaculture (fish farming) systems. Put simply, the agricultural system had a lower emergy-to-dollar ratio compared to the other systems. The fish farming system had a more favourable energy-money ratio compared to the animal husbandry and horticulture systems, primarily because of its semi-natural state. According to Zhang et al. (2012), if two systems have the same net income, the one with a lower emergy inflow would be more sustainable. The EMR values for mechanised, traditional, conservation, and natural habitat systems of shallot were determined as 1.67E+13, 1.86E+13, 1.72E+13, and 8.6E+12, respectively, according to Amiri et al. (2021).

4. Conclusion

This study aimed to implement a production system that maximises efficiency and economic-ecological productivity for two export products, Mazafati and Rabbi dates, in the Mirjaveh county from 2022 to 2023. Agricultural ecosystems are considered complex biological systems because of their diverse forms and functions. Hence, it is crucial to assess the sustainability of agricultural systems in order to identify appropriate production patterns, as part of a comprehensive and scientific approach. Emergy analysis has the ability to evaluate the environmental, economic, product quality, and social aspects of different systems. The primary objective

of this research was to generate a premium and nutritious product with optimal financial gain, given that dates are the predominant crop grown in Mirjaveh county. The Mazafati and Rabbi varieties dominate the cultivation area in the palm groves of Mirjaveh among the different types of dates. The chosen indices for this research were diverse and capable of measuring ecological, economic, market dimensions, and product quality.

The results obtained from emergy-based indices for these export products showed variations in the calculated values of the transformity with specific emergy. The calculation of the transformity revealed that the efficiency of the Mazafati date production system was lower than that of the Rabbi date system. Conversely, when considering the SpE calculation, the efficiency was lower for the system specific to Rabbi dates. When analysing indices in the Mazafati date production system, it was found that higher R% and EER values, as well as lower EIPS, ELR*, and EMR values, provided a slight advantage. However, the Rabbi date production system demonstrated greater sustainability in terms of higher EYR, lower EIR and EIR*, and lower ELR compared to the Mazafati date production system. However, the calculated values of these indices must not ignore the extra strain that both production systems place on the environment. Date farmers must prioritise this matter and enhance the quality of their product and the surrounding environment by optimising the utilisation of natural resources and substantially decreasing the reliance on non-renewable environmental resources and purchased inputs. Nevertheless, when considering the economic, commercial, and ecological aspects, the Mazafati date system exhibited a slight superiority compared to the Rabbi date production system.

Acknowledgement

The authors would like to express their sincere gratitude to University of Zabol for the financial support provided for this research through Grant No. IR-UOZ-GR-6673. We are also grateful to the Department of Agriculture of Mirjaveh County and the Jihad Keshavarzi Organization Jihad Organization of Sistan and Baluchestan Province for their valuable assistance in providing data and facilitating the collection of field data .The researchers also extend their appreciation to the date palm farmers who participated in the study for their time and for providing the necessary information.

References

Alipour, F., & Mahdavi, F. (2014). Halal (lawful) and Tayyib (clean) are the highest standards of food hygiene in the Quran. *Islam and Health Journal*, *1*(2), 41-50.

Amini, S., Rohani, A., Aghkhani, M. H., Abbaspour-Fard, M. H., & Asgharipour, M. R. (2020). Sustainability assessment of rice production systems in Mazandaran Province, Iran with emergy analysis and fuzzy logic. *Sustainable Energy Technologies and Assessments*, *40*, 100744. https://doi.org/10.1016/j.seta.2020.100744

Amiri, Z., Asgharipour, M. R., Campbell, D. E., & Armin, M. (2019). A sustainability analysis of two rapeseed farming ecosystems in Khorramabad, Iran, based on emergy and economic analyses. *Journal of Cleaner Production*, *226*, 1051-1066. https://doi.org/10.1016/j.jclepro.2019.04.091

Amiri, Z., Asgharipour, M. R., Campbell, D. E., Azizi, K., Kakolvand, E., & Moghadam, E. H. (2021). Conservation agriculture, a selective model based on emergy analysis for sustainable production of shallot as a medicinal-industrial plant. *Journal of Cleaner Production*, *292*, 126000. https://doi.org/10.1016/j.jclepro.2021.126000

Asgharipour, M. R., Amiri, Z., & Campbell, D. E. (2020). Evaluation of the sustainability of four greenhouse vegetable production ecosystems based on an analysis of emergy and social characteristics. *Ecological Modelling*, *424*, 109021. https://doi.org/10.1016/j.ecolmodel.2020.109021

Amiri, Z., Maghsoudi, A., Asgharipour, M. R., Nejati-Javaremi, A., & Campbell, D. E. (2022). The semi-intensive production model: A strategy based on emergy and economic analyses to realize sustainability in the ecosystem of Sistani beef cattle raising in Iran. *Journal of Cleaner Production*, *362*, 132304. https://doi.org/10.1016/j.jclepro.2022.132304

Asgharipour, M. R., Shahgholi, H., Campbell, D. E., Khamari, I., & Ghadiri, A. (2019). Comparison of the sustainability of bean production systems based on emergy and economic analyses. *Environmental monitoring and assessment*, *191*, 1-21. https://doi.org/10.1007/s10661-018-7123-3

Brown, M. T., Campbell, D. E., De Vilbiss, C., & Ulgiati, S. (2016). The geobiosphere emergy baseline: A synthesis. *Ecological Modelling*, *339*, 92-95. https://doi.org/10.1016/j.ecolmodel.2016.03.018

Brown, M. T., & Ulgiati, S. (2004). Energy quality, emergy, and transformity: HT Odum's contributions to quantifying and understanding systems. *Ecological Modelling*, *178*(1-2), 201-213. https://doi.org/10.1016/j.ecolmodel.2004.03.002

Campbell, D. E., Brandt-Williams, S. L., & Meisch, M. E. (2005). *Environmental accounting using emergy: Evaluation of the state of West Virginia*. Narragansett, RI, USA: US Environmental Protection Agency, Office of Research and Development, National Health and Environmental Effects Research Laboratory, Atlantic Ecology Division.

Cavalett, O., De Queiroz, J. F., & Ortega, E. (2006). Emergy assessment of integrated production systems of grains, pig and fish in small farms in the South Brazil. *Ecological Modelling*, *193*(3-4), 205-224. https://doi.org/10.1016/j.ecolmodel.2005.07.023

Chen, B., Chen, Z. M., Zhou, Y., Zhou, J. B., & Chen, G. Q. (2009). Emergy as embodied energy based assessment for local sustainability of a constructed wetland in Beijing. *Communications in Nonlinear Science and Numerical Simulation*, *14*(2), 622-635. https://doi.org/10.1016/j.cnsns.2007.05.035

Chen, W., Liu, W., Geng, Y., Brown, M. T., Gao, C., & Wu, R. (2017). Recent progress on emergy research: A bibliometric analysis. *Renewable and Sustainable*

Energy Reviews, *73*, 1051-1060. https://doi.org/10.1016/j.rser.2017.02.041

Cheng, H., Chen, C., Wu, S., Mirza, Z. A., & Liu, Z. (2017). Emergy evaluation of cropping, poultry rearing, and fish raising systems in the drawdown zone of Three Gorges Reservoir of China. *Journal of Cleaner Production*, *144*, 559–571. https://doi.org/10.1016/j.jclepro.2016.12.053

Fallahinejad, S., & Armin, M. (2022). Role of mechanization on the sustainability of sugar beet production using emergy approach. *Agriculture, Environment & Society*, *2*(1), 15–24. https://doi.org/10.22034/aes.2022.327793.1019

Fallahinejad, S., Armin, M., & Asgharipour, M. R. (2021). A survey on the ecological sustainability of introducing new crops in the cropping pattern using emergy approach. *Current Research in Environmental Sustainability*, *3*, 100083. https://doi.org/10.1016/j.crsust.2021.100083

Frankel, J., & Romer, D. (1999). Does trade cause growth? *The American Economic Review*, *89*(3), 379–399. https://doi.org/10.1257/aer.89.3.379

Ghaley, B. B., Kehli, N., & Mentler, A. (2018). Emergy synthesis of conventional fodder maize (Zea mays L.) production in Denmark. *Ecological Indicators*, *87*, 144–151. https://doi.org/10.1016/j.ecolind.2017.12.027

Gheicari, G., Asgharipour, M. R., Mousavi Nik, M., & Ghanbari, A. (2021). Effects of different cotton tillage methods on N_2O and NH_3 emissions in a cotton-wheat rotation. *Agriculture, Environment & Society*, 1(1), 1–9. https://doi.org/10.22034/aes.2021.144106

Guan, F. C., Sha, Z. P., Zhang, Y. Y., Wang, J. F., & Wang, C. (2016). Emergy assessment of three home courtyard agriculture production systems in Tibet Autonomous Region, China. *Journal of Zhejiang University. Science. B*, *17*(8), 628. https://doi.org/10.1631/jzus.B1500154

Houshyar, E., Wu, X. F., & Chen, G. Q. (2018). Sustainability of wheat and maize production in the warm climate of southwestern Iran: An emergy analysis. *Journal of Cleaner Production*, *172*, 2246–2255. https://doi.org/10.1016/j.jclepro.2017.11.187

Jafari, M., Asgharipour, M. R., Ramroudi, M., Galavi, M., & Hadarbadi, G. (2018). Sustainability assessment of date and pistachio agricultural systems using energy, emergy and economic approaches. *Journal of Cleaner Production*, *193*, 642–651. https://doi.org/10.1016/j.jclepro.2018.05.089

Kazemi, H., Shokrgozar, M., Kamkar, B., & Soltani, A. (2018). Analysis of cotton production by energy indicators in two different climatic regions. *Journal of Cleaner Production*, *190*, 729-736. https://doi.org/10.1016/j.jclepro.2018.04.195

Kohkan, S. A., Ghanbari, A., Asgharipour, M. R., & Fakheri, B. A. (2017). Emergy evaluation of Yaghuti grape of Sistan. *Arid Biome Scientific and Research Journal*, *7*(2), 73-84. https://doi.org/10.29252/aridbiom.7.2.73

Li, L. J., Lu, H. F., Campbell, D. E., & Ren, H. (2010). Emergy algebra: Improving matrix methods for calculating transformities. *Ecological Modelling*, *221*, 411-422. https://doi.org/10.1016/j.ecolmodel.2010.08.005

Lu, H. F., & Campbell, D. E. (2009). Ecological and economic dynamics of the Shunde agricultural system under China's small city development strategy. *Journal of Environmental Management*, *90*, 2589-2600. https://doi.org/10.1016/j.ecoleng.2009.08.001

Lu, H. F., Tan, Y. W., Zhang, W. S., Qiao, Y. C., Campbell, D. E., Zhou, L., & Ren, H. (2017). Integrated emergy and economic evaluation of lotus-root production systems on reclaimed wetlands surrounding the Pearl River Estuary, China. *Journal of Cleaner Production*, *158*, 367-379. https://doi.org/10.1016/j.jclepro.2017.05.016

Lu, H., Bai, Y., Ren, H., & Campbell, D. E. (2010). Integrated emergy, energy and economic evaluation of rice and vegetable production systems in alluvial paddy fields: Implications for agricultural policy in China. *Journal of Environmental Management*, *91*, 2727-2735. https://doi.org/10.1016/j.jenvman.2010.07.025

Martin, J. F., Diemont, S. A. W., Powell, E., Stanton, M., & Levy-Tacher, S. (2006). Emergy evaluation of the performance and sustainability of three agricultural systems with different scales and management. *Agriculture, Ecosystems & Environment*, *115*, 128-140. https://doi.org/10.1016/j.agee.2005.12.016

Mollazehi, M., & Shahiki Tash, M. N. (2013). *Examining the structure of the market and its continuity* (Master's thesis). Sistan and Baluchistan University.

Moonilall, N. I., Homenauth, O., & Lal, R. (2020). Emergy analysis for maize fields under different amendment applications in Guyana. *Journal of Cleaner Production*, *258*, 120761. https://doi.org/10.1016/j.ecolmodel.2019.108889

Nazarian, S. M., Zibaei, M., & Sheikh Zainuddin, A. (2020). Assessing the sustainability of agricultural systems with a consensual planning approach: Kohdasht region of Lorestan. *Journal of Agricultural Economics and Development*, *34*(3), 239-257.

Odum, H. T. (1996). Scales of ecological engineering. Ecological Engineering, 6(1-3), 7-19.

Odum, H. T. (2000). *Handbook of Emergy Evaluation: A Compendium of Data for Emergy Computation (Folio #2 Emergy global processes)*. Gainesville, FL: Center of Environmental Policy, University of Florida.

Ortega, E., Anami, M., & Diniz, G. (2002). Certification of food products using emergy analysis. In *Proceedings of the III International Workshop Advances in Energy Studies* (pp. 227–237).

Pejman, H. (2001). *Date palm planting and harvesting guide*. Office of Educational Services and Technology, Agricultural Education Publications.

Rafiei, H., Mirbagheri, S. Sh., & Akbarpour, H. (2017). Investigating the influencing factors on the fluctuations in the export price of Iranian dates. *Agricultural Economics Research*, 10(1), 149–170. https://doi.org/10.1016/j.ecolmodel.2017.07.022

Sadorsky, P. (2012). Energy consumption, output and trade in South America. *Energy Economics*, 34(2), 476–488. https://doi.org/10.1016/j.eneco.2011.10.009

Sha, Z. H., Guan, F., Wang, J., Zhang, Y., Liu, H., & Wang, C. H. (2015). Evaluation of raising geese in cornfields based on emergy analysis: A case study in southeastern Tibet. *Ecological Engineering*, *84*, 485–491. https://doi.org/10.1016/j.ecoleng.2015.09.024

Shah Hosseini, H. R., Ramrodi, M., & Kazemi, H. (2021). Economic analysis and evaluation of the sustainability of potato production based on greenhouse gas emissions (case study: the province of Golestan). *Scientific Research Journal of Agricultural Knowledge and Sustainable Production, 31*(3), 295–311.

Shah Hoseini, H. R., & Kazemi, H. (2022). Evaluation of sustainability of rainfed rapeseed production in Gorgan County using emergy analysis. *Journal of Emergy, Life Cycle and System Analysis in Agriculture*, *2*(1), 61–70. https://doi.org/10.22034/aes.2022.337172.1031

Su, Y., He, S., Wang, K., Shahtahmassebi, A. R., Zhang, L., Zhang, J., Zhang, M., & Gan, M. (2020). Quantifying the sustainability of three types of agricultural production in China: An emergy analysis with the integration of environmental pollution. *Journal of Cleaner Production*, *252*, 119650. https://doi.org/10.1016/j.jclepro.2019.119650

Wang, X., Chen, Y., Sui, P., Gao, W., Qin, F., Zhang, J., & Wu, X. (2014). Emergy analysis of grain production systems on large-scale farms in the North China Plain based on LCA. *Agricultural Systems*, *128*, 66–78. https://doi.org/10.1016/j.agsy.2014.04.002

Xi, Y. G., & Qin, P. (2009). Emergy evaluation of organic rice-duck mutualism system. *Ecological Engineering*, *35*(11), 1677–1683. https://doi.org/10.1016/j.ecoleng.2009.06.020

Yasini, H., Ghanbari, A., Asgharipour, M. R., & Seyedabadi, A. (2020). Assessing the sustainability of garlic, onion and wheat production systems in Sistan with integrated Emergy and economic analysis. *Journal of Agricultural Sciences and Sustainable Production, 30*, 269-288.

Yue, J., Yuan, X., Li, B., Ren, H., & Wang, X. (2016). Emergy and exergy evaluation of a dike-pond project in the drawdown zone (DDZ) of the Three Gorges Reservoir (TGR). *Ecological Indicators, 71*, 248-257. https://doi.org/10.1016/j.ecolind.2016.05.015

Zhai, X., Huang, D., Tang, S., Li, S., Guo, J., Yang, Y., Liu, H., Li, J., & Wang, K. (2017). The emergy of metabolism in different ecosystems under the same environmental conditions in the agro-pastoral ecotone of northern China. *Ecological Indicators, 74*, 198-204. https://doi.org/10.1016/j.ecolind.2016.11.028

Zhan, C., Zhao, R., & Hu, S. (2020). Emergy-based sustainability assessment of forest ecosystem with the aid of mountain eco-hydrological model in Huanjiang County, China. *Journal of Cleaner Production, 251*, 119638. https://doi.org/10.1016/j.agsy.2022.103594

Zhang, L. X., Song, B., & Chen, B. (2012). Emergy-based analysis of four farming systems: Insight into agricultural diversification in rural China. *Journal of Cleaner Production*, *28*, 33–44. https://doi.org/10.1016/j.jclepro.2011.10.042

Zhao, H., Zhai, X., Guo, L., Liu, K., Huang, D., Yang, Y., Li, J., Xie, S., Zhang, C., Tang, S., & Wang, K. (2019). Assessing the efficiency and sustainability of wheat production systems in different climate zones in China using emergy analysis. *Journal of Cleaner Production*, *235*, 724–732. https://doi.org/10.1016/j.jclepro.2019.06.251

Agriculture, Environment & Society

Journal homepage: www.aes.uoz.ac.ir

Examining the weaknesses, strengths, threats and opportunities of Shulabad watershed in Lorestan Province to provide management solutions

Ebrahim Karimi Sangchini*[a], Seyed Hossein Arami[b], Reza Chamanpira[a]

[a] Soil Conservation and Watershed Management Research Institute, Lotestan Agricultural and Natural Resources Research and Education Center, Agricultural Research, Education and Extension Organization (AREEO), Khorramabad, Iran
[b] Forests and Rangelands Research Department, Khuzestan Agricultural and Natural Resources Research and Education Center, Agricultural Research Education and Extension Organization (AREEO), Ahvaz, Iran

ARTICLE INFO

Article history:
Received: 18 November 2024
Accepted: 10 February 2025
Available online: 30 June 2025

Keywords:
Comprehensive management
Delphi technique
Stockholders
SWOT framework

ABSTRACT

The purpose of this research is to examine the weaknesses, strengths, threats and opportunities in the Shulabad Watershed, which will be a prelude to determining comprehensive management strategies. An examination was conducted on the key sources of income and economic status of watershed residents, and the most significant environmental challenges stemming from existing economic activities were identified. Subsequently, the SWOT framework was utilized for strategy identification. A Likert five-point spectrum questionnaire, completed by two groups comprising experts and local communities, was employed to gauge the relative weights of internal and external factors. The Delphi technique was employed to ascertain the relative weights of these factors. Considering these factors, strategies were devised for achieving management objectives by pairing each internal and external factor. The reliability of the questionnaires was calculated using Cronbach's alpha method of 0.89. The existence of lands prone to garden development and the conversion of low yielding rainfed lands to gardens with a rating of 0.253 were recognized as the most important components of strengths. Traditional animal husbandry, the imbalance between livestock and the capacity of pastures in the region, and excessive density of livestock in pastures were selected as the most important weaknesses with a rank of 0.25. The tendency of non-native people to invest was recognized as the most important component of opportunity with a rank of 0.215. Partiality and non-implementation of the land preparation program was selected as the most important threat in this watershed with a rating of 0.301. The stockholders of Shulabad Watershed have a desire to create gardens instead of rainfed cultivation with very low efficiency, so it is necessary to provide facilities and educational and promotion programs in order to expand this importance. Reverse migration can be provided by helping alternative livelihoods, especially the development of gardens and tourism.

Highlights

- Land suitable for orchards is a key strength for Shulabad Watershed.
- Overgrazing and livestock imbalance degrade Shulabad's environment.
- Non-native investment offers economic growth for Shulabad.
- Poor land management threatens Shulabad's sustainable development.
- Tourism potential in Shulabad is high but lacks promotion.

1. Introduction

The essence of management should be accompanied by comprehensiveness and integration. However, the concept of comprehensive or integrated watershed management emerged due to the separate management of resources within watersheds (sectoral management) and the resulting environmental hazards, as well as the decline in ecosystem services due to the disruption of watershed health (Reed et

* Corresponding author.
E-mail address: e.karimi64@gmail.com
https://doi.org/10.22034/jelsa.2025.475987.1083

al., 2009; Mirchi et al., 2010). Considering the natural, economic, and social conditions governing Iran's watersheds, there is a strong need to adopt and implement this model. The necessity of implementing different levels of management and planning, as well as adopting a "strategy" (which represents the highest level), in the country's watersheds requires a long-term "attitude" toward the "allocation" of resources and "scientific (Karimi Sangchini *et al*., 2017). Integrated watershed management has been proposed as a new paradigm for managing natural resources, emphasizing the socio-economic characteristics of the region to sustain livelihoods without vulnerability to essential resources and to enhance the well-being of the residents in these areas (Lee and Chung, 2007; McDuff et al., 2008; Ratha and Agrawal, 2015). The overarching goal of comprehensive watershed management is to develop sustainable rural livelihoods based on the integrated management of natural resources, with the active participation of all stakeholders (Promburom, 2010; Thapa et al., 2022). Integrated watershed management is presented as both a new concept and a fresh approach to planning and development concerning water, soil, and vegetation management, with special emphasis on economic, social, and environmental issues, seeking to create collaborative solutions within these domains. The foundational philosophy of watershed management advocates for a comprehensive, integrated approach to natural resource management. The purpose of this approach is to foster integration and coordination in managing the natural and social resources of watersheds through people-oriented programs (Gleick, 2003; Pahl-Wostl, 2009; Mutekanga, 2012; Yavuz and Baycan, 2014).

The application of the SWOT model is extensive, serving as a conceptual framework for system analysis. It allows for the examination of factors and the comparison of bottlenecks, threats, detrimental aspects, opportunities, demands, and conditions of the external environment while assessing the strengths and weaknesses of a strategy (Ebener and Smith, 2015; Azubuike et al., 2018; Mallick et al., 2020). Within this model, weaknesses, opportunities, and threats are categorized and discussed, leading to the formulation of strategies based on these factors (Marsall, 2006; Wheelen and Hunger, 2017; Grant, 2019; Patel et al., 2022). Specifically, SWOT is an acronym representing strengths, weaknesses, opportunities, and threats. SWOT analysis is a widely utilized tool for simultaneously analyzing internal and external environments, thereby determining a systematic approach for decision-making (Yuksel and Dagdeviren, 2007; Helms and Nixon, 2010; Shahba et al., 2017). This model aims to provide possible strategies by quantifying internal factors (weaknesses and strengths) and external factors (opportunities and threats) as well as the interaction between these factors (Nikolaou and Evangelinos, 2010; David, 2015; Sarsby, 2016). SWOT analysis systematically identifies factors that should best align with the strategy. The rationale behind this approach is that an effective strategy should maximize the system's strengths and opportunities while minimizing its weaknesses and threats. When applied correctly, this logic yields favorable outcomes for the selection and design of an effective strategy (Yavuz and Baycan, 2013; Bakalár et al., 2021; Nasiri Khiavi et al., 2024). Effective planning for the proper management of an execution plan necessitates a comprehensive understanding of issues, problems, and challenges, on one hand, and strengths and opportunities on the other. Thus, internal and external factors, including challenges and impediments, as well as potentials and opportunities, should be investigated to determine optimal strategies. Among the various models and methods available for strategic management and planning, the SWOT matrix method is regarded as one of the most common approaches for strategy formulation (Pahl and Richter, 2009; Giusti et al., 2016; Bassi et al., 2024). One of the critical steps in implementing integrated watershed management strategies is the determination and compilation of these strategies. Various methods and models are available for this purpose, each encompassing its own concepts, insights, and specific techniques. Among them, the SWOT model, which evaluates strengths, weaknesses, opportunities, and threats of the system, has gained widespread recognition. Today, this method is employed by designers to assess strategy as a contemporary tool for performance analysis and strategy formulation (Wickramasinghe, 2009; Heshmati et al., 2022). Consequently, the SWOT model is an effective group decision-making tool designed for establishing long-term or short-term strategies and informing critical decisions regarding various issues. This model can be applied to an organization or company, or it can focus on a particular geographical area or issue that is of relevance to us. The primary objective of this model is to develop strategies that enhance efficiency or improve situations (Kurttila, 2000; Policastro, 2001; Savari et al., 2022).

Designing a comprehensive watershed management model for the Shulabad Watershed is crucial in light of climate change, water resource depletion, droughts, floods, deforestation, and the degradation of forests and pastures. This model should encompass components and elements that comprehensively address watershed management while utilizing innovative and effective tools for conserving and efficiently utilizing natural resources (Lee and Chung, 2007; Gleick, 1998; Sanchez et al., 2014). Some of the components that should be considered in the comprehensive watershed management model for the Shulabad Watershed include: Analysis of the Current Situation: A thorough assessment of the current status of the watershed, including water resources, soil, forests, pastures, economic and social conditions, and the impacts of climate change. Identification and Analysis of Problems and Challenges (Worden, 2024): Assessing the primary issues in the watershed, such as water resource depletion, deforestation, and the impacts of floods and droughts. Setting Priorities and Objectives: Determining strategic priorities and management goals, including the preservation of water and soil resources, flood and drought control, and promoting sustainable development and utilization of forests and pastures (Karimi Sangchini et al., 2022). Formulating Strategies and Operational Plans: Developing strategies and operational plans to achieve management objectives, including the adoption of

innovative technologies, promotion of sustainable agriculture, and encouragement of green economic development. The Shulabad watershed faces numerous challenges related to soil erosion and susceptibility to flooding. The steep slopes of this mountainous region, combined with extensive grazing practices, have exacerbated the problems associated with this watershed. Alongside these challenges, the area possesses significant development potential in terms of tourism, owing to its rich natural and geological features, which are conducive to ecotourism and geotourism. The presence of the Chakan Waterfall and mountain ranges with elevations exceeding 4,000 meters can create opportunities for the development of this industry. Therefore, the purpose of this research is to assess the weaknesses, strengths, threats, and opportunities in the Shulabad Watershed, which will lay the groundwork for determining comprehensive management strategies.

2. Materials and Methods

2.1. The study area

The Shulabad Watershed is located between 33° 15′ to 43° 52′ N and 48° 04′ to 48° 46′ E. This watershed constitutes in the upstream areas of the Karun River basin, originating from the Persian Gulf and the Oman Sea sub-basins. The area of the Shulabad Watershed is 5,484 square kilometers, classified as a medium-sized basin. The average elevation of the entire study area is 2,495 meters above sea level. The average slope of the Shulabad Watershed is estimated at 9.53 percent, indicating a steep terrain. The average annual precipitation, based on the correlation between precipitation and elevation, is approximately 835.2 millimeters. About 262 millimeters, or approximately 31.41 percent of the total annual precipitation, falls as snow in this watershed. Roughly, 46 percent of the study area comprises rocky terrain, while approximately 35 percent is covered by sparse forests with medium density.

2.2. The SWOT Framework

The SWOT framework is a strategic analysis tool used to evaluate the internal (Strengths and Weaknesses) and external (Opportunities and Threats) factors of an organization or situation. Typically employed in the strategic planning process, this tool assists managers in making informed decisions based on a comprehensive analysis of the internal and external environment of the organization (Pahl and Richter, 2009; Azubuike et al., 2018). In the context of integrated watershed management, this framework serves as a valuable tool for assessing the current and future status of watersheds and water resource management. Specifically (Kangas et al., 2001; Ebener and Smith, 2015): Strengths: These encompass the characteristics, resources, and activities existing within the watershed that have the potential to create a competitive advantage for watershed management. For instance, abundant water resources, advanced technologies in water resource management, and strong collaboration with local communities and other relevant institutions. Weaknesses: These include limitations, weaknesses, and deficiencies present in the current watershed management. For example, declining water resources due to deforestation, challenges in water and wastewater management, and lack of coordination among stakeholders in watershed issues. Opportunities: These consist of trends, environmental changes, and opportunities available for improving the watershed situation. For instance, increasing attention to environmental conservation and sustainable development, growing international cooperation in water resource management. Threats: These encompass external factors such as competition, changes in laws and regulations, and other threats to watershed management. For example, decreasing water resources due to climate change competition for access to water resources, and conflicts in differing water use needs (Kurttila et al., 2000; Sarsby, 2016). Through the utilization of SWOT analysis, managers can develop strategies that capitalize on strengths to exploit opportunities, while also addressing weaknesses and threats to prepare plans for problem-solving and future threat mitigation (Pahl and Richter, 2009; Sarsby, 2016; Bassi et al., 2024).

2.3. Water quality index based on industrial uses

This study employed a research methodology that integrates library research, resource analysis, and interviews conducted via questionnaires to propose strategic frameworks for comprehensive watershed management in the Shulabad region. Initially, the Delphi method was utilized to identify factors influencing comprehensive watershed management. Subsequently, these factors were prioritized through questionnaires administered to a team of experts (Fabbri, 1998; Chang et al., 2010; Ruiz et al., 2012; Karimi Sangchini et al., 2022; Kibria et al., 2024). The Delphi method, originally developed for systematic prediction and interactive communication, relies on expert consensus and is predominantly employed in futures studies to uncover innovative and reliable ideas or to provide relevant information for decision-making (Wickramasinghe et al., 2009; Karimi Sangchini et al., 2017; Worden et al., 2024). The sample comprised 27 individuals, including experts and academic scholars, to determine the components of the SWOT model in the Shulabad Watershed area. Insights were gathered from university professors in Lorestan and personnel from the Research and Education Center for Agriculture and Natural Resources of Lorestan Province, alongside officials from the Agricultural Jihad and Natural Resources departments of Shulabad City, and watershed operators. In the final stage, in addition to identifying significant factors within each of the strength, weakness, opportunity, and threat criteria, requisite management strategies were defined based on the contextual specifics of Lorestan Province through SWOT analysis. SWOT analysis involves evaluating both internal factors (strengths and weaknesses) and external factors (opportunities and threats) pertinent to the subject under study. Strengths are characteristics that facilitate the achievement of organizational goals, while weaknesses are attributes that hinder goal attainment (Heshmati et al., 2022). Opportunities encompass external environmental

conditions that can positively impact goal achievement, whereas threats denote external environmental conditions that can impede goal attainment (Nasiri Khiavi et al., 2024). The strategies resulting from the SWOT analysis are presented in Table 1. To prioritize weaknesses, strengths, opportunities, and threats, it is essential not only to consider the weights obtained during the survey process from experts but also to assess the weight of each item within each criterion in relation to other items across different criteria (Kibria et al., 2024).

Table 1. Comparative SWOT matrix for strategy development (Policastro, 2001)

	External factors		
Internal factors	Opportunity	Threats	
Strengh	Offensive strategy	Conservative strategy	
Weakness	Competitive Strategy	Defensive Strategy	

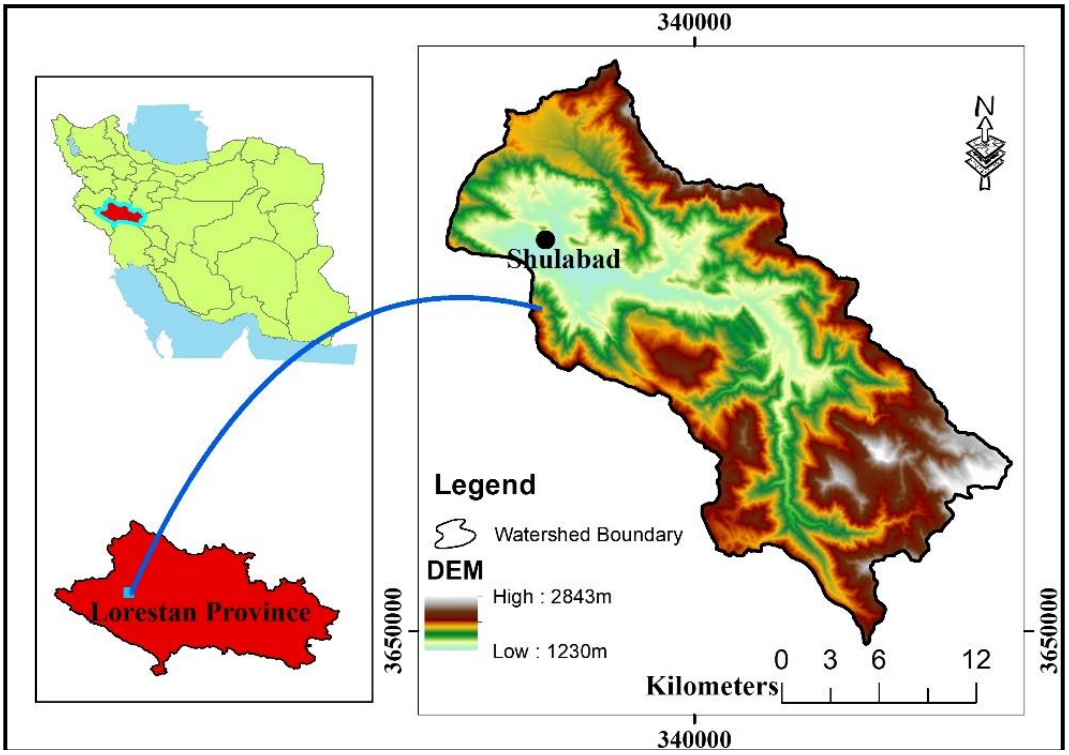

Figure 1. Location Shulabad Watershed in Lorestan Province and Iran

3. Results and discussion

The reliability of the questionnaires, considered as the trustworthiness of the measurement tool, was calculated using the Cronbach's alpha method, resulting in a coefficient of 0.89. This indicates that the questionnaires employed in this study exhibited appropriate reliability. The results obtained from expert surveys, involving experts, specialists, and stakeholders in the Shulabad Watershed area, regarding the strengths, weaknesses, opportunities, and threats facing comprehensive watershed management, were derived from the questionnaires. For ranking purposes, each criterion was assigned a position ranging from 1 to 4 based on its respective weight within one of the categories.The criteria for effectiveness included: The impact of threats on exacerbating weaknesses and hindering opportunities. The influence of weaknesses on exacerbating threats and failing to leverage strengths and opportunities. The effect of strengths on leveraging opportunities, reducing weaknesses, and addressing threats. The effect of capitalizing on opportunities to enhance strengths, mitigate weaknesses, and address threats (Savari and Shokati Amghani, 2022). Subsequently, the average score of each criterion (derived from expert evaluation) was divided by the total scores of the criteria for internal factors (weaknesses and strengths) to calculate the importance coefficient of each criterion relative to the total. The same methodology was applied to external factors (opportunities and threats). Multiplying the importance coefficient by the rank of each criterion yielded the final score for that criterion. This approach facilitates consensus among experts on the criteria and serves as the foundation for designing and implementing strategies for comprehensive watershed management. These strategies are formulated based on a comprehensive matrix juxtaposing internal factors (weaknesses and strengths) against external factors (opportunities and threats (Shahba et al., 2017). In the next step, the average score of each item (resulting from the experts' survey) was divided by the total scores of the internal factors (weaknesses and strengths) to obtain the importance coefficient of each item as a ratio of the total (see Table 2). The same procedure was applied to the external factors (opportunities and threats). By multiplying the importance coefficient by the impact rating of each item, the final score for that item was calculated

(see Table 3). This methodology allows for an understanding of the consensus among experts regarding the issues and establishes the cornerstone for the design and formulation of comprehensive management strategies for the Shulabad Watershed. To develop these strategies, the list of internal factors (weaknesses and strengths) was juxtaposed against the list of external factors (opportunities and threats) in a large matrix to address related issues. Table 4 displays the top items in each component. The ST area focuses on addressing upcoming threats and transforming threats into opportunities. The WT zone represents a fallback or reduction strategy aimed at decreasing the level of debilitating activities. The SO region emphasizes developmental strategies that prioritize strengths and opportunities. Finally, the WO area suggests that, based on the identified weaknesses and available opportunities, activities should shift from weaknesses toward opportunities.

Table 2. Results of the Internal Factors Evaluation (IFE) Matrix for Shulabad Watershed

Row	Component Type	Criteria List	Mean Importance	Adjusted Importance	Criterion Rank	Final Importance
1	Strengths	Adequate mountainous rainfall and abundant water resources in the watershed	4.80	0.062	2	0.123
2		Potential for alternative livelihoods (medicinal and industrial plants, beekeeping, and aquaculture development)	4.53	0.058	4	0.233
3		Availability of skilled human labor	3.40	0.044	1	0.044
4		Social acceptance and feasibility of implementing natural resource rehabilitation and restoration programs	3.53	0.045	2	0.091
5		Ecotourism and geotourism attractions	4.60	0.059	4	0.236
6		Potential for renewable energy production (solar and wind)	2.87	0.037	3	0.110
7		Livestock activities, livestock products, and expansion of livestock and aquaculture	4.60	0.059	3	0.177
8		Availability of suitable land for horticultural development and conversion of low-yield rainfed lands to orchards	4.93	0.063	4	0.253
1	Weaknesses	Distance from provincial and county centers and limited infrastructure development	5.00	0.064	3	0.192
2		Proliferation of smallholder ownership in agriculture, lack of appropriate cultivation patterns, and weakness in cooperative and group participation	4.93	0.063	3	0.190
3		Poverty, unemployment, and rural migration	4.47	0.057	3	0.172

Table 2. (Continued)

Row	Component Type	Criteria List	Mean Importance	Adjusted Importance	Criterion Rank	Final Importance
4		Excessive dependence of household livelihoods on natural resources	3.27	0.042	2	0.084
5		Lack of technical knowledge among operators in the cultivation and propagation of seedlings and fruit trees, cultivation of medicinal plants, and pest control	4.33	0.056	1	0.056
6		Deforestation, rangeland degradation, and land use change from forest and rangeland to agriculture	4.20	0.054	3	0.162
7		Severe cold in winter and lack of adequate tourism facilities in cold months	4.27	0.055	2	0.109
8		Traditional animal husbandry and imbalance between livestock and rangeland capacity in the area, excessive livestock density in rangelands	4.87	0.062	4	0.250
9		Non-compliance with the timing of livestock entry and exit to rangelands	4.73	0.061	2	0.121
10		Biophysical obstacles or environmental hazards (rough and impassable topography, avalanche risk, erosion, floods, mass and debris flows, riverbank erosion)	4.60	0.059	3	0.177
Total Score		If the table is to span more than one page, it must have a title on every page.	77.93	1	49	2.780

Table 3. Results of the External Factors Evaluation (EFE) Matrix for Shulabad Watershed

Row	Component Type	Criteria List	Mean Importance	Adjusted Importance	Criterion Rank	Final Importance
1	Opportunities	Non-native individuals' inclination toward investment	3.33	0.054	4	0.215
2		Possibility of supportive reverse migration	2.40	0.039	3	0.116
3		Availability of low-interest facilities for livestock breeders and farmers	3.33	0.054	3	0.161
4		Introduction of watershed tourism attractions to attract tourists and even international tourists	2.33	0.038	3	0.113
5		Capacity for the production of herbal products, proximity to major distillation and packaging factories of flowers and medicinal plants, such as workshops in Aligudarz and Mahallat	4.40	0.071	3	0.213
6		Seizing the opportunity to utilize graduates	3.47	0.056	2	0.112
1	Threats	Climate change impact (warming, evaporation, drought, flood, and desertification), reduction of biodiversity, and species extinction	4.67	0.075	3	0.226
2		Vulnerability of sales of products produced by farmers and gardeners to imports	3.93	0.063	2	0.127
3		Lack of pricing system for agricultural and livestock products	4.80	0.077	2	0.155

Table 3. (Continued)

Row	Component Type	Criteria List	Mean Importance	Adjusted Importance	Criterion Rank	Final Importance
4		Fragmented vision and failure to implement land improvement programs	4.67	0.075	4	0.301
5		Currency devaluation and the impact of inflation on the price of seeds, pesticides, and agricultural and livestock inputs	4.73	0.076	3	0.229
6		Spread of human, animal, and joint human-animal diseases from outside the watershed	4.13	0.067	1	0.067
7		Possibility of pests and plant diseases spreading from outside the watershed	3.33	0.054	1	0.054
8		Removal of government support in agriculture and incomplete coverage of agricultural and livestock product damages	4.20	0.068	3	0.203
9		Attraction of surrounding city migration	3.40	0.055	4	0.219
10		Passage of nomads outside the watershed and severe rangeland degradation	4.93	0.079	3	0.238
Total Score			62.07	1	44	2.747

Table 4. Top Indicators in Each Component of the SWOT Model for the Shulabad Watershed

Rank	Strengths	Rank	Weaknesses
1	Existence of suitable lands for agricultural development and conversion of low-productivity rainfed lands into orchards	1	Traditional animal husbandry and imbalance between livestock and rangeland capacity in the area, excessive grazing pressure on rangelands
2	Ecotourism and geotourism attractions	2	Distance from provincial and county centers and inadequate infrastructure development
3	Potential for alternative livelihoods (medicinal and industrial plants, beekeeping, and aquaculture development)	3	Spread of small-scale ownership in the agricultural sector, lack of appropriate cultivation patterns, and weakness in cooperatives and group participation
4	Existence of livestock activities and products, and aquaculture development	4	Biophysical obstacles or environmental hazards (rough and impassable topography, risk of landslides, water erosion, floods, mass, and debris flows, and riverbank erosion)
Rank	**Opportunities**	**Rank**	**Threats**
1	Interest of non-native individuals in investment	1	Partial view and non-implementation of land improvement programs
2	Capacity to produce medicinal plants, proximity to important distillation and packaging factories of medicinal plants including workshops in the city of Aligudarz and districts	2	Migration of nomads outside the watershed and severe degradation of rangelands
3	Availability of low-interest facilities to livestock farmers and agriculturists	3	Decrease in the value of the national currency and the impact of inflation on the price of seeds, pesticides, and agricultural and livestock inputs
4	Possibility of reverse migration support	4	Climate change effects (warming, evaporation, drought, floods, and desertification) leading to reduced biodiversity and species extinction

The researches of Bakalár et al. (2021) and Nasiri Khiavi et al. (2024) are also in this direction and they introduced the SWOT approach in the comprehensive management of water and soil resources. They also considered it important to use the opinions of local communities, experts and policymakers to formulate strengths, weaknesses, opportunities and threats.

The distance from provincial and county centers and limited infrastructure development with a weight of 192.0 has a very high effectiveness among weakness factors in the comprehensive management of the Shulabad Watershed. This is while the lack of technical knowledge among operators in planting and cultivating seedlings, fruit trees, medicinal plants, and combating plant diseases with a weight of 0.056 has very low effectiveness among weakness factors in the comprehensive management of the Shulabad Watershed. The main problem and weakness of the Shulabad Watershed is its distance from important population centers, which can lead to more problems. The long distance from population centers, coupled with difficult access, results in low welfare facilities. Due to the low agricultural land area and the lack of dependence on agriculture, technical knowledge in planting, maintaining, and harvesting agricultural products has received low priority.

In the research of Reed et al. (2009), Sanchez et al. (2014), Karimi Sangchini et al. (2007) and Worden et al. (2024) people's participation has been emphasized. It should also be noted that future management plans for this mountainous watershed with steep slopes should be considered. Unfortunately, skilled labor in this area has migrated due to lack of employment, limited welfare facilities, and urban attractiveness, posing challenges in this regard. However, alternative livelihood support, especially the development of orchards and tourism, can facilitate reverse migration.

Among the opportunities, the factor of non-native individuals' inclination to invest with a weight of 0.215 has

very high effectiveness, while the factors of introducing attractions of the watershed for attracting tourists, and even cross-border tourists, with a final weight of 113.0 have the lowest importance. Due to the significant tourism attractions in this area and the abundant water potential, the inclination of non-native individuals to invest in tourism, aquaculture, and agriculture sectors is high, but unfortunately, there is a weakness in introducing tourist attractions, especially to foreign tourists. One of the reasons for the low investment in these areas is the lack of welfare facilities, appropriate access roads, and the difficult access to the watershed. Partial views and failure to implement land improvement programs among the factors studied in threats with a weight of 301.0 have the highest effectiveness. Also, the possibility of the spread of plant pests and diseases from outside the watershed with a weight of 0.054 has the lowest effectiveness among the threats to the comprehensive management of the Shulabad Watershed. A major problem in many watershed areas of the country in the current conditions is partial views and failure to implement land improvement programs, which is hoped to be resolved by passing the land improvement and integrated watershed management plan, shifting from a partial approach to a holistic and systemic approach. In the researches of Thapa et al. (2022), Yavuz and Baycan, (2013), Karimi Sangchini et al. (2022) and Nasiri Khiavi et al. (2024) a comprehensive approach in watershed management is mentioned.

4. Conclusion

This study has been conducted to find the weaknesses, strengths, threats and opportunities of the Shulabad watershed, with the ultimate goal of achieving a comprehensive management of this watershed. To implement this objective, co-management approach and stakeholders' opinions were used to gather strengths (S), weaknesses (W), opportunities (O) and threats (T). In this regard, semi-structured interviews with local stakeholders, technical experts and policy makers were conducted to collect and formulate strengths, weaknesses, opportunities and threats, briefly known as SWOT.

Analysis of the identified strengths factors in the comprehensive management of the Shulabad Watershed shows that the presence of land suitable for horticultural development and the conversion of low-productivity rainfed lands to orchards with a weight of 0.25 has a higher effectiveness and importance among other factors. Also, the presence of skilled human resources in Shulabad Watershed with a weight of 0.4 has very low effectiveness and importance. This indicates that the stakeholders in the Shulabad Watershed prefer to establish orchards instead of low-yield rainfed cultivation, which requires facilitation and promotion programs to expand this initiative.

The problems of the watershed in terms of forest and pasture destruction, including traditional animal husbandry and imbalance between livestock and pasture capacity, excessive livestock density in pastures, premature grazing, excessive dependence of operators on natural resources, the passage of external nomads, and severe destruction of pastures provide grounds for proposing this strategy. Unfortunately, the lack of human resources for the protection and restoration of forests and pastures in this watershed is evident. It is recommended to prioritize the employment of human resources and engage community participation. The strategy of water and soil conservation measures and farm management can be considered as a defensive strategy (WT). This strategy, considering the biophysical obstacles or environmental hazards (including rough and impassable topography, risk of avalanches, water erosion, floods, mass movements, and riverbank erosion) in the Shulabad Watershed and the presence of steep and heavily eroded agricultural lands, is proposed. Allocating appropriate facilities for the development of mechanized agriculture and terracing steep lands is suggested.

Acknowledgements

This article is taken from a part of the results of a research project with the approved code 01-29-29-034-010953 in the Agricultural Research, Education and Extension Organization and from the respected officials of the SCWMRI, and Lorestan Agricultural and Natural Resources Research and Education Center.

References

Azubuike, S. I., Songi, O., Irowarisima, M., & Chinda, J. K. (2018). Identifying policy and legal issues for shale gas development in Algeria: A SWOT analysis. *The Extractive Industries and Society*, *5*(4), 469-480. https://doi.org/10.1016/j.exis.2018.10.005

Bakalár, T., Pavolová, H., & Tokarčík, A. (2021). Analysis and model of river basin sustainable management by SWOT and AHP methods. *Water*, *13*(17), 2427. https://doi.org/10.3390/w13172427

Bassi, D. B., Bahl, S. G., Gopal, S., Sethi, V., Backholer, K., Gavaravarapu, S. M., … Arora, M. (2024). Are advertising policies affirmative in restricting the marketing of foods high in fat, salt and sugar (HFSS) in India?: Evidence from SWOT Analysis. *The Lancet Regional Health – Southeast Asia*, *21*, 100315. https://doi.org/10.1016/j.lansea.2023.100315

Chang, C.-H., Lin, J.-J., Lin, J.-H., & Chiang, M.-C. (2010). Domestic open-end equity mutual fund performance evaluation using extended TOPSIS method with different distance approaches. *Expert Systems with Applications*, *37*(6), 4642-4649. https://doi.org/10.1016/j.eswa.2009.12.044

David, F. R. (2015). *Strategic management: Concepts and cases*. Pearson Education.

Ebener, D. R., & Smith, F. L. (2015). *Strategic planning: An interactive process for leaders*. Paulist Press.

Fabbri, K. P. (1998). A methodology for supporting decision making in integrated coastal zone management. *Ocean & Coastal Management, 39*(1–2), 51-62. https://doi.org/10.1016/s0964-5691(98)00013-1

Giusti, A., & Maggini, M. (2016). SWOT analysis of policies and programs on prevention and management of diabetes across Europe. *European Journal of Public*

Health, *26*(suppl_1), ckw168.030. https://doi.org/10.1093/eurpub/ckw168.030

Gleick, P. H. (1998). Water in crisis: Paths to sustainable water use. *Ecological Applications*, *8*(3), 571-579.

Gleick, P. H. (2003). Global freshwater resources: Soft-path solutions for the 21st century. *Science*, *302*(5650), 1524-1528. https://doi.org/10.1126/science.1089967

Grant, R. M. (2019). *Contemporary strategy analysis: Text and cases edition*. Wiley.

Helms, M. M., & Nixon, J. (2010). Exploring SWOT analysis – where are we now?: A review of academic research from the last decade. *Journal of Strategy and Management*, *3*(3), 215-251. https://doi.org/10.1108/17554251011064837

Heshmati, M., Gheitury, M., & Shadfar, S. (2022). Factors affecting possibility of ecotourism development and sustaining natural resources using SWOT approach in west Iran. *International Journal of Geoheritage and Parks*, *10*(2), 173-183. https://doi.org/10.1016/j.ijgeop.2022.03.004

Kangas, J., Pesonen, M., Kurttila, M., & Kajanus, M. (2001). WOT: Integrating the AHP with SWOT analysis. In *Sixth International Symposium on the Analytic Hierarchy Process – ISAHP 2001* (pp. 189-198). Bern, Switzerland.

Karimi Sangchini, E., Salehpour Jam, A., & Mosaffaie, J. (2022). Flood risk management in Khorramabad watershed using the DPSIR framework. *Natural Hazards*, *122*(1), 3101-3121. https://doi.org/10.1007/s11069-022-05538-7

Karimi Sangchini, E., Islam, I., Farajollahi, A., Arami, S. A., & Jafari, M. (2017). Development and prioritization of socio-economic strategies to elevate public participation in natural resource management using TOPSIS approach: Case study, Chaharmahal and Bakhtiari Province (Iran). *Journal of Applied Sciences and Environmental Management*, *21*(3), 476-485. https://doi.org/10.4314/jasem.v21i3.7

Kibria, E., Seekamp, E., Xiao, X., Dalyander, S., & Eaton, M. (2024). Multi-criteria decision approach for climate adaptation of cultural resources along the Atlantic coast of the southeastern United States: Application of AHP method. *Climate Risk Management*, *43*, 100587. https://doi.org/10.1016/j.crm.2024.100587

Kurttila, M., Pesonen, M., Kangas, J., & Kajanus, M. (2000). Utilizing the analytic hierarchy process (AHP) in SWOT analysis – a hybrid method and its application to a forest-certification case. *Forest Policy and Economics*, *1*(1), 41-52. https://doi.org/10.1016/s1389-9341(99)00024-7

Lee, K. S., & Chung, E.-S. (2007). Development of integrated watershed management schemes for an intensively urbanized region in Korea. *Journal of Hydro-environment Research*, *1*(2), 95-109. https://doi.org/10.1016/j.jher.2007.07.004

Mallick, S. K., Rudra, S., & Samanta, R. (2020). Sustainable ecotourism development using SWOT and QSPM approach: A study on Rameswaram, Tamil Nadu. *International Journal of Geoheritage and Parks*, *8*(3), 185-193. https://doi.org/10.1016/j.ijgeop.2020.06.001

Marsall, C. T., Mullins, G., & Allen, R. (2006). Teaching SWOT analysis.

McDuff, M., Appelson, G. S., Jacobson, S. K., & Israel, G. D. (2008). Watershed management in north Florida: Public knowledge, attitudes and information needs. *Lake and Reservoir Management*, *24*(1), 47-56. https://doi.org/10.1080/07438140809354692

Mirchi, A., Watkins Jr, D., & Madani, K. (2010). Modeling for watershed planning, management, and decision making. In *Watersheds: Management, restoration and environmental impact* (pp. 354-392).

Mutekanga, F. (2012). *Participatory policy development for integrated watershed management in Uganda's highlands* (Doctoral dissertation). Wageningen University.

Nasiri Khiavi, A., Vafakhah, M., & Sadeghi, S. H. (2024). Comparative applicability of MCDM-SWOT based techniques for developing integrated watershed management framework. *Natural Resource Modeling*, *36*(4), e12380. https://doi.org/10.1111/nrm.12380

Nikolaou, I. E., & Evangelinos, K. I. (2010). A SWOT analysis of environmental management practices in Greek mining and mineral industry. *Resources Policy*, *35*(3), 226-234. https://doi.org/10.1016/j.resourpol.2010.03.001

Pahl, N., & Richter, A. (2009). *SWOT analysis: Idea, methodology and a practical approach*. GRIN Verlag.

Pahl-Wostl, C. (2009). A conceptual framework for analysing adaptive capacity and multi-level learning processes in resource governance regimes. *Global Environmental Change*, *19*(3), 354-365. https://doi.org/10.1016/j.gloenvcha.2009.06.001

Patel, K., Nayak, B., Behera, T. R., Mandal, N., Rana, S., Gupta, N., … Palo, S. K. (2022). Factors influencing, SWOT analysis and emerged strategies for improving the use of digital data platforms in immunization program by frontline health care providers: A study from rural Eastern India. *International Journal of Community Medicine and Public Health*, *9*(11), 4091-4097. https://doi.org/10.18203/2394-6040.ijcmph20222901

Policastro, M. L. (2001). *Introduction to strategic planning*. Routledge.

Promburom, P. (2010). *Companion modeling and watershed management in Northern Thailand: The importance of local networks* (Doctoral dissertation). University of Lyon.

Ratha, D., & Agrawal, V. P. (2015). A digraph permanent approach to evaluation and analysis of integrated watershed management system. *Journal of Hydrology*, *525*, 188-196. https://doi.org/10.1016/j.jhydrol.2015.03.046

Reed, M. S., Graves, A., Dandy, N., Posthumus, H., Hubacek, K., Morris, J., & Stringer, L. C. (2009). Who's in and why? A typology of stakeholder analysis methods for natural resource management. *Journal of Environmental Management*, *90*(5), 1933-1949. https://doi.org/10.1016/j.jenvman.2008.12.012

Ruiz, M. C., Romero, E., Pérez, M. A., & Fernández, I. (2012). Development and application of a multi-criteria spatial decision support system for planning sustainable industrial areas in Northern Spain. *Automation in Construction*, *22*, 320-333. https://doi.org/10.1016/j.autcon.2011.09.009

Sanchez, G. M., Nejadhashemi, A. P., Zhang, Z., Woznicki, S. A., Habron, G., Marquart-Pyatt, S., & Shortridge, A. (2014). Development of a socio-ecological environmental justice model for watershed-based management. *Journal of Hydrology*, *518*(A), 162-177. https://doi.org/10.1016/j.jhydrol.2013.08.014

Sarsby, A. (2016). *SWOT analysis*. Spectaris Limited.

Savari, M., & Shokati Amghani, M. (2022). SWOT-FAHP-TOWS analysis for adaptation strategies development among small-scale farmers in drought conditions. *International Journal of Disaster Risk Reduction*, *67*, 102695. https://doi.org/10.1016/j.ijdrr.2021.102695

Shahba, R., Arjmandi, R., Monavari, M., & Ghodusi, J. (2017). Application of multi-attribute decision-making methods in SWOT analysis of mine waste management (case study: Sirjan's Golgohar iron mine, Iran). *Resources Policy*, *51*, 67-76. https://doi.org/10.1016/j.resourpol.2016.11.002

Thapa, P., Chaudhary, S., & Dasgupta, P. (2022). Corrigendum to "Contribution of integrated watershed management (IWM) to disaster risk reduction and community development: Lessons from Nepal" [*International Journal of Disaster Risk Reduction*, *76*, 103029]. *International Journal of Disaster Risk Reduction*, *79*, 103108. https://doi.org/10.1016/j.ijdrr.2022.103108

Wheelen, T. L., & Hunger, J. D. (2017). *Strategic management and business policy: Globalization, innovation and sustainability*. Pearson Education.

Wickramasinghe, V., Saman Kumara, V., & Takano, S. (2009). Application of combined SWOT and analytic hierarchy process (AHP) for tourism revival strategic marketing planning. In *Proceedings of the Eastern Asia Society for Transportation Studies*, *7*.

Worden, S., Svobodova, K., Côte, C., & Bolz, P. (2024). Regional post-mining land use assessment: An interdisciplinary and multi-stakeholder approach. *Resources Policy*, *89*, 104680. https://doi.org/10.1016/j.resourpol.2024.104680

Yavuz, F., & Baycan, T. (2013). Use of SWOT and analytic hierarchy process integration as a participatory decision making tool in watershed management. *Procedia Technology*, *8*, 134-143. https://doi.org/10.1016/j.protcy.2013.11.020

Yavuz, F., & Baycan, T. (2014). Application of combined Analytic Hierarchy Process (AHP) and SWOT for integrated watershed management. *International Journal of the Analytic Hierarchy Process*, *6*(1), 39-55. https://doi.org/10.13033/ijahp.v6i1.193

Yuksel, E., & Dagdeviren, M. (2007). Using the analytic network process in a SWOT analysis: A case study for a textile firm. *Information Sciences*, *177*(15), 3364-3382. https://doi.org/10.1016/j.ins.2007.02.001

Agriculture, Environment & Society

Journal homepage: www.aes.uoz.ac.ir

Investigating the relationship between SPI and UNEP aridity indices with trend of the dust storm index in the central region of Iran

Ebrahim Yousefi Mobarhan*[a]

[a] Soil Conservation and Watershed Management Research Institute, Semnan Agricultural and Natural Resources Research and Education Center, Agricultural Research, Education and Extension Organization (AREEO), Semnan, Iran

ARTICLE INFO

Article history:
Received: 20 November 2024
Accepted: 21 February 2025
Available online: 30 June 2025

Keywords:
Correlation
Drought
DSI
Semnan
SPI
UNEP Index

ABSTRACT

The dust phenomenon has many dangers for human society and is of special importance for the residents of Iran. Different researchers have studied this phenomenon from different angles. In terms of the significance of the subject and the dangers arising from it, it is still at the top of the topics of interest of researchers all over the world. This research aims to use DSI, UNEP and SPI Indices in the evaluation and zoning of dust storms in Semnan Province. In this research, the temporal distribution of dust storms in Semnan, taking into account the weather conditions and the average wind speed of the study area during the years 2003 to 2017, was investigated in five synoptic stations. The homogeneity of climatic parameters and dust storm indices and the trends of these two variables were calculated using linear regression in the SPSS software environment, and after examining the changing trend of the UNEP index, the resulting information was zoned in the ArcGIS software environment. Correlation between drought indices, rainfall standard, and DSI shows that the DSI index has increased during the analyzed period at the same time as the severity of drought increased and its correlation with SPI during the 15 years was significant (R^2=0.89). These results showed that increasing the amount of drought index has a positive effect on increasing the amount of drought index, also the occurrence of dust storms has increased with the increase of the drought index.

Highlights

- DSI in Semnan rose from 2003-2017, peaking in 2011, tied to worsening drought (R^2=0.89 with SPI).
- UNEP index zones Semnan as arid, highly prone to desertification across all stations.
- SPI shows moderate drought in Damghan (-0.15), normal conditions elsewhere in Semnan.
- Dust storms surged west-to-east, linked to moderate dust days (MDS), per DSI zoning.
- June-July high winds and low moisture drive dust storms, per climatic data analysis.

1. Introduction

Droughts, which occur frequently as a natural disaster, can have various impacts on water resources including the supply and quality of water, as well as the availability of both surface and subsurface water. In addition, proper management of water resources may also be affected by droughts, as reported by several studies (van Loon et al., 2014; Amin et al., 2016; FAO, 2017; Scanlon et al., 2017). Four types of droughts are generally acknowledged, with the first one being meteorological drought. This type of drought is due to insufficient precipitation (Beguería et al., 2014; Das et al., 2016; Ahmadalipour et al., 2017; Hameed et al., 2018). The second type of drought is agricultural drought, which takes into account the deficit of moisture in the soil (Gao et al., 2014; Mishra et al., 2015; Nichol & Abbas, 2015; Vicente-Serrano et al., 2015; Yan et al., 2017; Karimi Sangchini et al., 2020). The third type of drought is hydrological drought, which refers to a deficiency of both surface and subsurface water (Barker et al., 2016; van Loon & Laaha, 2015; Zhang, 2017). The fourth type of drought is socio-economic drought, which considers the inadequacy of the water resources system caused by the other types of droughts (Huang et al., 2016; Maia et al., 2015). With the rise in global temperatures, the rate at which water moves

* Corresponding author.
E-mail address: e.yousefi.m@gmail.com
https://doi.org/10.22034/jelsa.2025.489843.1089

around the planet is increasing causing more frequent and severe instances of extreme weather like floods and droughts (Guo et al., 2019; Han et al., 2019; Ren et al., 2019; Yu et al., 2020). Drought is often measured using drought indices. However, because the concept of drought is multifaceted and difficult to define precisely, no single measure can fully capture all aspects of drought severity and the impacts it has (Vicente-Serrano et al., 2020; Lloyd-Hughes, 2014). According to Sun et al. (2019), there has been a growing trend of droughts that vary in their intensity and duration, lasting anywhere from one month to several years (Yousefi Mobarhan et al., 2023, Yousefi Mobarhan et al., 2024). Additionally, Middleton (2017) notes that dust storms have become a significant natural hazard worldwide, particularly in regions that are arid or semi-arid. This occurrence is noticeable in regions that undergo consistent droughts, minimal precipitation and moisture, unstable and susceptible soil, insufficient flora, and powerful winds (Goudie, 2018). Conversely, if an area has appropriate vegetation and beneficial environmental and ecological circumstances, the number of these storms is infrequent. They are more likely to happen in hot and arid climates with sparse and dispersed vegetation (Xiao et al., 2008; Tan, 2016; Goudie & Middleton, 2006). Due to its location on the desertification and wind erosion belt and having over 30% of its territory being arid or semi-arid, Iran is at risk of this occurrence. The recent prolonged periods of drought have led to significant portions of Iran being affected by dust storms. These storms are more frequent and severe in the eastern and western parts of the country compared to other regions, with the southeast being recognized as one of the primary sources of dust globally (Arami et al., 2018; Fiedler et al., 2014; Miri, 2020; Miri et al., 2009; Rashki et al., 2013).

The impacts of dust storms on the environment are extensive. Apart from the source regions where millions of tons of soil particles are lost, they also affect transportation and sedimentation environments. These storms cause air pollution due to the surge in dust particle concentration, posing a threat to human health, reducing visibility leading to accidents on roads, destroying farmlands, reducing crop yields, and burying residential areas. These detrimental consequences are among the effects of this phenomenon (Middleton, 2017; Miri et al., 2007; Wang et al., 2006; Xiao et al., 2008). Overall, it can be concluded that the wide expanse of dry and semi-arid climates in Iran and neighboring countries, coupled with the inappropriate utilization of water and soil resources, have led to wind erosion and the occurrence of dust and quicksand phenomena. These phenomena impact population centers, industrial regions, agricultural lands, and infrastructure structures annually (Yousefi Mobarhan & Khaleghi, 2024). Based on the research carried out in this area, it can be asserted that climate data has not been utilized for dust storm classification in Semnan province so far. The occurrence of dust storms and quicksand movements is viewed as a critical land degradation process and a significant obstacle in Iran, particularly in Semnan province. As climatic factors significantly contribute to this phenomenon, their consideration is crucial (Yousefi Mobarhan et al., 2021). Hence, it is crucial to investigate and comprehend these factors that contribute to the emergence and escalation of dust phenomena in order to prevent environmental crises in the future. This study aims to assess and categorize the dust phenomenon in Semnan province by analyzing the climatic data collected from synoptic stations. The primary objective is to explore the relationship between drought patterns, UNEP[1] method, SPI[2], and DSI[3] from 2003 to 2017 in Semnan province.

2. Materials and methods

Semnan province is located between 34˚ 17´ to 37˚ 51´ N and 51˚ 58´ to 57˚ 58´ E and approximate area of 98,000 square kilometers. This region is located on the southern slopes of the Alborz Mountain range and covers more than half of its surface area with desert plains. The elevation of the province gradually decreases from the north to south, with a difference of more than 3000 meters in height. The average altitude above sea level is 1067 meters, and it can be divided into three distinct regions: mountainous, foothills, and lowland areas. The temperature in this province ranges from 12.8 to 23.7 degrees Celsius, and the average temperature is 18.3 degrees Celsius. The annual rainfall is around 136 mm. Figure 1 shows the geographical location of the study area and the position of the synoptic stations within Semnan Province.

2.1. Analysis of climatic data

To assess both the climatic aspects and the movement of sand dunes in the region, the quality control data from Semnan Meteorological Organization was utilized. To achieve this goal, five synoptic stations were carefully chosen within the study area based on both the availability of data and the research objectives. The data collected from these stations spanned the period from 2003 to 2017, and Table 1 provides detailed information on the specifications of the selected stations.

Table 1. the characteristics of the synoptic stations of Semnan Province

Rows	Station Name	Longitude	Latitude	Sea Level (M)	Average Precipitation (mm)
1	Biyarjomand	55.81	36.09	1099	122
2	Damghan	54.32	36.15	1155	107
3	Semnan	53.42	35.59	1127	136
4	Shahroud	54.39	36.38	1325	164
5	Garmsar	52.36	35.24	899	184

2.2. Determining the Dust Storm Index (DSI)

[1] United Nations Environment Programme
[2] Standardized Precipitation Index
[3] Dust Storm Index

The DSI index was computed for a 15-year period at the synoptic stations situated in Semnan province using Eq, 1. The overall value of the DSI index was then established for Semnan province by aggregating the values obtained from each station. The annual changes in the DSI trend were analyzed through statistical and experimental means, and the gathered information was eventually categorized into zones.

$$DSI = \sum_{i=1}^{n} [(5 \times SDS) + MDS + (0.05 \times LDE)]_i \quad (1)$$

SDS = Stormy days with severe dust, total observations of dust codes, maximum daily code 33-35

MDS = Stormy days or average dust, total observations of dust codes, maximum daily code 30, 32, and 98

LDE = Days of storms or local dust, the sum of observations of dust codes, daily maximum code 07 and 09

The Dust Storm Index (DSI) was recorded at several stations during a specific period to determine the impact of drought on fine dust. Trend analysis was conducted by comparing the trends of these variables from 2003 to 2017, using least square linear regression against the relevant climate data (Yousefi et, al. 2021).

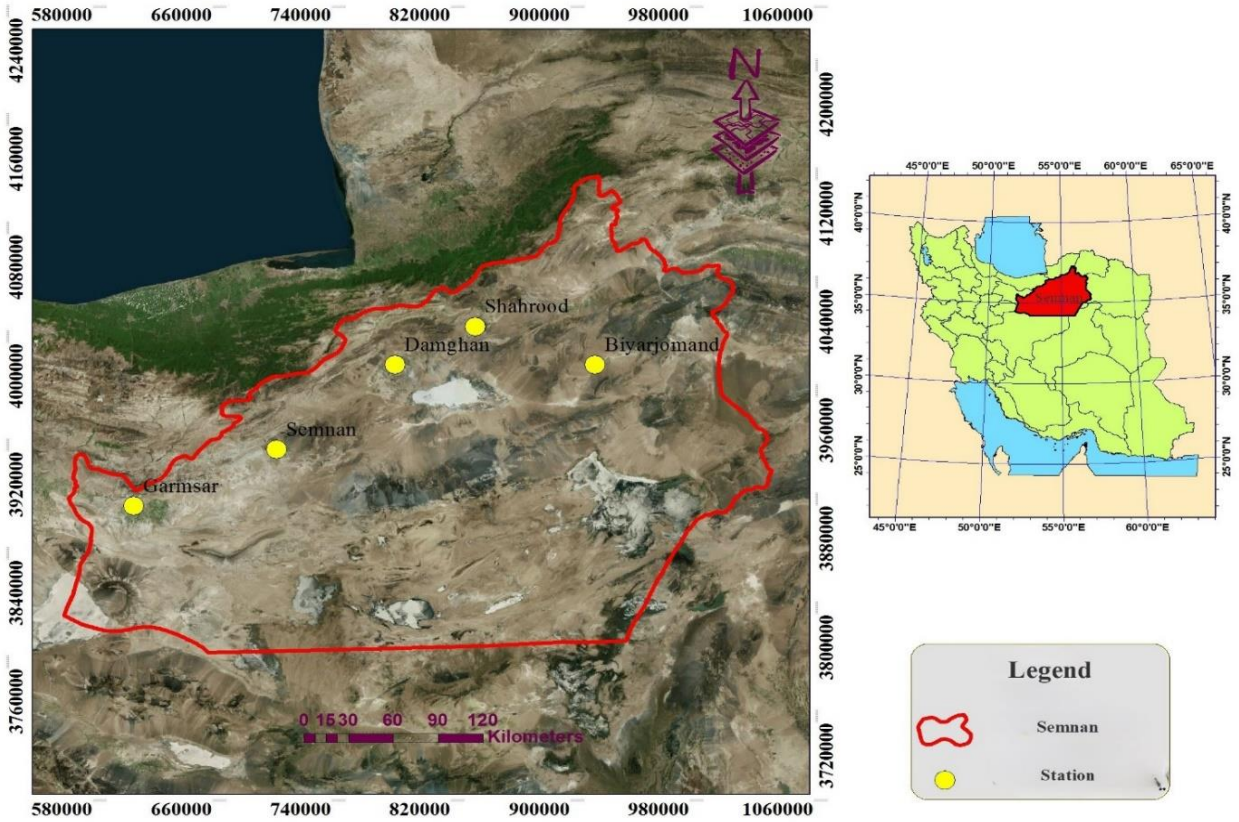

Figure 1. Geographical location of synoptic stations in the study area

2.3. Determining the Standard Rainfall Index (SPI)

To develop effective strategies for managing drought, monitoring systems play a crucial role. To quantify this phenomenon, drought indices are utilized. One such index is the Standard Precipitation Index (SPI), which measures rainfall deficits across various time scales ranging from one to 48 months (McKee et al., 1993).

The SPI is a precipitation-based drought index that assumes two hypotheses: firstly, that precipitation variability outweighs other variables like temperature and potential evaporation/transpiration, and secondly, that other variables have insignificant time trends. As one of the most commonly used indices in drought monitoring, SPI helps assess dry periods by including a time scale in its calculations. Monitoring systems for calculating SPI are vital for developing plans to manage and mitigate drought. Overall, drought indices like SPI quantify the phenomenon of rainfall deficit across various time scales. The SPI relies solely on precipitation and operates under two assumptions: firstly, that precipitation variability is significantly greater than that of other variables like temperature, evaporation, and transpiration; and secondly, that other variables do not have significant time trends. This index is widely used in drought monitoring and assesses dry periods by including a time scale.

SPI and SPEI calculations are based on average values over the area of interest, with a value of 0 indicating near-average conditions for that particular region. However, the same value for SPEI can indicate varying degrees of water stress in different regions, depending on their respective long-term averages (Parsons et al., 2019).

The time scale for drought assessment varies based on the effects it has on hydrological and agricultural resources. The time scale can range from one month to several years.

Table 2. Classification of SPI index

Severity of drought	SPI
Acute fear	<2.00
Extreme fear	1.99 – 1.55
Moderate fear	1.49 – 1.00
Normal	0.00 – 0.99
Moderate drought	0.00 - -0.99
Extreme drought	-1.00 - -1.49
Acute drought	-1.50 - -1.99

SPI calculations are solely based on precipitation data. In this study, rainfall data from a three-month period within the desired time scale was used to calculate SPI values for each station. The calculation of SPI involves Eq. 2 and two classification values are presented in the table (Yousefi Mobarhan & Zandifar, 2023).

$$SPI = \frac{X_{ik} - \overline{X_t}}{\delta i}, \quad (2)$$

2.4. Determining the aridity index of UNEP

This study utilized the UNEP aridity index (UNEP, 1991) to evaluate the level of dryness in the air and climate. The index is recognized by the United Nations Convention to Combat Desertification (UNCCD) and is a useful scientific tool for assessing the climatic conditions of regions and the likelihood of desertification. Several studies including Zare et al. (2016), Tavousi (2018), Tavosi et al. (2019), Abtahi and Darvish (2019), and Zandifar et al. (2020) have confirmed its effectiveness. Eq. 3, defined as the ratio between precipitation and potential evaporation and transpiration, is used to determine the prevailing climate and risk of desertification according to Table 3, which is based on the UNEP drought index (Yousefi Mobarhan et al., 2024).

$$I = \frac{P}{ETP} \quad (3)$$

I: UNEP index,
P: average annual precipitation (mm)
ETP: average potential evapotranspiration (mm).

Table 3. Climate zoning based on the UNEP aridity index

Climate type	Dryness index	The danger of desertification
Ultra Arid	I<0.05	Desert
Arid	0.05<I<0.2	Very Intense
Semi-Arid	0.02<I<0.5	Intense
Dry, Sub-Humid	0.5<I<0.65	Moderate
Sub-Humid	0.65<I<0.75	Low
Wet and very humid	0.75<I	NON

3. Results and analysis

3.1. Analysis

To gather comprehensive information on the condition of dusty days and dust storms in the study area, a statistical index spanning 15 years (from 2003 to 2017) was used. Graphs showing the long-term changes in precipitation, temperature, annual wind speed, evaporation, and transpiration were created using data from the synoptic stations in the Semnan province. Figure 2 displays the annual potential, while Figure 3 represents the monthly potential. The highest amount of rainfall on both the annual and monthly scales occurred in 2007 and during April and May, respectively, in the Semnan province (as illustrated in Figure 2). The data presented in Figure 2 reveals that July and August experienced the highest average, maximum and minimum temperatures, while January had the lowest. On a seasonal level, the maximum and minimum temperature events occurred during summer and winter, respectively.

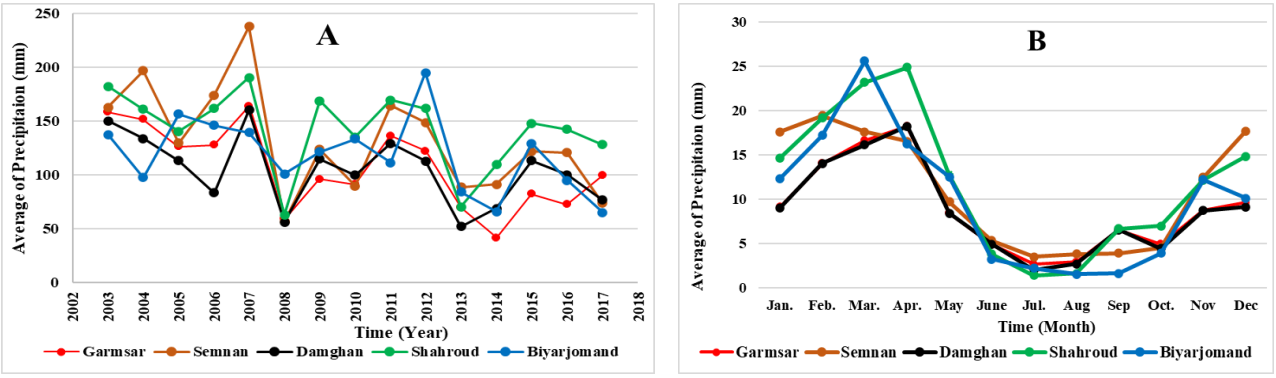

Figure 2. displays a graphical representation of the enduring alterations in yearly (A) and monthly (B) rainfall patterns observed at synoptic stations within Semnan province.

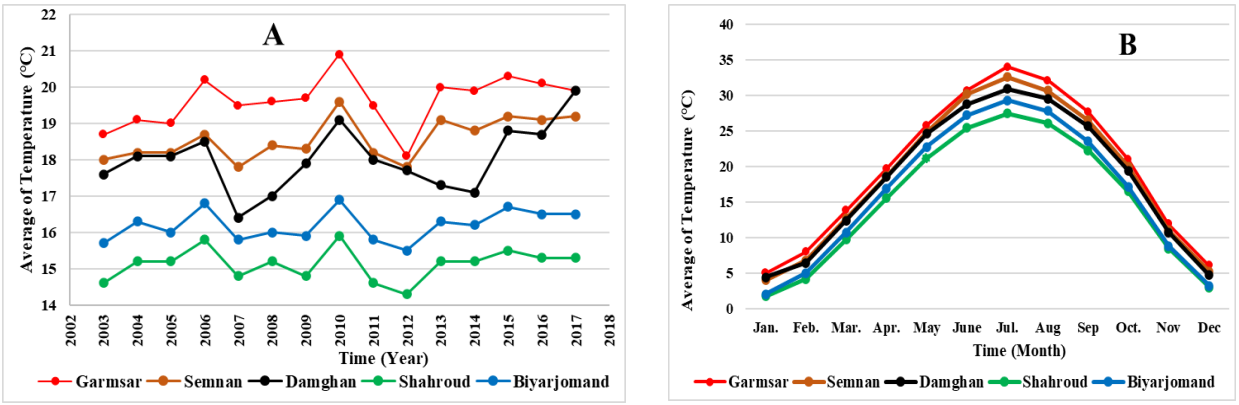

Figure 3. depicts a graphical representation showcasing the enduring alterations in yearly (A) and monthly (B) temperature patterns observed at synoptic stations within Semnan province.

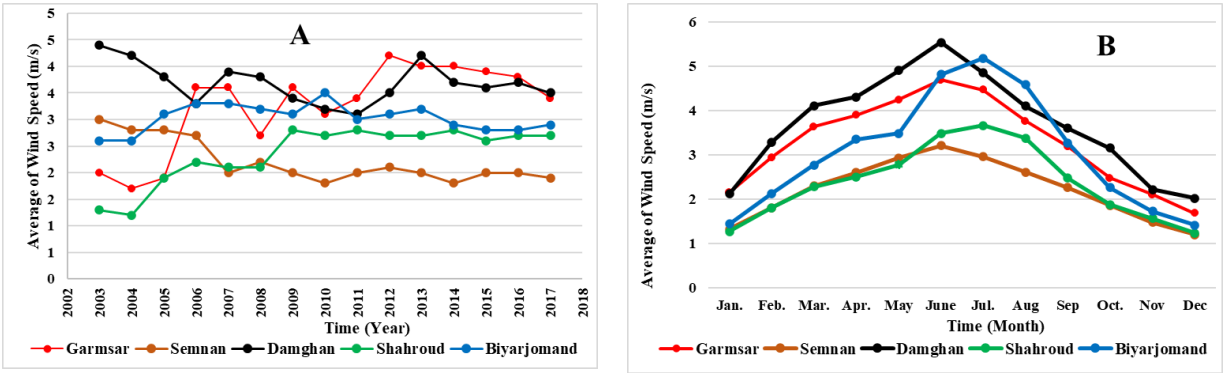

Figure 4. illustrates a graphical representation of the enduring modifications in the yearly (A) and monthly (B) wind velocity at the synoptic stations located in Semnan province.

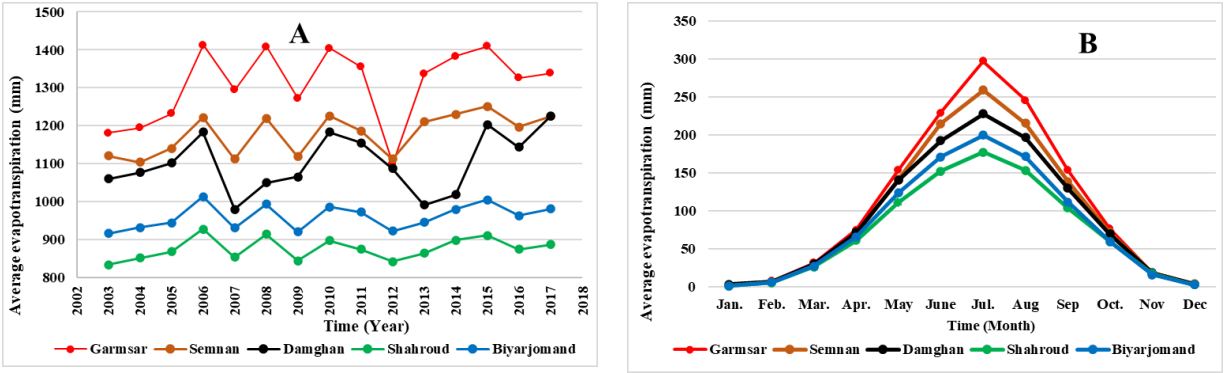

Figure 5. presents a schematic depiction of the long-term fluctuations in the yearly (A) and monthly (B) potential evapotranspiration at the synoptic stations situated in Semnan province.

Figure 3 shows that the highest surface wind speed was recorded in June and July in most of the synoptic stations of Semnan province. The analysis of potential evaporation and transpiration from 2003 to 2017 indicates that July witnessed the highest amount of these events in Semnan province, which coincides with the peak of temperature events during the same month. Other months did not observe such high levels of potential evaporation and transpiration. According Figure 4, the presence or absence of moisture is a crucial factor in the formation of dust storms alongside unstable air. If the unstable air contains adequate moisture, it leads to the occurrence of rain and thunderstorms, whereas insufficient moisture results in a dust storm. Results from the correlation analysis between monthly average temperature and the dust pollution index indicate a positive correlation between these variables. Conversely, the relationship between the monthly average relative humidity and the dust pollution index is inverse in nature (Saavedra et al., 2012).

3.2. Status of FAO-UNEP drought index

The UNEP aridity index, which is an effective tool approved by the United Nations Convention to Combat Desertification, was utilized in this study to measure the dryness factor of the air and climate. This index has been cited in various studies as a way to assess climatic conditions and desertification risk in different areas. The first relationship, represented by a ratio of precipitation and potential evapotranspiration, is used to determine the prevailing climate and desertification risk level of a region.

Table 2 outlines the weather conditions according to the UNEP drought index (Zare et al., 2016; Tavousi, 2018; Tavosi et al., 2019; Abtahi and Darvish, 2019; Zandifar et al., 2020).

3.3. Status of SPI index

To map out the distribution of drought in the province, data from synoptic stations and changes in SPI in Semnan were analyzed, resulting in Figure 6. Out of the eight synoptic stations in Semnan, five were chosen for analysis: Biyarjomand, Damghan, Garmsar, Semnan, and Shahroud. Damghan station was found to be in the moderate drought category with an SPI index value of -0.15, while Garmsar, Semnan, and Shahroud stations scored 0.77, 0.91, and 0.26 respectively, placing them in the normal class. The Biyarjomand station scored the highest at 1.15, indicating average precipitation levels. Table 4 summarizes these classifications. Additionally, a weak correlation between DSI and SPI indices with a correlation coefficient of 0.46 was found, suggesting an unfavorable correlation between them. Moreover, meteorological drought was found to have no impact on dust storms according to the results of the correlation analysis between SPI and DSI shown in Figure 6. The distribution of drought was determined based on the Standard Rainfall Index.

Table 4. Classification of drought based on the stations of Semnan province

Rows	Station Name	SPI	Drought class
1	Biyarjomand	1.15	Moderate fear
2	Damghan	-0.15	Moderate drought
3	Garmsar	0.77	Normal
4	Semnan	0.91	Normal
5	Shahroud	0.26	Normal

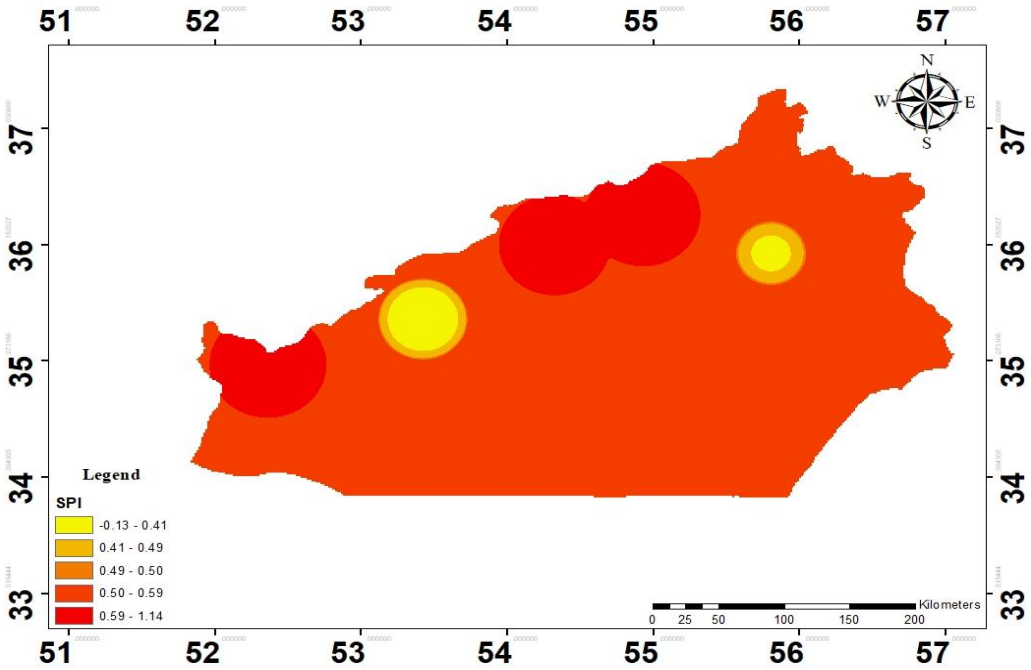

Figure 6. Drought distribution map of Semnan Province in the period of 2003-2017

3.4. Status of Dust Storm Index (DSI)

The study examined the trend of the DSI index at different stations over a period of time. The results indicated that at Garmsar, Semnan, Damghan, and Shahroud stations, there was a direct and significant correlation between the DSI index and time, meaning that as time increased, the frequency of dust during the year also increased. On the other hand, at the Biarjmand station, there was a significant inverse relationship between the two variables, indicating that as time increased, the intensity and frequency of dust decreased. Moreover, the analysis of the DSI index trend in Semnan province revealed that the index has been increasing with time, reaching its highest value in 2011 and its lowest value in 2008 (as shown in Figure 7).

To compare spatial-temporal changes in various stations, the intensity of changes in the DSI index was calculated and then divided into zones using ArcGIS software. This resulted in a map depicting the 15-year trends in increasing and decreasing changes (Figure 8). The green points on the map indicate a decrease in dust, while the red and orange points represent an increase in dust over the mentioned period. The observed increase in dust from west to east of the province is likely due to the rise in stormy days with medium dust (MDS) frequency.

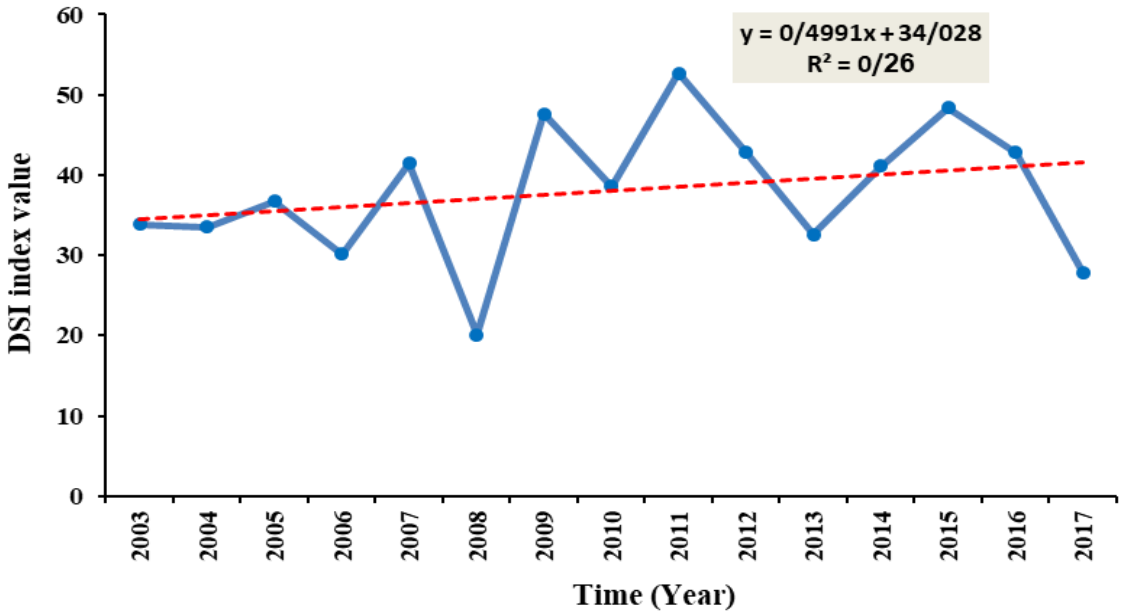

Figure 7. Trend of dust storm index (DSI) during the studied years in Semnan province

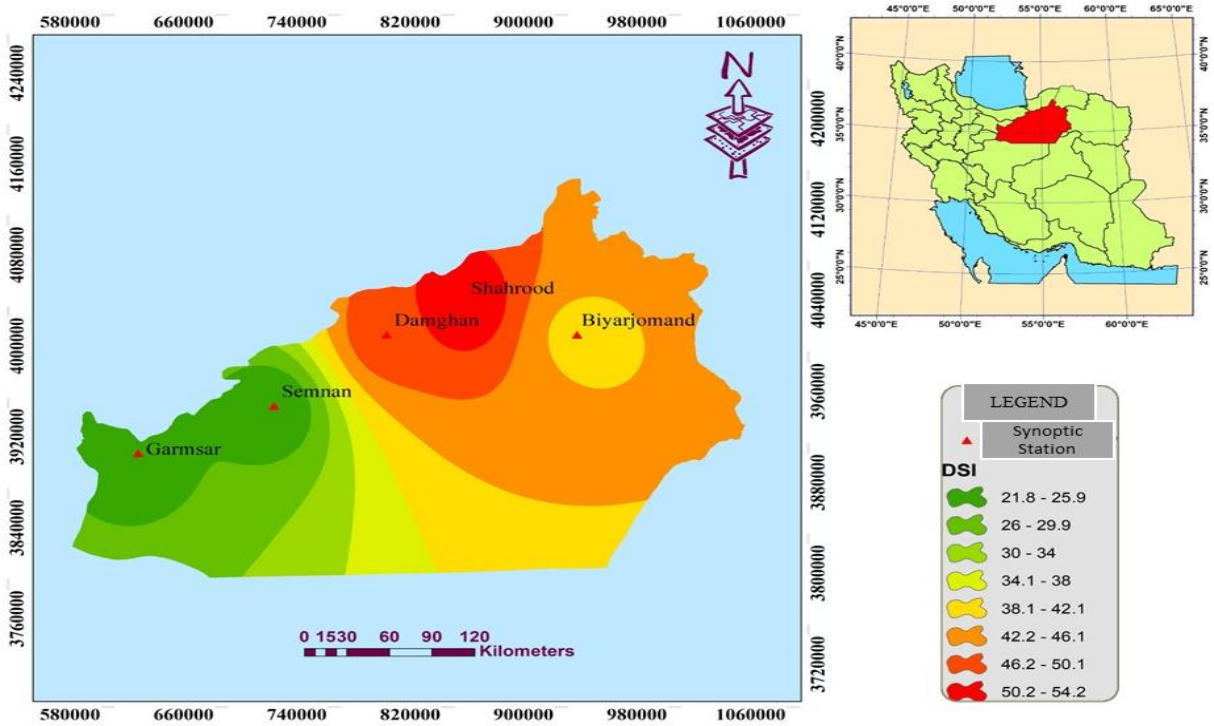

Figure 8. Regionalization of DSI index changes in different regions of the province in a 15-year statistical period (2003-2017)

Upon closer analysis of the relationship between drought indices, rainfall standards, and DSI, it was found that the severity of drought increased during the same period as the rise in DSI index, and there was a significant correlation between DSI and SPI over the 15-year period with an R^2 value of 0.89. Table five also indicates a strong correlation between drought index, DSI, and SPI in the region. In fact, during dry seasons, the DSI value decreases, while during wet seasons, the dust index value increases (as shown in Figure 9).

3.5. Reviewing the situation of the drought index (FAO-UNEP)

Table 5 displays the categorization of arid regions using the UNEP index for five stations in the area under investigation, which indicates that this region falls within the dry climate zone and is highly susceptible to desertification according to the UNEP climate index (Figure 10).

Table 5. Classification of dry areas based on the UNEP index

Rows	Station Name	Dryness index	Climate and weather	The danger of desertification
1	Garmsar	0.16	Arid	Very Intense
2	Semnan	0.12	Arid	Very Intense
3	Damghan	0.1	Arid	Very Intense
4	Shahroud	0.11	Arid	Very Intense
5	Biyarjomand	0.08	Arid	Very Intense

Figure 9. The degree of correlation between drought indices, SPI, DSI & FAO-UNEP

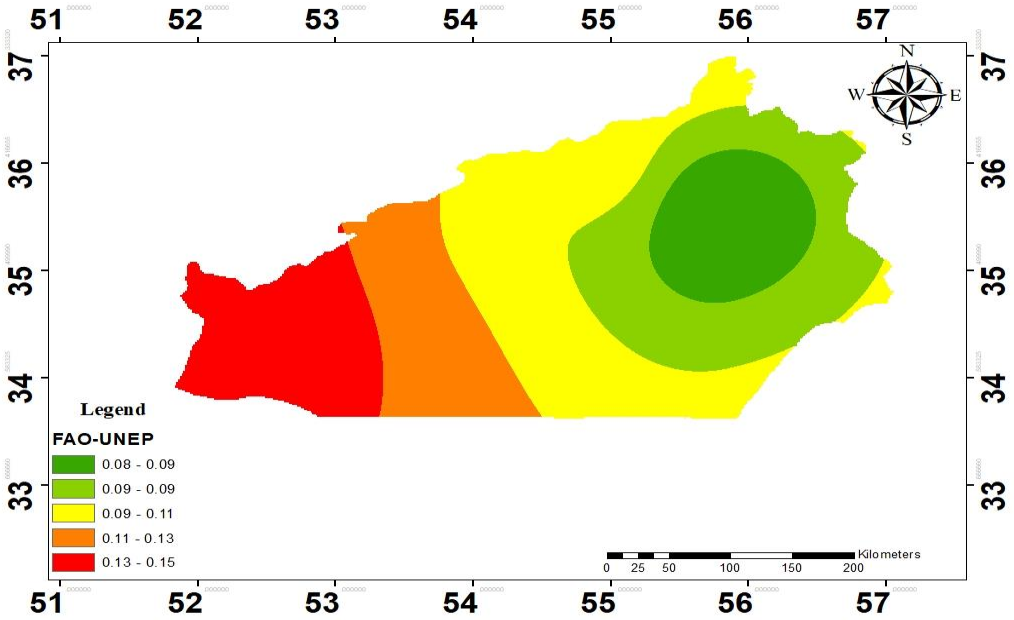

Figure 10. Drought distribution map of Semnan province with FAO-UNEP method in the period of 2003-2017

4. Conclusions

Dry area ecosystems have a highly variable climate, making them susceptible to changes in weather patterns and climate change. Dust storms have long been a source of trouble for inhabitants of dry and semi-arid areas. This study focuses on Semnan province, one of Iran's dry regions, to investigate the frequency of dust days at both yearly and monthly scales by considering local climatic conditions, such as rainfall, temperature, and wind speed. The findings indicate that over the 15-year period from 2003-2017, the average annual temperature increased significantly, leading to drought stress in the region. Moreover, the temperature rise has caused greater evaporation and transpiration and resulted in decreased moisture levels. The recent rainfall has caused an increase in surface water loss on Earth. By analyzing wind speed data on a monthly basis for each station, it was found that the months of June and July, with the highest prevailing wind speeds, have the greatest likelihood of dust storms occurring in the province. Conversely, the months of December and January had the lowest incidence of dust storms, which is consistent with findings from previous studies by Nabavi et al. (2019). Based on the UNEP index, the severity of drought in the studied area is quite intense and at risk of severe desertification. The analysis of the trend in the dust storm index for the time period of 2003-2017 across Semnan province indicated a significant increase with changes occurring at a 95% confidence level. However, the lack of significance in changes during the last decade suggests that policy decisions related to dust management in the region have had an impact (Asghari-Podeh, 2014). The division of changes in the DSI index across various regions of the province over the 15-year statistical period indicates that dust levels have risen from the west to the east due to an increase in the frequency of moderate dust storm days (MDS). In examining the relationship between drought and the DSI index, it was found that although the DSI index increased during the studied period along with an increase in drought severity, there was no significant correlation between the two factors over the 15 years. Nevertheless, the trend in the DSI index corresponds to a dry trend pattern, which aligns with the findings of Rahi et al.'s research (2022) and Yousefi Mobarhan & Khaleghi (2024).

References

Abtahi, S. M., & Darvish, M. (2019) Investigation of plant cover destroys in dry lands by using FAO & UNEP method (Case study: sub basin of Kashan). *Geography (Regional Planning)*, *9*(34), 381-391.

Ahmadalipour, A., Moradkhani, H., & Svoboda, M. (2017). Centennial drought outlook over the CONUS using NASA-NEX downscaled climate ensemble. *International Journal of Climatology*, *37*(5), 2477-2491. https://doi.org/10.1002/joc.4859

Amin, M. T., Mahmoud, S. H., & Alazba, A. A. (2016). Observations, projections and impacts of climate change on water resources in Arabian Peninsula: current and future scenarios. *Environmental Earth Sciences*, *75*, 1-17. https://doi.org/10.1007/s12665-016-5684-4

Arami, S. A., Ownegh, M., Mohammadian Behbahani, A., Akbari, M., & Zarasvandi, A. (2018). Statistical Analysis of Spatio-Temporal Pattern of Dust Storms in West and Southwest of Iran. *Journal of Water and Soil*

Conservation, *25*(1), 61-83. https://doi.org/10.22069/jwsc.2018.14107.2883

Asghari Podeh, Z., Shafiizadeh, M., Fakharan, S., & Gilani, A. (2014). Evaluation and zoning of spatio-temporal changes of dust storms using DSI index in Khuzestan province. In *The Second National Conference on Climate Change and Development Engineering, Stable Agriculture and Natural Resources*, Tehran. https://civilica.com/doc/437359.

Barker, L. J., Hannaford, J., Chiverton, A., & Svensson, C. (2016). From meteorological to hydrological drought using standardised indicators. *Hydrology and Earth System Sciences*, *20*(6), 2483-2505. https://doi.org/10.5194/hess-20-2483-2016

Beguería, S., Vicente-Serrano, S. M., Reig, F., & Latorre, B. (2014). Standardized precipitation evapotranspiration index (SPEI) revisited: Parameter fitting, evapotranspiration models, tools, datasets and drought monitoring. *International Journal of Climatology*, *34*(10), 3001–3023. https://doi.org/10.1002/joc.3887

Das, P. K., Dutta, D., Sharma, J. R., & Dadhwal, V. K. (2016). Trends and behaviour of meteorological drought (1901–2008) over Indian region using standardized precipitation–evapotranspiration index. *International Journal of Climatology*, *36*(2), 909–916. https://doi.org/10.1002/joc.4392

Parsons, D. J., Rey, D., Tanguy, M., & Holman, I. P. (2019). Agricultural systems ecological modeling. *Agricultural Systems*, *198*, 127–138.

FAO, (2017). *Drought characteristics and management in Central Asia and Turkey*. Rome.

Fiedler, S., Schepanski, K., Knippertz, P., Heinold, B., & Tegen, I. (2014). How important are atmospheric depressions and mobile cyclones for emitting mineral dust aerosol in North Africa? *Atmospheric Chemistry and Physics*, *14*(17), 8983–9000. https://doi.org/10.5194/acp-14-8983-2014

Gao, Z., Xu, N., Fu, C., & Ning, J. (2014). Evaluating drought monitoring methods using remote sensing: A dynamic correlation analysis between heat fluxes and land cover patterns. *IEEE Journal of Selected Topics in Applied Earth Observations and Remote Sensing*, *8*(1), 298–303. https://doi.org/10.1109/jstars.2014.2359657

Goudie, A. (2018). Dust storms and ephemeral lakes. *Desert*, *23*(1), 153–164.

Goudie, A. S., & Middleton, N. J. (2006). *Desert dust in the global system*. Springer Science & Business Media.

Guo, Y., Huang, S., Huang, Q., Wang, H., Fang, W., Yang, Y., & Wang, L. (2019). Assessing socioeconomic drought based on an improved Multivariate Standardized Reliability and Resilience Index. *Journal of Hydrology*, *568*, 904–918. https://doi.org/10.1016/j.jhydrol.2018.11.055

Hameed, M., Ahmadalipour, A., & Moradkhani, H. (2018). Apprehensive drought characteristics over Iraq: results of a multidecadal spatiotemporal assessment. *Geosciences*, *8*(2), 58. https://doi.org/10.3390/geosciences8020058

Han, Z., Huang, S., Huang, Q., Leng, G., Wang, H., Bai, Q., ... & Du, M. (2019). Propagation dynamics from meteorological to groundwater drought and their possible influence factors. *Journal of Hydrology*, *578*, 124102. https://doi.org/10.1016/j.jhydrol.2019.124102

Huang, S., Huang, Q., Leng, G., & Liu, S. (2016). A nonparametric multivariate standardized drought index for characterizing socioeconomic drought: A case study in the Heihe River Basin. *Journal of Hydrology*, *542*, 875–883. https://doi.org/10.1016/j.jhydrol.2016.09.059.

Karimi Sangchini, E., Ownegh, M., Sadoddin, A., & Yousefi Mobarhan, E. (2020). Predicting the impacts of land cover management scenarios on the run-off volume and river pollutants using the L-THIA model for the Hablehrud basin. *Watershed Management Research*, *33*(3), 36–52.

Lloyd-Hughes, B. (2014). The impracticality of a universal drought definition. *Theoretical and Applied Climatology*, *117*, 607–611. https://doi.org/10.1007/s00704-013-1025-7

McKee, T. B., Doesken, N. J., & Kleist, J. (1993). The relationship of drought frequency and duration to time scales. In *Proceedings of the 8th Conference on Applied Climatology*, *17*(22), 179-183.

Maia R., Vivas, E., Serralheiro, R., & de Carvalho, M. (2015). Socioeconomic evaluation of drought effects: Main principles and application to Guadiana and Algarve case studies. *Water Resources Management*, *29*, 575–588. https://doi.org/10.1007/s11269-014-0883-9

Middleton, N. J. (2017). Desert dust hazards: A global review. *Aeolian Research*, *24*, 53–63. https://doi.org/10.1016/j.aeolia.2016.12.001

Miri, A. (2020). Dust storms analysis in the Sistan region using DDI and DSI indices and wind speed, visibility and PM10 parameters. *Journal of Water and Soil Conservation*, *27*(1), 1–23. https://doi.org/10.22069/jwsc.2020.16883.3225

Miri, A., Ahmadi, H., Ekhtesasi, M. R., Panjehkeh, N., & Ghanbari, A. (2009). Environmental and socio-economic impacts of dust storms in Sistan Region, Iran. *International Journal of Environmental Studies*, *66*(3), 343–355. https://doi.org/10.1080/00207230902720170

Miri, A., Ahmadi, H., Ghanbari, A., & Moghaddamnia, A. (2007). Dust storms impact on air pollution and public health under hot and dry climate.

Mishra, A. K., Ines, A. V., Das, N. N., Khedun, C. P., Singh, V. P., Sivakumar, B., & Hansen, J. W. (2015). Anatomy of a local-scale drought: Application of assimilated remote sensing products, crop model, and statistical methods to an agricultural drought study. *Journal of Hydrology*, *526*, 15–29. https://doi.org/10.1016/j.jhydrol.2014.10.038

Nabavi, S. S., Moradi, H., & Shrifikia, M. (2019). Evaluation of dust storm temporal distribution and the relation of the effective factors with the frequency of occurrence in Khuzestan Province from 2000 to 2015. *Scientific-Research Quarterly of Geographical Data*

(SEPEHR), *28*(111), 191–203. https://doi.org/10.22131/sepehr.2019.37518

Nichol, J. E., & Abbas, S. (2015). Integration of remote sensing datasets for local scale assessment and prediction of drought. *Science of the Total Environment*, *505*, 503–507. https://doi.org/10.1016/j.scitotenv.2014.09.099

Rahi, G. R. , Bahraini, F. , KhosroShahi, M. & Biabani, L. (2022). The effect of drought on dust storm frequency (case study: Bushehr province). *Journal of Water and Soil Conservation*, *29*(1), 31-51. https://doi: 10.22069/jwsc.2022.19677.3511

Rashki, A., Rautenbach, C. D., Eriksson, P. G., Kaskaoutis, D. G., & Gupta, P. (2013). Temporal changes of particulate concentration in the ambient air over the city of Zahedan, Iran. *Air Quality, Atmosphere & Health*, *6*, 123–135. https://doi.org/10.1007/s11869-011-0152-5

Ren, K., Huang, S., Huang, Q., Wang, H., Leng, G., Cheng, L., ... & Li, P. (2019). A nature-based reservoir optimization model for resolving the conflict in human water demand and riverine ecosystem protection. *Journal of Cleaner Production*, *231*, 406–418. https://doi.org/10.1016/j.jclepro.2019.05.221

Saavedra, S., Rodríguez, A., Taboada, J. J., Souto, J. A., & Casares, J. J. (2012). Synoptic patterns and air mass transport during ozone episodes in northwestern Iberia. *Science of the Total Environment*, *441*, 97–110. https://doi.org/10.1016/j.scitotenv.2012.09.014

Scanlon, B. R., Ruddell, B. L., Reed, P. M., Hook, R. I., Zheng, C., Tidwell, V. C., & Siebert, S. (2017). The food-energy-water nexus: Transforming science for society. *Water Resources Research*, *53*(5), 3550–3556. https://doi.org/10.1002/2017wr020889

Sun, F., Mejia, A., Zeng, P., & Che, Y. (2019). Projecting meteorological, hydrological and agricultural droughts for the Yangtze River basin. *Science of the Total Environment*, *696*, 134076. https://doi.org/10.1016/j.scitotenv.2019.134076

Tan, M. (2016). Exploring the relationship between vegetation and dust-storm intensity (DSI) in China. *Journal of Geographical Sciences*, *26*, 387–396. https://doi.org/10.1007/s11442-016-1275-2

Tavosi, T., Shoja, F., & Asgari, E. (2019). Amendment of climate zones of northeastern Iran based on a combination of changes in aridity index. *Desert Management*, *7*(13), 117–134. https://doi.org/10.22034/jdmal.2019.36538

Tavousi, T. (2018). Investigating the trend of fluctuations in annual precipitation and UNEP aridity index of climatic zones in the west and northwest of Iran. *Scientific-Research Quarterly of Geographical Data (SEPEHR)*, *27*(105), 85–96. https://doi.org/10.22131/sepehr.2018.31475

Van Loon, A. F., & Laaha, G. (2015). Hydrological drought severity explained by climate and catchment characteristics. *Journal of Hydrology*, *526*, 3–14. https://doi.org/10.1016/j.jhydrol.2014.10.059

Van Loon, A. F., Ploum, S. W., Parajka, J., Fleig, A. K., Garnier, E., Laaha, G., & Van Lanen, H. A. (2014). Hydrological drought typology: Temperature-related drought types and associated societal impacts. *Hydrology and Earth System Sciences Discussions*, *11*(9), 10465–10510. https://doi.org/10.5194/hessd-11-10465-2014

Vicente-Serrano, S. M., Cabello, D., Tomás-Burguera, M., Martín-Hernández, N., Beguería, S., Azorin-Molina, C., & El Kenawy, A. (2015). Drought variability and land degradation in semiarid regions: Assessment using remote sensing data and drought indices (1982–2011). *Remote Sensing*, *7*(4), 4391–4423. https://doi.org/10.3390/rs70404391

Vicente-Serrano, S. M., Quiring, S. M., Peña-Gallardo, M., Yuan, S., & Domínguez-Castro, F. (2020). A review of environmental droughts: Increased risk under global warming? *Earth-Science Reviews*, *201*, 102953. https://doi.org/10.1016/j.earscirev.2019.102953.

Wang, ., Yuan, W., & Shang, K. (2006). The impacts of different kinds of dust events on PM10 pollution in northern China. *Atmospheric Environment*, *40*(40), 7975–7982. https://doi.org/10.1016/j.atmosenv.2006.06.058.

Xiao, F., Zhou, C., & Liao, Y. (2008). Dust storms evolution in Taklimakan Desert and its correlation with climatic parameters. *Journal of Geographical Sciences*, *18*, 415–424. https://doi.org/10.1007/s11442-008-0415-8

Yan, H., Moradkhani, H., & Zarekarizi, M. (2017). A probabilistic drought forecasting framework: A combined dynamical and statistical approach. *Journal of Hydrology*, *548*, 291–304. https://doi.org/10.1016/j.jhydrol.2017.03.004

Yousefi Mobarhan, E., & Khaleghi, A. (2024). Analyzing the trend of changes in the Dust Storm Index (DSI) and its relationship with the meteorological drought in the arid climate (Case study: Semnan Province). *Environmental Sciences*, *22*(2), 289–304. https://doi.org/10.48308/envs.2024.1369

Yousefi Mobarhan, E., & Zandifar, S. (2023). Zoning of changes in the decreasing groundwater table and temporal monitoring of drought in the Ghorove-Dehgolan plain. *Iranian Journal of Rainwater Catchment Systems*, *11*(1), 17–35. https://doi.org/20.1001.1.24235970.1402.11.1.2.8

Yousefi Mobarhan, E., Ghodrati, M., & Khosroshahi, M. (2021). Monitoring and forecasting of effective climatic factors on the mobility of sand dunes in Semnan province. *Journal of Water and Soil Resources Conservation*, *10*(4), 127–142. https://doi.org/10.30495/wsrcj.2021.18085

Yousefi Mobarhan, E., Karimi Sangchini, E., & Lotfinasabasl, S. (2023). Scaling and corrosion quality zoning of groundwater in the aquifer of the Ghorove–Dehgolan plain. *Journal of Emergy, Life Cycle and System Analysis in Agriculture*, *2*(2), 179–186. https://doi.org/10.22034/jelsa.2024.416742.1053

Yousefi Mobarhan, E., Khaleghi, A., & Zandifar, S. (2024). Examining the evolving patterns of recent droughts and climate categorization's impact on groundwater reserves through the utilization of GRI and SPI indices in the southern plain of the Sefidroud Basin, Iran.

Research Square, Preprint. https://doi.org/10.21203/rs.3.rs-4447426/v1

Yousefi Mobarhan, E., Karimi Sangchini, E., & Lotfinasabasl, S. (2024). Temporal and spatial investigation of underground water quality with emphasis on industrial uses in Sefirod watershed. *Modelling and Management of Water and Soil*. https://doi.org/10.22098/mmws.2023.12220.1211

Yu, M., Liu, X., & Li, Q. (2020). Responses of meteorological drought–hydrological drought propagation to watershed scales in the upper Huaihe River basin, China. *Environmental Science and Pollution Research, 27*, 17561–17570. https://doi.org/10.1007/s11356-019-06413-2

Zandifar, S., Khosroshahi, M., Ebrahimikhusfi, Z., & Naeimi, M. (2020). Predicting mobility of sands in the future based on sensitivity analysis test (Case study: Manjil City). *Journal of Arid Regions Geographic Studies, 11*(39), 18–35.

Zare, M., Poormohammadi, S., & Sodaizade, H. (2016). Climatic parameters, aridity indices, reference evapotranspiration, and statistical distribution in Iran. *Geography and Environmental Planning, 27*(2), 103–118. https://doi.org/10.22108/gep.2016.21818

Agriculture, Environment & Society

Journal homepage: www.aes.uoz.ac.ir

Life Cycle Assessment of Major Crops in the Lenjanat Watershed, Isfahan Province

Majid Dekamin[a], Seyed Morteza Ghaemmaghami[b], Amin Toranjian[*b]

[a] Department of Plant Production and Genetics, Faculty of Agriculture, Malayer University, Malayer, Hamadan, Iran
[b] Department of Water and Soil Science, Faculty of Agriculture, Malayer University, Malayer, Hamadan, Iran

ARTICLE INFO

Article history:
Received: 12 February 2025
Accepted: 20 April 2025
Available online: 8 May 2025

Keywords:
Agro-Environmental Analysis
Crop Production
Environmental Impacts
Resource Efficiency
Sustainable Agriculture

ABSTRACT

Agriculture is a cornerstone of societal production, playing a pivotal role in food security, economic development, and environmental sustainability. However, the escalating use of chemical inputs and fossil fuels in agricultural systems has raised significant concerns about their environmental sustainability. This study applies the life cycle assessment methodology—specifically the CML 2001 baseline method developed by Leiden University and in accordance with ISO 14044 standards—to evaluate the environmental impacts of four major crops: wheat, barley, alfalfa, and rice, cultivated in the Lenjanat watershed of Isfahan Province, Iran. The functional unit was defined as the production of one ton of each crop, with the system boundary encompassing all farm activities from land preparation to harvest. Data were collected for the agricultural year 2020–2021 and analyzed using SimaPro 9.2 software and the Ecoinvent database. The results indicated that rice had the highest global warming potential at 4137.85 kg CO_2-eq ton^{-1}, primarily due to its high water demand and diesel fuel consumption. Wheat exhibited the highest acidification potential at 28.11 kg SO_2-eq ton^{-1} and the highest eutrophication potential at 11.79 kg PO_4^{3-}-eq ton^{-1}, driven by excessive nitrogen and phosphate fertilizer use. Alfalfa, while showing the lowest global warming potential and eutrophication potential, had the highest photochemical oxidant formation potential at 0.392 kg C_2H_4-eq ton^{-1} due to frequent harvesting operations. The study underscores the critical role of nitrogen fertilizers, diesel fuel, and phosphate fertilizers in environmental impacts. To mitigate these effects, adopting organic inputs, modern irrigation technologies, reduced tillage, and optimized fuel use are recommended. These strategies can significantly enhance agricultural sustainability in the Lenjanat region.

Highlights

- The study assessed the environmental impacts of four crops using Life Cycle Assessment.
- Rice had the highest global warming potential due to water use and diesel fuel.
- Wheat showed the highest acidification and eutrophication potential from fertilizer use.
- Alfalfa's frequent harvesting led to high photochemical oxidant formation.
- The study suggests improving irrigation, fertilizer use, and machinery efficiency.

1. Introduction

Agriculture is one of the most fundamental production sectors in any society, playing a vital role in ensuring food security, economic development, and environmental sustainability. However, several challenges have emerged, including increasing population, climate change, limited natural resources, and growing competition over land and water use. These challenges have placed immense pressure on agricultural systems, particularly in terms of resource management and environmental impact. The growing reliance on external inputs, such as chemical fertilizers, pesticides, and fossil fuels, has led to significant environmental consequences, including soil and water contamination, greenhouse gas emissions, reduced biodiversity, and the degradation of ecosystems (Hoekstra et al., 2012; Dekamin et al., 2024). Approximately 20% of

* Corresponding author.
E-mail address: A.toranjian@malayeru.ac.ir
https://doi.org/10.22034/aes.2025.528191.1105

global greenhouse gas emissions originate from agricultural activities, with a large share attributed to nitrogen fertilizers and fossil fuels used in sowing, cultivation, and harvesting operations (Hoekstra et al., 2012; Nemecek et al., 2024). These realities underline the urgent need for accurate, cost-effective, and data-driven methods to assess and mitigate the environmental impacts of agricultural production.

One of the most internationally recognized approaches for environmental impact assessment is Life Cycle Assessment (LCA). Defined under ISO 14040 and ISO 14044 standards, LCA evaluates all inputs and outputs of a product or process from raw material extraction to final disposal. In the agricultural sector, LCA is commonly applied with a "cradle-to-farm-gate" system boundary, which encompasses input consumption, energy use, farming operations, and the associated emissions and outputs (Roy et al., 2009; Dekamin et al., 2018; Dekamin et al., 2022). Over recent years, the application of LCA in agricultural studies has expanded significantly. This method provides a systematic tool for quantifying environmental impacts at every stage of crop production, from input procurement to on-farm use (ISO, 2006).

Numerous studies worldwide, including in Europe, Australia, and beyond, have assessed the environmental impacts of crop production using LCA. In Iran, research by Mirhaji and Khojastehpour (2011) in South Khorasan, Koocheki et al. (2018) in Khorasan Razavi, and Aliqolinya (2015) in the Urmia Lake basin, all emphasized the essential role of LCA in assessing agricultural sustainability. In the field of agriculture, LCA is mainly employed to identify environmental hotspots in cropping and horticultural systems (Afshar et al., 2022). Several studies have applied LCA in horticultural production, including Nikkhah et al. (2017), who evaluated peach production in Mazandaran and Golestan provinces, and Mohseni et al. (2019), who assessed the energy use and environmental impacts of grape production. Similarly, Ghasempour and Ahmadi (2018) employed LCA to evaluate corn, wheat, and soybean production systems.

International studies in China (Zhu et al., 2018), Spain (Martin-Gorriz et al., 2020), and Italy (Pergola et al., 2022) have used LCA to evaluate the environmental performance of various agricultural crops. Across all these studies, nitrogen fertilizers, diesel fuel, and pesticides have been identified as the major contributors to environmental degradation. In the study by Zamani et al. (2024), the IMPACT 2002+ method was employed to assess environmental effects, revealing that walnut production caused the highest negative impacts across multiple categories, including human health, ecosystem quality, resource use, and climate change.

The Lenjanat region in Isfahan Province—one of the central agricultural hubs of Iran—faces intensive water consumption, a high dependency on chemical inputs, and traditional farming structures. These characteristics highlight the need for comprehensive environmental assessments. The region's four major crops—wheat, barley, alfalfa, and rice—differ significantly in their input requirements and productivity, making them suitable candidates for Life Cycle Assessment aimed at informing sustainable agricultural management.

Agriculture in Lenjanat, located in Isfahan Province, is vital to the local economy. However, the region faces challenges due to its semi-arid climate, characterized by low annual rainfall (ranging from 200 to 250 mm) and high summer temperatures exceeding 35°C. These climatic conditions significantly increase the demand for irrigation, which relies primarily on surface water from the Zayanderud River and groundwater. Due to limited water availability, farming practices in Lenjanat heavily depend on chemical inputs, such as nitrogen fertilizers and pesticides, to enhance crop yields. The region grows crops like wheat, barley, alfalfa, and rice, each requiring specific water and input management strategies. This, combined with traditional farming practices, underscores the need for sustainable approaches to ensure long-term agricultural productivity and environmental balance in the region.

Despite a growing body of global research applying LCA in agriculture, there is a significant gap in localized data, particularly in arid and semi-arid regions like Lenjanat. Existing studies often rely on generalized data that may not fully capture the unique environmental conditions and farming practices of these regions. Additionally, there is a lack of comprehensive supply chain analysis that accounts for the full range of inputs and outputs in agricultural production. This study aims to address these gaps by providing detailed, localized LCA data for four major crops in Lenjanat. By offering a more context-specific assessment of environmental impacts, this research is crucial for developing sustainable agricultural management strategies in the region.

The primary objective of this analysis is to identify key processes and inputs contributing to environmental impact categories, offering strategies for optimizing resource use and mitigating environmental damage. The findings of this study are expected to highlight critical hotspots in input and energy consumption, which will provide a foundation for management strategies aimed at reducing environmental impacts and enhancing sustainability in crop production systems. Additionally, the insights gained from this study may help agricultural policymakers optimize cropping patterns and input use in areas with similar ecological and climatic conditions.

2. Materials and Methods

2.1. Study Area

The Lenjanat region consists of three main counties: Lenjan, Mobarakeh, and Dehaghan. Lenjan County is located in the western part of Isfahan Province and covers an area of 1,172 km², which represents approximately 1.1% of the total area of Isfahan Province. Lenjan is situated 35 km southwest of Isfahan city, with an average elevation of 1,700 meters above sea level. Lenjanat County, with its center in Zarinsahr, is located in the southwestern part of Isfahan Province and lies within the Central Plateau of Iran. Climatically, this area falls under the semi-arid and arid regions of the country. Geographically, it is positioned at approximately 51° longitude and 32° latitude. The average

annual rainfall in this county ranges from 200 to 250 mm, which is below the national average of Iran, and its distribution is uneven, mainly occurring in winter. Additionally, the summer temperatures in this area exceed 35°C, and the high evaporation rates further increase the water demand for crops.

Due to the limited availability of water resources, agriculture in this region is primarily irrigated using water from the Zayanderud River and underground water resources. The significant reduction in the Zayanderud River flow in recent years, along with the declining groundwater levels, has posed major challenges to the sustainability of agricultural production. The region has a long history of cultivating crops such as wheat, barley, forage corn, alfalfa, potatoes, and vegetables, which constitute a substantial part of the local economy.

Given that Lenjanat shares the characteristic features of dry regions, including low rainfall, high temperatures, limited water resources, and high dependence on chemical agricultural inputs, it can serve as a representative area for studying the environmental impacts of crop production in arid climates of Iran. Evaluating the consequences of input consumption, pollutant emissions, and water resource use in such regions can significantly contribute to sustainable agricultural management strategies under similar ecological conditions.

2.2. Study Objective and Scope

The primary objective of this research is to assess the environmental impacts of producing four major crops, namely wheat, barley, alfalfa, and rice, in the Lenjanat watershed in Isfahan Province using the LCA method. The scope of this assessment includes all environmental inputs and outputs related to farm operations, from land preparation to crop harvest. The selection of these crops was based on their significant cultivation area, economic importance in the region, and differences in their water and input requirements.

2.3. LCA Theoretical Framework

The LCA method is based on international standards ISO 14040 and ISO 14044 and includes four main stages: (1) goal and scope definition, (2) life cycle inventory analysis (LCI), (3) life cycle impact assessment (LCIA), and (4) interpretation of results (ISO, 2006a; ISO, 2006b). This approach is highly suitable for analyzing the cumulative environmental impacts of a production system throughout its life cycle, especially in agricultural systems where the diversity and interdependence of inputs are high (Guinée, 2002).

2.4. Functional Unit

For this study, the functional unit was defined as the production of one ton of each agricultural crop. This unit serves as the basis for comparing the environmental impacts of different products and helps evaluate the efficient consumption of resources and the generation of pollution across various crops (Roy et al., 2009).

2.5. System Boundaries

The system boundary of this study is "cradle-to-farm-gate," which includes all activities occurring within the farm, such as land preparation, sowing, input consumption (seeds, fertilizers, pesticides, fuel, and labor), farm operations, irrigation, and harvest. Post-harvest processes such as packaging, transportation, and processing are not included in this study's scope (Nemecek & Schnetzer, 2010).

2.6. Data Collection

Isfahan Province, a comprehensive and structured data collection approach was adopted. The primary source of data was field surveys conducted among local farmers, complemented by expert consultations and secondary data from reputable databases. The study focused on both traditional and modern agricultural practices across different irrigation methods and crop types. For this study, data were collected from farms across the Lenjanat watershed, Isfahan Province. These calculations were performed using Cochran's formula, which considers a 95% confidence level and a 5% margin of error. The results of these calculations are presented in Table 1, which shows both the initial and final sample sizes for each crop.

Table 1. initial and final sample sizes for each crop

Crop	Initial Sample Size (n_0)	Final Sample Size (n)
Wheat	101	47
Barley	82	41
Alfalfa	68	36
Rice	59	33

A detailed questionnaire was designed to gather essential information on farming operations, energy inputs, and resource use. The questionnaire was divided into several sections, including (1) demographic information of farmers (e.g., age, education, years of experience), (2) farm characteristics such as total area, cultivated area, and crop variety, (3) input quantities used during the production cycle (e.g., seeds, fertilizers, manure, pesticides, fuel, water, electricity), and (4) operation-specific details for land preparation, sowing, crop maintenance, and harvesting activities. Additional questions addressed labor inputs (e.g., type and number of workers) and transportation logistics for both inputs and harvested products.

In order to enhance the accuracy and reliability of the data, face-to-face interviews were conducted with selected farmers across the Lenjanat watershed. These interviews were complemented by consultations with agricultural experts, including extension officers, researchers, and faculty members from regional universities. The dual approach of farmer interviews and expert validation ensured that the collected data reflected actual field

practices while compensating for potential gaps in farmer recall or knowledge.

To capture upstream environmental impacts associated with the production and use of agricultural inputs (e.g., fuel combustion, fertilizer manufacturing), secondary data were sourced from well-established life cycle inventory databases. These databases were accessed via the SimaPro software platform, which was used to model and assess the full life cycle of each crop under study.

2.7. Software and Database

For process modeling and impact assessment, SimaPro 9.2 software was used. This software is one of the most powerful LCA tools, allowing the incorporation of local data and the use of standard global databases such as EcoInvent (Pré Consultants, 2020). Processes related to fertilizer production, diesel fuel, energy consumption, and other inputs were modeled through connections to the EcoInvent database.

2.8. Environmental Impact Assessment (LCIA) Method

For environmental impact analysis, the CML 2001 – baseline method, developed by Leiden University, was employed. This is one of the most widely used LCIA approaches recommended for evaluating agricultural products (Guinée et al., 2002).

In this study, four key environmental impact categories were evaluated:

- Global Warming Potential (GWP) in kg CO_2eq ton^{-1}
- Acidification Potential (AP) in kg SO_2eq ton^{-1}
- Eutrophication Potential (EP) in kg PO_4^{3-}eq ton^{-1}
- Photochemical Oxidant Formation Potential (POFP) in kg C_2H_4eq ton^{-1}

These indicators represent the most significant negative environmental consequences in agricultural systems and have been commonly used in similar studies (Brentrup et al., 2004; Nemecek et al., 2011).

2.9. Model Assumptions

Some of the key assumptions for the modeling are as follows:

- The production of inputs (fertilizers, pesticides, seeds) occurs outside the farm, and their data are sourced from the EcoInvent database.
- Irrigation operations are conducted via gravity-fed systems, with the primary water source being surface water from the Zayanderud River or local wells.
- Farm machinery is diesel-powered and commonly used.
- Post-harvest operations (such as storage, transportation, and processing) are not included within the system boundary.

2.10. Uncertainty and Data Accuracy Analysis

To assess the accuracy of the data, quality control methods proposed by ISO standards were applied, and farm data were cross-checked with official sources such as the Agricultural Planning and Economics Bureau of Isfahan Province and agricultural statistics reports. Additionally, some sensitive data (such as fertilizer and fuel consumption) were modeled with a ±20% variation to assess the impact of fluctuations on the environmental impact categories (Notarnicola et al., 2017). Monte Carlo simulations (1,000 iterations) were conducted in SimaPro 9.2 to evaluate the effect of ±20% variation on fertilizer and fuel inputs.

3. Results

3.1. Life Cycle Inventory Analysis

All raw materials, chemical and organic fertilizers, and pesticides used, as well as the fuel for farm machinery, are considered as input findings, or in other words, all the operations from sowing to harvest are included in the life cycle assessment process. Table 2 provides the inputs and outputs for crop production in the Lenjanat watershed.

Table 2. inputs and outputs for crop production per ha in Lenjanat watershed

	Wheat	Barley	Alfalfa	Rice
Machinery (kg)	300.8	340.8	20	40.2
Nitrogen (kg)	160.6	220.8	50	10.1
Phosphorus (kg)	120.1	90	0	112
Potassium (kg)	3	3.2	0	0.6
Herbicide (l)	6.5	1.1	2	0.3
Fungicide (l)	1.5	2.4	0.5	0.6
Insecticide (l)	5.2	4.4	2	1
Organic Fertilizer (kg)	5200	4375	2000	1000
Irrigation Water (m^3)	5757	5175	10000	14180
Electricity (kWh)	1950	1660	4860	1738
Seed (kg)	300	300	30	300
Irrigation Wastewater (m^3)	4029	3556	3556	3556
Nitrous Oxide (kg)	62	68	48.4	48.4
Ammonia (kg)	56	50	90.4	90.4
Nitrate (kg)	1.22	3	1.22	1.22
Phosphorus (kg)	0.81	0.5	0.5	0.5
Herbicide (l)	3.51	0	0	0
Fungicide (l)	1.62	1.24	1.24	1.24
Insecticide (l)	0.62	0.24	0.24	0.24
Crop Yield (kg)	4300	4500	10000	5500

3.2. Life Cycle Impact Assessment (LCIA) Results

The results from the LCA for the four crops-wheat, barley, alfalfa, and rice- were analyzed across various environmental impact categories. This analysis helps identify which products exert the most pressure on the environment and highlights the key inputs and processes contributing to each impact category. The results for the four major environmental impact indicators—GWP, AP, EP, and POFP—are reported below in Table 3.

Table 3. environmental impact categories for 1 ton of each crop produced in Lenjanat

Impact Category	Rice	Barley	Alfalfa	Wheat
Global Warming Potential (kg CO_2-eq)	4137.8	3469.3	1381.1	3616.9
Photochemical Oxidant Formation (kg C_2H_4-eq)	0.182	0.186	0.392	0.162
Acidification Potential (kg SO_2-eq)	7.34	21.705	11.356	28.113
Eutrophication Potential (kg PO_4^{3-}-eq)	6.02	11.24	1.86	11.79

3.3. Global Warming Potential (GWP)

GWP is an indicator used to measure the environmental impact of greenhouse gases emitted due to human activities. According to Table 4 and Figure 1, rice exhibited the highest GWP among the four crops studied, with a value of 4137.8 kg CO_2-eq ton^{-1}. This is primarily due to its very high water requirements, frequent irrigation, and consequently, the large amount of diesel fuel used for pumping irrigation water, along with the heavy application of nitrogen fertilizers.

In contrast, alfalfa showed the lowest GWP at 1381.1 kg CO_2-eq ton^{-1}, due to its multi-year growth cycle, nitrogen fixation, and lower need for tillage and frequent mechanized operations. Over 70% of the impact in this category is attributed to electricity use, manure, and mineral fertilizers. Other inputs have a relatively minor effect on this category. This aligns with findings from Zhu et al. (2018), which also reported high GWP for rice due to methane emissions and irrigation energy use. The comparison suggests that water management strategies and alternative irrigation methods could significantly reduce rice's environmental impact. Pishgar-Komleh et al, (2020), which also reported that rice has a significant carbon footprint, primarily due to methane emissions from flooded fields and fossil fuel use in irrigation. However, Ahmad et al, (2023) presents a slightly lower GWP for rice, suggesting that variations in irrigation methods and fertilizer application can influence emissions.

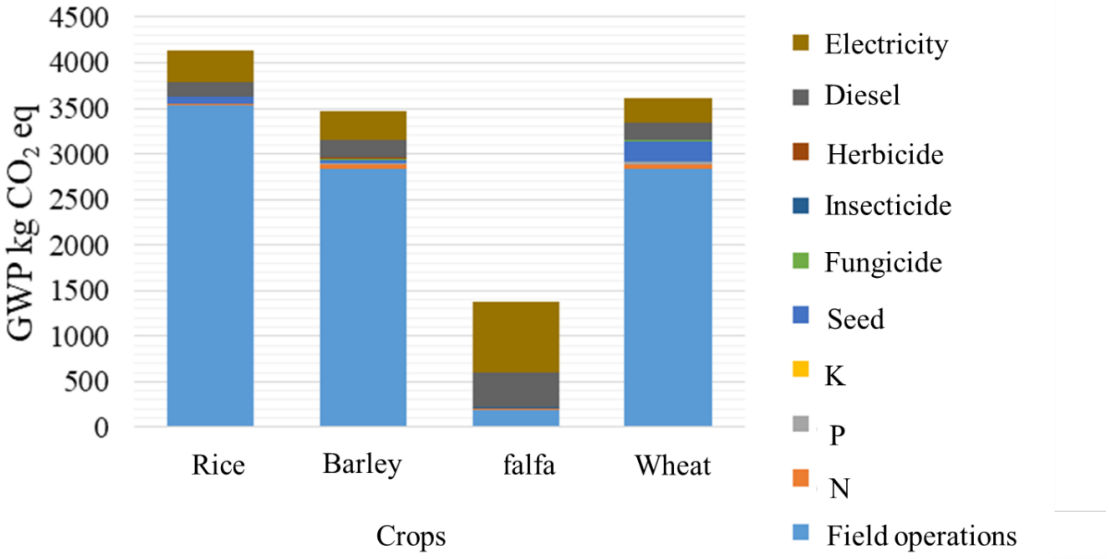

Figure 1. Global Warming Potential (GWP) for wheat, barley, alfalfa and rice produced in the Lenjanat watershed (units: kg CO_2-eq ton^{-1} product)

3.4. Acidification Potential (AP)

AP results from the release of gases such as SO_2, NH_3, and NO_x, which can cause acid rain and degrade soil and water resources. As shown in Table 4 and Figure 2, wheat has the highest AP value, with 28.113 kg SO_2-eq ton^{-1}. This high value is mainly due to the heavy application of urea fertilizers and ammonia emissions from its evaporation from soil surfaces. The ammonia released is converted to nitrates in the atmosphere and falls as nitric acid during rainfall, contaminating both soil and water. In comparison, rice and alfalfa showed much lower AP values, with 7.34 and 1.86 kg SO_2-eq ton^{-1}, respectively, due to their lower fertilizer consumption and reduced ammonia evaporation. This is consistent with findings from Koocheki et al. (2018), which also highlighted the role of nitrogen fertilizers in acidification and eutrophication. The comparison underscores the need for optimized fertilizer application techniques to mitigate these environmental effects. Pishgar-Komleh et al, (2020) stating that wheat production leads to high ammonia volatilization and nitrate leaching, which contribute to acidification.

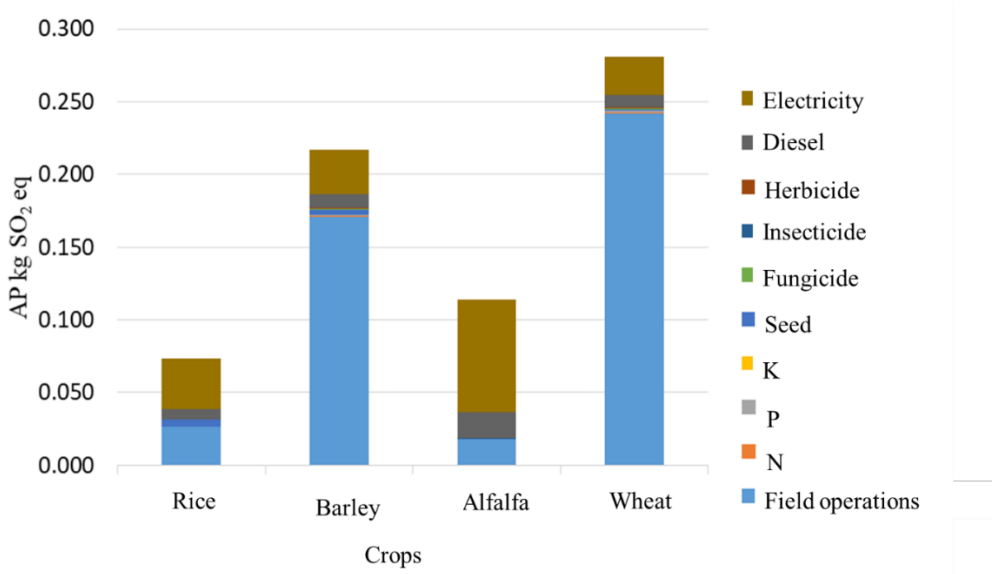

Figure 2. Acidification Potential (AP) for wheat, barley, alfalfa and rice produced in the Lenjanat watershed (units: kg SO_2-eq ton^{-1} product)

3.5. Eutrophication Potential (EP)

EP refers to the enrichment of surface and groundwater resources with nutrients, often caused by the leaching of nitrates and phosphates from fertilizers. As seen in Table 4 and Figure 3, wheat exhibited the highest EP at 11.79 kg PO_4^{3-}-eq ton^{-1}, mainly due to the excessive use of phosphate fertilizers and their non-optimal distribution, leading to surface runoff and leaching in the soils of the region. In contrast, alfalfa demonstrated a significantly lower EP value of 1.86 kg PO_4^{3-}-eq ton^{-1}, attributed to its natural nitrogen fixation and limited fertilizer requirements. Nuraeefar et al, (2024), also confirms that wheat has a significant eutrophication impact, but it attributes this more to irrigation runoff rather than direct fertilizer application.

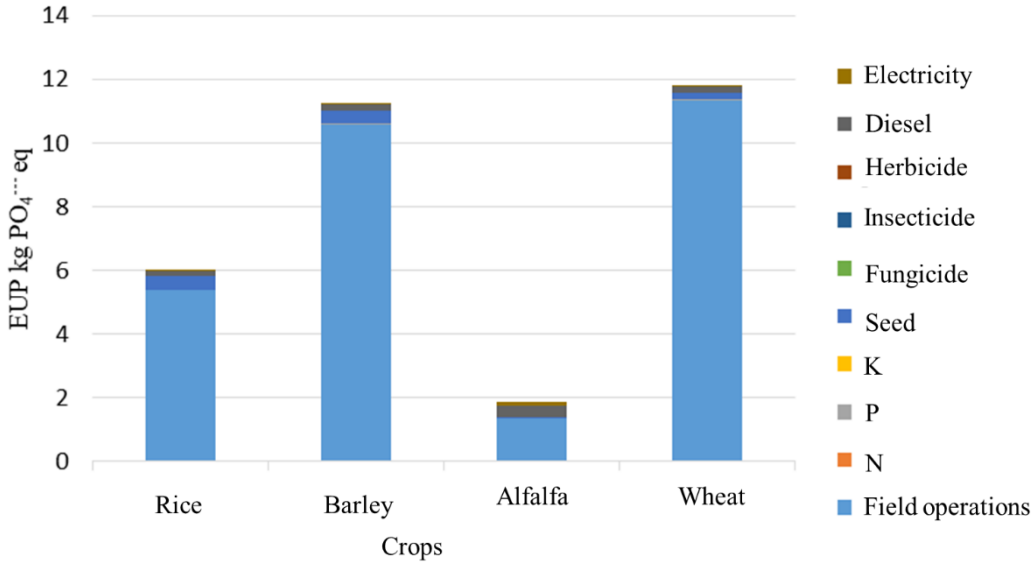

Figure 3. Eutrophication Potential (EP) for wheat, barley, alfalfa and rice produced in the Lenjanat watershed (units: kg PO_4^{-3}-eq ton^{-1} product)

3.6 Photochemical Oxidant Formation Potential (POFP)

POFP, also known as smog formation, is primarily influenced by the release of volatile organic compounds (VOCs) and nitrogen oxides from fuel consumption and fertilizers. Based on the data presented in Table 4 and Figure 4, alfalfa recorded the highest POFP at 0.392 kg C_2H_4-eq ton^{-1}. This may seem unexpected initially, but it is due to the repeated harvesting operations in alfalfa farms (more than four times per year), each of which requires the use of diesel-powered machinery and fueling.

Despite its favorable performance in other impact categories, the frequent harvesting operations in alfalfa farms lead to increased emissions of compounds contributing to photochemical smog. Rice ranked second

with 0.182 kg C_2H_4-eq ton^{-1}, followed by wheat with 0.162 kg C_2H_4-eq ton^{-1}.

This aligns with Ghasempour and Ahmadi (2018), which also noted increased emissions from mechanized harvesting in alfalfa production. The comparison suggests that improving mechanization efficiency and adopting alternative harvesting methods could reduce POFP.

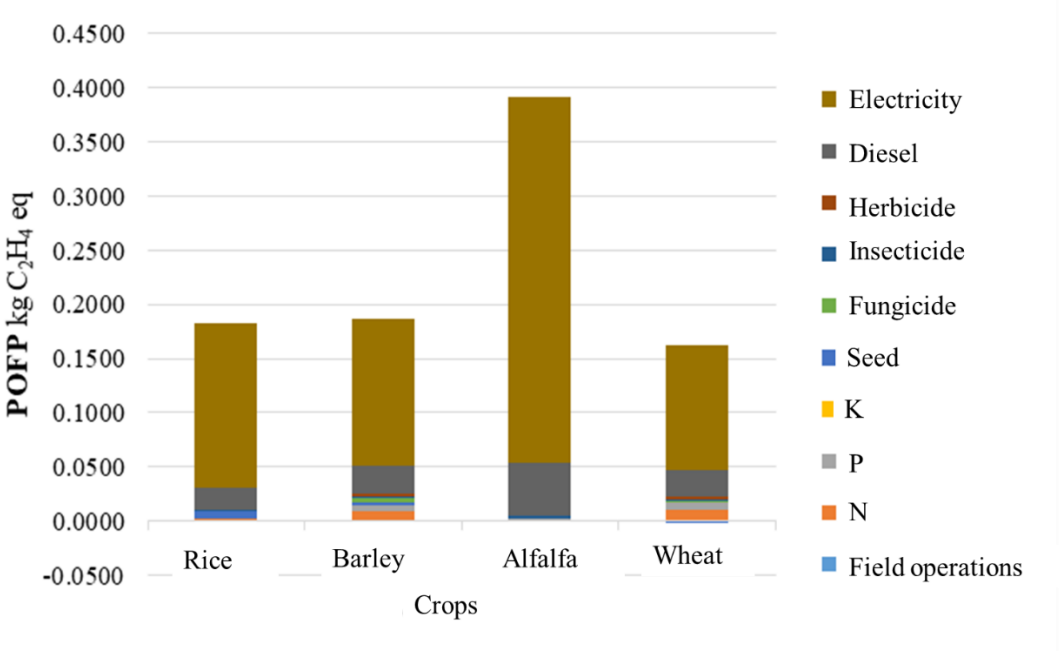

Figure 4. Photochemical Oxidant Formation Potential (POFP) for wheat, barley, alfalfa and rice produced in the Lenjanat watershed (units: kg C_2H_4-eq ton^{-1} product)

3.7. Key Inputs Driving Environmental Impacts

The three main inputs contributing most significantly to environmental impacts were nitrogen fertilizers (urea), diesel fuel, and phosphate fertilizers. Specifically, nitrogen fertilizers accounted for 40-60% of the GWP and AP. Phosphate fertilizers were the main driver of EP, contributing between 60-80%, while diesel fuel played a significant role in both GWP and POFP. These findings are consistent with those reported in previous studies by Guinée (2002) and Notarnicola et al. (2017).

3.8. Environmental Performance of Crops

From an environmental perspective, alfalfa exhibited the best overall performance and could be recommended as a suitable option for sustainable agriculture in the region. Rice, despite its high nutritional value, contributed the most to GWP and requires a thorough reconsideration of input usage and irrigation methods. Wheat demonstrated the highest values for AP and EP, indicating that fertilizer management is crucial for this crop.

4. Discussion

The results from LCA of the four major crops—wheat, barley, alfalfa, and rice—cultivated in the Lenjanat region provide important insights into the environmental impacts of agricultural practices in semi-arid regions. The results revealed significant differences in the environmental performance of each crop, primarily due to variations in input consumption, water requirements, farming operations, and the intensity of mechanized activities. This section discusses these findings in detail, compares them with previous studies, and offers recommendations for improving the sustainability of agricultural practices in Lenjanat and other similar regions.

Rice exhibited the highest GWP among the crops studied, with a value of 4137.8 kg CO_2-eq ton^{-1} produced. This high GWP can largely be attributed to two key factors: the high water demand for rice cultivation and the associated use of diesel fuel for irrigation, coupled with the significant nitrogen fertilizer application. The water-intensive nature of rice farming, particularly in the Lenjanat region, where irrigation is heavily reliant on surface water from the Zayanderud River and groundwater, exacerbates the GWP of this crop. Rice cultivation, especially under conventional irrigation systems, is a major source of greenhouse gas emissions, including methane and carbon dioxide. Studies such as those by Brentrup et al. (2004) and Singh et al. (2010) have similarly emphasized the contribution of flooded rice systems to global warming, mainly due to methane emissions and fossil fuel consumption.

Rice's high GWP in this study reflects a broader global trend where rice cultivation, especially in regions with inefficient irrigation systems, remains a significant source of greenhouse gas emissions. The dependence on diesel-powered irrigation systems, which are common in the Lenjanat region, further compounds this environmental burden. Therefore, addressing the inefficiencies in irrigation systems and transitioning to more sustainable methods, such as drip or sprinkler irrigation, could significantly reduce the GWP associated with rice farming.

In contrast, alfalfa showed the lowest GWP at 1381.1 kg CO_2-eq ton^{-1} produced. The lower GWP of alfalfa can be attributed to its ability to fix nitrogen naturally, reducing the need for synthetic nitrogen fertilizers. Additionally, alfalfa's multi-year growth cycle and lower mechanization requirements compared to annual crops like rice and wheat contribute to its relatively lower GWP. Alfalfa's lower GWP is a significant finding, as it suggests that leguminous crops, with their natural nitrogen fixation capabilities and lower water and energy requirements, could offer more sustainable alternatives to conventional cereal crops, particularly in regions like Lenjanat that face water scarcity and limited energy resources.

Wheat, which recorded the highest AP and EP values among the crops, shows a clear need for better nutrient management practices. The AP of wheat was 28.11 kg SO_2-eq ton^{-1}, primarily driven by the over-application of nitrogen fertilizers, particularly urea, and ammonia emissions from soil surfaces. Ammonia volatilization is a significant concern in wheat farming, as it contributes to the formation of acid rain, which leads to soil and water pollution. The excessive application of nitrogen fertilizers in wheat farming has been a recurring issue in many studies worldwide, including Mirhaji and Khojastehpour (2011), which also highlighted the negative effects of over-fertilization on both water quality and soil health. The high AP in wheat production reflects broader trends in conventional farming practices, where nutrient management is often suboptimal, leading to nutrient imbalances that harm the environment.

The high EP of wheat, recorded at 11.79 kg PO_4^{3-}-eq ton^{-1}, is similarly attributed to the excessive use of phosphate fertilizers. Phosphorus runoff from agricultural fields is a well-known environmental concern, as it can lead to nutrient pollution in rivers, lakes, and other water bodies, contributing to eutrophication and algal blooms. The overuse of phosphate fertilizers in wheat production, combined with inefficient fertilizer application techniques, leads to the leaching of phosphorus into the environment, where it contributes to water quality deterioration. These findings are consistent with the research of Roy et al. (2009), which identified phosphorus as a key driver of eutrophication in agricultural systems.

Rice, despite its high water usage, showed much lower AP (7.34 kg SO_2-eq ton^{-1}) and EP (0.81 kg PO_4^{3-}-eq ton^{-1}) values compared to wheat. The lower fertilizer requirements for rice, along with its relatively lower ammonia volatilization, contributed to its more favorable performance in these impact categories. However, it is important to note that rice still poses significant environmental challenges, particularly in terms of water management and fuel consumption. Therefore, improving fertilizer management, especially in the case of wheat, could significantly reduce the environmental impacts of crop production in Lenjanat.

Alfalfa exhibited the highest POFP value among the crops at 0.392 kg C_2H_4-eq ton^{-1}, which is somewhat surprising given its relatively favorable performance in other environmental impact categories. The high POFP of alfalfa can be attributed to the frequent harvesting operations required for this perennial crop. Alfalfa is typically harvested more than four times per year, which necessitates the use of diesel-powered machinery. The emissions from these mechanized operations contribute to the formation of photochemical oxidants, commonly known as smog. While alfalfa's lower GWP and EP make it a more sustainable crop compared to other alternatives, the environmental burden from frequent harvesting remains a concern. This finding underscores the importance of improving mechanization in alfalfa production, particularly by adopting more energy-efficient machinery and exploring alternative harvesting techniques.

In comparison, rice (0.182 kg C_2H_4eq ton^{-1}) and wheat (0.162 kg C_2H_4eq ton^{-1}) showed lower POFP values. The lower POFP values for these crops can be attributed to less frequent mechanized operations, particularly in the case of rice, where water management and irrigation are the primary environmental concerns. The findings suggest that while wheat and rice have lower POFP, they still pose significant environmental challenges in other categories, particularly GWP and AP.

The primary drivers of environmental impacts across all four crops were nitrogen fertilizers, diesel fuel, and phosphate fertilizers. Specifically, nitrogen fertilizers were responsible for 40-60% of the GWP and AP in wheat and rice production, highlighting the importance of optimizing nitrogen use. Diesel fuel, particularly for irrigation and mechanized operations, was a major contributor to both GWP and POFP, emphasizing the need to transition to more energy-efficient irrigation and mechanization practices. Phosphate fertilizers were the main contributor to EP, particularly in wheat production, where excessive use led to phosphorus runoff and leaching into water bodies.

These findings are consistent with previous research, which has identified these inputs as major environmental burdens in agricultural systems. The study by Notarnicola et al. (2017) also emphasized the importance of nitrogen and phosphorus management in reducing the environmental impacts of crop production. The results of this study suggest that improving fertilizer management, reducing fuel consumption, and transitioning to more efficient technologies can significantly reduce the environmental burden of crop production in the Lenjanat region.

Based on the findings of this study, several strategies can be implemented to reduce the environmental impacts of crop production in Lenjanat. First, improving water management practices, particularly for rice farming, is essential. Adopting efficient irrigation systems, such as drip or sprinkler irrigation, can reduce water consumption and diesel fuel use, significantly lowering the GWP of rice production. Additionally, improving the efficiency of fertilizer use, particularly nitrogen and phosphate fertilizers, can help reduce the AP and EP associated with wheat and other crops. Implementing precision farming techniques, such as variable rate application of fertilizers, can optimize input use and minimize environmental pollution.

In the case of alfalfa, improving mechanization is key to reducing POFP. The adoption of more energy-efficient machinery or exploring less mechanized harvesting methods could reduce the emissions associated with frequent harvesting. Moreover, the use of organic fertilizers and the promotion of crop rotation systems could further reduce the environmental burden of alfalfa production.

From a policy perspective, the results of this study highlight the need for sustainable agricultural policies in the Lenjanat region. Key recommendations include: Reforming cropping patterns to favor low-input and drought-resistant crops, such as legumes and other sustainable alternatives. Diversifying irrigation systems by replacing gravity-fed systems with more efficient methods such as drip or sprinkler irrigation. Providing financial incentives for farmers to adopt sustainable practices, such as the use of organic fertilizers and efficient irrigation technologies. Establishing local environmental databases to track LCA changes over time and support evidence-based decision-making in agricultural policy.

5. Conclusions

This study demonstrated that LCA can be a powerful tool for evaluating and improving the environmental sustainability of agricultural systems. The results indicate that the environmental impacts of crop production in the Lenjanat region vary significantly depending on the crop type, input structure, water consumption, and level of mechanization. These findings emphasize that sustainable agriculture in this region can only be achieved through optimizing input use, improving water management, adopting more efficient technologies, and implementing data-driven policies based on LCA results.

In terms of environmental impacts, rice was found to have the highest GWP, primarily due to high diesel fuel consumption for irrigation and extensive use of nitrogen fertilizers. This finding aligns with previous studies that have emphasized the need for improved irrigation practices and reduced fossil fuel consumption. The adoption of more efficient irrigation systems, such as drip or sprinkler irrigation, could significantly reduce the GWP associated with rice production. Additionally, improving irrigation practices in the Lenjanat region could help reduce water consumption and improve water use efficiency.

Wheat, which exhibited the highest AP and EP, highlighted the urgent need for better nutrient management and reduced reliance on chemical fertilizers. Specifically, excessive use of nitrogen and phosphate fertilizers has led to water and soil pollution in the region. In this context, adopting precision agriculture techniques, such as optimized fertilizer use and efficient irrigation systems, could significantly reduce the environmental impacts associated with wheat. Additionally, using organic fertilizers and slow-release fertilizers could help reduce chemical fertilizer use and mitigate environmental pollution.

Alfalfa, with the lowest GWP and EP, was considered a more sustainable option for agriculture in the region. This crop benefits from its natural nitrogen fixation ability, reducing the need for synthetic nitrogen fertilizers. However, due to the frequent harvesting required for this perennial crop, diesel-powered machinery contributes to increase POFP. To address this, improving mechanization efficiency or exploring alternative harvesting methods could help reduce the emissions associated with frequent harvesting. Therefore, while alfalfa performs better in many environmental categories, attention must still be paid to improving mechanization and reducing fossil fuel consumption.

The analysis of key inputs revealed that nitrogen fertilizers (especially urea), diesel fuel, and phosphate fertilizers were the primary drivers of environmental impacts. Specifically, nitrogen fertilizers contributed the most to GWP and AP, while phosphate fertilizers were the main contributors to EP in wheat production. Diesel fuel played a significant role in both GWP and POFP, emphasizing the need for the modernization of irrigation systems and mechanization practices. These findings are consistent with previous research that has identified these inputs as major environmental burdens in agricultural systems. The study suggests that optimizing fertilizer use, reducing fuel consumption, and transitioning to more efficient technologies can significantly reduce the environmental burden of crop production in the Lenjanat region.

The results of this study emphasize the need for resource management strategies in Lenjanat that focus on reducing fuel consumption, improving irrigation methods, optimizing fertilizer use, and educating farmers on reducing environmental impacts. Given the environmental challenges faced by Lenjanat, such as reduced water resources, soil erosion, and water source pollution, it is crucial to adopt policies that specifically promote sustainable agricultural practices. The findings can serve as a basis for regional policy-making aimed at improving agricultural practices and enhancing environmental sustainability in this area.

Key policy recommendations that could be implemented based on this study include:

- Reforming cropping patterns to favor low-input and drought-resistant crops, such as legumes that require less nitrogen fertilizer.
- Diversifying irrigation systems by replacing gravity-fed systems with more efficient systems, such as drip or sprinkler irrigation, which would reduce water consumption and diesel fuel use.
- Providing financial incentives for the use of sustainable inputs and practices, such as organic fertilizers and efficient irrigation technologies.
- Establishing local environmental databases to track LCA changes over time and support data-driven decision-making in agricultural policy.

In conclusion, this study has demonstrated that LCA can be an effective tool for analyzing and improving the sustainability of agricultural systems. The findings show that the environmental impacts of crops in the Lenjanat region vary significantly due to differences in input structure, water consumption, and mechanization levels. Based on these findings, it can be concluded that sustainable agriculture in this region will only be

achievable through a combination of changes in cropping patterns, optimized input use, the adoption of efficient technologies, and data-driven policymaking. Implementing these recommendations could help reduce the environmental impacts of agriculture in Lenjanat and other regions with similar environmental conditions.

References

Afshar, R. K., & Dekamin, M. (2022). Sustainability assessment of corn production in conventional and conservation tillage systems. *Journal of Cleaner Production*, *351*, 131508. https://doi.org/10.1016/j.jclepro.2022.131508

Ahmad, A., Zoli, M., Latella, C., & Bacenetti, J. (2023). Rice cultivation and processing: Highlights from a life cycle thinking perspective. *Science of The Total Environment*, *871*, 162079. https://doi.org/10.1016/j.scitotenv.2023.162079

Aliqolinya, A. (2015). Water footprint of agricultural products in the Lake Urmia basin. *Iranian Journal of Irrigation and Drainage*, *9*(3), 1-12. https://doi.org/10.22059/ijid.2015.47718

Brentrup, F., Küsters, J., Kuhlmann, H., & Lammel, J. (2004). Environmental impact assessment of agricultural production systems using the life cycle assessment methodology. *European Journal of Agronomy*, *20*(3), 247-264. https://doi.org/10.1016/j.eja.2003.12.003

Dekamin, M., Barmaki, M., Kanooni, A., & Meshkini, S. R. M. (2018). Cradle to farm gate life cycle assessment of oilseed crops production in Iran. *Engineering in Agriculture, Environment and Food*, *11*(4), 178-185. https://doi.org/10.1016/j.eaef.2018.04.003

Dekamin, M., Kheiralipour, K., & Afshar, R. K. (2022). Energy, economic, and environmental assessment of coriander seed production using material flow cost accounting and life cycle assessment. *Environmental Science and Pollution Research*, *29*(55), 83469-83482. https://doi.org/10.1007/s11356-022-21585-0

Dekamin, M., Norooz-Valashedi, R., & Toranjian, A. (2024). Environmental, energy, and economic (3E) assessment of viticulture systems. *Environmental Science and Pollution Research*, 1-18. https://doi.org/10.1007/s11356-024-35575-x

Ghasempour, A., & Ahmadi, A. (2018). Evaluation of environmental effects in producing three main crops (corn, wheat, and soybean) using life cycle assessment. *Agricultural Engineering International: CIGR Journal*, *20*(2), 126-137. https://doi.org/10.7714/aei.2018.5987

Guinée, J. B. (2002). *Handbook on Life Cycle Assessment*. Springer. https://doi.org/10.1007/978-1-4020-0215-9

Hoekstra, A. Y., Mekonnen, M. M., Chapagain, A. K., Mathews, R. E., & Richter, B. D. (2012). Global monthly water scarcity: Blue water footprints versus blue water availability. *PLoS One*, *7*(2), e32688. https://doi.org/10.1371/journal.pone.0032688

International Organization for Standardization. (2006). ISO 14040:2006 Environmental management — Life cycle assessment — Principles and framework (2nd ed.). https://www.iso.org/standard/37456.html

ISO. (2006a). *Environmental management - Life cycle assessment - Principles and framework (ISO 14040:2006)*. https://www.iso.org/standard/37456.html

ISO. (2006b). *Environmental management - Life cycle assessment - Requirements and guidelines (ISO 14044:2006)*. https://www.iso.org/standard/37456.html

Koocheki, A., Vafabakhsh, J., & Khorramdel, S. (2018). Evaluation of environmental impacts of important field crops by Life Cycle Assessment (LCA) in Khorasan-e Razavi Province. https://doi.org/10.22067/gsc.v16i3.70560

Martin-Gorriz, B., Gallego-Elvira, B., Martínez-Alvarez, V., & Maestre-Valero, J. F. (2020). Life cycle assessment of fruit and vegetable production in the Region of Murcia (south-east Spain) and evaluation of impact mitigation practices. *Journal of Cleaner Production*, *265*, 121656. https://doi.org/10.1016/j.jclepro.2020.121656

Mirhaji, M., & Khojastehpour, M. (2011). Environmental assessment of sugar beet production using LCA approach (Case study: Khusf Agro-industrial company). *Iranian Journal of Biosystems Engineering*, *42*(4), 677-688. https://doi.org/10.22067/jag.v4i2.15017

Mohseni, P., Borghaee, A. M., & Khanali, M. (2019). Energy consumption analysis and environmental impact assessment of grape production in Hazavah region of Arak city. *Journal of Agricultural Machinery*, *9*(1), 177-193. https://doi.org/10.22067/jam.v9i1.67645

Nemecek, T., & Schnetzer, J. (2010). Environmental impacts of Swiss agricultural products: Methodology and results for carrots, barley, potatoes, onions, and pork. Agroscope Reckenholz-Tänikon Research Station ART.

Nemecek, T., Dubois, D., Huguenin-Elie, O., & Gaillard, G. (2011). Life cycle assessment of Swiss farming systems: I. Integrated and organic farming. *Agricultural Systems*, *104*(3), 217-232. https://doi.org/10.1016/j.agsy.2010.10.002

Nemecek, T., Roesch, A., Bystricky, M., Jeanneret, P., Lansche, J., Stüssi, M., & Gaillard, G. (2024). Swiss agricultural life cycle assessment: a method to assess the emissions and environmental impacts of agricultural systems and products. *The International Journal of Life Cycle Assessment*, *29*(3), 433-455. https://doi.org/10.1007/s11367-023-02255-w

Nikkhah, A., Royan, M., Khojastehpour, M., & Bacenetti, J. (2017). Environmental impacts modeling of Iranian peach production. *Renewable and Sustainable Energy Reviews*, *75*, 677-682. https://doi.org/10.1016/j.rser.2016.11.041

Notarnicola, B., Sala, S., Anton, A., McLaren, S. J., Saouter, E., & Sonesson, U. (2017). The role of life cycle assessment in supporting sustainable agri-food systems. *Journal of Cleaner Production*, *140*, 399-409. https://doi.org/10.1016/j.jclepro.2016.06.071

Nuraeefar, K., Parashkoohi, M. G., & Zamani, D. M. (2024). Enhancing the efficiency of energy use and reducing the environmental effects of alfalfa and silage barley production. *Environmental and Sustainability Indicators*, *22*, 100348. https://doi.org/10.1016/j.indic.2024.100348

Pergola, M., Persiani, A., D'Ammaro, D., Pastore, V., D'Adamo, C., Palese, A. M., & Celano, G. (2022). Environmental and energy analysis of two orchard systems: A case study in Mediterranean environment. *Agronomy*, *12*(10), 2556. https://doi.org/10.3390/agronomy12102556

Pishgar-Komleh, S. H., Zylowski, T., Rozakis, S., & Kozyra, J. (2020). Efficiency under different methods for incorporating undesirable outputs in an LCA+ DEA framework: A case study of winter wheat production in Poland. *Journal of Environmental Management*, *260*, 110138. https://doi.org/10.1016/j.jenvman.2020.110138

Pré Consultants (2020). *SimaPro 9.2 Software Manual*. Amersfoort, the Netherlands.

Roy, P., Nei, D., Orikasa, T., Xu, Q., Okadome, H., Nakamura, N., & Shiina, T. (2009). A review of life cycle assessment (LCA) on some food products. *Journal of Food Engineering*, *90*(1), 1-10. https://doi.org/10.1016/j.jfoodeng.2008.06.016

Singh, R. P., & Agrawal, M. (2010). Variations in heavy metal accumulation, growth and yield of rice plants grown at different sewage sludge amendment rates. *Ecotoxicology and Environmental Safety*, *73*(4), 632-641. https://doi.org/10.1016/j.ecoenv.2010.01.020

Zamani, A., Rostamian, R., & Norouzi, G. (2024). Comparative assessment of environmental impacts and water scarcity footprint of horticultural crops in Iran. *Environmental Research*, *257*, 119082. https://doi.org/10.1016/j.envres.2024.119082

Zhu, Z., Jia, Z., Peng, L., Chen, Q., He, L., Jiang, Y., & Ge, S. (2018). Life cycle assessment of conventional and organic apple production systems in China. *Journal of Cleaner Production*, *201*, 156-168. https://doi.org/10.1016/j.jclepro.2018.08.204

Agriculture, Environment & Society

Journal homepage: www.aes.uoz.ac.ir

Environmental impacts of mung bean production systems based on life cycle assessment methodology and IMPACT 2002+ model

Amin Fathi[a,b], Kamran Kheiralipour*[a]

[a] Mechanical Engineering of Biosystems Department, Ilam University, Ilam, Iran
[b] Department of Agronomy, Ayatollah Amoli Branch, Islamic Azad University, Amol, Iran

ARTICLE INFO

Article history:
Received: 27 December 2024
Accepted: 21 February 2025
Available online: 10 March 2025

Keywords:
Agronomy
Emissions
Environment
Impact assessment
Input-output
Midpoint and endpoint indicators.

ABSTRACT

Environment is one of the key elements in sustainable production. The present study was conducted to investigate the environmental impacts of mung bean production systems in Dareh Shahr, Ilam, Iran. The required data were collected through questionnaires and face-to-face interviews with 78 mung bean farmers in 2022-2023. Inputs and output data were calculated and then environmental impacts were calculated using the life cycle assessment methodology and IMPACT 2002+ impact assessment model. The results showed that the mung bean production process in farms, potassium production in the factory, and seed production in the farm were the main contributors to almost all environmental indicators. Human health was the main indicator in mung bean production. Other main indicators were ranked as climate change, resources, and ecosystem quality. The total environmental damage of mung bean production was equal to 263.90 mPt. The results of the present research found hotspots in mung bean production which are useful to practically decrease environmental impacts via decreasing inputs and increasing output.

Highlights

- LCA shows mung bean production's total environmental damage is 263.90 mPt in Dareh Shahr, Iran.
- Human health tops environmental indicators, followed by climate change and resources.
- Farms, potassium, and seed production are key contributors to mung bean's eco-impact.
- Global warming potential of mung bean is 787.85 kg CO_2 eq./ton, higher than wheat.
- Biofertilizers and direct planting can reduce environmental burdens of mung bean.

1. Introduction

Sustainable production is a path considering economic, environmental, and social aspects, besides the technical perspective (Kheiralipour, 2022). To move on sustainable production path, environmental aspect is assessed via studying material, energy, and environmental indicators to reduce the consumption/use of different inputs and consequently decrease emissions (Kheiralipour and Sheikhi, 2021; Dekamin and Kheiralipour. 2023; Ramedani et al., 2024; Pourmehdi and Kheiralipour, 2024; Kheiralipour et al., 2024a). In this regard, environmental indicators of different production systems are studied using life cycle assessment (LCA) as a main research method (Kheiralipour et al., 2021).

Life cycle assessment is a method in which all environmental impacts associated with a product (including goods and services) are assessed throughout its life cycle, from the extraction or collection of raw materials to the consumption stage, and then recycling or disposal of the resulting waste. In this method, all resources used to produce the product and all emissions released into the environment are quantified and assessed (Pennington et al., 2004; Kheiralipour, 2020).

Life cycle assessment is a systematic and step-by-step process that consists of four phases: defining the purpose

* Corresponding author.
E-mail address: k.kheiralipour@ilam.ac.ir
https://doi.org/10.22034/jelsa.2025.496117.1095

and scope of the study (scope), inventory analysis, impact assessment, and interpretation (Guinee, 2002). The methodology has been applied to assess the environmental impacts of different production systems in industry (Kheiralipour et al., 2022; Jiang et al., 2023; Kheiralipour et al., 2024b), agriculture (Kheiralipour et al., 2017; Payandeh et al., 2017; Ramedani et al., 2019; Bamber et al., 2022; Kheiralipour et al., 2023), and agricultural processing plants (Pourmehdi and Kheiralipour, 2020; Gholamrezaee et al., 2021; Jalilian et al., 2021; Dominguez Aldama et al., 2023; Kheiralipour & Sheikhi, 2024).

Environmental impacts of different agronomic products such as canola (Kheiralipour et al., 2017), coriander (Dekamin et al., 2022), oat (Viana et al., 2022), and wheat (Pourmehdi and Kheiralipour, 2023) have been investigated. However, the goal of the present research is to investigate the environmental impacts of mung bean production systems. Studying the environmental impacts of this agronomic product is essential to take the first step in reducing its environmental burdens. Moreover, it finds environmental hotspots by ranking the environmental contributors to prioritize the management strategies in the reduction of the burdens.

Mung bean (*Vigna radiata* L.) belongs to the legume family (Lambrides & Godwin, 2007) and is one of the most important crops due to their high nutritional properties (Tong, 2020; Ganesan & Xu, 2018; Fathi & Kheiralipour, 2025). Although about 90% of the mung bean is produced in Asia, mostly in India, China, Pakistan, and Thailand countries, it is cultivated in Africa and Australia (Lambrides & Godwin, 2007). According to the importance of mung bean and protecting the environment, the novel goal of the present research is to assess the environmental impacts of the crop.

Different impact assessment models have been used to calculate environmental impacts including CLM-IA baseline (Kheiralipour et al., 2022; Kheiralipour et al., 2024c), ReCiPe 2016 (Shrestha et al., 2020; Jiang et al., 2021), and IMPACT 2002+ (Jolliet et al., 2003; Rybaczewska-Blazejowska & Jezierski, 2024). However, the goal of the present research is to investigate the environmental impacts of mung bean production systems in Dareh Shahr, Ilam, Iran, using the IMPACT 2002+ model.

2. Materials and methods

The present LCA study was conducted based on the ISO 14040 standard in four main phases (ISO, 2006). In the first phase of the life cycle assessment, the product, process, or activity is defined and described. The system under study, the system boundaries, and the functional unit are also identified (Guinee, 2002).

Defining the purpose and scope is the most important stage of life cycle assessment; because it is the most important leader for the next phase and the selection of the impact categories under study.

Life cycle assessment is a “cradle to grave” approach; however, it is possible to consider the system boundary as part of the entire process in order to focus on the processes. It is also possible to express the results based on the selected boundary and on a smaller scale (Kheiralipour, 2020). The goal of the present research was to investigate the environmental impacts of mung bean production systems via a gate-to-gate LCA study in Dareh Shahr, Ilam, Iran. The functional unit was 1 tone mung bean grain. The allocation process was neglected because the output in the farms was only mung bean grain. The boundary of the present research was considered to be included from tillage to harvesting operations and transportation, post-harvest processing, and distribution were excluded.

In the inventory analysis phase, all necessary resources in the system for the production of the product and all outputs and environmental emissions should be determined. This phase included calculating inputs and emissions. The data collection in the present research was based on the questionnaire method and face-to-face interviews.

The information about different inputs and their amounts and the amount of mung bean output was collected. The inputs were seed, fertilizers (nitrogen, phosphorous, and potassium), sprays (pesticide and herbicide), labor, machinery, fuel, oil, electricity, and water in different agricultural operations The data related to the input and output materials were randomly collected for the mung bean farms in Darreh Shahr, Ilam, Iran. The input and emissions were calculated per the functional unit. All emissions to air, soil, and water must be calculated or measured. The emissions related to input consumption/use were calculated according to the IPCC 14040 (IPCC, 2006).

As in agriculture, the Ecoinvent2.0 database is more used, the emissions related to input production were obtained from the available in the used software.

In the third phase, impact assessment, it must first be determined which impact categories should be considered and what method should be used to assess their impact. As in agriculture, SimaPro (PRé, 2006) is more used, this software was used to calculate the midpoint and endpoint environmental impacts of mung bean production in the characterization step. The IMPACT 2002+ model was applied to categorize the environmental impacts. Other steps in the third phase including normalization and weighting were done after characterization.

In the interpretation phase, the results of the impact assessment and the calculations are evaluated to identify the hotspots in the production path that have the most adverse environmental impacts. The options with less adverse impacts on the environment can be evaluated. In this phase, conclusions are drawn and an LCA report is prepared (Kheiralipour, 2021; Kheiralipour, 2023). In the last phase, the contributions of the process and all inputs were assessed in this phase.

3. Results and Discussion

3.1. Environmental indicators

The midpoint and endpoint environmental indicators and their values in mung bean LCA study based on the IMPACT 2002+ model were presented in Table 1 and 2, respectively.

Table 1. The values of the midpoint environmental indicators in mung bean production systems.

No.	Indicator	Unit	Value
1	Carcinogens	kg C_2H_3Cl eq.	18.23
2	Non-carcinogens	kg C_2H_3Cl eq.	8.96
3	Respiratory inorganics	kg PM2.5 eq.	0.79
4	Ionizing radiation	Bq C-14 eq.	4386.18
5	Ozone layer depletion	kg CFC-11 eq.	5.87×10^{-5}
6	Respiratory organics	kg C_2H_4 eq.	0.21
7	Aquatic ecotoxicity	kg TEG water	260421.70
8	Terrestrial ecotoxicity	kg TEG soil	8361.43
9	Terrestrial acidification/nutrification	kg SO_2 eq.	74.13539
10	Land occupation	m2org.arable	67.85
11	Aquatic acidification	kg SO_2 eq.	24.69
12	Aquatic eutrophication	kg PO_4 P-lim	0.593042
13	Global warming	kg CO_2 eq.	787.85
14	Non-renewable energy	MJ primary	11891.05
15	Mineral extraction	MJ surplus	14.11

Table 2. The values of the endpoint environmental damages of mung bean production.

Indicator	Unit	Value
Human health	DALY	6.32×10^{-4}
Ecosystem quality	PDF*m^2×yr	230.27
Climate change	kg CO_2 eq.	787.85
Resources	MJ primary	11905.16

Pourmehdi and Kheiralipour (2023) calculated the environmental impacts of dryland and irrigated wheat production systems based on the CML Baseline model. As ozone layer depletion and global warming indicators are the same in IMPACT 2002+ and CML Baseline models, their values can be compared. The value of the global warming indicator in mung bean was 787.85 kg CO_2 eq./ton which was higher than the corresponding values of dryland (588 kg CO_2 eq./ton,) and irrigated (308 kg CO_2 eq./ton) wheat. The value of global warming in the production of 1 ton of wheat flour was 693 kg CO_2 eq (Pourmehdi and Kheiralipour, 2020), However, the value of the global warming indicator for mung bean was lower than that of coriander seed (897.38 kg CO_2 eq., Dekamin et al., 2022), chicken (5782.38 kg CO_2 eq., Payandeh et al., 2017), turkey bird (3630 kg CO_2 eq., Kheiralipour et al., 2017), and ostrich production (16800 kg CO_2 eq., Ramedani et al., 2019). Also, ozone layer depletion of mung bean had a higher value (5.87×10^{-5} kg CFC-11 eq./ton) than the corresponding values of dryland and irrigated wheat production systems (3.54×10^{-5} and 1.90×10^{-5} kg CFC-11 eq./ton, respectively).

3.2. Normalized indicators

The normalizing step was done using the IMPACT 2002+ model. The highest to lowest endpoint indicators were ranked as human health, climate change, resources, and ecosystem quality. The values of the indicators were 8.92×10^{-2}, 7.96×10^{-2}, 7.83×10^{-2}, and 1.68×10^{-2}, respectively (Figure 1).

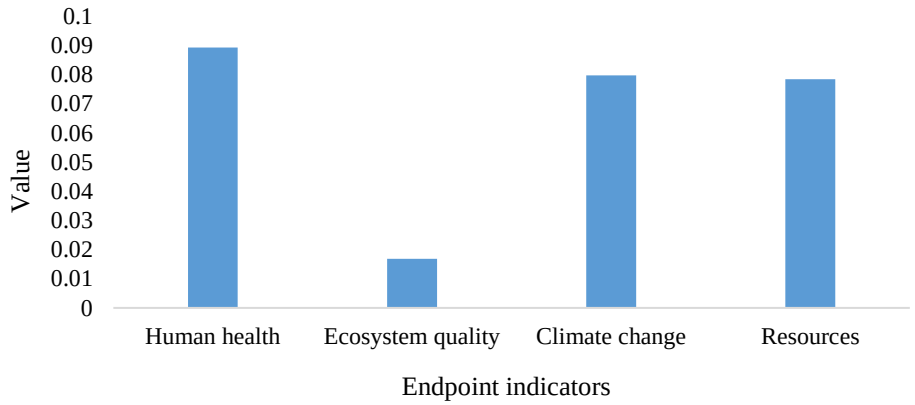

Figure 1. The normalized endpoint environmental damages of mung bean production.

3.3. Weighted indicators

The results of the weighting stage of endpoint environmental damages of mung bean production based on the Impact 2002+ model have been shown in Table 3. The first endpoint indicator in mung bean production systems was human health with a weighted value of 89.18 mPt. The second to fourth indicators were climate change, resources, and ecosystem quality, with values of 79.57, 78.34, and 16.81 mPt, respectively.

The advantage of the IMPACT 2002+ model is calculating the total damage impact of production systems, compared to the CML Baseline impact assessment model. The total damage impact of 1 ton of mung bean production in the present research has been estimated as 263.90 mPt.

Table 3. The values of the weighted endpoint environmental damages of mung bean production.

Indicator	Unit	Value
Human health	mPt	89.18
Ecosystem quality	mPt	16.81
Climate change	mPt	79.57
Resources	mPt	78.34
Total	mPt	263.90

3.4. Environmental contributors

The contributions of each factor in the midpoint and endpoint environmental indicators have been presented in Tables 4 and 5. The main contributor to all midpoint and endpoint indicators was the process (mung bean production in the farms). The second contributor to carcinogens, non-carcinogens, ionizing radiation, ozone layer depletion, respiratory organics, terrestrial ecotoxicity, non-renewable energy, and mineral extraction was potassium fertilizer. The corresponding factor for respiratory inorganics, terrestrial acid/nutria, aquatic ecotoxicity, aquatic acidification, aquatic eutrophication, and global warming indicators was seed input. Also, the second contributor to human health, ecosystem quality, and climate change endpoint indicator was seed. Lack of the information about seed production in databases was a limitation of the present research. This caused over estimating the contribution of seed in environmental impacts in mung bean production because instead of that, soybean seed was selected in SimaPro software.

Table 4. The values of each factor corresponded to the midpoint environmental indicators of mung bean production. *Process means the mungbean production in the farms.

Factor	Carcinogens	Non-carcinogens	Respiratory inorganics	Ionizing radiation	Ozone layer depletion	Respiratory organics	Aquatic ecotoxicity	Terrestrial ecotoxicity
Process	18.23009	8.96194	0.792738	4386.178	5.87E-05	0.205981	260421.7	8361.432
Seed	0	0.225506	0.550479	0	0	6.7E-05	226901.3	1020.824
Machinery	0.09114	-0.05328	0.010341	37.80238	7.53E-07	0.003149	-1559.16	-1511.17
Fuel	0.054364	-0.04274	0.00215	0	2.44E-08	0.003596	-283.19	0.47252
Lubricant	0.126524	0.200749	0.021211	1491.041	8.57E-06	0.054833	2198.17	560.6722
Nitrogen	0.028634	0.030902	0.001314	33.86752	6.28E-07	0.013798	203.6656	53.36281
Potassium	4.733545	5.351907	0.143139	1852.379	3.07E-05	0.061239	16258.02	5051.77
Phosphorous	0.229937	0.370029	0.010974	130.0214	1.72E-06	0.003903	1274.854	453.1436
Herbicide	0.095148	0.147634	0.009158	78.40036	6.06E-07	0.001387	500.6477	187.5579
Insecticide	0.183464	0.357923	0.010165	517.5986	1.58E-06	0.002998	4117.104	1458.821
Electricity	0.073605	0.147295	0.003867	199.4702	4.89E-07	0.001034	1750.717	627.9045

Factor	Terrestrial acid/nutria	Land occupation	Aquatic acidification	Aquatic eutrophication	Global warming	Non-renewable energy	Mineral extraction
Process	74.13539	67.84896	24.69323	0.593042	787.848	11891.05	14.10772
Seed	66.67962	0	22.97163	0.537317	312.251	0	0
Machinery	0.230248	56.92684	0.044106	0.006384	5.947096	68.92205	0.22634
Fuel	0.081681	0	0.014615	0.000498	13.00472	147.7827	0.224088
Lubricant	0.503183	0.234474	0.130386	0.003663	21.35105	2934.953	0.154229
Nitrogen	0.023565	0.019246	0.007655	0.000361	1.147453	66.28975	0.052515
Potassium	5.112735	6.748269	1.066944	0.027805	223.0732	4756.395	11.97614
Phosphorous	0.427686	0.555062	0.079403	0.002351	14.41521	249.9917	0.802822
Herbicide	0.176668	0.646204	0.12616	0.007944	5.38705	94.10621	0.26757
Insecticide	0.182964	1.769509	0.055369	0.003929	16.50746	335.7808	0.207067
Electricity	0.068512	0.870361	0.020876	0.001576	5.556864	116.9086	0.08029

Machinery was the second contributor to the land occupation indicator. The potassium fertilizer was the third main factor for respiratory inorganics and aquatic ecotoxicity, terrestrial acid/nutria, land occupation, aquatic acidification, aquatic eutrophication, and global warming indicators. The third main factor for ionizing radiation, ozone layer depletion, respiratory organics, and non-renewable energy was lubricant oil, for carcinogens, non-carcinogens, and mineral extraction was phosphorous fertilizer, and for terrestrial ecotoxicity was insecticide. Also, the third contributor to human health, ecosystem quality, and climate change endpoint indicator was potassium fertilizer.

According to Pourmehdi and Kheiralipour (2023), the main contributor for almost all indicators in wheat production was nitrogen fertilizer except for eutrophication and acidification indicators which the wheat production process in farms was the main contributor for them.

Managing the different operations in mung bean production causes a reduction in inputs and an increase in output and consequently decreases the environmental impacts and climate change mitigation. Sustainable agriculture practices such as increasing biodiversity cause to decrease the environmental impacts. Governmental programs such as education, incentives, and fines can be effective in this regard. The consumption of biofertilizers leads to a decrease in the application of chemical fertilizers (Sharifi and Kheiralipour, 2025) and using direct planting equipment causes reduced machinery use and fuel and oil consumption. These strategies lead reduction in environmental impacts of mung bean production.

Table 5. The contribution values corresponded to each factor in the endpoint environmental damages of mung bean production.

Factor	Human health	Ecosystem quality	Climate change	Resources
Process	6.32×10^{-4}	230.27	787.85	11905.16
Seed	3.86×10^{-4}	88.81	312.25	0.00
Machinery	7.36×10^{-6}	50.26	5.95	69.15
Fuel	1.55×10^{-6}	7.45×10^{-2}	13.00	148.01
Lubricant	1.62×10^{-6}	5.32	21.35	2935.11
Nitrogen	1.12×10^{-6}	0.48	1.15	66.34
Potassium	1.29×10^{-4}	53.45	223.07	4768.37
Phosphorous	9.40×10^{-6}	4.70	14.42	250.79
Herbicide	7.11×10^{-6}	2.40	5.39	94.37
Insecticide	8.75×10^{-6}	13.87	16.51	335.99
Electricity	3.37×10^{-6}	6.07	5.56	116.99

4. Conclusions

Environmental impacts of mung bean production systems were assessed in the present research. The environmental impacts were investigated in characterization, normalization, and weighting steps. The total damage impact of the production was 263.90 mPt. The contribution of mung bean production process in the farms and all inputs to all indicators were studied to find the environmental hotspots.

Decreasing inputs and increasing output cause decreasing environmental impacts of mung bean production. Based on the results of the present research, different attempts must be made to decrease the environmental impact of mung bean production by focusing firstly on the hotspots and then the other contributing factors. Application of biofertilizers in the farms instead of chemical fertilizers, pest control using biological agents, and using new technologies and methods to manage different operations such as direct planting and new irrigation systems are recommended. Governmental programs can be useful in educating the farmers to better manage operations, crop rotation, and biodiversity and consequently move on the sustainable production path. These suggestions not only can decrease inputs, increase output, and reduce environmental impacts, but also can decrease production costs and increase economic profits in mung bean production. The limitation of the present research was the lack of mung bean seed production in the LCA databases. This caused over estimating the contribution of seed in environmental impacts in mung bean production because instead of that, soybean seed was selected in SimaPro software. So, the results of the present research can be used in the future by providing environmental impacts of mung bean.

Acknowledgment

The authors acknowledge Ilam University for supporting this research. They also tank to the mung bean farmers who answered the questioners for gathering the information in the present research.

References

Bamber, N., Johnson, R., Laage, E., Dias, G., Tyedmers, P., & Pelletier, N. (2022). Life cycle inventory and emissions modelling in organic field crop LCA studies: review and recommendations. *Resources, Conservation and Recycling, 185,* 106465. https://doi.org/10.1016/j.resconrec.2022.106465

Dekamin, M., & Kheiralipour, K. (2023). Material and energy flow cost accounting (MEFCA) of grape production in Malayer City. *Journal of Agricultural Economics & Development, 37,* 325-340. https://doi.org/10.22067/jead.2023.80448.1174

Dekamin, M., Kheiralipour, K., & Keshavarz Afshar, R. (2022). Energy, economic, and environmental assessment of coriander seed production using material flow cost accounting and life cycle assessment. *Environmental Science and Pollution Research.* https://doi.org/10.1007/s11356-022-21585-0

Dominguez Aldama, D., Grassauer, F., Zhu, Y., Ardestani-Jaafari, A., & Pelletier, N. (2023). Allocation methods in life cycle assessments (LCAs) of agri-food co-products and food waste valorization systems: Systematic review and recommendations. *Journal of Cleaner Production, 421,* 138488. https://doi.org/10.1016/j.jclepro.2023.138488

Fathi, A., & Kheiralipour, K. (2025). Investigating the energy consumption and carbon footprint in mung bean production ecosystems in Iran. *Biosystems Engineering and Renewable Energies*, 1, 59-63. https://doi.org/10.22069/bere.2025.23066.1012

Ganesan, K., & Xu, B. (2018). A critical review on phytochemical profile and health promoting effects of mung bean (Vigna radiata). *Food Science and Human Wellness, 7(1),* 11-33. https://doi.org/10.1016/j.fshw.2017.11.002

Gholamrezaee, H., Kheiralipour, K., & Rafiee, S. (2021). Investigation of energy and environmental indicators in sugar production from sugar beet. *Journal of Environmental Studies Sciences, 6(2),* 3540-3548.

Guinee, J. B. (2002). *Handbook on life cycle assessment operational guide to the ISO standards.* Kluwer Academic, New York, USA. https://doi.org/10.1007/bf02978897

IPCC. (2006). IPCC 14040. *IPCC guidelines for national greenhouse gas inventories.* In: Eggleston, H. S., Buendia, L., Miwa, K., Ngara, T., Tanabe, K., Editors. Prepared by the national greenhouse gas inventories programme. IGES, Japan.

ISO. (2006). *ISO 14040 Environmental Management-Life Cycle Assessment-Principles and Framework.*

Jalilian, M. M., Kheiralipour, K., & Mirzaee Ghaleh, E. (2021). Comparison of environmental indicators in Sangak and Lavash bread production in Eslamabad-e-Gharb, Kermanshah. *Journal of Environmental Sciences Studies, 5(4),* 3198-3203.

Jiang, J., Chu, C., Song, L., Gao, X., Huang, B., Zhang, Y., Zhang, Y., Liu, Y., Hou, L., Ju, M., & Cao, Z. (2023). From prospecting to mining: A review of enabling technologies, LCAs, and LCCAs for improved construction and demolition waste management. *Waste Management, 159*, 12-26. https://doi.org/10.1016/j.wasman.2023.01.017

Jiang, Z., Zheng, H., & Xing, B. (2021). Environmental life cycle assessment of wheat production using chemical fertilizer, manure compost, and biochar-amended manure compost strategies. *Science of the Total Environment, 760*, 143342. https://doi.org/10.1016/j.scitotenv.2020.143342

Jolliet, O., Margni, M., Charles, R., Humbert, S., Payet, J., Rebitzer, G., & Rosenbaum, R. (2003). IMPACT 2002+: a new life cycle assessment methodology. *The International Journal of Life Cycle Assessment, 8(6)*, 324-330. https://doi.org/10.1007/bf02978505

Kheiralipour, K. (2022). *Sustainable Production: Definitions, Aspects, Elements.* 1st Ed., Nova Science Publishers, New York, USA. https://doi.org/10.52305/pmeu7193

Kheiralipour, K. (2021). Environmental Life Cycle Assessment of Poultry Production Systems. In: Jacob-Lopes, E., Zepka, L. Q., & Depra, M. C., Editors. *Interdisciplinary applications of the life cycle assessment tool.* 1st Ed., Nova Science Publishers, New York, USA.

Kheiralipour, K. (2020). *Environmental Life Cycle Assessment.* 1st Ed., Ilam University Publication, Ilam, Iran.

Kheiralipour, K., Brandao, M., Holka, M., & Chorynski, A. (2024a). A review of environmental impacts of wheat production in different agrotechnical systems. *Resources, 13(7)*, 93. https://doi.org/10.3390/resources13070093

Kheiralipour, K., Jafari Samrin, H., & Soleimani, M. (2017). Determining the environmental impacts of canola production by life cycle assessment, case study: Ardabil Province. *Iranian Journal of Biosystems Engineering, 48*, 517-526. https://doi.org/10.22059/ijbse.2017.218793.664864

Kheiralipour, K., Khoobbakht, M., & Karimi, M. (2024b). Effect of biodiesel on environmental impacts of diesel mechanical power generation by life cycle assessment. *Energy, 289*, 129948. https://doi.org/10.1016/j.energy.2023.129948

Kheiralipour, K., Rafiee, S., Karimi, M., Nadimi, M., & Paliwal, J. (2024c). The environmental impacts of commercial poultry production systems using life cycle assessment: a review. *World's Poultry Science Journal, 80*, 1-22. https://doi.org/10.1080/00439339.2023.2250326

Kheiralipour, K., Payandeh, Z., & Khoshnevisan, B. (2017). Evaluation of environmental impacts in turkey production system in Iran. *Iranian Journal of Applied Animal Science, 7*, 507-512.

Kheiralipour, K., & Sheikhi, N. (2024). Comparing the environmental impacts of seven bread-baking systems. *International Journal of Environmental Science and Technology, 22*, 4951-4960. https://doi.org/10.1007/s13762-024-06174-7

Kheiralipour, K., & Sheikhi, N. (2021). Material and energy flow in different bread baking types. *Environment, Development and Sustainability, 23*, 10512-10527. https://doi.org/10.1007/s10668-020-01069-2

Kheiralipour, K., Tashanifar, E., Hemati, A., Motaghed, S., & Golmohammadi, A. R. (2022). Environmental impact investigation of natural gas refinery process based on LCA CML-IA baseline method. *Gas Processing Journal, 9(2)*, 1-14. https://doi.org/10.22108/gpj.2021.127680.1100

Lambrides, C. J., & Godwin, I. D. (2007). Mung bean. In: Kole, C., Editor. *Genome Mapping and Molecular Breeding in Plants-Pulses, Sugar and Tuber Crops*, Springer, Heidelberg, Germany.

Payandeh, Z., Kheiralipour, K., Karimi, M., & Khoshnevisan, B. (2017). Joint data envelopment analysis and life cycle assessment for environmental impact reduction in broiler production systems. *Energy, 127*, 768-774. https://doi.org/10.1016/j.energy.2017.03.112

Pennington, D. W., Potting, J., Finnveden, G., Lindeijer, E., Jolliet, O., Rydberg, T., & Rebitzer, G. (2004). Life cycle assessment part 2: current impact assessment practice. *Environment International, 30*(5), 721-39. https://doi.org/10.1016/j.envint.2003.12.009

Pourmehdi, K., & Kheiralipour, K. (2024). Net energy gain efficiency, a new indicator to analyze energy systems, case study: comparing wheat production systems. *Results in Engineering, 22*, 102211. https://doi.org/10.1016/j.rineng.2024.102211

Pourmehdi, K., & Kheiralipour, K. (2023). Compression of input to total output index and environmental impacts of dryland and irrigated wheat production systems. *Ecological Indicators, 148*, 110048. https://doi.org/10.1016/j.ecolind.2023.110048

Pourmehdi, K., & Kheiralipour, K. (2020). Assessing the effects of wheat flour production on the environment. *Advances in Environmental Technology, 2*, 111-117. https://doi.org/10.22104/aet.2021.4704.1280

PRé. (2006). *PRé Consultants. SimaPro Database Manual*, Amersfoort, The Netherlands.

Ramedani, Z., Alimohammadian, L., Kheialipour, K., Delpisheh, P., & Abbasi, Z. (2019). Comparing energy state and environmental impacts in ostrich and chicken production systems. *Environmental Science and Pollution Research, 27*, 28284-28293. https://doi.org/10.1007/s11356-019-05972-8

Ramedani, Z., Lotfi, M., Veisi, A., & Kheiralipour, K. (2024). Comparison of material and energy indicators in sunflower and pumpkin seed production systems. *Sustainability Research: Technology Development and Assessment, 10*. https://doi.org/10.22098/sr.2024.14811.1020

Rybaczewska-Blazejowska, M., & Jezierski, D. (2024). Comparison of ReCiPe 2016, ILCD 2011, CML-IA baseline and IMPACT 2002+ LCIA methods: a case study based on the electricity consumption mix in

Europe. *The International Journal of Life Cycle Assessment*, *29*, 1799-1817. https://doi.org/10.1007/s11367-024-02326-6

Sharafi, S., & Kheiralipour, K. (2025). Long-term trends of chemical fertilizer consumption and productivity in cultivating five major crops in Iran. *Energy Nexus*, 18, 100444. https://doi.org/10.1016/j.nexus.2025.100444

Shrestha, P., Karim, R. A., Sieverding, H. L., Archer, D. W., Kumar, S., Nleya, T., Graham, C. J., & SMge, J. J. (2020). Life cycle assessment of wheat production and wheat-based crop rotations. *Journal Environment Quality*, *49*, 1515-1529. https://doi.org/10.1002/jeq2.20158

Tong, L.-T. (2020). Gluten-free noodles. In: Hou, G. G., Editor. *Asian Noodle Manufacturing*, Woodhead Publishing, Cambridge, UK. https://doi.org/10.1016/b978-0-12-812873-2.00007-8

Viana, L. R., Dessureault, P.-L., Marty, C., Loubet, P., Levasseur, A., Boucher, J.-F., & Paré, M. C. (2022). Would transitioning from conventional to organic oat grains production reduce environmental impacts? A LCA case study in North-East Canada. *Journal of Cleaner Production*, *349*, 131344. https://doi.org/10.1016/j.jclepro.2022.131344

Agriculture, Environment & Society

Journal homepage: www.aes.uoz.ac.ir

Assessment of industrial crops biodiversity in Kermanshah province during 2013-2022

Farzad Mondani *[a], Afsaneh Yarmohammadi [b], Mahmoud Khoramivafa [a]

[a] Department of Plant Production and Genetic, Razi University, Kermanshah, Iran
[b] Ph.D Student in Agroecology, Department of Plant Production and Genetics, Razi University, Kermanshah, Iran

ARTICLE INFO

Article history:
Received: 15 December 2024
Accepted: 22 February 2025
Available online: 1 May 2025

Keywords:
Shannon-Wiener biodiversity index
Sorenson's similarity index
Species diversity
Species richness

ABSTRACT

Agroecosystem health is a function of biodiversity; however, less attention has been paid to the importance of this issue in agricultural systems. Therefore, this study evaluated the biodiversity of industrial crops in Kermanshah Province. The required data, including industrial crops and their cultivation areas, were collected from the statistics and information bank of the agricultural organization for the years 2013-2022. Then biodiversity indices including species richness, Shannon-Wiener, evenness, and Sorenson's similarity were calculated. Among the counties, Kermanshah, Sarpol-e Zahab, and Sahneh had the highest species richness in most years, while Gilan-e Gharb county showed the lowest species richness. The highest Shannon-Wiener index value for the entire province was 1.11 at 2013, and the lowest was 0.78 at 2015. The counties of Sarpol-e Zahab, Gilan-e Gharb, Kermanshah, and Ravansar had the highest Shannon-Wiener biodiversity index values in most crop years, while Songhor county had the lowest value of this index, such that at 2013, the value of this index was 0.104 and decreased annually by approximately 0.8 units to about 0.020 at 2022. Among the province's counties, the highest Sorenson's similarity index was observed between Kermanshah and Islamabad (1.0), and the lowest was between Sahneh and Songhor counties (0.8). The highest evenness index was found in Islamabad-e Gharb, Ravansar, Gilan-e Gharb, and Sahneh with values of 0.05, 0.16, 0.17, and 0.094, respectively, while the lowest was in Songhor with a value of 0.003.

Highlights

- Shannon-Wiener index fell from 1.11 (2013) to 0.912 (2022); Songhor hit 0.020.
- Sorenson similarity highest (1.0) Kermanshah-Islamabad; lowest (0.8) Sahneh-Songhor.
- Evenness peaked in Ravansar (0.16), Gilan-e Gharb (0.17); Songhor lowest (0.003).
- Five industrial crops studied; cultivation area grew most in Kermanshah, shrank in Kangavar.

1. Introduction

Biodiversity refers to all living organisms and their interrelationships, representing genetic diversity, species diversity of living organisms, and the diversity of ecosystems in which these organisms live (Alibeygi et al., 2019). Agricultural diversity, as a component of biodiversity, is a combination of life forms and their interactions with each other and the physical environment that has made Earth habitable for humans (Lima and Pereira, 2023). Agricultural biodiversity has been recognized as one of the most important factors in establishing and enhancing agricultural sustainability, as maintaining and increasing biodiversity in agricultural ecosystems creates a balance between food production and other ecosystem services (Jackson et al., 2007; Shrestha et al., 2010). Furthermore, biodiversity can act as a support system in environmental processes and ecosystem service formation. Currently, many plant and animal species worldwide are at risk of extinction, with habitat destruction due to various human activities being the primary cause (Hilton-Taylor and Brackett, 2000).

Assessing agricultural biodiversity requires estimating the geographical area covered by species, varieties belonging to these species, population size, and existing

* Corresponding author.
E-mail address: f.mondani@razi.ac.ir
https://doi.org/10.22034/jelsa.2025.494204.1093

genetic diversity (Brown, 2000). Such assessments require the development and implementation of various methods. Species richness is the simplest method for evaluating biodiversity. Species richness indicates the total number of species or varieties present at a point in time (Hubbell, 2001). Species evenness expresses the number of individuals or areas belonging to each species or variety. The Shannon-Wiener and Simpson diversity indices combine the concepts of richness and evenness, providing computational and numerical methods for determining ecosystem diversity (McCune and Grace, 2002).

Koocheki et al. (2004b), in a study on the biodiversity of horticultural crops and vegetables in Iran, found that 31 horticultural species and 14 vegetable species were cultivated throughout the country. These researchers considered the diversity of horticultural and vegetable crops in the country's provinces to be relatively appropriate. In another study on cereals, it was reported that the lowest Shannon-Wiener index in the entire country belonged to Gilan province, indicating the dominance of rice species (Nasiri Mahalati et al., 2005). Estimates indicate that improved varieties have led to the loss of 90% of local varieties worldwide. The functioning of natural and agricultural ecosystems is based on biodiversity, and the destruction of biodiversity poses a serious threat to the survival of agricultural ecosystems and ultimately global food security (Blackshaw et al., 2001). Assessment of agricultural systems biodiversity in Ilam province also showed that over twelve years, the overall trend of changes in agricultural systems diversity decreased (Asgharipour et al., 2019). Additionally, an evaluation of the biodiversity status of agricultural and horticultural crops in Golestan province over 15 years revealed a decrease in agricultural crop biodiversity (Kazemi et al., 2018). Pourghasemian and Moradi (2016) found in their research that the highest and lowest evenness indices for horticultural crops belonged to Isfahan (0.83) and Semirom (0.192) counties respectively, and the highest and lowest Shannon-Wiener biodiversity indices in agricultural crops were observed in forage plants (0.929) and cucurbits (0.442) respectively.

Assessment of agricultural plant diversity in Kermanshah province also showed that, in general, the biodiversity of irrigated farms is higher than that of rainfed farms, demonstrating the impact of water resources on biodiversity (Asgari et al., 2018). Research results by Mondani et al. (2015) indicated that 16 medicinal plant species were cultivated in Kermanshah province, and among the counties of this province, Harsin, Kermanshah, and Kangavar had the highest number of species, while Qasr-e Shirin and Islamabad-e Gharb had the lowest. They reported that among the province's counties, the highest and lowest Shannon-Wiener biodiversity indices belonged to Kermanshah (1.28) and Sahneh (0.47), respectively. Allahyari et al. (2015) also showed that 29 crop species were cultivated in Kermanshah province, indicating relatively diverse agricultural products, with the highest number of crop species observed in Kermanshah, Sahneh, and Harsin counties, and the lowest in Paveh. They also stated that among the counties, the highest 10-year average Shannon-Wiener diversity index for agricultural crops belonged to Harsin (1.7) and the lowest to Dalahu (1).

Among the country's provinces, Kermanshah, with an area of over 2.3 million hectares, plays a significant role in agricultural production due to its diverse climatic conditions. In preliminary general assessments conducted by Koocheki et al. (2004c), the biodiversity status of agricultural products in this province was reported as favorable. However, to maintain and increase agricultural biodiversity, such studies need to be conducted more precisely at the county level within the province. Undoubtedly, the protection and proper utilization of existing biodiversity in agricultural ecosystems depends primarily on understanding its characteristics and spatial distribution, which itself requires studying biodiversity at various levels, including ecosystem levels, crop species, and their genotypes. Therefore, given the importance of this issue, this study was conducted to evaluate the trends in biodiversity changes of industrial crops by county in Kermanshah province over 10 years from 2013 to 2022.

2. Materials and Methods

2.1. Study area and data collection

This study was conducted in Kermanshah province (between 33° to 35° N latitude and 45° to 47° E longitude) located in western Iran at 2024 (Figure 1). The required data were obtained from the Statistics and Information Technology Department of the Ministry of Agriculture Jihad (MJA, 2024). These data included the cultivation area of agricultural products, particularly industrial plants, by species in 9 counties of Kermanshah province, recorded during the period from 2013 to 2022. Data collection was conducted either through in-person visits to the Agricultural Jihad Organization or retrieved from the organization's information database.

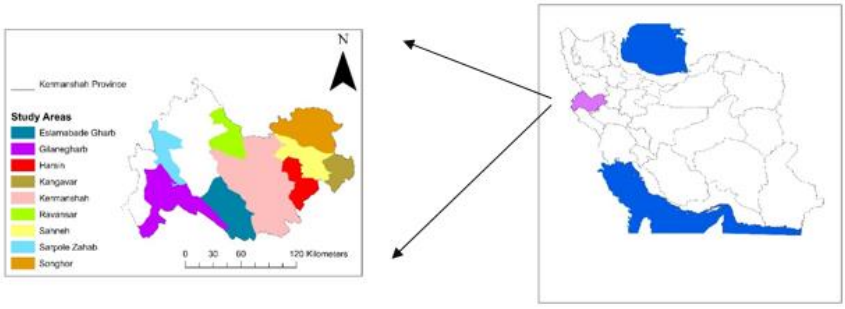

Figure 1. The study area in Kermanshah province by county

2.2. Measured biodiversity indices

2.2.1. Species richness

Species richness indicates the number of species present in an area, which was estimated by counting the number of industrial crop species cultivated in the province and by county (Barnes, 1998).

2.2.2. Shannon-Wiener index

The Shannon-Wiener index (H) is a more suitable index for measuring biodiversity, calculated based on species richness and relative abundance of species according to Equation 1 (Shannon and Wiener, 1949).

$$H = -\Sigma[(ni/N)\times\ln(ni/N)] \quad (1)$$

In this equation, ni is the number of individuals of each species (*i*th species), and N is the total number of individuals in an area. In this index, ni/N represents the proportion or relative frequency of a species. In this study, for calculating the Shannon diversity index, ni/N was considered as the cultivation area of each genotype of the *i*th species relative to the total cultivation area of that species. Additionally, to calculate the Shannon-Wiener diversity index for all industrial agricultural crops in the province (H'), equation (1) was used, but here ni/N represented the ratio of cultivation area of the *i*th industrial crop species to the total cultivation area of agricultural crops in the province.

2.2.3. Evenness index

With the Shannon-Wiener diversity index (H) known, the evenness index was calculated using Equation 2 (Magurran, 1988).

$$E = H/\ln(S) \quad (2)$$

In this equation, E is the evenness index, and S is the number of species (cultivation area of plant species). This index is a measure of the intensity of distribution uniformity of the number or cultivation area among genotypes of an agricultural species, and its value is equal to or less than 1. E=1 indicates equal cultivation area among all genotypes of an agricultural species, while E<1 indicates non-uniform distribution.

2.2.4. Sorenson's similarity index

Similarity indices show the difference in species composition and diversity changes in different habitats. There are several similarity indices, with Sorenson's similarity index (S) being the most common (Equation 3) (Magurran, 2004).

$$S = 2Vij/(Vi + Vj) \quad (3)$$

In this equation, Vij represents the number of common species present in both areas A and B, Vi and Vj represent the number of species present in area A but not in area B, and the number of species present in area B but not in area A, respectively. Sorenson's similarity index varies between zero (complete dissimilarity) and one (complete similarity between two areas or counties). Finally, Excel software version 2016 was used for data analysis and creating figures and tables. Linear regression was used to perform statistical analyses.

3. Results and discussion

3.1. Species richness

The results showed that, regardless of the province's counties, 5 industrial crop species including sugar beet, canola, confectionery sunflower, sesame, and cotton were cultivated in Kermanshah province (Table 1). The species richness of agricultural crops varied across different counties of the province during 2013 to 2022 (Table 1). Among the counties, Kermanshah, Sarpol-e Zahab, and Sahneh had the highest species richness in most years, while Gilan-e Gharb showed the lowest species richness. Among industrial agricultural crops from 2013 to 2022, the cultivation share of sugar beet, canola, and sunflower was higher than other plants. Kermanshah county, compared to other counties, has a larger area, which is why most of the agricultural crops cultivated in the province are also present in this county, such that during the years under study, approximately 80 percent of all agricultural species cultivated in the province were observed in this county. In Gilan-e Gharb county, the industrial plants cultivated represented about 60 percent of all species cultivated in the province. Biodiversity is considered one of the necessities of sustainable agriculture; therefore, improving biodiversity through the introduction of agricultural crops that have functions similar to off-farm inputs reduces the dependency of agricultural ecosystems and leads to increased self-sufficiency and sustainability (Mahdavi Damghani et al., 2007).

3.2. Changes in cultivation area

Results showed that among the province's counties, Kermanshah County had the highest cultivation area of industrial plants while Kangavar County had the lowest (Table 2). The trend of changes in cultivation area for other counties was increasing during these 10 years. In Kermanshah County, the cultivation area of industrial plants for the base year (2013) was approximately 1,490 hectares, which increased to 6,629 hectares at 2022 with a growth rate of about 455 hectares per year (Table 2). It appears that greater access to suitable equipment and increased extraction of groundwater resources during these 10 years compared to previous years were the main reasons for the increase in cultivation area. Results also showed that the trend of changes in cultivation area in Kangavar county was decreasing during the studied years, with a reduction of 244 hectares per year for this county (Table 2).

3.3. Shannon-Wiener biodiversity index

Regardless of the studied counties, the Shannon-Wiener biodiversity index value for the entire province was approximately 1.0 (Figure 2). The total Shannon-Wiener biodiversity index in different counties varied between 0.78 and 1.0. The highest value of this index was observed at 2013 (1.11), and the lowest was observed at 2015 (0.78). The Shannon-Wiener biodiversity index of industrial plants for the entire province decreased from 1.11 to 0.912 during the studied period, with an annual decrease of approximately 0.005 units. It appears that the low Shannon-

Wiener biodiversity index for Kermanshah province as a whole may be due to one or two industrial plants being dominant species in most counties (Table 1), which could lead to increased sensitivity of agricultural ecosystems to environmental and management changes. Another study has also stated that a low Shannon-Wiener biodiversity index indicates the dominance of a few specific species (Mondani et al., 2015).

Table 1. Species richness of industrial crops in the counties of Kermanshah province during 2013-2022

Counties	Year									
	2013	2014	2015	2015	2017	2018	2019	2020	2021	2022
Islamabad-e Gharb	Sugar beet Rapeseed	Sugar beet Rapeseed	Sugar beet	Sugar beet Rapeseed	Sugar beet Rapeseed	Sugar beet Rapeseed	Sunflower Sugar beet Rapeseed	Sunflower Sugar beet Rapeseed	Sugar beet Rapeseed	Sunflower Sugar beet
Ravansar	Rapeseed	Rapeseed	Sugar beet	Sugar beet	Sugar beet Rapeseed	Sugar beet Rapeseed	Sugar beet Rapeseed	Sugar beet Rapeseed	Sugar beet Rapeseed	Sunflower Sugar beet Rapeseed
Sarpol-e Zahab	Sunflower Sugar beet Sesame	Rapeseed Sesame	Sugar beet Rapeseed	Sunflower Sugar beet Rapeseed Sesame	Sugar beet Rapeseed Sesame	Sunflower Sugar beet Rapeseed Sesame	Sugar beet Rapeseed	Sugar beet Rapeseed Sesame	Sugar beet Rapeseed Sesame	Sugar beet Rapeseed Sesame
Songhor	-	Sesame	Sunflower	Sunflower Sugar beet Sesame	Sunflower Sugar beet	Sunflower Sugar beet	Rapeseed	Rapeseed	Cotton Rapeseed	Rapeseed
Sahneh	Sunflower Sugar beet Rapeseed	Sugar beet	Sugar beet	Sunflower Sugar beet Rapeseed	Sunflower Sugar beet Rapeseed	Sunflower Sugar beet Rapeseed	Sugar beet Rapeseed	Sugar beet Rapeseed	Sugar beet Rapeseed	Sugar beet Rapeseed
Kermanshah	Sugar beet Rapeseed	Sunflower Sugar beet Rapeseed	Sugar beet Rapeseed Sesame	Sunflower Sugar beet Rapeseed Sesame	Sunflower Sugar beet Rapeseed Sesame	Sunflower Sugar beet Rapeseed Sesame	Sugar beet Rapeseed	Sugar beet Rapeseed	Sunflower Sugar beet Rapeseed	Sunflower Sugar beet Rapeseed
Kangavar	Sunflower Sugar beet Rapeseed	Sugar beet Rapeseed	Sunflower Sugar beet Rapeseed	Sunflower Sugar beet Rapeseed	Sunflower Sugar beet Rapeseed	Sunflower Sugar beet Rapeseed	Sugar beet Rapeseed	Sugar beet Rapeseed	Sugar beet Rapeseed	Sunflower Sugar beet Rapeseed
Gilan-e Gharb	Rapeseed	Rapeseed	Rapeseed	Rapeseed	Rapeseed	Rapeseed	Sugar beet Rapeseed	Sugar beet Rapeseed	Sugar beet Rapeseed	Sugar beet Rapeseed
Harsin	Sugar beet Rapeseed	Sugar beet Rapeseed	Sugar beet	Sunflower Sugar beet Rapeseed	Sunflower Sugar beet Rapeseed	Sunflower Sugar beet Rapeseed	Sugar beet Rapeseed	Sugar beet Rapeseed	Sugar beet Rapeseed	Sugar beet Rapeseed
Total Province	4	5	5	5	4	4	3	4	6	5

Table 2. Changes in the cultivation area of industrial crops by county in Kermanshah province during 2013-2022.

Counties	Lowest	Heights	Equation	R^2	Yearly change
Islamabad-e Gharb	3327	4898	y = 62.812x - 122456	0.118	62.8
Ravansar	85	462	y = 24.897x - 49914	0.3303	24. 9
Sarpol-e Zahab	66	712	y = 56.195x - 113108	0.5866	56.2
Songhor	697	3083	y = 195.16x - 391507	0.5308	195.2
Sahneh	3388	5176	y = 157x - 312304	0.3667	157.0
Kermanshah	1490	7109	y = 481.67x - 967626	0.6962	481.7
Kangavar	1819	4999	y = -244.73x + 496995	0.4255	-244.7
Gilan-e Gharb	20	352	y = 31.837x - 64043	0.632	31.837
Harsin	352	1514	y = 125.86x - 252917	0.8127	125.86

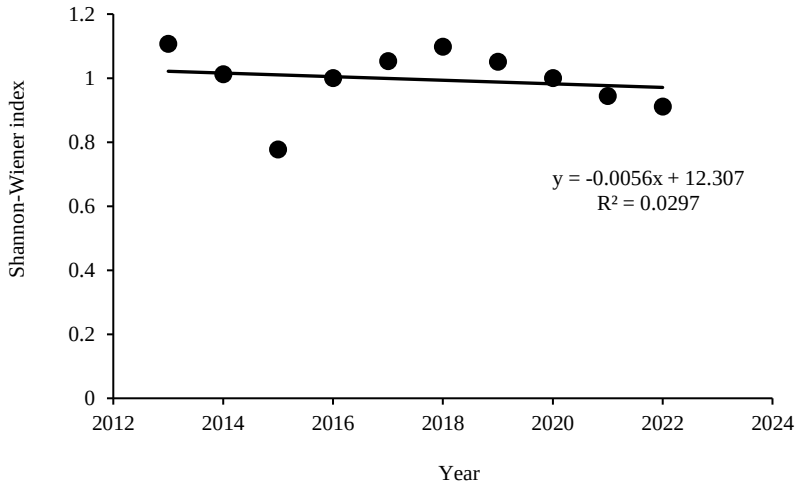

Figure 2. Changes in Shannon-Wiener biodiversity of total industrial crops in Kermanshah province during 2013-2022.

Except for Songhor County, the Shannon-Wiener biodiversity index increased among Kermanshah province's counties during the studied years (Table 3). Sarpol-e Zahab, Gilan-e Gharb, Kermanshah, and Ravansar had the highest Shannon-Wiener biodiversity index values in most crop years, while Songhor had the lowest value during these 10 years. This index value was 0.104 at 2013, and decreased annually by approximately 0.8 units, reaching 0.020 at 2022 (Table 3). In Gilan-e Gharb county, the increase in the Shannon-Wiener biodiversity index was higher compared to other counties, such that in the base year (2013), this index value was zero and increased annually by approximately 0.11 units, reaching 0.96 at 2022 (Table 3).

Table 3. Changes in the Shannon-Wiener Index of Industrial Products by County in Kermanshah Province during 2013-2022.

Counties	Lowest	Heights	Equation	R^2	Yearly change
Islamabad-e Gharb	0.01	0.63	y = 0.0379x - 76.083	0.2996	0.038
Ravansar	0.06	0.99	y = 0.0896x - 180.17	0.5114	0.090
Sarpol-e Zahab	0.49	1.20	y = 0.0219x - 43.328	0.1122	0.022
Songhor	0.020	0.24	y = -0.0038x + 7.8079	0.0257	0.004
Sahneh	0.62	1.07	y = 0.0133x - 26.012	0.0737	0.013
Kermanshah	0.55	1.08	y = 0.0102x - 19.687	0.0282	0.010
Kangavar	0.52	1.03	y = 0.0115x - 22.334	0.0539	0.012
Gilan-e Gharb	0	0.99	y = 0.1197x - 240.99	0.7902	0.120
Harsin	0.23	0.91	y = 0.0098x - 19.215	0.0185	0.010

A high Shannon-Wiener biodiversity index indicates that dominance is not limited to one specific species, all species have similar population numbers, and they possess higher diversity, cultivation area, and species richness. The decrease in Shannon-Wiener index value is due to reduced species richness or dominance of one species and reduced evenness. Fields with a Shannon-Wiener index of zero indicate the presence of only one species (Niazmoradi et al., 2023; Kazemi et al., 2020).

Climatic conditions are among the factors influencing agricultural crop biodiversity. Climate changes have been cited as determining factors for biodiversity in agricultural ecosystems, and the impact of climatic diversity on species diversity is usually more important than other environmental factors (Alaei Bazkiaei et al., 2022; Stocking, 1999). Diversity is not determined solely by the number of species; species abundance is also an important factor in increasing diversity. The Shannon-Wiener biodiversity index is calculated based on the cultivation area of each species and its ratio to the total cultivation area (Magurran, 2004). Furthermore, this index is a combination of species richness and relative abundance and is considered one of the most practical indices for diversity assessment (Thrupp, 1998).

3.4. Sorenson similarity index

The Sorenson similarity index showed relatively high values in the province's counties during 2013-2022 (Table 4), such that the counties had the highest similarity in industrial plant cultivation, and what caused differences between counties was the cultivation area of industrial plants. The highest Sorenson similarity was observed between Kermanshah and Islamabad-e Gharb counties (1), and the lowest was between Sahneh and Songhor counties (0.8). It appears that one reason for the similarity of cultivated species in Kermanshah province's counties was their geographical proximity, which created relatively similar environmental conditions. Overall, the similarity between counties regarding industrial crop species was high, due to the shared presence of several species among all counties, which led to an increase in the Sorenson index value. A high Sorenson similarity index indicates similar diversity in industrial plants cultivated in these regions (Koozehgar Kalaji et al., 2022). It appears that the diversity of existing agricultural systems aligns with climatic diversity, and soil characteristics of agricultural areas also influence this matter, which is also affected by climatic features (Koocheki et al., 2011).

Table 4. Changes in the Evenness index of industrial products by county in Kermanshah province during 2013-2022.

Counties	Lowest	Heights	Equation	R^2	Yearly change
Islamabad-e Gharb	0	0.08	y = 0.0045x - 9.0032	0.2949	0.0045
Ravansar	0.01	0.17	y = 0.0138x - 27.709	0.4405	0.0138
Sarpol-e Zahab	0.10	0.24	y = -0.0015x + 3.2774	0.0103	-0.0015
Songhor	0.002	0.031	y = -0.0007x + 1.4905	0.0577	-0.0007
Sahneh	0.07	0.12	y = 0.0012x - 2.3721	0.0515	0.0012
Kermanshah	0.068	0.125	y = 0.0002x - 0.3904	0.0013	0.0002
Kangavar	0.067	0.131	y = 0.0025x - 5.0074	0.1606	0.0025
Gilan-e Gharb	0	0.18	y = 0.0208x - 41.779	0.6858	0.0208
Harsin	0.038	0.135	y = 7E-05x - 0.0636	5E-05	7E-05

Gliessman (1992) showed that from an ecological perspective, climate and soil physical and chemical properties, which are themselves functions of climate, are the basis for the formation and diversity in agricultural ecosystems. Therefore, it appears that the spatial distribution and grouping of some counties were based on their climatic characteristics. Another study also found that in regions with unfavorable climatic and soil fertility conditions, fewer vegetable species are cultivated, and the cultivation area is unevenly distributed among species, leading to the dominance of fewer agricultural crops and ultimately greater similarity in agricultural systems (Koocheki et al., 2004a). The main application of the Sorenson similarity index is to examine the degree of similarity or compare regions in terms of species similarity (Magurran, 2004). The numerical value of this index ranges between zero and one; when all species in two regions are similar, the index value equals one, indicating 100%

similarity (Kazemi et al., 2020). Reasons for this level of similarity can include uniform soil fertility, relatively similar agricultural management, available water, uniform field slopes, and proximity of plots to each other (Koozehgar Kalaji et al., 2022).

3.5. Evenness index

The results of this study showed that the highest evenness index for industrial crops was observed in Islamabad-e Gharb, Ravansar, Gilan-e Gharb, and Sahneh counties, with values of 0.05, 0.16, 0.17, and 0.094, respectively (Table 5). The lowest evenness index for industrial crops was observed in Songhor County with values of 0.003 (Table 5). In this county, the largest cultivation area was allocated to confectionery sunflower, and due to the uneven distribution of land among industrial crops, this index decreased during 2013-2022 (Alaei Bazkiaei et al., 2022), indicating that monoculture has become more prevalent over time (Table 5).

Table 5. Changes in the Sorenson index of industrial products by city in Kermanshah province during 2013-2022.

Counties	Lowest	Heights	Equation	R^2	Yearly change
Islamabad-e Gharb whit Kermanshah	0.8	1	y = 0.0154x - 30.169	0.3154	0.015
Ravansar whit Sarpol-e Zahab	0.4	0.85	y = 0.0357x - 71.317	0.4634	0.036
Songhor whit Sahneh	0.4	1	y = 0.0131x - 25.696	0.0333	0.013
Kangavar whit Kermanshah	0.8	1	y = 0.0263x - 52.198	0.8497	0.026
Gilan-e Gharb whit Harsin	0.5	1	y = 0.0438x - 87.621	0.566	0.044

A low evenness index indicates the dominance of a particular crop. Higher species evenness indicates that the cultivation area of plant species is more uniform and the dominance of one or few plant species is lower (Koocheki et al., 2011). Counties with greater crop diversity and more balanced cultivation areas relative to each other have higher evenness. An evenness index of 1 means that the cultivation area of all species was equal; therefore, when the evenness index relative to all agricultural species in the province is less than one, it indicates greater unevenness in the cultivation area of agricultural species (Razavi et al., 2012). Additionally, the evenness or heterogeneity index is directly influenced by the Shannon-Wiener biodiversity index and species richness (Alaei Bazkiaei et al., 2022).

4. Conclusion

Understanding the benefits of biodiversity and distribution patterns of agricultural plants can be useful in policy-making related to sustainable agriculture objectives. The results of this study showed that in Kermanshah province, Kermanshah, Sarpol-e Zahab, and Sahneh counties had the highest species richness, while Gilan-e Gharb county had the lowest value in most crop years. The Shannon-Wiener biodiversity index for all agricultural crops decreased during 2013-2022. Sarpol-e Zahab, Gilan-e Gharb, Kermanshah, and Ravansar had the highest Shannon-Wiener biodiversity index values in most crop years, while Songhor county showed the lowest value of this index. The Sorenson similarity index showed relatively high values in the province's counties. All counties in the province had the highest similarity in industrial crop cultivation, and what caused differences between counties was the cultivation area of industrial crops. Furthermore, results showed that the highest evenness index for industrial crops was observed in Islamabad-e Gharb, Ravansar, Gilan-e Gharb, and Sahneh counties. These results indicate that the dominance of a single crop during the studied years was lower in these countries. The lowest evenness index for industrial crops was observed in Songhor county, as the largest cultivation area in this county was allocated to confectionery sunflowers.

Understanding and comprehending the effects of agricultural crop biodiversity and its impacts on agricultural production systems requires comprehensive data collection about different cultivated varieties for all counties and the distribution of these crops. Unfortunately, due to a lack of access to accurate statistics regarding variety names for most industrial crops, assessment of biodiversity at the variety level was not possible. It is hoped that in the future, through better and more accurate access to information about cultivated varieties at the county level, a more precise assessment of biodiversity benefits can be conducted.

References

Alaei Bazkiaei, P., Kazemi, K., & Shahhoseini, H. (2022). Assessment of the biodiversity of agricultural products in Mazandaran Province. *Journal of Agricultural Science and Sustainable Production, 32*(3), 333–352. https://doi.org/10.22034/saps.2021.48635.2757

Alibeygi, A., Montazersaheb, Z., & Shahmoradi, M. (2019). Identifying the influencing factors on understanding of biodiversity among agriculture and natural resources students of Razi University. *Quarterly Journal of Environmental Education and Sustainable Development, 7*(2), 39–48. https://doi.org/10.30473/ee.2019.5601

Allahyari, S., Jalali Honarmand, S., Mondani, F., & Khoramivafa, M. (2015). Evaluation of crop biodiversity in Kermanshah province during 2003–2012. *Iranian Journal of Field Crops Research, 13*(2), 340–348. https://doi.org/10.22067/gsc.v13i2.30281

Asgari, A., Koocheki, A., & Nassiri Mahalati, M. (2018). Evaluation of biodiversity indices for some agronomical plants in Kermanshah province. *Journal of Agroecology, 10*(2), 340–352. https://doi.org/10.22067/jag.v10i2.34755

Asgharipour, R. M., Kamari, F., Ramroudi, M., & Alizadeh, Y. (2019). Evaluation of agrobiodiversity in Ilam province (during 2004–2016). *Environmental Sciences, 17*(4), 121–132. https://doi.org/10.29252/envs.17.4.121

Barnes, B. V. (1998). *Forest ecology*. John Wiley & Sons.

Blackshaw, R. E., Larney, F. J., Lindwall, C. W., Watson, P. R., & Derksen, D. A. (2001). Tillage intensity and crop rotation affect weed community dynamics in a

winter wheat cropping system. *Canadian Journal of Plant Science*, *81*(4), 805–813. https://doi.org/10.4141/p01-023

Brown, A. H. (2000). The genetic structure of crop landraces and the challenge to conserve them in situ on farms. In S. B. Brush (Ed.), *Genes in the field: On-farm conservation of crop diversity* (pp. 29–48). International Plant Genetic Resources Institute. https://doi.org/10.1201/9781420049824.sec2

Gliessman, S. R. (1992). Agroecology in the tropics: Achieving a balance between land use and preservation. *Environmental Management*, *16*, 681–689. https://doi.org/10.1007/bf02645658

Hilton-Taylor, C., & Brackett, D. (2000). *IUCN red list of threatened species*. IUCN. https://coilink.org/20.500.12592/qzn5ws

Hubbell, S. P. (2001). *The unified neutral theory of biodiversity and biogeography*. Princeton University Press.

Jackson, L. E., Pascual, U., & Hodgkin, T. (2007). Utilizing and conserving agrobiodiversity in agricultural landscapes. *Agriculture, Ecosystems & Environment*, *121*(3), 196–210. https://doi.org/10.1016/j.agee.2006.12.017

Kazemi, H., Bakhshande Larimi, S., Gholikhani, S., & Rassam, G. (2020). Diversity assessment of crop and horticultural products in Zanjan province. *Journal of Agroecology*, *12*(2), 179–193. https://doi.org/10.22067/jag.v12i2.69227

Kazemi, H., Niazmoradi, M., Pourshirazi, S., & Sharifi, N. (2018). Assessment of the status of biodiversity of agricultural and horticultural crops in Golestan Province in the years 1998–2014. *Journal of Agroecology*, *8*(2), 47–67.

Koocheki, A., Nasiri Mahalati, M., & Najafi, F. (2004b). The agrobiodiversity of medicinal and aromatic plants in Iran. *Iranian Journal of Field Crops Research*, *2*(2), 208–215. https://doi.org/10.22067/gsc.v2i2.1256

Koocheki, A., Nasiri Mahalati, M., Asgharipour, M. R., & Khodashenas, A. (2004a). Biodiversity of fruits and vegetables in Iran. *Iranian Journal of Field Crops Research*, *2*(1), 79–88. https://doi.org/10.22067/gsc.v2i1.1166

Koocheki, A., Nassiri Mahalati, M., Moradi, R., & Alizadeh, Y. (2011). Meta-analysis of agrobiodiversity in Iran. *Journal of Agroecology*, *1*(2), 1–16.

Koocheki, A., Nassiri Mahalati, M., Zare Feizabadi, A., & Jahanbin, M. (2004c). Evaluation of agricultural systems diversity in Iran. *Research and Development*, *63*, 70–83.

Koozehgar Kaleji, M., Kazemi, H., Kamkar, B., Amirnezhad, H., & Hosseinalizadeh, M. (2022). Investigation of plant biodiversity in an agricultural landscape (Case study: Dasht-e-Naz, Sari). *Journal of Plant Production Research*, *29*(4), 1–24. https://doi.org/10.22069/jopp.2021.18919.2790

Lima, N. P., & Pereira, D. I. (2023). Living and dying on planet earth: An approach to the values of geodiversity. *Geoheritage*, *15*, 4. https://doi.org/10.1007/s12371-022-00776-8

Magurran, A. E. (1988). *Ecological diversity and its measurement*. Croom Helm. https://doi.org/10.1007/978-94-015-7358-0

Magurran, A. E. (2004). *Measuring biological diversity*. Blackwell Science.

Mahdavi Damghani, A., Koocheki, A., Rezvani Moghaddam, P., & Nassiri Mohallati, M. (2007). Evaluation of agrobiodiversity and its effects on the sustainability of a wheat-cotton cropping system in Khorassan. *Environmental Science*, *4*(3), 61–68. https://scj.sbu.ac.ir/article_96091.html

McCune, B., & Grace, J. B. (2002). *Analysis of ecological communities*. MjM Software Design.

Ministry of Jihad-e-Agriculture of Iran (MJA). 2024. Agricultural Jihad Organization of Kermanshah Province.

Mondani, F., Jalilian, A., & Ahmadi, M. (2015). Survey of the distribution and biodiversity of medicinal plants in Kermanshah province. In *The First International Conference and the Fourth National Conference on Medicinal Plants and Sustainable Agriculture*. https://civilica.com/doc/453615/

Nasiri Mahalati, M., Koocheki, A., & Mazaheri, D. (2005). Diversity of crop species in Iran. *Desert*, *10*(1), 33–50.

Niazmoradi, M., Kazemi, H., Gherekhloo, J., Soltani, A., & Kamkar, B. (2023). Study of diversity and weed population structure of wheat agroecosystems in Bandar-e-Torkeman county, Golestan province. *Weed Research Journal*, *15*(1), 37–52. https://doi.org/10.1038/s41598-025-03443-4

Pourghasemian, N., & Moradi, R. (2016). Assessing biodiversity of agronomical and horticultural productions of Isfahan province. *Journal of Agroecology*, *8*(2), 212–226. https://doi.org/10.22067/jag.v8i2.37582

Razavi, S. A., Rahmani, R., & Sattarian, A. (2012). The investigation of effective factors on biodiversity using MLR (Case study; Vaz Research Forest). *Journal of Wood and Forest Science and Technology*, *16*(1), 33–50. https://dorl.net/dor/20.1001.1.23222077.1388.16.1.3.3

Shannon, C. E., & Wiener, W. W. (1949). *The mathematical theory of communication*. University of Illinois Press.

Shrestha, R. P., Schmidt-Vogt, D., & Gnanavelrajah, N. (2010). Relating plant diversity to biomass and soil erosion in a cultivated landscape of the eastern seaboard region of Thailand. *Applied Geography*, *30*(4), 606–617. https://doi.org/10.1016/j.apgeog.2010.01.005

Stocking, M. (1999). Agrodiversity: A positive means of addressing land degradation and sustainable rural livelihoods. In A. J. Conacher (Ed.), *Land degradation* (Vol. 58, pp. 1–18). Springer. https://doi.org/10.1007/978-94-017-2033-5_1

Thrupp, L. A. (1998). *Cultivating diversity: Agrobiodiversity and food security*. World Resource Institute.

Agriculture, Environment & Society

Journal homepage: www.aes.uoz.ac.ir

Effect of GA_3 on morphological and yield traits in single and triple capsule sesame accessions under field conditions

Seyyed Fazel Fazeli Kakhki [a], Shahram Riahinia [*b], Morteza Goldani [c]

[a] Khorasan razavi agricultural and natural resources research and education center, AREEO, Mashhad, Iran
[b] Department of Agriculture, Payame Noor University, Tehran, Iran
[c] Department of Agronomy and Plant Breeding, College of Agriculture, Ferdowsi University of Mashhad, Mashhad, Iran

ARTICLE INFO

Article history:
Received: 30 July 2024
Accepted: 15 March 2025
Available online: 30 March 2025

Keywords:
1000-seed weight
Biomass
Length of branch
Node of triple capsule per plant
Number of capsules per plant

ABSTRACT

Phytohormones, such as gibberellic acid (GA_3), are integral to the regulation of plant development, influencing processes that enhance genetic potential and performance. To determine the effect of GA_3 on some morphological and yield components of sesame (*Sesamum indicum* L.), an experiment was conducted in a factorial arrangement based on a complete block design in three replications. The first factor involved two sesame genotypes: one producing a single capsule per leaf axil (CAP1) and another producing triple capsules per leaf axil (CAP2). The second factor was the concentration of GA_3 applied, with treatments at 0 ppm (control), 50 ppm, and 100 ppm. Significant differences were observed in plant morphology and yield components as influenced by GA_3 treatment. Notably, the CAP2 genotype treated with 50 ppm GA_3 as a seed priming agent exhibited the greatest plant height (102 cm). This treatment also resulted in the highest number of nodes with triple capsules and the maximum number of capsules per plant. In terms of biomass, the fresh and dry weights were significantly increased by 72% and 73%, respectively, in the CAP2 genotype primed with 50 ppm GA_3, compared to the lowest values recorded under the 100 ppm GA_3 foliar spray treatment. Furthermore, the 1000-seed weight was maximized under the 50 ppm GA_3 seed priming treatment in the CAP2 genotype. These findings underscore the efficacy of 50 ppm GA_3 seed priming in enhancing morphological and yield attributes in sesame, particularly in genotypes with triple capsules per leaf axil. The study suggests potential agronomic benefits in utilizing GA_3 to optimize sesame crop performance.

Highlights

- The study investigates the effects of GA_3 on the growth and yield components of two sesame varieties.
- The study focuses on different concentrations and application methods consisting of seed priming and foliar spraying.
- The study identifies that 50 ppm GA_3 is the most effective concentration for improving growth and yield traits in sesame.
- The paper shows that GA_3 treatment significantly improved yield components, with CAP2 plants.

1. Introduction

Sesame (*Sesamum indicum* L.) is a significant annual oilseed crop cultivated predominantly in tropical and subtropical regions. However, it exhibits relatively high yield performance in temperate climates (Alegbejo et al., 2003). The seeds of sesame are notably rich in oil content, comprising 50-60% oil, along with 20% protein and 14-20% carbohydrates. The presence of endogenous antioxidants such as sesamol and sesaminol, in combination with tocopherols, contributes to the excellent oxidative stability of sesame oil (Ball et al., 2000).

Sesame has a comparatively low yield potential relative to other crop species, which can be attributed to factors such as its low harvest index, susceptibility to diseases, tendency for seed-shattering, and indeterminate growth habits (Ashri, 1994). Notably, all currently available commercial sesame cultivars in Iran and other regions exhibit an indeterminate growth habit. Research indicates

* Corresponding author.
E-mail address: riahinia@pnu.ac.ir
https://doi.org/10.22034/aes.2025.470641.1080

that cultivars with a determinate growth habit produce lower yields compared to indeterminate types under standard planting densities (Ashri, 1995).

The branching trait has been observed in some ecotypes of sesame, particularly under high input conditions, where it can enhance capsule production. In sesame, capsules are a primary yield component, forming at the axils of leaves. The development of capsules typically begins from the axils of leaves located at about the fourth to sixth node pairs and continues up to the apex of the plant. This trait is controlled by a recessive gene and results in the formation of triple capsules. However, the occurrence of this triple capsule is limited and dependent on agronomic management, climatic conditions and sesame variety type. (Langham and Wiemers, 2002).

The length of the culm or branch in sesame plants is influenced by the availability of moisture and agricultural inputs. Optimal agronomic management, characterized by sufficient water and nutrient supply, can enhance growth parameters such as the elongation of the main stem and branches. This, in turn, leads to an increased number of capsules per plant.

Gibberellic acid (GA_3), a phytohormone, plays a crucial role in promoting plant growth and development when applied in small quantities and at low concentrations. Gibberellins are terpenoid compounds composed of isoprene units that contribute to increased stem elongation and cell division. The elongation of stems in response to the exogenous application of gibberellic acid (GA_3) is primarily due to its effects on both cell division and cell enlargement. While cell division is an essential component of the growth process, it alone does not account for growth; it must be accompanied by cell enlargement. This synergistic effect of cell division and enlargement is what drives growth in response to the application of GA_3 (Moore, 2012). The exogenous application of gibberellic acid has also been reported to enhance stem elongation, dry matter accumulation and yield in soybean (Maske et al., 1998; Deotale et al., 1998).

Chory et al. (1987) demonstrated that the application of GA_3-induced changes in a specific group of translatable mRNAs and the accumulation of polypeptides in pea and corn plants, which are associated with genetic modifications that enhance stem growth. GA_3 application enhances polyamine biosynthesis and promotes internode elongation in pea seedlings (Dai et al., 1982; Ross et al. 2003).

Additionally, Kaur et al. (2000) reported that seed priming with gibberellic acid accelerated flowering and ripening, thereby increasing yield in chickpeas. Studies have also shown that the application of GA_3 results in increased yield and yield components in wheat (*Triticum aestivum* L.) (Zarehmanesh et al., 2010) and corn (*Zea mays* L.) (Ghodrat et al., 2010).

With the growing global population and the rising demand for oil, it is imperative to investigate factors that affect crop yield. This study was conducted to explore the effects of different concentrations of gibberellic acid (GA_3) applied as a seed primer and foliar spray. The objective was to determine the optimal exogenous concentration and application timing of GA_3 to effectively enhance the growth and yield of the sesame plant (*Sesamum indicum* L.).

2. Material and method

To investigate the effects of gibberellic acid (GA_3) on some agronomic traits and yield components of sesame plants, a field experiment was conducted using a factorial arrangement based on a complete block design with three replications, at the Khorasan razavi agricultural and natural resources research and education center in Mashhad, Iran. The first factor in the experiment involved two types of seeds derived from plants grown over three consecutive years. Initially, 13 accessions of sesame seeds were obtained from the Oilseeds Section of the Agriculture Organization of Khorasan. Preliminary tests were conducted to assess the performance of these accessions (Nezami et al., 2014). In the initial year, seeds were collected from plants that produced three capsules per leaf axil. Over the next three years, these seeds were grown in pots to obtain pure lines with consistently triple capsules per leaf axil. From these plants, seeds were harvested and categorized based on capsule formation: one group with three capsules per leaf axil (CAP2) and another with single capsules per leaf axil (CAP1). These two types of seeds served as the first factor in the experiment. The second factor in the experiment involved the application of three concentrations of gibberellic acid (GA_3): 0, 50, and 100 ppm. These concentrations were applied at two stages in the sesame plant's life cycle: seed priming and foliar spray 65 days after planting (DAP). This setup resulted in six treatment combinations, assigned to zero, 50, and 100 ppm in prime; zero, 50, and 100 ppm were used in the form of foliar spraying in 65 DAP, Consequently, the total treatments included combinations of the GA_3 concentrations for seed priming and foliar application, resulting in six treatments designated as T1, T2, T3, T4, T5, and T6.

The seeds were disinfected with fungicides prior to planting on May 10. After the seedlings reached the four-leaf stage, they were thinned to maintain a spacing of 7 cm between plants in a row. Concurrently, weed control was carried out using mechanical methods. The field was irrigated weekly. Upon crop maturation, 10 plants from each plot, excluding those affected by marginal effects, were selected for measurement. The morphological and yield component traits assessed included plant height, number of branches, branch length, number of nodes with single capsules, number of nodes with multiple capsules, total capsules per plant, seeds per capsule, 1000-seed weight, fresh weight, and dry weight per plant. Data analysis was conducted using SAS software version 9.2, and mean comparisons were made using Duncan's multiple range test at a significance level of $p < 0.05$.

3. Results

3.1. Comparison of CAP1 and CAP2 Treatments

The results presented in Table 1 indicated significant differences between plants grown from seeds with single

capsules per leaf axil (CAP1) and those from seeds with triple capsules per leaf axil (CAP2) in several traits. Specifically, CAP1 plants exhibited 32% more branches, averaging 3.82 branches per plant, compared to CAP2 plants. However, CAP2 plants showed 24% more nodes with multiple capsules and an 18% higher number of seeds per capsule compared to CAP1 plants. No significant differences were observed between the treatments for other measured traits (Table 1).

Table 1. Analysis of Variance (ANOVA) for various traits of sesame plants under field conditions in Mashhad

S.O.V	Df	Length of plant	Number of branches	Length of branch	Node of one capsule	Node of multiple capsules	Number of capsules per plant	Number of seeds per capsule	Weight 1000 seed	Fresh weight	Dry weight
Block	2	27.4 ^{ns}	3.11*	283^{ns}	8.86^{ns}	14.6^{ns}	654.6**	166.2*	0.24*	1024**	73.5**
Capsule (CAP)	1	0.21^{ns}	12.2**	74.1^{ns}	2.83^{ns}	73.1**	1216**	71.7^{ns}	0.02^{ns}	5.7^{ns}	17.7^{ns}
Gibbereline (GA_3)	5	127*	23.2**	645**	38.3*	8.57^{ns}	175*	110^{ns}	0.27**	1576**	44*
Capsule×Gibberelin	5	552**	12.7**	1248**	2.18^{ns}	102.1**	1317**	350**	0.4**	2551**	183**
Error	22	33.7	0.687	122	11.35	6.71	106	44.5	0.06	135	11.57

ns, * and ** are non-significant and significant at the 5 and 1% probability level respectively

3.2. Effects of gibberellic acid (GA_3)

Application of 50 ppm GA_3 as a seed primer resulted in the maximum plant height, reaching 94.2 cm. The lowest plant height, 69.3 cm, was observed in the T1 treatment (control). The highest number of branches (6.8) and branch length (64.6 cm) were recorded in the T2 and T5 treatments, respectively. The lowest number of nodes with single capsules was observed in T2 with 7.8, while the highest was found in the T1 treatment (Table 3). Foliar application of 50 ppm GA_3 resulted in the highest number of capsules per plant (62.2) and the highest number of seeds per capsule (49.1). Additionally, the 50 ppm GA_3 treatment achieved the maximum fresh and dry weights, with values of 85.5 g and 22.7 g per plant, respectively (Table 3).

Table 2. Mean comparison of traits in sesame plants with one capsule (CAP1) vs. triple capsules (CAP2) per leaf axil

Treatment	Length of a plant (cm)	Number of branches per plant	Length of branch (cm)	Node of one capsule per plant	Node of triple capsule per plant	Number of capsules per plant	Number of seeds per capsule	Weight 1000 seed (g)	Fresh weight (g)	Dry weight (g)
CAP1	87.37	3.89	50.25	13.09	8.65	52.7	38.3	2.58	65.3	17.2
CAP2	87.22	2.72	47.38	12.53	11.50	64.4	42.2	2.64	66.0	19.1
significant	ns	**	ns	ns	**	**	ns	ns	ns	ns

CAP1 and CAP2: Denote the types of plants based on the capsule trait (one vs. triple capsules per leaf axil).

Table 3. Mean comparison of traits under different gibberellin (GA_3) treatments in sesame plants with one capsule (CAP1) vs. multiple capsules (CAP2) per leaf axil

Treatment	Length of a plant (cm)	Number of branches per plant	Length of branch (cm)	Node of one capsule per plant	Node of triple capsule per plant	Number of capsules per plant	Number of seeds per capsule	Weight 1000 seed (g)	Fresh weight (g)	Dry weight (g)
T1	79.3 ^{d}	3^{c}	52.1^{abc}	16.3^{a}	9.9^{a}	62.8^{a}	39.6^{bc}	2.2^{b}	80.7^{ab}	18.9^{bc}
T2	94.2 ^{a}	6.8 ^{a}	37.1 ^{d}	14.1 ^{abc}	7.8 ^{a}	56.1 ^{ab}	37.3 ^{c}	2.4 ^{b}	85.5 ^{a}	22.7 ^{a}
T3	82.9 ^{bc}	4.1^{b}	54.7^{ab}	14.5^{ab}	10^{a}	61.4^{a}	41.1^{b}	2.3^{b}	70.8^{bc}	19.2^{abc}
T4	88.5 ^{ab}	2.1 ^{cd}	39.2 ^{cd}	10.6 ^{bc}	10.9 ^{a}	57.9 ^{ab}	38.5 ^{bc}	2.4^{b}	51.5 ^{de}	15.7 ^{cd}
T5	87.2 ^{bc}	2.3 ^{c}	64.6 ^{a}	10.8 ^{bc}	11.1 ^{a}	62.2 ^{a}	49.1 ^{a}	2.9^{a}	44.5 ^{e}	15.1 ^{d}
T6	81.4 ^{c}	1.3 ^{d}	45 ^{bcd}	10.4 ^{c}	10.5 ^{a}	48.7 ^{b}	38.9 ^{bc}	2.7^{a}	61 ^{cd}	17.5 ^{bcd}

For each trait, the averages that have at least one common letter, do not differ significantly according to Duncan's test at the 5% probability level.

T1 to T6: Treatment codes representing different GA_3 concentrations and application methods.

3.3. Interaction of CAP and GA_3 Treatments

The analysis of variance revealed significant interactions between the CAP types and GA_3 treatments for all measured traits, except for the number of nodes with single capsules per leaf axil (Table 1). The longest plants were observed in the CAP2 group with 50 ppm GA_3 priming, measuring 102 cm, while the shortest plants were in the T1 × CAP1 treatment group (Table 4). The number of branches per plant ranged from 1 in the T6 × CAP2 treatment to 10 in the T1 × CAP1 treatment. The maximum branch length was obtained from the CAP2 group with 50 ppm GA_3 priming, which was approximately 81% longer than the minimum branch length observed in the CAP1 group with 50 ppm GA_3 priming. There was no significant difference in the interaction between GA_3 and CAP treatments (both CAP1 and CAP2) regarding the number of nodes with single capsules per leaf axil (Tables 1 and 4).

The highest number of nodes with triple capsules per leaf axil and the greatest number of capsules per plant were observed in the CAP2 treatment with 50 ppm GA_3 seed priming. According to Table 4, as the concentration of GA_3 increased, these two traits also increased. However, the efficacy of GA_3 was more pronounced in the CAP1 treatment compared to CAP2, resulting in higher values for these traits in CAP1 under the same GA_3 concentrations.

The highest number of seeds per capsule was obtained from the T1 × CAP2 treatment. The maximum 1000-seed weight was recorded in the CAP2 treatment with foliar

application of 50 ppm GA_3, while the lowest was observed in the T4 × CAP1 treatment. The number of seeds per capsule was also highest in the T2 × CAP2 treatment, showing an increase of approximately 32% compared to the corresponding CAP1 treatment, which had 37.5 seeds per capsule. Fresh and dry weights were greatest in the CAP2 treatment with 50 ppm GA_3 seed priming, showing increases of approximately 72% and 73%, respectively, compared to the lowest values, which were recorded in the T6 × CAP2 treatment (Table 4). Overall, most traits studied responded positively to gibberellic acid in plants grown from seeds with triple capsules, particularly with the application of 50 ppm GA_3 as seed priming.

Table 4. Mean Comparison of Interaction Between Gibberellin (GA_3) and Capsule Type on Agronomic Traits in Sesame Plants

Interaction effect of treatments	Length of plant (cm)	Number of branches per plant	Length of branch (cm)	Node of one capsule per plant	Node of triple capsule per plant	Number of capsules per plant	Number of seeds per capsule	Weight 1000 seed (g)	Fresh weight (g)	Dry weight (g)
T1 × CAP1	80.3 ^{d}	10.0^{a}	46.5^{bcd}	16.9^{a}	5.7^{ef}	46.1^{c}	24.1^{e}	2.8^{abc}	50.8^{c}	15.6^{de}
T2 × CAP1	85.6 ^{cd}	4.3^{bc}	16.2^{e}	13.5^{a}	6.3^{def}	49.8^{c}	37.5^{cd}	2.7^{abc}	55.4^{c}	16.4^{cde}
T3 × CAP1	82. 7 ^{cd}	3.6^{bcd}	60.5^{b}	14.3^{a}	10.4^{bcd}	67.8^{ab}	43.8^{abc}	2.2^{ef}	90.1^{b}	19.7^{cd}
T4 × CAP1	86.1^{cd}	2.00^{ef}	38.4^{d}	12.9^{a}	13.7^{abc}	77.8^{a}	47.8^{abc}	1.9^{f}	55.9^{c}	17.6^{cde}
T5 × CAP1	90.9 ^{bc}	1.6 ^{ef}	58 ^{bc}	11.1^{a}	14.6 ^{ab}	73.0 ^{a}	36.6 ^{cd}	2.3 ^{def}	47.6 ^{cd}	17.5 ^{cde}
T6 × CAP1	98.3^{ab}	1.6^{ef}	53.1^{bcd}	11.4^{a}	9.6^{de}	71.7^{ab}	46.1^{abc}	2.7^{bcd}	91.8^{ab}	27.5^{ab}
T1 × CAP2	98.3^{ab}	3.6 ^{bcd}	57.8 ^{bc}	15.7 ^{a}	14.2 ^{ab}	62.4^{abc}	52.0 ^{a}	2.4^{cde}	86.1^{b}	22.1^{c}
T2 × CAP2	102 ^{a}	1.6^{ef}	86.6 ^{a}	14.7 ^{a}	18.0 ^{a}	79.6 ^{a}	55.9 $^{a.}$	2.5 ^{bcde}	110 ^{a}	28.1 ^{a}
T3 × CAP2	83.1^{cd}	4.6^{b}	48.9^{bcd}	14.8^{a}	9.6^{cde}	55^{bc}	38.3^{cd}	2.5^{cde}	80.8^{b}	21.7^{c}
T4 × CAP2	90.9b^{c}	2.3^{def}	40^{cd}	11.0^{a}	8.00^{de}	47.0^{c}	50.4^{ab}	3.1^{a}	47.2^{cd}	13.8^{e}
T5 × CAP2	83.4^{a}	3.00^{cde}	42.5^{bcd}	12.5^{a}	7.60^{de}	46.8^{c}	40.4^{bcd}	2.6^{bcde}	41.4^{cd}	12.7^{ef}
T6 × CAP2	64.5^{e}	1.00^{f}	37.0^{d}	11.9 ^{a}	3.00^{f}	25.7^{d}	31.7^{de}	2.9^{ab}	30.2^{d}	7.6^{f}

For each trait, the averages that have at least one common letter, do not differ significantly according to Duncan's test at the 5% probability level.
T1 × CAP1 to T6 × CAP2: Interactions between the six GA_3 treatments and the two capsule types.

4. Discussion

Primary growth in plants, characterized by the initiation of new leaves and branches, begins with the development of blossom buds in the shoots. This phase of growth, which follows the opening of the blossom buds, is crucial for the establishment of the plant's vegetative structure. Secondary growth, which results in an increase in the diameter of the shoot, occurs subsequent to primary growth. This process is essential for the thickening of the plant's stems and branches. Hormonal signals, produced by actively growing buds, play a critical role in regulating these growth activities in plants (Moore, 2012).

Interactions between environmental factors and plant hormones play a crucial role in manifesting the internal potential of plants. Plant hormones, or phytohormones, are key regulators of developmental activities and are primarily responsible for the plant's response to external physical conditions. According to Keshavarzi et al (2013), applying 100 ppm GA_3 during the stem elongation phase of corn (*Zea mays* L.) resulted in a 14% increase in plant height compared to the control. In the present study, seed priming with 50 ppm GA_3 in the CAP2 treatment led to an approximately 15% increase in plant height compared to the control. This suggests that the application of exogenous GA_3, in conjunction with the plant's endogenous GA_3, enhances cell division and elongation in the internodal regions, thereby promoting stem elongation (Moore, 2012).

In a study by Ashraf et al. (2002), the application of GA_3 in wheat (*Triticum aestivum* L.) was found to enhance dry weight and the photosynthetic process. Similarly, research by Keshavarzi et al. (2013) reported that foliar spraying of 150 ppm GA_3 resulted in the highest biomass in corn, with an increase of 21% compared to the control. The present study demonstrated that increasing the concentration of GA_3 from zero to 50 ppm in seed priming resulted in only a 5% increase in fresh weight compared to the control. Additionally, applying GA_3 at various concentrations as a foliar spray led to a decrease in both fresh and dry weight compared to seed priming.

These findings suggest that foliar application of GA_3 has a limited effect on the fresh and dry weight of sesame plants. Keshavarzi's model (2013) predicted that higher concentrations of GA_3 applied as foliar spray decrease biomass in corn plants. This effect might be attributed to the physiological role of GA_3 when used as a seed primer, potentially stimulating the production of amylase enzymes, which break down starch into glucose, thereby promoting growth (Paleg, 1965). This mechanism might explain the observed differences in biomass accumulation between foliar application and seed priming with GA_3.The application of exogenous GA_3 can stimulate the synthesis of new RNA, which is crucial for producing hydrolase enzymes. Additional evidence indicates that GA_3 enhances the synthesis of polyadenylated RNA (poly A RNA), leading to the production of specific polypeptides in seeds that promote growth (Moore, 2012). This effect was also observed in a study by Akter et al (2007), where the application of 50 ppm GA_3 resulted in the highest number of fertile siliques per plant (244.00) in mustard, compared to 152 siliques in the control.

In the present study, seed priming with 50 ppm GA_3 in the CAP2 treatment produced the highest number of nodes with multiple capsules (18), whereas the control in CAP1 had the lowest number (5.7). This suggests that GA_3 application may enhance the translocation of assimilates to reproductive organs, thereby increasing the growth and number of nodes with multiple capsules per plant, up to certain levels of GA_3 application (Uddin et al., 1986). This translocation likely contributes to the observed increase in reproductive structures, facilitating greater yield potential in sesame plants.

5. Conclusion

The findings from this experiment indicate that seed priming with 50 ppm GA_3 in CAP2 (plants grown from seeds with triple capsules per leaf axil) resulted in the greatest improvements in several key traits. These included maximum plant height, the number of nodes with triple capsules per plant, the number of seeds per capsule, and the fresh and dry weight per plant. This demonstrates the potential of GA_3 application to optimize the growth and yield of sesame plants under these conditions.

References

Akter, A., Ali, E., Islam, M. Z., Karim, R., & Razzaque, A. H. M. (2007). Effect of GA_3 on growth and yield of mustard. *International Journal of Sustainable Crop Production*, *2*, 16–20.

Alegbejo, M. D., Iwo, G., Abo, M. E., & Idowu, A. A. (2003). *Sesame:* A potential industrial and export oil seed crop in Nigeria. *Journal of Sustainable Agriculture*, *23*, 59–76. https://doi.org/10.1300/j064v23n01_05

Ashraf, M., Karim, F., & Rasul, E. (2002). Interactive effects of gibberellic acid (GA_3) and salt stress on growth, ion accumulation and photosynthetic capacity of two spring wheat (*Triticum aestivum* L.) cultivars differing in salt tolerance. *Plant Growth Regulation*, *36*(1),49–59. https://doi.org/10.1023/a:1014780630479

Ashri, A. (1994). Genetic resources of sesame: Present and future perspectives. In R. K. Arora & K. W. Riley (Eds.), *Sesame biodiversity in Asia: Conservation, evaluation and improvement* (pp. 25–39). IPGRI.

Ashri, A. (1995). Sesame research overview: Current status, perspectives, and priorities. In M. R. Bennett & I. M. Wood (Eds.), *Proceedings of the 1st Australian Sesame Workshop* (pp. 1–17). NT Department of Primary Industry and Fisheries.

Ball, R. A., Purcell, L. C., & Vories, E. D. (2000). Short-season soybean yield compensation in response to population and water regime. *Crop Science*, *40*, 1071–1078. https://doi.org/10.2135/cropsci2000.4041070x

Chory, J., Voytas, D. F., Olszewski, N. E., & Ausubel, F. M. (1987). Gibberellin-induced changes in the population of translatable mRNAs and accumulation of polypeptides in dwarfs of maize and peas. *Plant Physiology*, *83*, 15–23. https://doi.org/10.1104/pp.83.1.15

Dai, Y., Kaur-Sawhney, R., & Galston, A. W. (1982). Promotion by gibberellic acid of polyamine biosynthesis of light-grown dwarf peas. *Plant Physiology*, *69*, 103–105. https://doi.org/10.1104/pp.69.1.103

Deotale, R. D., Mask, V. G., Sorte, N. V., Chimurkar, B. S., & Yerne, A. Z. (1998). Effect of GA_3 and NAA on morpho-physiological parameters of soybean. *Journal of Soils and Crops*, *8*, 91–94.

Ghodrat, V., Tadiion, S., & Jafari Haghighi, B. (2010). Studies effect of indol-boric acid and GA on yield and yield component of corn *(Zea mays). Proceedings of the 11th Agronomy and Plant Breeding Congress*, Shahid Beheshti University, Iran.

Kaur, S., Gupta, A. K., & Kaur, N. (2000). Effect of GA_3, kinetin, and indole acetic acid on carbohydrate metabolism in chickpea seedlings germinating under water stress. *Plant Growth Regulation*, *30*, 61–70. https://doi.org/10.1023/a:1006371219048

Keshavarzi, M., Jafari Haghighi, B., & Bagheri, A. (2013). The evaluation of auxin and gibberellin hormone on quantitative and qualitative characteristics of forage corn. *Plant Ecophysiology*, *5*(15), 26–35.

Langham, D. R., & Wiemers, T. (2002). Progress in mechanizing sesame in the US through breeding. In J. Janick & A. Whipkey (Eds.), *Trends in new crops and new uses.* American Society for Horticultural Science.

Maske, V. G., Deotale, R. D., Sorte, N. B., Gorammagar, H. B., & Chore, C. N. (1998). Influence of GA_3 and NAA on growth and yield contributing parameters of soybean. *Journal of Soils and Crops*, *8*, 20–21.

Moore, T. C. (2012). *Biochemistry and physiology of plant hormones* (2nd ed.). Springer-Verlag.

Nezami, A., Fazeli Kakhki, S. F., Zarghani, H., Shabahang, J., & Gandomzadeh, M. R. (2014). Preliminary study of yield and yield components of some sesame ecotypes *(Sesamum indicum* L.*)* common in Khorasan province. *Iranian Journal of Field Crops Research*, *12*(2), 189–195.

Paleg, L. G. (1965). Physiological effects of gibberellins. *Annual Review of Plant Biology*, *16*, 291–322. https://doi.org/10.1146/annurev.pp.16.060165.001451

Ross, J. J., O'Neil, D. P., & Rathbone, D. A. (2003). Auxin–gibberellin interactions in pea: Integrating the old with the new. *Journal of Plant Growth Regulation*, *22*, 99–108. https://doi.org/10.1007/s00344-003-0021-z

Uddin, M. M., Samad, A., Khan, M. R., Begum, S., & Salam, M. A. (1986). Effect of sowing dates on the yield and some of its components of mustard and rapeseed. *Bangladesh Journal of Scientific and Industrial Research*, *21*, 160–165.

Zarehmanesh, H., Salahvarzian, A., & Naghashzadeh, R. (2010). Effect of different concentrations and timing of GA on yield and yield component of wheat *(Triticum aestivum). Proceedings of the 11th Agronomy and Plant Breeding Congress*, Shahid Beheshti University, Iran.

Agriculture, Environment & Society

Journal homepage: www.aes.uoz.ac.ir

Development of an electrochemical sensor for environmental pollutant detection based on cobalt sulfide and graphene nanocomposite

Neda Babaee Dezfouli [a], Zhila Safari [*a], Halimeh Rajabzadeh [a]

[a] Department of Chemistry, Dez.C., Islamic Azad University, Dezful, Iran

ARTICLE INFO

Article history:

Received: 30 April 2025

Accepted: 20 June 2025

Available online: 25 June 2025

Keywords:

Cobalt Sulfide

Cobalt Sulfide-Graphene Nanocomposite

Electrocatalytic Oxidation

Hydrazine

ABSTRACT

Hydrazine is a toxic and carcinogenic substance that can enter the human body through multiple pathways, leading to poisoning and other adverse health effects. Given its ecological significance in various aqueous environments and its widespread industrial applications, accurate quantification and monitoring of hydrazine in environmental systems are crucial. Electroanalytical techniques for hydrazine assessment demonstrate considerable promise owing to their cost-effectiveness, exceptional detection limits, and rapid analytical response. In this study, a new, simple, and cost-effective electrode is proposed and presented for the measurement of hydrazine. This electrode is a modified electrode based on a nanocomposite composed of cobalt sulfide and graphene nanoparticles. The modified cobalt sulfide-graphene electrode, after preparation, was used as a nanocomposite sensor for the electrocatalytic measurement of hydrazine through cyclic voltammetry. Due to the presence of nanoparticles in its structure, this electrode exhibits sensitivity and selectivity in the electroanalysis of hydrazine. The effects of various parameters, such as scan rate (from 10 to 300 mV/s), pH (from 3 to 10), and different concentrations of hydrazine (from 0.2 to 2 mM), were investigated. The nanocomposite was characterized using field emission scanning electron microscopy (FESEM). To determine the diffusion coefficient of hydrazine, chronoamperometry techniques were used, and the diffusion coefficient of hydrazine in this study was calculated to be 8.48×10-9 cm²/s. The detection limit was determined using differential pulse voltammetry, calculated to be 0.081 mM.

Highlights

- A novel cobalt sulfide-graphene nanocomposite electrode was proposed for electrocatalytic hydrazine sensing.
- The presence of nanoparticles ensured high sensitivity and selectivity in hydrazine electroanalysis.
- The proposed sensor achieved a low limit of detection (0.081 mM) via Differential Pulse Voltammetry (DPV).
- The diffusion coefficient of hydrazine was determined as 8.48×10^{-9} cm^2/s using chronoamperometry.

1. Introduction

Electrochemical sensing platforms are highly regarded for their numerous advantages, including ease of use, cost-effectiveness, high specificity, and improved detection capabilities. As a result, these devices have become essential analytical tools in various fields, such as food quality control, environmental monitoring, clinical diagnostics, biomedical evaluation, and counterterrorism security. Electrochemical sensors are mainly categorized into three types: amperometric, potentiometric, and impedimetric. The development of new electrode substrates with enhanced charge transport properties, structural durability, and larger active surface areas is crucial for maximizing the effectiveness of electrochemical sensing systems (Fazeli-Nasab et al., 2022; Meng et al., 2024).

In contemporary scientific research, ultrathin planar nanomaterials particularly graphene-based architectures have garnered considerable attention owing to their exceptional physicochemical characteristics and versatile utility in electronic components, photonic devices, catalytic systems, and electrochemical energy storage solutions. These atomically layered materials have become pivotal in the evolution of next-generation electrochemical sensing

* Corresponding author.
E-mail address: Zhilasafari@yahoo.com
https://doi.org/10.22034/aes.2025.532560.1107

platforms. The expansive interfacial domain of graphene nanostructures enables exceptional analyte adsorption capacity, facilitating ultra-sensitive detection. Furthermore, the abundant surface functionalities on modified graphene variants permit diverse strategies for immobilizing biorecognition elements, enabling precise electrochemical interrogation of biomacromolecules such as proteins and oligonucleotides. Significant research efforts have been devoted to developing advanced hybrid nanocomposites through strategic material integration for enhanced sensor applications (Iqbal et al., 2024; Traipop et al., 2024).

A recent study utilized electropolymerization through repetitive potential cycling to immobilize a synthetic recognition layer onto an unmodified graphite substrate. This functionalized transducer was then used for trace-level quantification of lead. The fabrication process took place under ambient conditions, with optimal analytical performance observed at pH 8.0 using Britton-Robinson buffer as the supporting electrolyte. Comprehensive electrochemical characterization was conducted using cyclic voltammetry and differential pulse voltammetry, while high-resolution electron microscopy was employed to assess the topological features(Wang et al., 2022).

In a study (Motaharian and Milani, 2015), A novel voltammetric detection platform was engineered utilizing a molecularly imprinted polymer (MIP)-functionalized carbon composite electrode for selective quantification of the benzodiazepine compound diazepam. The synthetic recognition elements were fabricated through precipitation-induced polymerization protocol and subsequently integrated as the bioactive interface in the electrochemical transducer assembly. Comparative analytical evaluation revealed the MIP-modified carbon composite electrode exhibited significantly enhanced molecular recognition capability for diazepam compared to its non-imprinted polymer (NIP) counterpart. The developed biosensing platform demonstrated successful application in detecting therapeutic concentrations of diazepam in complex biological matrices, specifically human blood serum specimens.

It has been conducted (Najafi and Sohuli, 2018) research on the development of a sensor for fentanyl determination. This investigation developed a novel electroanalytical platform through functionalization of a glassy carbon substrate with multi-walled carbon nanostructures and ferric oxide nanoparticles for ultrasensitive fentanyl detection in aqueous media. The engineered transducer's surface architecture was characterized using high-resolution field emission scanning electron microscopy. Electrochemical characterization was conducted through cyclic potential sweeps, while quantitative analysis employed pulsed potential techniques. The optimized sensor demonstrated dual linear response ranges (80 nM - 1 μM and 1 - 100 μM) for fentanyl quantification, achieving a remarkably low detection threshold of 45 nM. The anodic oxidation current showed excellent correlation with analyte concentration across both dynamic ranges, confirming the platform's robust performance for opioid monitoring.

It has been developed (Wang et al., 2007) it has been developed an innovative voltammetric biosensing platform utilizing polypeptide-graphenic nanodot heterostructures as dual signal-enhancing components for precise quantification of hydrosoluble micronutrients in commercial dietary supplements. The study pioneered the electrochemical polymerization of biocompatible polystyrene-graphenic nanodot hybrids as an advanced interfacial engineering approach for glassy carbon electrode functionalization, creating a novel electroanalytical interface. Through potential-controlled synthesis employing cyclic voltammetric deposition (1.5-2.0 V potential window), quantum-confined carbon nanostructures were successfully immobilized on polycarboxylate matrices, as confirmed by high-resolution field emission microscopy demonstrating stable nanodot dispersion within the polymeric network. The engineered transducer exhibited exceptional electrocatalytic activity, enabling sensitive detection of target micronutrients via both cyclic and differential pulse voltammetric techniques, with the nanocomposite architecture significantly enhancing analytical performance through synergistic signal amplification mechanisms.

It has been conducted a novel multiplexed electrochemical detection platform through electrosynthetic polymerization of conductive β-cyclodextrin-based macromolecular networks onto reduced graphene-functionalized screen-printed transducers. The engineered biosensing interface exhibited outstanding analytical performance for the simultaneous quantification of ascorbate, dopamine, and urate biomarkers. The supramolecular polymeric film showed excellent signal reproducibility and long-term operational stability. The crosslinked β-cyclodextrin architecture's host-guest recognition capabilities, paired with the enhanced electron transfer properties of the reduced graphene substrate, facilitated the selective and simultaneous detection of all three electroactive analytes in complex matrices (Ping et al., 2012) . It has been employed (Golabi et al., 2001) a vitreous carbon electrode functionalized with pyrocatechol violet (PCV) for the electrochemical catalysis of hydrazine oxidation. The investigation utilized cyclic voltammetric analysis to derive kinetic parameters, achieving a quantification threshold of 4.2 micromolar for hydrazine detection.

2. Materials and methods

The experimental electrochemical analysis was conducted utilizing an Autolab PGSTAT028N potentiostat-galvanostat system integrated with a conventional three-electrode electrochemical cell interfaced with computational data acquisition software. The electrochemical cell configuration comprised: (i) a Metrohm-sourced saturated silver/silver chloride (Ag/AgCl/KCl) reference electrode, (ii) a high-purity graphite rod serving as the counter electrode, and (iii) a platinum substrate functioning as the modified working electrode, with the latter being fabricated in-house. All electrode potentials were standardized against the Ag/AgCl reference electrode. The raw voltammetric data acquired by

the potentiostat were subsequently exported to spreadsheet software for quantitative analysis and graphical representation (Nigde et al., 2022).

2.1. Preparation of cobalt sulfide-graphene (CoS_2-GR) nanocomposite

Graphene oxide (GO) is a single-layer structure derived from graphite oxide, which is essentially a graphite base sheet interspersed with epoxy and hydroxyl functional groups, along with carbonyl and carboxyl groups at the edges. Graphite oxide does not occur naturally and is synthetically produced. Since producing pure graphene is relatively difficult and expensive, graphene derivatives, such as graphene oxide, are used for its production. The fundamental distinction between graphitic oxide and graphenic oxide resides in their lamellar architecture—graphitic oxide exists as a multilamellar stacked system, while graphenic oxide comprises isolated or oligolamellar sheets. This structural divergence gives graphenic oxide unique advantages, especially as a transitional precursor for synthesizing monoatomic or few-atomic-layer graphene matrices. The material has garnered significant scientific interest due to its exceptional physicochemical properties, such as enhanced surface reactivity and tunable electronic characteristics, which result from its reduced dimensionality compared to multilayered graphene. Additionally, graphene oxide functions as an electrical insulator and enhances the tensile strength of composite materials by disrupting the connections within the graphene network (Uzdrowska et al., 2025).

The fabrication of CoS_2-graphene hybrid nanostructures began with the preparation of graphene oxide (GO) nanosheets through a modified Hummers oxidation process. The resulting GO powder was then subjected to ultrasonic exfoliation in 80 mL of ultrapure water (18.2 MΩ·cm resistivity) to create a homogeneous colloidal dispersion. Stoichiometric amounts of cobalt(II) chloride hexahydrate (2 mmol) and thiourea (4 mmol) were added to this aqueous suspension as metal and sulfur precursors, respectively. The reaction mixture was then sonicated for 60 minutes to ensure thorough homogenization. Following this, the precursor solution was transferred to a PTFE-lined stainless steel hydrothermal reactor for solvothermal treatment at 453 K (180°C) for 24 hours under autogenous pressure. After cooling to ambient temperature (298 K), the reaction products were isolated by centrifugation at 10,000 rpm. The resulting black nanocomposite sediment was purified through multiple washing cycles with deionized water and absolute ethanol to remove any residual reactants. Finally, the product was dried under reduced pressure (10^{-2} Torr) at 333 K (60°C) for 24 hours to yield the desired CoS_2-GR nanocomposite (Huo et al., 2024).

2.2. Characterization of cobalt sulfide-graphene nanoparticles

Field emission scanning electron microscopy (FESEM) images and energy-dispersive X-ray spectroscopy (EDX) results from the SEM analysis of cobalt sulfide-graphene nanoparticles are shown in Figure 1 and 2. The FESEM images reveal a uniform dispersion of interconnected nanoparticles on the graphene surface, which is attributed to the electrostatic attraction between the cobalt sulfide nanoparticles and the graphene surface. This electrostatic attraction leads to a uniform distribution on the final surface (Choi et al., 2024). The FESEM images indicate that the sheets have an average diameter of 30 nanometers. EDX analysis confirms the presence of sulfur, cobalt, and carbon atoms in the sample.

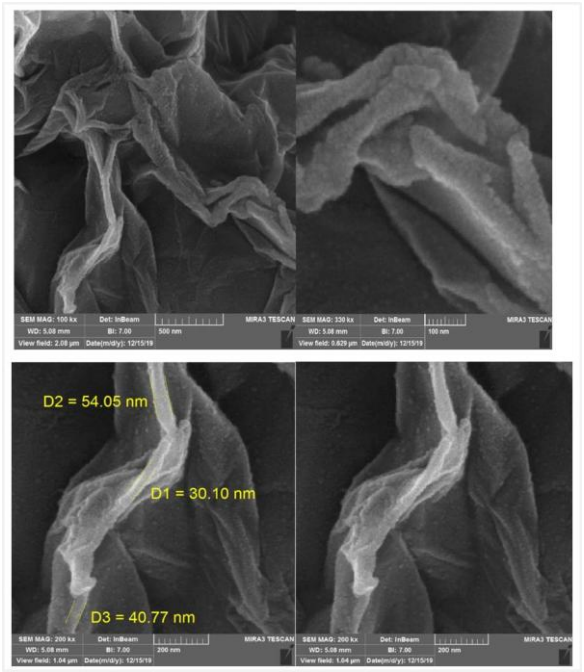

Figure 1. High-resolution FESEM micrograph depicting the surface topography of cobalt sulfide-decorated graphene hybrid nanostructures.

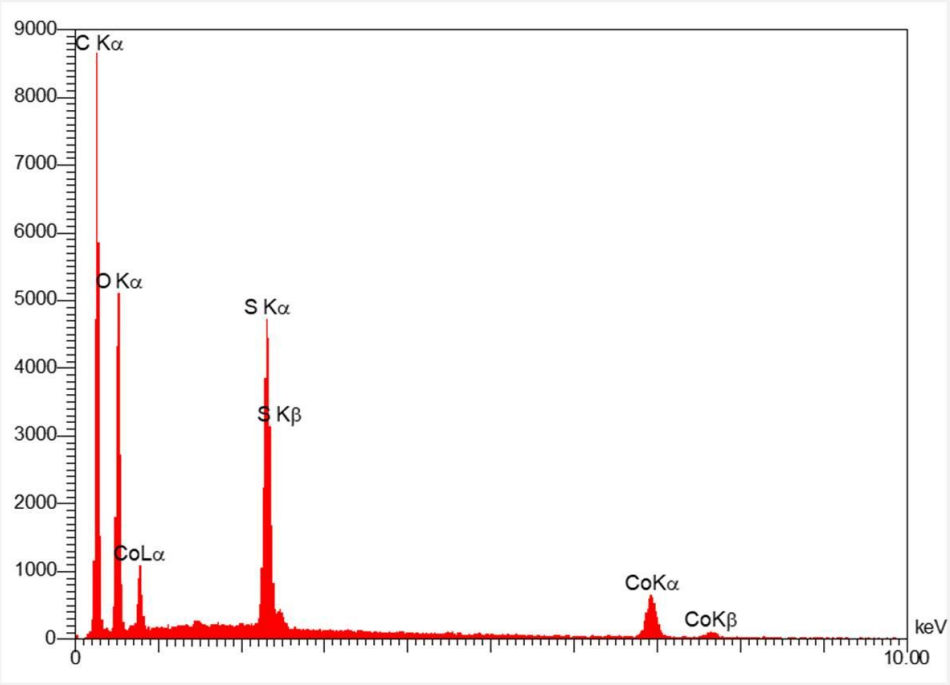

Figure 2. EDX elemental analysis spectra confirming the composition of cobalt sulfide-graphene nanocomposites.

2.3. Immobilization of the nanocomposite material on the working electrode

To prepare the suspension for electrode modification, 10.0 mg of the dry CoS_2-GR nanocomposite powder was dispersed in 1.0 mL of deionized water via 30 minutes of ultrasonication to form a homogeneous 10 mg mL^{-1} suspension. For electrode modification, a 5 µL aliquot of the well-dispersed CoS_2-GR suspension (10 mg mL^{-1}) was precisely pipetted and deposited at the center of the pristine platinum working electrode surface, resulting in a total nanocomposite loading of 50 µg. The solvent was allowed to evaporate under ambient conditions for 20 to 25 minutes, forming a uniform thin-film coating of the nanocomposite on the electrode surface. Following complete solvent evaporation, the modified electrode was rinsed gently with deionized water to remove any loosely adsorbed material and was subsequently used for electrochemical characterization.

2.4. Hydrazine measurement method using cyclic voltammetry

Cyclic voltammetry is an advanced potentiostatic technique derived from linear potential sweep methodology. It involves applying a time-dependent triangular waveform potential to the working electrode, alternating between oxidative and reductive polarization. This widely used electroanalytical method is essential for gaining mechanistic insights into charge transfer processes, particularly during the initial characterization of novel electrochemical systems. Its significance stems from the direct quantitative relationship between faradaic peak current density and the concentration of electroactive analytes, making it the most versatile and comprehensive method for investigating redox-active species. Its operational flexibility and straightforward experimental setup have led to its widespread adoption in various electrochemical research fields, including inorganic coordination complexes, organic redox systems, and biomolecular electron transfer processes. In the voltammetry method, three electrodes are used: the working electrode, the reference electrode, and the auxiliary electrode. The potential is applied between the working and reference electrodes, while the current is measured between the working and auxiliary electrodes (Bourgeois, 2001). In this system, the three electrodes are connected to a galvanostat. The working electrode, along with the other two electrodes, is placed in different solutions, and an appropriate potential and sweep rate depending on the type of experiment are applied. In this way, it was used for all experiments, including determining the optimal pH, examining the effect of sweep rate on electrochemical behavior, concentration effect, and determining hydrazine in various samples.

3. Results

This investigation aims to engineer an advanced electrochemical transducer through surface functionalization, establishing a robust analytical protocol for hydrazine quantification with enhanced sensitivity, precision, rapid response, operational simplicity, and economic viability. To elucidate the electrochemical behavior and quantify the active surface area of both pristine and functionalized electrodes, cyclic voltammetric analysis was conducted in a reversible redox probe system utilizing potassium ferrocyanide ($K_4[Fe(CN)_6]$). The experimental protocol involved immersing both electrode variants in 10 mM ferrocyanide electrolyte and executing potential sweeps across a scan rate spectrum of 10-300 mV s^{-1} (refer to Figures 3-4). Distinct oxidation and reduction peaks corresponding to the $[Fe(CN)_6]^{3-/4-}$ redox couple were evident for both electrodes, with notably augmented current densities observed on the cobalt sulfide-graphene

nanocomposite modified surface. These observations align with the Randles-Ševčík theoretical framework, which predicts linear dependence of peak current on the square root of scan rate for diffusion-controlled reversible systems (Herbei et al., 2023; Mirceski et al., 2024). The linearity of this graph confirms that the electron transfer process on the surface of the modified electrode is diffusion-controlled and that the active surface area of the modified electrode has increased (Figures 5 and 6).

The voltammetric profiles shown in Figures 5 and 6 illustrate a notable reduction in peak potential separation (ΔEp) for the functionalized electrode compared to its unmodified version. This decrease in polarization potential is directly linked to improved charge transfer kinetics at the nanostructured interface, indicating enhanced electrochemical reversibility due to the modified surface architecture. The lower ΔEp value quantitatively confirms the increased electron transfer efficiency achieved through electrode functionalization, as the catalytic nanocomposite layer effectively lowers activation barriers for the redox process.

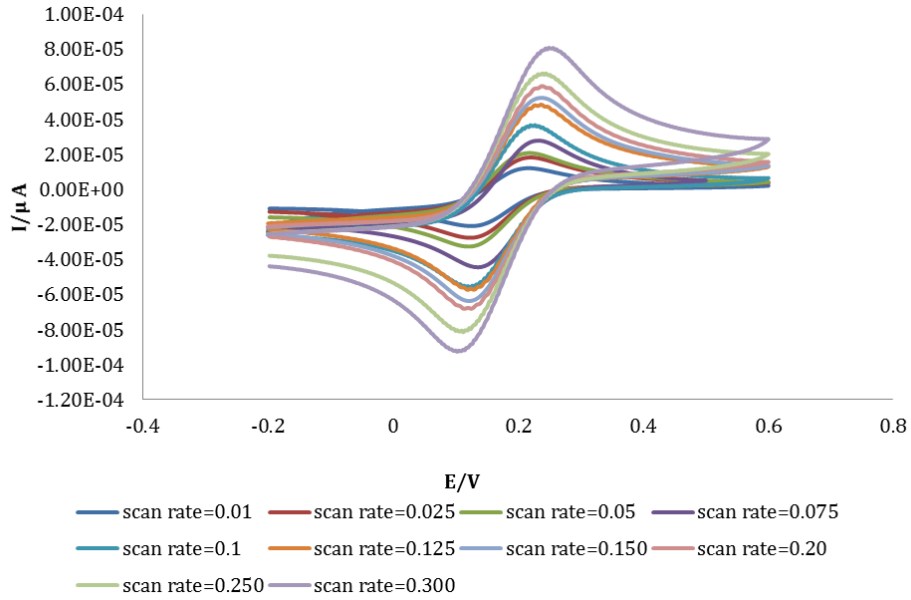

Figure 3. Cyclic voltammetry profiles of $K_4[Fe(CN)_6]$ at varying potential sweep rates using a bare (unmodified) electrode.

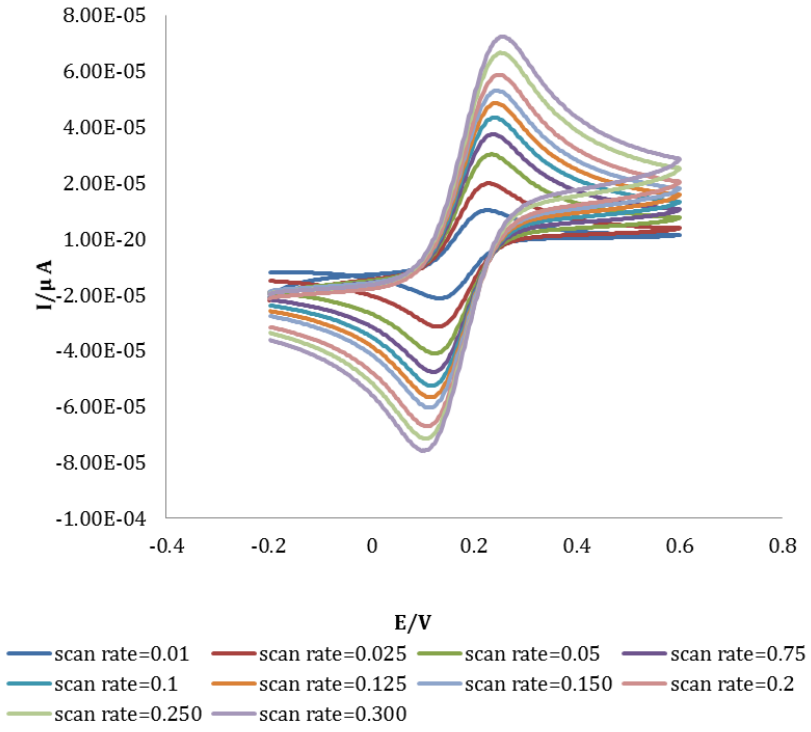

Figure 4. Cyclic voltammetric response of $K_4[Fe(CN)_6]$ at multiple scan rates on a cobalt sulfide-graphene modified electrode.

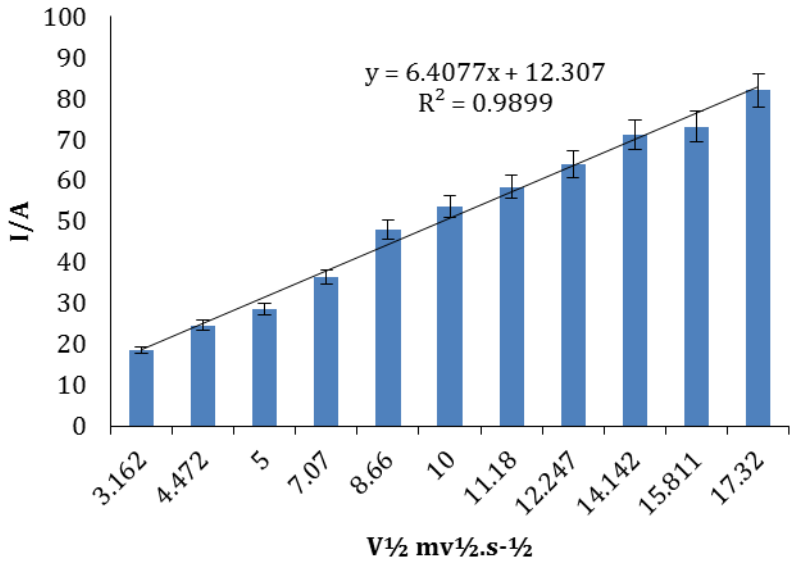

Figure 5. Linear correlation between anodic peak current and the square root of scan rate for the unmodified electrode.

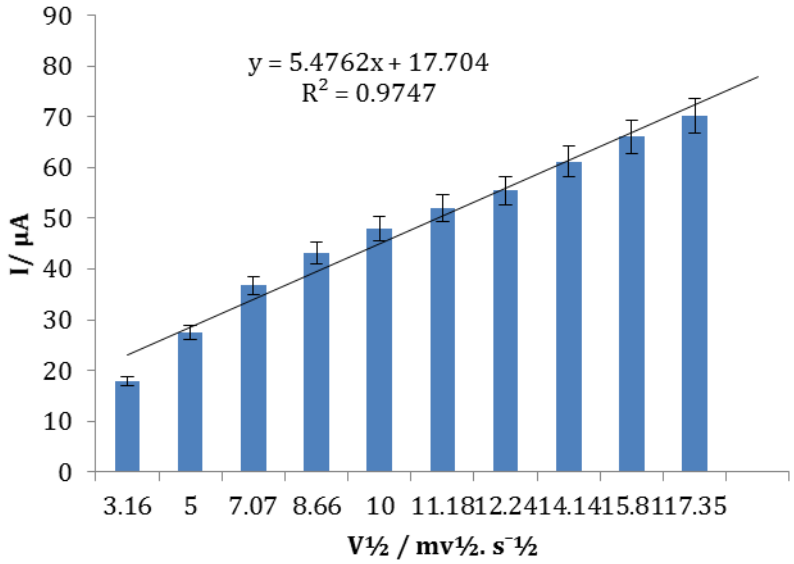

Figure 6. Dependence of anodic peak current on the square root of scan rate for the cobalt sulfide-graphene functionalized electrode.

The operational durability of the cobalt disulfide-graphene hybrid material was assessed through continuous cyclic voltammetric scanning over 50 cycles in a potassium ferrocyanide electrolyte (Figure 7). The electrochemical analysis revealed remarkable stability, with both oxidation and reduction potentials showing negligible shifts ($\Delta E < 5$ mV) throughout the testing period. Quantitative evaluation indicated only a minimal current decrease of 3.8 ± 0.2% in peak current density, confirming the excellent structural integrity and interfacial adhesion of the nanocomposite coating. These results highlight the exceptional electrochemical robustness of the surface-bound cobalt sulfide-graphene nanostructure under repeated redox cycling conditions.

The electrochemical behavior of the modified electrode was systematically investigated as a function of nanocomposite loading concentration, given the critical influence of material composition on charge transfer kinetics. Voltammetric characterization was performed using electrodes functionalized with 5 µL and 10 µL aliquots of cobalt disulfide-graphene nanohybrid suspension in potassium ferrocyanide electrolyte. Comparative analysis of oxidative peak currents revealed superior electrocatalytic activity for the 5 µL modified electrode, which was consequently selected as the optimal configuration for subsequent experiments.

A systematic evaluation of hydrazine electrooxidation pathways was conducted through cyclic voltammetric analysis of 2 mM hydrazine solutions across varying pH conditions (Figure 9). The voltammetric profiles revealed a cathodic shift in oxidation potential concomitant with increasing alkalinity, accompanied by moderate current enhancement at pH 9. Optimal electrocatalytic performance was observed at pH 9, demonstrating

maximum faradaic current density. The oxidation potential exhibited a non-monotonic dependence on pH, increasing progressively from pH 6 to 9 before decreasing at more alkaline conditions. This characteristic potential-pH relationship suggests a proton-coupled electron transfer mechanism governed by the following redox process: The observed electrochemical behavior confirms that hydrazine oxidation within the pH 6-9 window proceeds through a concerted proton-electron transfer process involving stoichiometric equivalence of both species. (Golabi et al., 2001; Michalkiewicz et al., 2024):

$$N_2H_4 \rightarrow N_2 + 4H^+ + 4e^- \quad (1)$$

Cyclic voltammetric analysis was employed to investigate the electrocatalytic oxidation kinetics of hydrazine (2 mM) at a cobalt disulfide-graphene nanocomposite-modified electrode (Profile α), with comparative studies performed on an unfunctionalized electrode (Profile β) and a background control in hydrazine-free phosphate buffer (Profile γ), all measurements conducted under standardized conditions (pH 9, 50 mV/s scan rate) as depicted in Figure 10. The nanohybrid-modified surface demonstrated significantly enhanced electrochemical activity, evidenced by pronounced current amplification and favorable potential shifts relative to the unmodified substrate, while the control measurement established the baseline electrochemical signature of the supporting electrolyte system (Karami-Kolmoti and Zaimbashi, 2023).

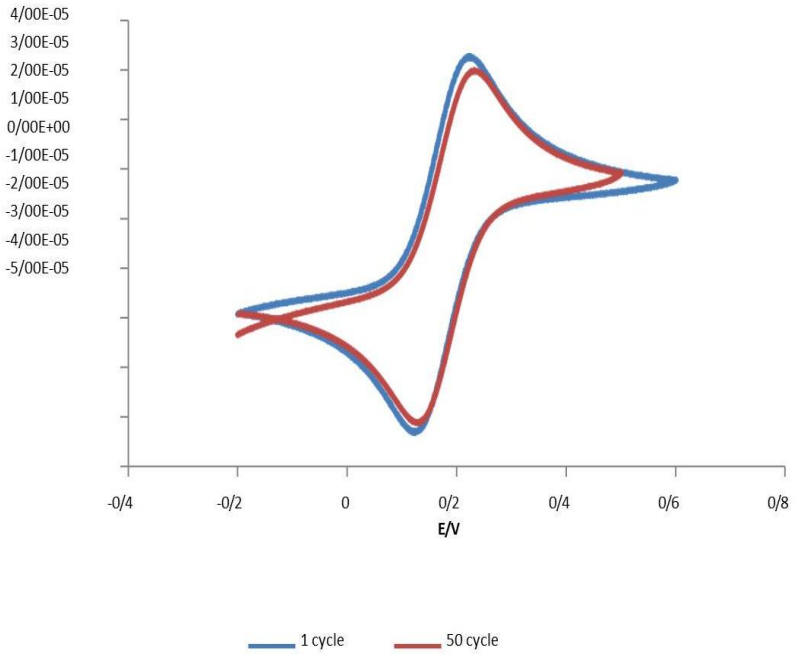

Figure 7. Successive cyclic voltammetry scans of $K_4[Fe(CN)_6]$ at 50 mV/s using the cobalt sulfide-graphene nanocomposite-modified electrode.

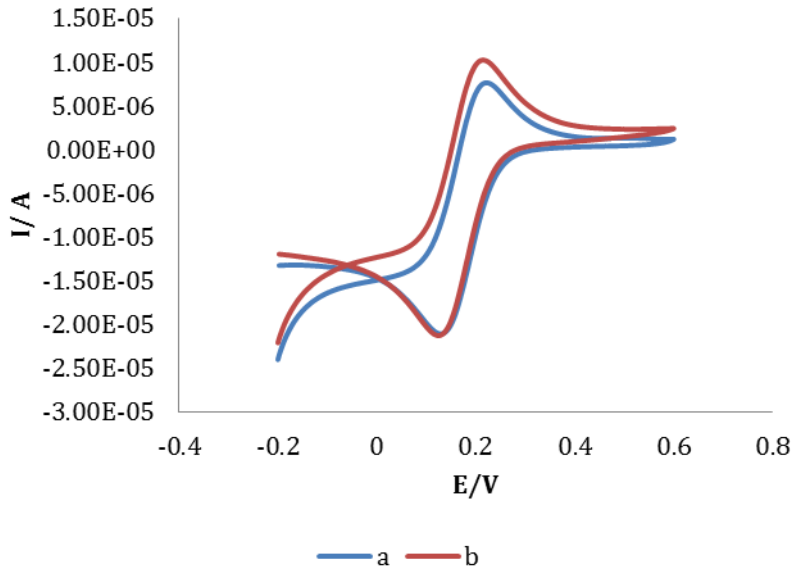

Figure 8. Comparative electrode modifications: (a) 10 µL deposition, (b) 5 µL deposition.

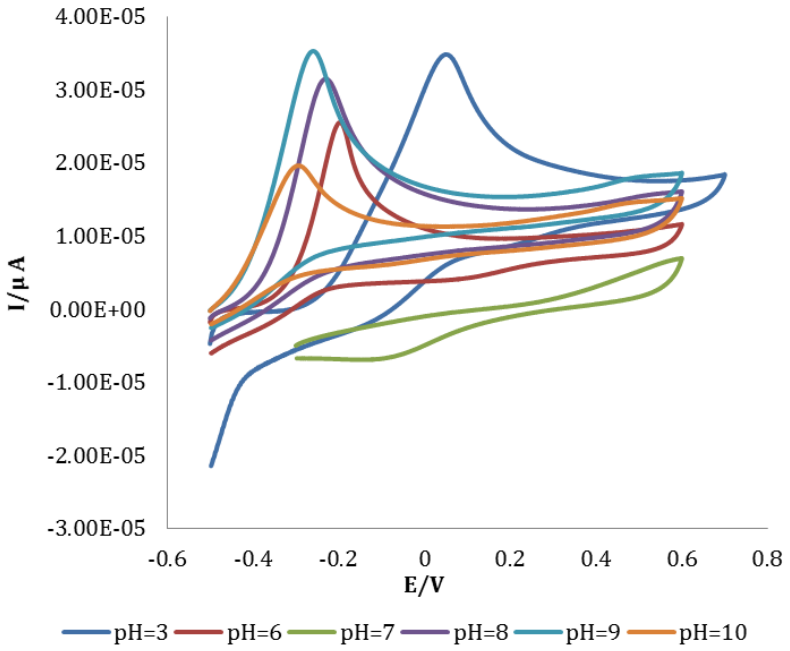

Figure 9. pH-dependent cyclic voltammetric behavior of hydrazine solutions.

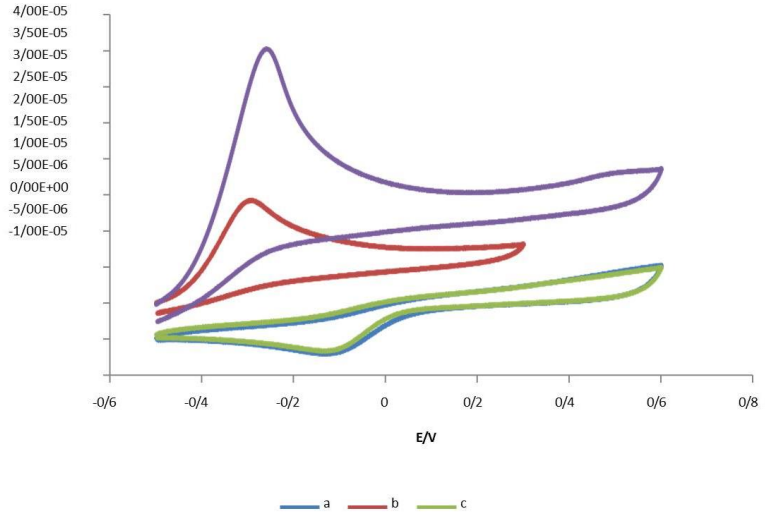

Figure 10. Comparative CV responses in pH 9 phosphate buffer: (a) Modified electrode with 2 mM hydrazine, (b) Unmodified electrode with 2 mM hydrazine, (c) Unmodified electrode (blank).

The voltammetric response of the functionalized electrode was characterized across multiple scan rates in pH 9 phosphate buffer electrolyte containing 2 mM hydrazine. Subsequent quantitative analysis revealed a linear correlation ($R^2 > 0.99$) between oxidative peak current density and the square root of scan rate (Figure 11), demonstrating diffusion-controlled charge transfer kinetics at the nanostructured interface. This relationship confirms the electrochemical reaction follows the Randles-Ševčík behavior, where mass transport limitations dominate the redox process at the modified electrode surface.

To determine the diffusion coefficient of hydrazine (D) on the nanoparticle-modified electrode, we employed chronoamperometry. A potential of 300 mV relative to the reference electrode was applied, and chronoamperograms were recorded under optimal conditions for various concentrations of hydrazine. Based on the Cottrell equation, the variation of current as a function of the inverse square root of time was plotted for different concentrations of hydrazine over a specific time range (Figure 12). The slope value for each concentration was obtained, and according to the Cottrell relationship, it was observed that the variation of current with the inverse square root of time is linearly diffusion-controlled (Figure 13) (Sheikh-Mohseni and Pirsa, 2016).

Next, the graph of the variation in the slopes of the $I - t^{\frac{-1}{2}}$ lines in Figure 13 and 14 were plotted against the concentration of hydrazine. From the slope of this graph, the diffusion coefficient of hydrazine was found to be 8.48 $\times 10^{-9}$ cm^2 s^{-1}.

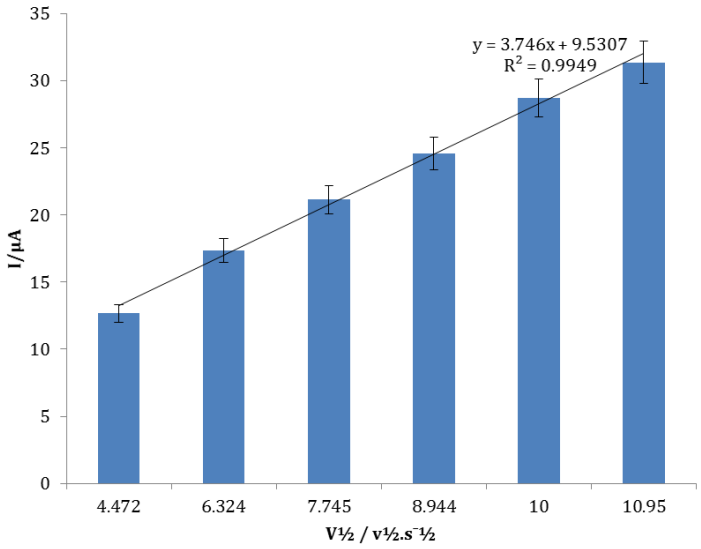

Figure 11. Chronoamperometric recordings of the modified electrode in pH 9 buffer with incremental hydrazine concentrations

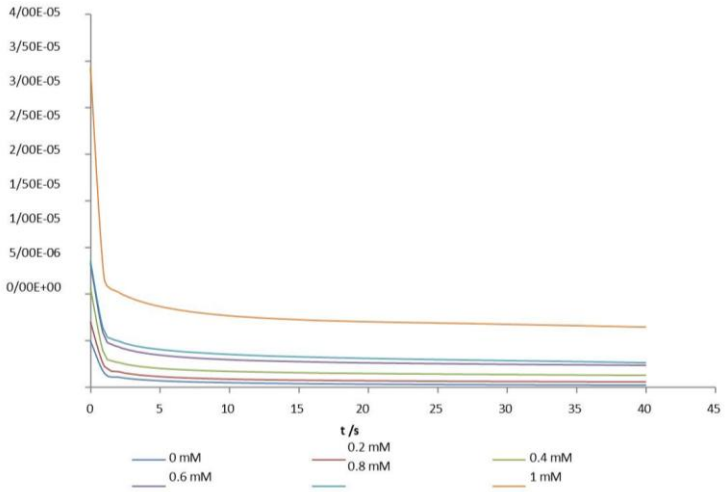

Figure 12. Chronoamperograms of the modified electrode in a buffer solution with pH = 9 in the presence of different concentrations of hydrazine.

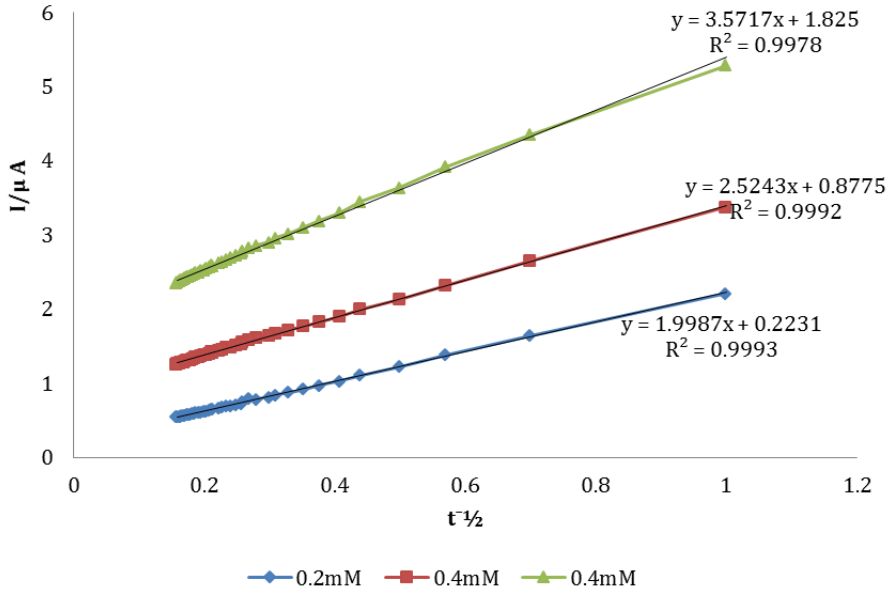

Figure 13. Cottrell plot (current vs. $t^{-1/2}$) for varying hydrazine concentrations in pH 9 buffer.

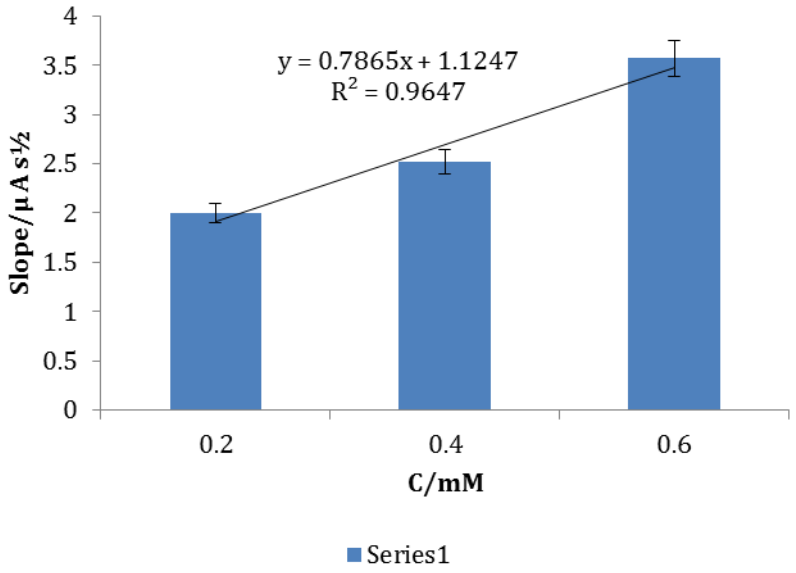

Figure 14. Slope analysis of I-$t^{-1/2}$ linear regressions as a function of hydrazine concentration.

Differential pulse voltammetry (DPV) was chosen as the primary analytical method because it offers superior resolution and increased sensitivity compared to traditional voltammetric techniques. This method allowed for the accurate development of a calibration profile and the determination of the hydrazine detection threshold. Quantitative analysis was performed under optimized conditions (applied potential: -0.6 to -0.1 V vs. reference, pH 9 phosphate buffer electrolyte) using a nanostructured electrode. The voltammetric response showed a linear relationship between oxidative current amplitude and hydrazine concentration within the 0.1-2 mM range. The progressive augmentation of anodic peak intensity with increasing analyte concentration ($\Delta I/\Delta C$ = 12.3 μA/mM, R^2 = 0.998) confirms both the electrochemical stability of the cobalt disulfide-graphene nanocomposite and its sustained catalytic activity during successive analyte introduction. This behavior substantiates the material's potential for continuous monitoring applications requiring stable electrocatalytic performance (Figure 15) (Karami-Kolmoti and Zaimbashi, 2023).

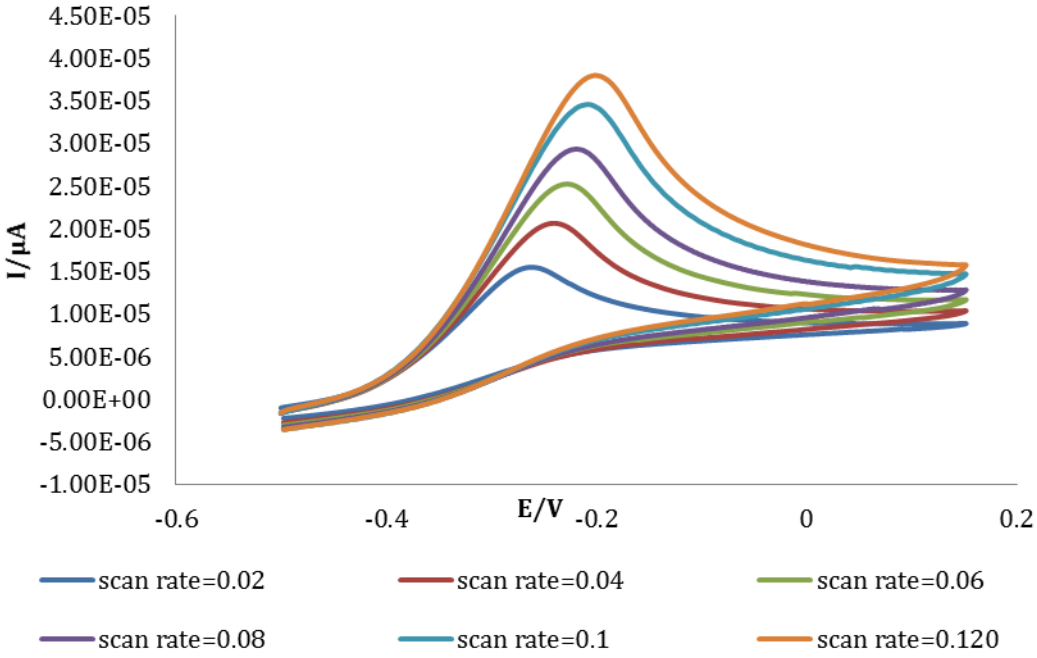

Figure 15. Anodic peak current vs. square root of scan rate for the nanocomposite-modified electrode.

In Figures 16 and 17, the peak current of the differential pulse voltammogram is shown as a function of hydrazine concentration. The calibration curve for hydrazine is linear in the concentration range of 0.2 to 2 mM. In this concentration range, the sensitivity is 0.0051 µA/µM. At higher concentrations of hydrazine, the generation of nitrogen gas at the electrode surface increases and affects the diffusion of hydrazine. Therefore, the slope of the calibration curve decreases at higher concentrations. The gas production at lower concentrations is not sufficient to hinder the diffusion of hydrazine toward the electrode. From the slope of the calibration curve, the detection limit of the sensor for hydrazine was calculated to be 0.081 mM.

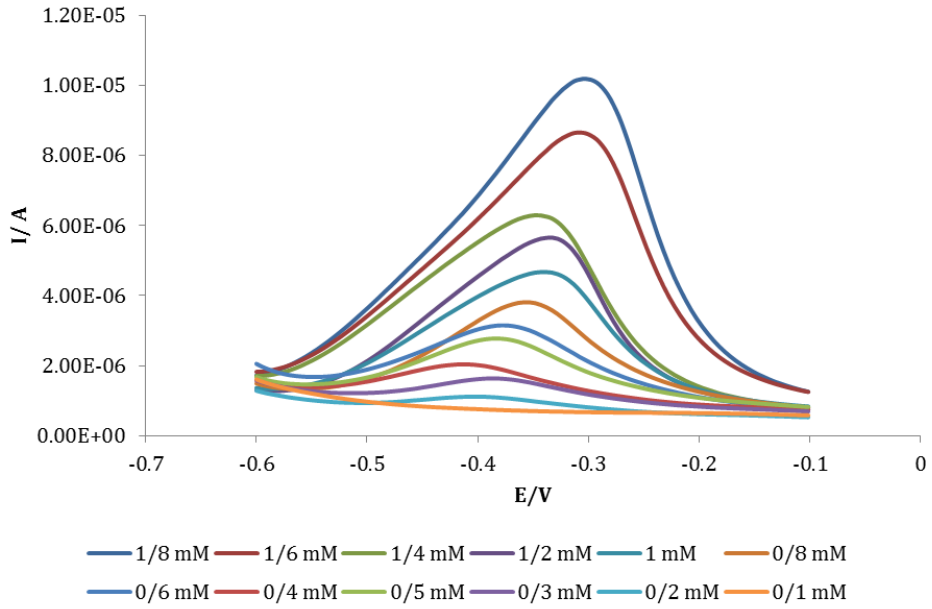

Figure 16. Differential pulse voltammetry responses for hydrazine detection at different concentrations (pH 9 buffer).

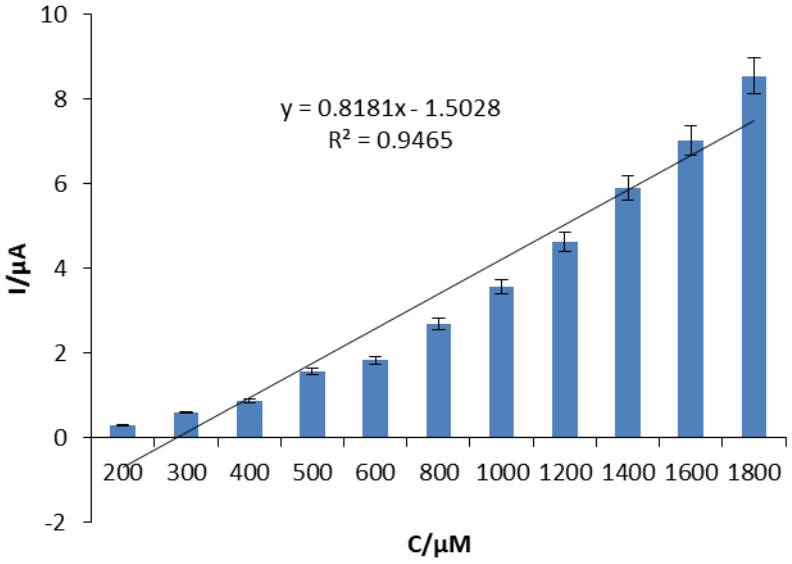

Figure 17. Standard calibration curve for hydrazine quantification (0.2–2 mM range)

4. Discussion

According to Nicholson's theory, the peak potential separation (ΔEp) of a reversible redox couple serves as an important indicator of electron transfer kinetics at the electrode surface. The relationship demonstrates an inverse correlation between ΔEp and the electron transfer rate constant (k^o) - as k^o increases, the ΔEp value decreases correspondingly. This fundamental principle arises because faster electron transfer kinetics allow the redox system to maintain equilibrium more effectively during potential scanning, resulting in narrower peak separation. The theoretical foundation for this relationship is based on the Butler-Volmer formalism of electrode kinetics. In this framework, rapid electron transfer enables efficient charge propagation across the electrode-electrolyte interface. When the standard rate constant (k^o) is sufficiently high—typically greater than 0.1 cm/s for a one-electron process—the system exhibits nearly reversible behavior,

characterized by minimal peak separation (ΔEp), approaching the theoretical value of 59 mV for n=1 at 25°C. In contrast, slower electron transfer results in increased peak separation due to higher overpotential requirements. This principle serves as a valuable diagnostic tool for assessing the effectiveness of electrode modifications and for understanding charge transfer mechanisms in electrochemical systems (Mirceski et al., 2024; Raeisi-Kheirabadi et al., 2022). Therefore, the presence of sulfide-graphene nanoparticles on the electrode surface not only increases the active surface area but also improves the electron transfer rate. Another conclusion that can be drawn from Figures 3 and 4 is that a scan rate of 50 millivolts per second is the optimal rate for this study.

The voltammetric response (Curve α) shows a significant increase in oxidative current characteristics, evidenced by a 300% rise in peak amplitude and an expanded integrated peak area compared to the unmodified substrate. This notable current enhancement confirms the catalytic effectiveness of the cobalt disulfide-graphene nanocomposite, with the threefold increase in current directly linked to the electron mediation properties of the nanohybrid. These results are consistent with previous observations of accelerated charge transfer kinetics during ferrocyanide oxidation, indicating reliable catalytic behavior across various redox systems. The synergistic effects between the metallic sulfide and carbon nanostructure components improve both electron conduction and the electroactive surface area, ultimately contributing to the enhanced electrochemical performance (Saei and Asadpour-Zeynali, 2023).

Nanoparticles are essential as electrocatalysts in the electrochemical oxidation of hydrazine, as they greatly enhance the electron transfer rate. Their high surface-to-volume ratio and unique electronic properties promote faster charge transfer kinetics, resulting in more efficient electrochemical reactions. Additionally, nanoparticles increase the effective surface area of the electrode, offering more active sites for hydrazine oxidation. This expansion of the active surface area leads to a higher electrochemical current, indicating improved catalytic activity. The increase in current observed on nanoparticle-modified electrodes confirms their effectiveness in enhancing the electrochemical oxidation of hydrazine. This enhancement arises from both improved electron transfer efficiency and a greater number of available reaction sites. Consequently, the modified electrode demonstrates a stronger response to hydrazine oxidation compared to unmodified electrodes. Moreover, the amplified current response correlates with higher measurement sensitivity, enabling more precise and reliable detection of hydrazine. This improvement is especially advantageous in applications that require low detection limits, such as environmental monitoring, fuel cell technology, and chemical sensing. Thus, nanoparticle-modified electrodes present a promising strategy for optimizing electrochemical sensors and catalytic systems, combining enhanced reactivity with superior sensitivity. In summary, nanoparticles significantly enhance the electrocatalytic performance of electrodes by accelerating electron transfer, expanding the active surface area, and increasing current response, ultimately improving sensitivity in hydrazine detection (Hatip et al., 2021; Miao et al., 2021; Wang et al., 2021).

The study concludes that the electrocatalytic oxidation of hydrazine on the modified electrode surface is controlled by diffusion. Initially, increasing the scan rate leads to a sharp rise in the anodic peak current, indicating a strong dependence on diffusion. However, as the scan rate continues to increase, the peak current rises more slowly, suggesting that diffusion is becoming the limiting factor. This behavior confirms that the reaction kinetics are determined by the mass transport of reactants to the electrode surface, rather than by the electron transfer process itself. The findings emphasize the crucial role of diffusion in influencing the efficiency of hydrazine oxidation at different scan rates (Alsoghier et al., 2024).

5. Conclusion

In conclusion, this study successfully engineered an advanced electrochemical transducer through functionalization with a cobalt sulfide-graphene nanocomposite, establishing a highly effective protocol for hydrazine sensing. The modified electrode demonstrated superior performance, evidenced by a significantly enhanced active surface area, a reduced peak potential separation (ΔEp) confirming faster charge transfer kinetics, and exceptional stability with only a 3.8% current loss over 50 cycles. The sensor operated via a diffusion-controlled mechanism, as confirmed by Randles-Ševčík analysis, and achieved optimal electrocatalytic hydrazine oxidation at pH 9. The differential pulse voltammetry (DPV) method provided a highly sensitive and linear response ($R^2 = 0.998$) across a 0.2–2 mM concentration range, yielding a detection limit of 0.081 mM. This work validates the functionalized electrode as a robust, sensitive, and stable platform for reliable hydrazine quantification.

References

Alsoghier, H. M., Abd-Elsabour, M., Alhamzani, A. G., Abou-Krisha, M. M., & Assaf, H. F. (2024). Real samples sensitive dopamine sensor based on poly 1,3-benzothiazol-2-yl ((4-carboxlicphenyl) hydrazono) acetonitrile on a glassy carbon electrode. *Scientific Reports*, *14*(1), 16601. https://doi.org/10.1038/s41598-024-65192-0

Choi, H. N., Kim, H., Kim, M. J., & Sun, Y. K. (2024). Constructing the interconnected charge transfer pathways in sulfur composite cathode for all-solid-state lithium-sulfur batteries. *ACS Applied Materials & Interfaces*, *16*(8), 11076–11083. https://doi.org/10.1021/acsami.3c18675

Fazeli-Nasab, B., Shahraki-Mojahed, L., Beigomi, Z., Beigomi, M., & Pahlavan, A. (2022). Rapid detection methods of pesticides residues in vegetable foods. *Chemical Methodologies*, *6*(1), 24–40. https://doi.org/10.22034/chemm.2022.1.3

Golabi, S., Zare, H., & Hamzehloo, M. (2001). Electrocatalytic oxidation of hydrazine at a pyrocatechol violet (PCV) chemically modified

electrode. *Microchemical Journal*, *69*(2), 13–23. https://doi.org/10.1016/s0026-265x(00)00158-2

Hatip, M., Koçak, S., & Dursun, Z. (2021). Sensitive determination of hydrazine using poly(phenolphthalein), Au nanoparticles and multiwalled carbon nanotubes modified glassy carbon electrode. *Turkish Journal of Chemistry*, *45*(1), 167–180. https://doi.org/10.3906/kim-2009-12

Herbei, E. E., Alexandru, P., & Busila, M. (2023). Cyclic voltammetry of screen-printed carbon electrode coated with Ag-ZnO nanoparticles in chitosan matrix. *Materials*, *16*(8). https://doi.org/10.3390/ma16083266

Huo, Y., Yu, T., Xue, Y., Zhang, G., Song, S., Shao, Y., & Han, X. (2024). Three CoS/CoO microspheres and their mixed matrix membranes for the highly efficient photocatalytic degradation of methyl blue. *RSC Advances*, *14*(35), 25811–25819. https://doi.org/10.1039/d4ra03261f

Iqbal, A. A., Harcen, C. S., & Haque, M. (2024). Graphene (GNP) reinforced 3D printing nanocomposites: An advanced structural perspective. *Heliyon*, *10*(7), e28771. https://doi.org/10.1016/j.heliyon.2024.e28771

Karami-Kolmoti, P., & Zaimbashi, R. (2023). An electrochemical sensing platform based on a modified carbon paste electrode with graphene/Co_3O_4 nanocomposite for sensitive propranolol determination. *ADMET & DMPK*, *11*(2), 227–236. https://doi.org/10.5599/admet.1705

Meng, J., Zahran, M., & Li, X. (2024). Metal-organic framework-based nanostructures for electrochemical sensing of sweat biomarkers. *Biosensors*, *14*(10). https://doi.org/10.3390/bios14100495

Miao, R., Yang, M., & Compton, R. G. (2021). The electro-oxidation of hydrazine with palladium nanoparticle modified electrodes: Dissecting chemical and physical effects—Catalysis, surface roughness, or porosity? *Journal of Physical Chemistry Letters*, *12*(28), 6661–6666. https://doi.org/10.1021/acs.jpclett.1c01955

Michalkiewicz, S., Skorupa, A., Jakubczyk, M., & Bebacz, K. (2024). Application of a carbon fiber microelectrode as a sensor for apocynin electroanalysis. *Materials*, *17*(7). https://doi.org/10.3390/ma17071593

Mirceski, V., Guziejewski, D., & Gulaboski, R. (2024). Genuine anodic and cathodic current components in cyclic voltammetry. Scientific Reports, *14*(1), 17314. https://doi.org/10.1038/s41598-024-67840-x

Motaharian, A., & Milani, H. M. (2015). Electrochemical sensor based on molecularly imprinted polymer nanoparticles for determination of diazepam drug. *Journal of Applied Research in Chemistry*, *9*(3), 51–59. https://sid.ir/paper/180276/en

Najafi, M., & Sohuli, S. (2018). Electrochemical sensor for fentanyl determination by modified electrode with carbon nanotube and iron (III) oxide nanoparticles. *Journal of Applied Research in Chemistry*, *12*(1), 103–110. https://sid.ir/paper/180110/en

Nigde, M., Agir, I., Yildirim, R., & Isildak, I. (2022). Development and comparison of various rod-shaped mini-reference electrode compositions based on Ag/AgCl for potentiometric applications. *Analyst*, *147*(3), 516–526. https://doi.org/10.1039/d1an01754c

Ping, J., Wu, J., Wang, Y., & Ying, Y. (2012). Simultaneous determination of ascorbic acid, dopamine and uric acid using high-performance screen-printed graphene electrode. *Biosensors and Bioelectronics*, *34*(1), 70–76. https://doi.org/10.1016/j.bios.2012.01.016

Raeisi-Kheirabadi, N., Nezamzadeh-Ejhieh, A., & Aghaei, H. (2022). Cyclic and linear sweep voltammetric studies of a modified carbon paste electrode with nickel oxide nanoparticles toward tamoxifen: Effects of surface modification on electrode response kinetics. *ACS Omega*, *7*(35), 31413–31423. https://doi.org/10.1021/acsomega.2c03441

Saei, J. N., & Asadpour-Zeynali, K. (2023). Enhanced electrocatalytic activity of fluorine-doped tin oxide (FTO) by trimetallic spinel $ZnMnFeO_4$/$CoMnFeO_4$ nanoparticles as a hydrazine electrochemical sensor. *Scientific Reports*, *13*(1), 12188. https://doi.org/10.1038/s41598-023-39321-0

Sheikh-Mohseni, M. A., & Pirsa, S. (2016). Nanostructured conducting polymer/copper oxide as a modifier for fabrication of L-dopa and uric acid electrochemical sensor. *Electroanalysis*, *28*(9), 2075–2080. https://doi.org/10.1002/elan.201600089

Traipop, S., Jesadabundit, W., Khamcharoen, W., Pholsiri, T., Naorungroj, S., Jampasa, S., & Chailapakul, O. (2024). Nanomaterial-based electrochemical sensors for multiplex medicinal applications. *Current Topics in Medicinal Chemistry*, *24*(11), 986–1009. https://doi.org/10.2174/0115680266304711240327072348

Uzdrowska, K., Knap, N., Konieczna, L., Kamm, A., Kuban-Jankowska, A., Gieraltowska, J., ... Gorska-Ponikowska, M. (2025). Combined graphene oxide with 2-methoxyestradiol for effective anticancer therapy in vitro model. *International Journal of Nanomedicine*, *20*, 933–950. https://doi.org/10.2147/ijn.s498947

Wang, H., Dong, Q., Lei, L., Ji, S., Kannan, P., Subramanian, P., & Yadav, A. P. (2021). *Co* nanoparticle-encapsulated nitrogen-doped carbon nanotubes as an efficient and robust catalyst for electro-oxidation of hydrazine. *Nanomaterials*, *11*(11). https://doi.org/10.3390/nano11112857

Wang, L., Huang, P. F., Wang, H. J., Bai, J. Y., Zhang, L. Y., & Zhao, Y. Q. (2007). Covalent modification of glassy carbon electrode with aspartic acid for simultaneous determination of hydroquinone and catechol. *Annali di Chimica*, *97*(5–6), 395–404. https://doi.org/10.1002/adic.200790024

Wang, X., Wu, D., Yuan, D., & Wu, X. (2022). A nano-lead dioxide-composite electrochemical sensor for the determination of chemical oxygen demand. *Journal of Environmental Chemical Engineering*, *10*(3), 107464. https://doi.org/10.1016/j.jece.2022.107464

Guide for Authors

Preface

The Journal of *Agriculture, Environment and Society (AES)* welcomes articles in various areas of agriculture from all over the world. Contributions must be original and have not previously been published elsewhere. Please be ensure that there are no conflicts between the authors before submitting. Before being published, manuscripts submitted to *Agriculture, Environment and Society (AES)* are critically reviewed. The purpose of the review is to reassure readers that the papers have been approved by competent and unbiased professionals. The manuscript should be submitted only via the *Agriculture, Environment and Society (AES)* Editorial System (https://aes.uoz.ac.ir/). All papers are available free of charge at the Journal's webpage.

Types of article

The following types of contribution are published in Agriculture, Environment and Society (AES):

Original research article: It should describe novel and well validated findings, and experimental techniques should be described in sufficient detail to allow the study to be verified. Research papers of 6000-8000 words in length, with tables, illustrations and references, in which hypotheses are tested and results reported.

Review article: Review and perspective on current issues are accepted and encouraged. The format and length of review papers are more flexible than for a full paper. Typical reviews are less than 12000 words including references.

Short Communications: It is appropriate for recording the results of small-scale research or providing information on novel models or hypotheses, innovative methodologies, procedures, or apparatus. Research papers of 2500-3500 words in length, with tables, illustrations and references.

Structure of Articles

Text should be written in a succinct and cohesive manner, with an emphasis on significant points, conclusions, breakthroughs, or discoveries, as well as their broader relevance. All running text should be saved as a Word document. All writings should be written using Times New Roman font. Both American and British English format are accepted, but not their mixture. The font size for title is 14 point and for the main text is 12 point. The subtitles should be written in Bold and font size of 12 point. Figures and tables can be put within the text or at the bottom. Figures should have a high enough resolution to allow for refereeing.

The original research articles should contain the following sections:

Title

The title should be clear, intelligible to experts in different disciplines, and represent the substance of the article. There may be no abbreviations in the title. The title, authors, and affiliations should all be included on a title page as the first page of the manuscript file.

Name(s) of the author (s) not visible in the manuscript (Double Blind Reviews).

Abstract

The title's information does not need to be duplicated in the abstract. The abstract should not be more than 350 words long. It must include the study's goal, methods, findings, and conclusions. Abbreviations should be used sparingly and explained when first used. The abstract is presented separately from the article in a single paragraph after the title page in the manuscript file.

Keywords

Provide a maximum of six keywords appear immediately after the abstract with alphabetical order. Keywords should cover the most precise phrases in the article and should not be the same as the terms used in the title.

Introduction

The introduction should provide background that puts the manuscript into context and allows readers outside the field to understand the purpose and significance of the study. It should define the problem addressed and why it is important, with a brief review of the key literature and conclude with a brief statement of the overall aim of the work.

Material and methods
Provide sufficient details to allow the work to be reproduced by an independent researcher. Methods that are already published should be summarized, and indicated by a reference. If quoting directly from a previously published method, use quotation marks and also cite the source. Any modifications to existing methods should also be described.

Results
Results should be clear and concise.

Discussion
This should explore the significance of the results of the work, not repeat them. A combined Results and Discussion section is often appropriate. Together, these sections should describe the results of the experiments, the interpretation of these results, and the conclusions that can be drawn. Authors should explain how the results relate to the hypothesis presented as the basis of the study and provide a succinct explanation of the implications of the findings, particularly in relation to previous related studies and potential future directions for research.

Conclusions
The main conclusions of the study may be presented in a short Conclusions section, which may stand alone or form a subsection of a Discussion or Results and Discussion section.

Appendices
If there is more than one appendix, they should be identified as A, B, etc. Formulae and equations in appendices should be given separate numbering: Eq. (A.1), Eq. (A.2), etc.; in a subsequent appendix, Eq. (B.1) and so on. Similarly for tables and figures: Table A.1; Fig. A.1, etc.

Acknowledgements
Acknowledgements of persons, grants, money, and so forth should be included before the reference list in a distinct section.

References
Please ensure that every reference cited in the text is also present in the reference list (and vice versa). In the text, papers with more than two authors should be cited by the last name of the first author, followed by et al., space, and the year of publication (example: Jones et al., 2020). If the cited manuscript has two authors, the citation should include both last names, space, and the publication year (example: Smith and Ebrahim, 2018).

In the Reference section, a maximum of ten authors of the cited paper may be given. All references cited in the text must be listed in the Reference section alphabetically by the last names of the author(s) and then chronologically.

Format for Journal paper
Author, A. A., Author, B. B., & Author, C. C., (Year of publication). Title of article. *Name of Journal*, *Volume number*(issue number), pages. **Doi link**

Example:

Golshani, F., Asgharipour, M. R., Ghanbari, A., & Seyedabadi, E. (2023). Environmental accounting for croplands, livestock husbandry, and integrated systems based on emergetic indicators. *Energy, Ecology and Environment*, *8*(1), 28-49. **https://doi.org/10.1007/s40974-022-00262-5**

Format for Books
Author, A. A., (Year of publication). Title of work: Capital letter also for subtitle. Location: Publisher.

Strunk Jr., W., & White, E. B., (2000). The Elements of Style, fourth ed. Longman, New York.

Chapter in an Edited Book
Author, A. A., & Author, B. B., (Year of publication). Title of chapter, in: Title of book (Eds.). Publisher, Location, pages of chapter.

Mettam, G. R., Adams, L. B., (2009). How to prepare an electronic version of your article, in: Jones, B. S., Smith, R. Z. (Eds.), Introduction to the Electronic Age. E-Publishing Inc., New York, pp. 281–304.

Note: To ensure accurate and efficient referencing, it is recommended to use reference management software such as EndNote for in-text citations and reference lists. The appropriate style (AES style) for EndNote can be downloaded from journal website.

Tables and Figures
Please submit tables and figures as editable text and not as images. All figures and tables should be embedded while correctly positioned.

Tables
Please avoid using vertical lines in tables. Please use "Table" in both text and captions. Number tables consecutively in accordance with their appearance in the text. Place footnotes to tables below the table body and indicate them with superscript lowercase letters. Avoid vertical rules. Be sparing in the use of tables and ensure that the data presented in tables do not duplicate results described elsewhere in the article. The table caption appears above the table using Times New Roman font with font size of 10 points in bold. Use no border for the tables. Footnotes to tables should appear beneath the tables and should be designated by a lower-case superscript letter, †, or z, y, x, etc.

Figures
Ensure that each illustration has a caption. Supply captions separately, not attached to the figure. A caption should comprise a brief title (not on the figure itself) and a description of the illustration. Keep text in the illustrations themselves to a minimum but explain all symbols and abbreviations used (preferably in the caption). The caption should allow the reader to understand the main elements of what is being shown without needing to refer to then main text. The figure caption appears below the figure and written using Times New Roman font with font size of 10 points in bold. Use no border for the figures. The font size within the figure should not smaller than 8 point and bigger than 10 point. Try to present the figures in gray scale instead of color illustration. Use (Figure) at the end of the sentence and captions and use Figure in text.

Math formulae
Present simple formulae in the line of normal text where possible. In principle, variables are to be presented in italics. Number consecutively any equations that have to be displayed separately from the text in the right margin (if referred to explicitly in the text).

Suggest Reviewers
With the manuscript, the author should include a list of three qualified, independent, prospective reviewers who could perform quality peer reviews of your document. Be sure to include their complete names, affiliations, and current e-mail addresses.

University of Zabol

Agriculture, Environment & Society

Faculty of Agriculture, University of Zabol, Zabol, Iran
P.O. Box 538-98615, Tel: +98-54-31232102
Website: http://aes.uoz.ac.ir
Email: aes@uoz.ac.ir